The Use of Receptor Chimeras to Study the Function of the Carboxyl Terminal Domain in Prostacyclin Receptor Signalling

A thesis presented for degree of
Doctor of Philosophy

by

Hannah Murdoch

Division of Biochemistry and Molecular Biology

Institute of Biomedical and Life Sciences
University of Glasgow

August 2002

ProQuest LLC.
789 East Eisenhower Parkway
P.O. Box 1346
Ann Arbor, MI 48106 – 1346

List of Contents

List of Figures

List of Tables

Abbreviations

α	alpha subunit of G protein
α-AR	alpha-adrenergic receptor
A	adenine
AC	adenylyl cyclase
ADP	adenosine-5'-diphosphate
Ala (A)	alanine
Asn (N)	asparagine
Asp (D)	aspartate
Arg (R)	arginine
AT	angiotensin
ATP	adenosine-5'-triphosphate
β	beta subunit of G protein
β-AR	beta-adrenergic receptor
βARK	β-AR kinase
βγ	beta-gamma dimer of G protein
B_{max}	maximum binding sites

BSA	bovine serum albumin
C	cytosine
cAMP	adenosine 3', 5'-cyclic monophosphate
CCK	cholecystokinin
CCV	clathrin-coated vesicle
cDNA	complementary DNA
Ci	Curie
C-tail	carboxyl terminal tail
Cys (C)	cysteine
DMEM	Dulbecco's Modified Eagle's Medium
DMSO	dimethyl sulphoxide
DNA	deoxyribonucleic acid
DPM	disentegrations per minute
DTT	dithriothreitol
EC_{50}	concentration of agonist producing half-maximal response
EDTA	ethylenediamine tetra-acetic acid
fmol	femtomole

γ	gamma subunit
G	guanine
G_i	inhibitory G protein
G_s	stimulatory G protein
GDP	guanosine 5'-diphosphate
GF109203X	bisindolylmaleimide I hydrochloride
GFP	green fluorescent protein
Gln (Q)	glutamine
Glu (E)	glutamate
Gly (G)	glycine
GnRH	gonadotropin releasing hormone
GPCR	G protein coupled receptor
GRK	GPCR kinase
GTP	guanosine 5'-triphosphate
^3H	tritium
H89	N-[2-((*p*-bromocinnamyl)amino)ethyl]-5-isoquinolinesulfonamide, 2HCl

HA	haemagglutinin
HA-IP	HA-tagged IP-R
HA-IP-β_2	HA-IP with β_2-AR carboxyl tail
HA-IP-TRH	HA-IP with TRH receptor carboxyl tail
HEK	human embryonic kidney
HEPES	(N-[2-hydroxeythl] piperazine-N'-[2-ethanesulphonic acid])
His (H)	histidine
HRP	horseradish peroxidase
IBMX	isobutylmethylxanthine
Ile (I)	isoleucine
IP-R	prostacyclin receptor
IP-GFP	GFP-tagged IP-R
IP-β_2-GFP	IP-GFP with β_2-AR receptor carboxyl tail
IP-TRH-GFP	IP-GFP with TRH receptor carboxyl tail
kDa	kiloDalton
K_d	dissociation constant

L (l)	litre
LB	L-broth
Leu (L)	leucine
Lys (K)	lysine
µg	microgram
µl	microlitre
µM	micromolar
M	molar
MES	4-morpholineethanesulfonic acid
Met (M)	methionine
min	minute(s)
ml	millilitre
mg	milligram
mm	millimetre
mM	millimolar
MOPS	4-morpholinepropanesulfonic acid
mRNA	messenger ribonucleic acid

NBCS	new born calf serum
ng	nanogram
nm	nanometre
nM	nanomolar
N terminus	amino terminus
^{32}P	phosphorus-32
PAGE	polyacrylamide gel electrophoresis
PAR	protease-activated receptor
PBS	phosphate-buffered saline
PCR	polymerase chain reaction
PG	prostaglandin
PKA	protein kinase A
PKC	protein kinase C
pM	picomolar
PMA	phorbol 12-myristate
pmol	picomole
Pro (P)	proline

R	receptor
RFP	red fluorescent protein
SDS	sodium dodecyl sulphate
SEM	standard error of the mean
Ser (S)	serine
T	thymine
TCA	trichloroacetic acid
Thr (T)	threonine
TM	transmembrane
Tris	tris(hydroxymethyl)aminomethane
TRH	thyrotropin releasing hormone
Trp (W)	tryptophan
TSH	thyrotropin stimulating hormone
TX	thromboxane
Tyr (Y)	tyrosine
Val (V)	valine

Summary

To investigate the role of the carboxyl terminal in the regulation of the prostacyclin (IP) receptor, chimeric receptors expressing the carboxyl termini of either the thyrotropin-releasing hormone-1 (TRH) receptor or the β_2-adrenoreceptor (β_2-AR) were generated. Furthermore, C-terminally green fluorescent protein (GFP)-tagged forms of the receptors were built and stably expressed in HEK293 cells, thus enabling direct visualisation of receptor localisation and trafficking in intact cells.

Pharmacological analysis of the receptor-GFP fusion proteins demonstrated that each bound [^{3}H] iloprost with similar affinity and coupled to increased cAMP production. Sequestration studies revealed that iloprost-induced internalisation of the prostacyclin receptor was augmented by the addition of the TRH carboxyl tail. Conversely, the β_2-tailed chimeras exhibited internalisation properties comparable to those of the full-length prostacyclin receptors. The receptors' internalisation kinetics were unaffected by the addition of the GFP moiety.

Agonist-mediated sequestration of the constructs was abolished by treatments inducing clathrin depletion. In addition, sequestered receptors were found to colocalise in endosomes containing transferrin, as determined by confocal microscopy. Visual assessment of the dynamic interaction between β-arrestins and the receptor proteins demonstrated that sequestration of the full-length receptor proceeded primarily via an arrestin-independent mechanism. Switching of the receptor's carboxyl domain for the equivalent β_2-AR sequence did not confer β-arrestin sensitivity to the receptor. In contrast, the TRH-tailed receptors exhibited an increased binding affinity for β-arrestins, internalising in complexes with β-arrestin 2. In a cellular milieu deficient of β-arrestins and GRKs, the prostacyclin receptor and its chimeric forms retained the ability to undergo agonist-mediated sequestration.

Analysis of receptor regulation revealed that the GFP-tagged IP receptor elicited rapid signal attenuation in response to iloprost challenge. A less striking desensitisation response was evident with receptors expressing the different carboxyl tails. During desensitisation of the receptor-GFP proteins, iloprost challenge induced rapid receptor

phosphorylation which was, in part, mediated by the second messenger kinases PKA and PKC. PKA was demonstrated to be a major desensitising kinase of the receptors while PKC phosphorylation was identified as a possible determinant for receptor sequestration. Upon agonist withdrawal, the internalised GFP-tagged full-length receptor recycled rapidly back to the plasmalemmal surface, which was followed by the restoration in receptor responsiveness. By comparison, the agonist-activated chimeric receptors failed to recycle, and therefore resensitise, after agonist removal. Subsequently, the intracellularly retained chimeric receptors were sorted predominantly via a degradative pathway. Taken together, these data highlight the importance of the carboxyl terminal domain in prostacyclin receptor function.

Chapter 1

Introduction

1.1 Cell Signalling

Communication between individual cells is an essential prerequisite for the co-ordinated functioning of a multicellular organism. Cells have the ability to process vast amounts of information provided to them by extracellular signals (such as hormones, neurotransmitters, and growth factors) and physical signals (such as light). Most of these signals do not enter the cell, but affect membrane-bound receptors which are dedicated to the recognition of such messenger molecules. The most abundant receptor family is the G protein-coupled receptor (GPCR) family. In vertebrates, this family contains 1000-2000 members, thus constituting one of the largest protein families in nature.

GPCRs are involved in the recognition and transduction of messages as diverse as light, Ca^{2+} ions, odorants, small molecules such as nucleotides, amino acid residues, and peptides, as well as proteins. GPCRs characteristically activate one or more members of the guanine-nucleotide-binding signal transducing proteins (G proteins) that convey the information received by the receptor to cellular effectors such as enzymes and ion channels. These effectors influence levels of second messengers that regulate a wide variety of cellular processes including cell growth and differentiation.

1.1.1 GPCRs and G proteins: Historical perspective

In 1957, Sutherland and Rall described the basic properties of an enzyme now known as adenylyl cyclase, its activators adrenaline, glucagon, and sodium fluoride, and its product cAMP (Rall *et al.*, 1957; Sutherland and Rall, 1958). At this stage, G proteins and hormone receptors were unknown. Ten years later the hormone-sensitive enzyme was still thought of as a protein complex in which its catalytic activity was regulated allosterically by the direct binding of a hormone ligand to a specific site on a regulatory subunit. By the end of the 1960s, however, studies of fat cell adenylyl cyclase by Birnbaumer and Rodbell (1969) determined that hormone receptors and adenylyl cyclase are distinct entities. A few years later the separateness of receptor and cyclase was directly demonstrated by Orly and Schramm (1976), and in 1981, the purification

of a β-adrenergic receptor (β-AR) was reported, the first GPCR to be characterised (Shorr *et al.*, 1981).

Further study of the molecular mechanisms governing hormonal activation of adenylyl cyclase revealed a critical role for GTP in the process (Rodbell and Birnbaumer, 1971). A GTP-binding protein was subsequently separated from the enzyme complex by Pfeufer and Helmreich in 1975, and by 1977 Ross and Gilman reported that activation of a GTP-insensitive cyclase could be restored by the addition of a 40 kDa GTP-binding protein which is now known as $G_{s\alpha}$.

In the late 1970s, Cassel and Selinger (1978) first noted the GTPase activity of $G_{s\alpha}$ when adrenaline was used to stimulate adenylyl cyclase activity. They postulated that interaction of the hormone-activated receptor with G_s triggered the release of bound GDP and subsequent GTP binding. The hydrolysis of bound GTP to GDP led to G_s inactivation and the completion of the cycle. They also noted that hormone-stimulated GTPase activity could be inhibited by cholera toxin-catalysed ADP-ribosylation of $G_{s\alpha}$ resulting in constitutive activation of adenylyl cyclase.

Further research showed that G_α proteins formed complexes with two other proteins, which became known as the β (35-36 kDa) and γ (6-10 kDa) subunits. The β and γ subunits were found to be tightly bound together to function as a βγ dimer. βγ dimers have since been shown to be involved in the activation of signalling pathways within cells independently of the G_α subunit (Clapham and Neer, 1997). Using cDNA cloning techniques, by the late 1980s, an array of G_α subunits had been identified including the G_i proteins (which are associated with inhibition of adenylyl cyclase), G_o (which are involved in ion channel activation), and transducin (the G-protein coupling rhodopsin to cGMP phosphodiesterase in rod photoreceptors) (Spiegel, 1987). In 1990 the G_q family (which regulate phospholipase C activity) were reported (Strathmann and Simon, 1990).

1.1.2 Structural features of GPCRs

Nearly 2000 GPCRs have been reported since bovine opsin was first cloned in 1983 and the β-AR receptor in 1986. The superfamily has been classified into over 100

subfamilies according to sequence homology, ligand structure, and receptor function. All GPCRs share a common structural homology which comprises an extracellular N-terminal segment, seven transmembrane spanning domains which are linked by three extracellular and three intracellular loops, and an intracellular C-terminal segment (Figure 1.1a).

The N-terminal segment of most GPCRs exhibit at least one consensus sequence (Asn-X-Ser/Thr) for N-linked glycosylation, although for some receptors there may also be predicted glycosylation sites in the first and second extracellular loops. In some receptors glycosylation seems to be functionally important for cell surface expression (George *et al.*, 1986). The secretin/vasointestinal peptide GPCR sub-family, which bind neuropeptides and peptide hormones, possess a relatively large N-terminus with at least 6 highly conserved cysteine residues which are thought to be involved in ligand binding (Strader *et al.*, 1995). Members of the metabotropic glutamate receptor family possess the longest N-terminal segments which not only provides the ligand binding site but is also involved in receptor activation (Takahashi *et al.*, 1993).

The seven transmembrane (TM) spanning domains are thought to form a barrel shape, orientated roughly perpendicular to the plane of the membrane in an anti-clockwise fashion with three extracellularly and three intracellularly connecting loops, forming a ligand binding pocket (Figure 1.1b). Sequence analysis has shown that each of the TM domains comprise 20-25 predominantly hydrophobic amino acids. By extrapolation from the structure of rhodopsin these stretches are predicted to form α-helical membrane spanning domains of unequal length which can extend beyond the lipid bilayer (Unger *et al.*, 1997). The orientation of the TMs imposes a stereo- and geometric specificity on a ligand's entry into and binding to the TM core. The core primarily contains TMs II, III, V, and VI (which are extremely hydrophobic) whereas TMs I, IV, and VII (which are more hydrophilic) are more exposed to the bilayer (Sealfon *et al.*, 1997). Hydrogen bonds and salt bridges between residues of the same TM as well as other TMs are critical for maintaining a tightly packed TM core (Pebay-Peyroula *et al.*, 1997).

Figure 1.1

a) Schematic representation of the general structure of GPCRs.

GPCRs comprise 7 α-helical transmembrane domains which are linked by 3 intracellular and 3 extracellular loops. The N-terminal region contains sites for glycosylation and the C-terminal region contains sites for lipid modification and phosphorylation.

b) Arrangement of the transmembrane domains of a prototypical GPCR in the lipid bilayer.

The 7 transmembrane regions are arranged in the plasma membrane as a closed loop in an anti-clockwise direction from TM1 to TM7. The stability of the structure is maintained by intramolecular disulphide bonds and salt bridges.

Figure 1.1

a)

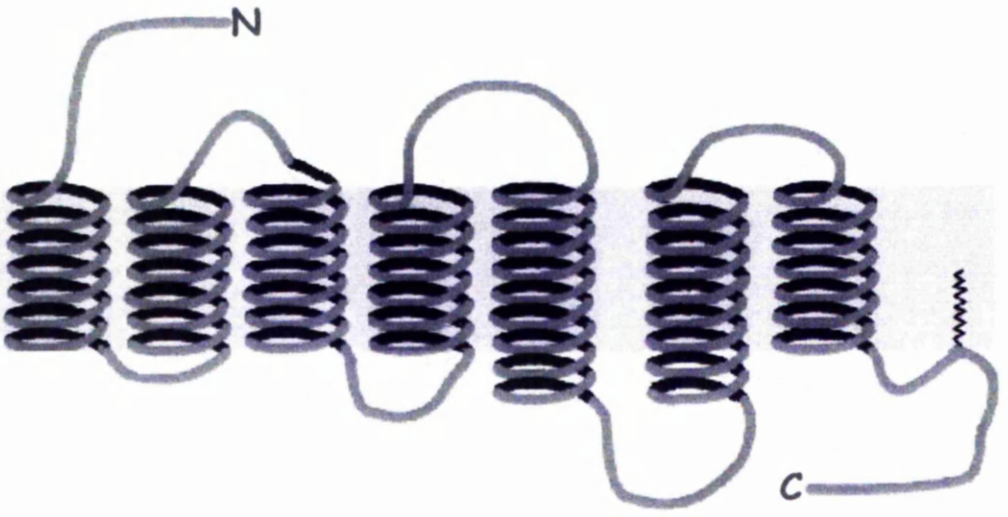

b)

Two conserved cysteine residues in extracellular loops 1 and 2 are known to be linked by a disulphide bond in bovine rhodopsin, the thyrotropin-releasing hormone (TRH) receptor, the thromboxane receptor, and the gonadotropin-releasing hormone (GnRH) receptor. This disulphide linkage is thought to constrain the loops and receptor, specifically pulling the second extracellular loop over and thus preventing the opening of the TM core on the extracellular side (Ji and Ji, 1995). Substitution of cysteine residues in the first and second extracellular loops of the β_2-AR receptor (Cys^{106} and Cys^{184}) induced destabilisation of the tertiary structure and alterations in the receptor's ligand binding properties (Dohlman *et al.*, 1990). The first or second extracellular loops may also contain sites for N-linked glycosylation.

The intracellular loops are predicted to be between 10 and 40 amino acids in length with the notable exception of the third intracellular loop, which can be more than 150 residues long. The intracellular loops are involved in the interaction of the receptor with the heterotrimeric G proteins. Both the second and the third intracellular loops have been reported to be crucial for coupling to G_α subunits. The amino acid sequence of the second intracellular loop is among the most highly conserved in the GPCR superfamily and substitutions in some of its highly conserved residues has been shown to severely impair G protein coupling. The amino and carboxyl terminal portions of the third intracellular loop in the muscarinic and catecholamine receptors appear to be critical determinants of G protein coupling and activation (Wess *et al.*, 1990; Cotecchia *et al.*, 1992). The third intracellular loop is also a target for phosphorylation by G protein receptor kinases (GRKs), and in case of the β_2-AR, second messenger kinases such as cAMP-dependent protein kinase (PKA) (Benovic *et al.*, 1985).

The intracellular C-terminal tail varies considerably in length (12-359 amino acids) with the exception of the mammalian GnRH receptor which completely lacks an intracellular C-terminal domain (Sealfon *et al.*, 1997). A fourth cytoplasmic loop can be formed when the C-tail is palmitoylated. The C-tail is usually rich in serine and threonine residues that are potential sites for phosphorylation by GRKs and second messenger kinases for receptor desensitisation (Freedman and Lefkowitz, 1996).

1.1.3 Ligand binding and receptor activation

Ligand binding and receptor signalling are clearly dissociable functions involving distinct interactions of the ligand with several domains of the GPCR. The regions of the receptor responsible for binding and activation is dependent on the GPCR subfamily as well as the size and structure of the ligand.

The binding of biogenic amines to their receptors is characterised by a complex of interactions involving key residues in TMs III, V and VI (Strader *et al.*, 1987). In these receptors, the amine of the ligand interacts with the carboxyl group of an aspartate residue in TM III, whereas the catechol ring interacts with residues in TMs V and VI. Interactions of the ligand with TMIII are important for binding, while interactions with TMs V and VI are more important for receptor activation (Strader *et al.*, 1997).

Photo-affinity labelling and mutational analysis showed that the β-ionone ring of retinal associates with TMs III, V, and VI of rhodopsin, in particular TM VI Trp^{265} and Tyr^{268} (Han, 1997). Light absorption causes an all-*trans* isomerisation of retinal and as a result, key hydrogen bonds and salt bridges between TMs III and VI are broken, leading to a rearrangement of TMs III, VI, and VII, thereby generating a signal (Han, 1997).

Small peptides, such as angiotensin, bind to regions of the first extracellular loop and TMs II-VII, highlighting the role of both extracellular and TM domains in ligand binding and receptor activation. The C-terminal part of the ligand enters the TM core and the C-terminal carboxyl group pairs with Lys^{199} in TM V, while the N-terminal part of the ligand ion pairs with the His^{183} of the second extracellular loop and Asp^{281} of the third extracellular loop. Mutational studies suggest the interaction with the aspartate residue is necessary for signal generation (Noda *et al.*, 1995; Feng *et al.*, 1995)

For glycoprotein hormone receptors, which characteristically possess a 350-400 residue amino terminus, the N-terminal region is solely capable of high affinity ligand binding. Leucine-rich repeats in the N-terminus are thought to be important in the ligand binding, whereas contact with the extracellular loops and/or membrane-associated domains are required for receptor activation (Ji and Ji, 1995).

For the metabotropic glutamate receptors, the ~300 amino acid amino-terminal half of N-terminal segment not only functions as the ligand binding site, but also mediates the signal specificity for effector stimulation i.e. phospholipase C activation or inhibition of adenylyl cyclase (Takahashi *et al.*, 1993).

1.2 Heterotrimeric G Proteins

1.2.1 Introduction

GPCRs characteristically bind G proteins that in turn act as mediators of receptor-stimulated effector activation. Upon receptor activation, bound GDP, in the guanine nucleotide-binding site of the GTPase domain of the G_α subunit, is released and exchanged for GTP (due to high intracellular concentrations of GTP). GTP binding promotes α-subunit dissociation from the βγ dimer, which in turn allows both the G_α subunit and the βγ dimer to activate effectors. G protein deactivation is rate-limiting for turn off of the cellular response and occurs when the intrinsic GTPase activity of the G_α subunit hydrolyses the GTP to GDP, and the G_α subunit subsequently reassociates with the $G_{\beta\gamma}$ unit (Figure 1.2).

1.2.2 G_α subunit

To date, more than 20 different G_α subunits have been identified corresponding to 16 gene products, which have been divided into 4 subfamilies according to their sequence homology (Figure 1.3). The G_s family includes $G_{s\alpha}$ and G_{olf} which mediate adenylyl cyclase activation and the closure of Ca^{2+} ion channels. The G_i family includes $G_{i\alpha 1\text{-}3}$, which function mainly to inhibit adenylyl cyclase activity, G_t (αt and αt2) which stimulate cGMP phosphodiesterase, G_o (αoA and αob) which are involved in Ca^{2+} ion channel closure (Hsu *et al.*, 1990) and the G_{gust} and G_z proteins. G_{gust} is expressed in the taste buds and is thought to couple to cGMP phosphodiesterase. G_z is expressed in neuronal cells where it inhibits adenylyl cyclase (Taussig and Gilman, 1985). The G_q family ($G_{q\alpha}$, $G_{11\alpha}$, $G_{14\alpha}$, $G_{15\alpha}$, and $G_{16\alpha}$) predominantly couples to phosphoinositide turnover (Strathmann and Simon, 1990). The G_{12}/G_{13} family is ubiquitously expressed

Figure 1.2

The G protein cycle.

Activated receptors (R*) associate with the trimer (α-GDP$\beta\gamma$) triggering dissociation of GDP. GTP then binds with the trimer in its "empty" state ($\alpha_e\beta\gamma$) and induces a conformational change which leads to the dissociation of α-GTP from the complex, releasing $\beta\gamma$. After GTP hydrolysis, α-GDP reassociates with $\beta\gamma$.

Figure 1.2

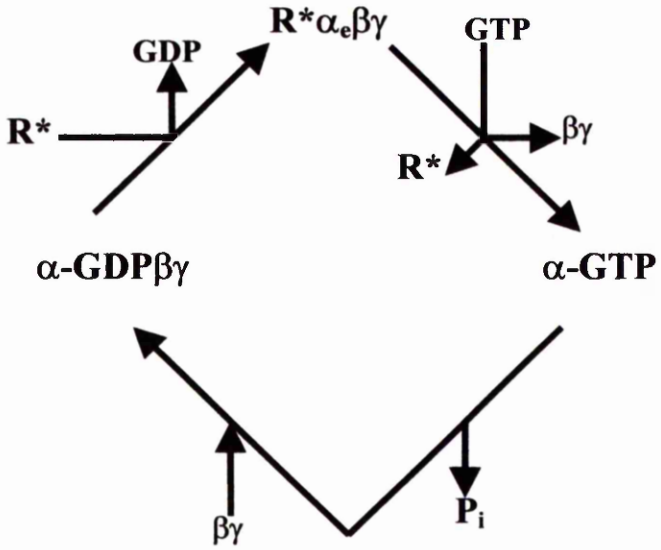

Figure 1.3

G protein α subunit family.

Four distinct classes of G_α have been identified. The α subunits are grouped according to their shared amino acid identity.

Figure 1.3

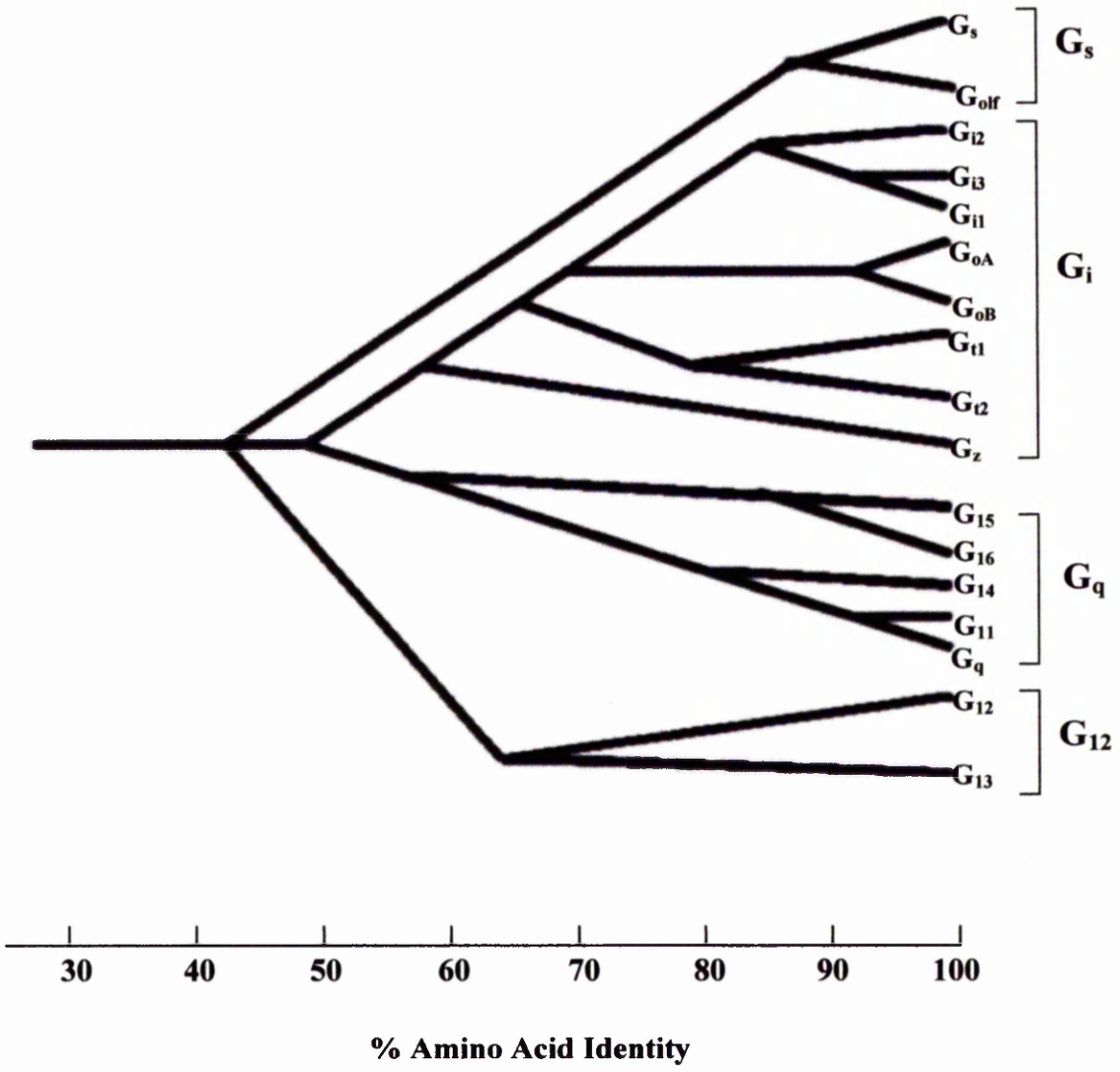
G_s
G_{olf}
G_{i2}
G_{i3}
G_{i1}
G_{oA}
G_{oB}
G_{t1}
G_{t2}
G_z
G_{15}
G_{16}
G_{14}
G_{11}
G_q
G_{12}
G_{13}
G_s
G_i
G_q
G_{12}
30
40
50
60
70
80
90
100
% Amino Acid Identity

and has been shown to be involved in the regulation of Na^+/H^+ ion exchange in cells (Hooley *et al.*, 1996) and the maintenance of the cell cytoskeleton through the activation of the small GTPase Rho (Klages *et al.*, 1999).

1.2.3 $G_{\beta\gamma}$ subunit

The $G_{\beta\gamma}$ complex comprises two polypeptides G_β and G_γ which function as a monomeric unit. As with the G_α subunits, there are multiple β and γ proteins. At present, genes encoding 6 β and 12 γ subunits have been identified. Most $G_{\beta\gamma}$ pairs are functional although there are exceptions. The γ_1 protein (and all the other γ proteins) can combine with β_1 but is unable to pair with β_2. The region on the γ subunit which determines this specificity for β_1 over β_2 is located in a 14 amino acid sequence on the γ subunit (Spring and Neer, 1994). Evidence that βγ units could regulate effectors came from studies of cardiac atrial cells where βγ dimers were shown to activate a K^+ ion channel (Logothetis *et al.*, 1987). βγ proteins have since been demonstrated to regulate numerous effectors including activation of phospholipase Cβ isoforms (Camps *et al.*, 1992), inhibition of adenylyl cyclase type I, stimulation of adenylyl cyclase types II and IV (Tang and Gilman, 1991), GRK regulation (Pitcher *et al.*, 1992) and MAP kinase activation (Crespo *et al.*, 1994).

1.2.4 Structural features of G proteins

G_α subunits contain two domains, a domain involved in binding and hydrolysis of GTP that is structurally homologous to the GTPases of monomeric G proteins and elongation factors, and a unique helical domain which buries the bound GTP in the protein core. The GTPase domain consists of 5 α helices surrounded by 6 β strands which bind the phosphate and the guanine moiety of GTP. Also present in the core is a binding site for Mg^{2+} ions which are essential for catalysis (Sprang, 1997). Substantial rearrangement of three segments of the α subunit occurs upon GTP hydrolysis. These are designated Switch I (the loop between the first α helix and the second β strand), Switch II (the loop preceding the second α helix) and Switch III (the loop between the third α helix and the fifth β strand) (Lambright *et al.*, 1994). When GTP is bound, basic residues in Switch II

form ionic interactions with residues in Switch III. Upon GTP hydrolysis, these linkages are broken as Switch II and III collapse. Switches II and III are the proposed effector-binding regions in activated $G_{s\alpha}$ (Sprang, 1997).

The β subunit of heterotrimeric G proteins comprises an N-terminal helix followed by a 7 membered β-propeller structure based on its 7 WD-40 repeats (Sondek *et al.*, 1996). The γ subunit contains two helices but no inherent tertiary structure. The γ subunit interacts with β through an N-terminal coiled-coil, whereas the remainder interacts extensively with the β propeller (Sondek *et al.*, 1996).

The interaction of the G_α with the $G_{\beta\gamma}$ unit involves the G_α N-terminal helical domain binding to the propeller structure of the β subunit (Lambright *et al.*, 1996). Upon receptor activation and the exchange of GDP for GTP, conformational changes in the G_α subunit cause a reduction in the α helical content of the G_α (Lambright *et al.*, 1996) which leads to separation of the βγ dimer from the α subunit.

1.2.5 Lipid modification of G proteins

All G_α subunits undergo covalent modification at or near their N-termini by the attachment of the fatty acids myristate and/or palmitate. N-myristoylation, which occurs in members of the G_i family, is a co-translational modification of the glycine residue at the extreme N-terminus after the removal of the initiating methionine residue (Gordon *et al.*, 1991). All G protein α subunits, with exception of αt, can be palmitoylated. Palmitate is attached through a labile, reversible thioester bond to a cysteine residue near the N-terminus (Parenti *et al.*, 1993). G_γ subunits are covalently modified by the fixture of the 20-carbon isoprenoid geranylgeranyl, or in the case of retinal-specific γ_1, the 15-carbon isoprenoid farensyl. Prenylation occurs via a stable thioether bond to a cysteine residue located in the C-terminal "CAAX" motif. Following covalent modification the C-terminal three amino acids are removed by proteolysis and the new C-terminus is carboxymethylated (Higgins and Casey, 1994). Although non-prenylated γ mutants have been shown to form stable dimers with β, prenylation of γ is essential for normal βγ function.

For G proteins, lipid modification acts as a hydrophobic membrane anchor. Both palmitoylation and myristoylation are thought to contribute to membrane association, with palmitoylation providing a stronger interaction with the lipid bilayer due to its greater hydrophobicity. Non-palmitoylated mutants of $G_{s\alpha}$ (which are not myristoylated) have been reported to exhibit a markedly decreased capacity to associate with the membrane (Wedegaertner *et al.*, 1993). $\beta\gamma$ dimers also help guide α subunits to membranes and prenylation of the γ chains is a prerequisite for correct targeting of the $\beta\gamma$ to the membrane (Silvius and l'Heureux, 1994), and indeed binding of $\beta\gamma$ to the α subunit, receptors and effectors (Casey *et al.*, 1994).

1.3 Receptor/G protein coupling

1.3.1 Structural features of GPCRs important for coupling

Considering the general structure of GPCRs, receptor-G protein coupling domains lie within the intracellular portion of the receptor which include the loops, the distal parts of the TM domains, and the C-terminal tail.

Deletion studies of the β_2-AR demonstrated the importance of the regions of the amino and carboxy segments of the third intracellular loop and the N-terminal segment of the cytoplasmic tail as being critical for β_2-AR activation of adenylyl cyclase (O'Dowd *et al.*, 1988).

For the m1 and m2 muscarinic receptors, mutational analysis revealed that the aspartate and arginine residues of the highly conserved DRY motif located at the beginning of the second intracellular loop are crucial for efficient coupling (Wess, 1993).

Studies of the rhodopsin receptor identified residues 143-150 of the second intracellular loop and residues 236-239 and 244-249 of the third intracellular loop as domains essential for the activation of transducin (Konig *et al.*, 1989). In addition, a synthetic peptide from the fourth intracellular loop (created by palmitoylation of a cysteine residue in the C-tail) was capable of interacting with transducin (Konig *et al.*, 1989).

Investigations of the porcine calcitonin and murine GnRH receptors revealed the first intracellular loop to be of importance in G protein coupling. In the former (which is G_s and $G_{q/11}$-coupled), substitution of the first intracellular loop with the equivalent sequence from a human receptor isoform (containing a unique insertion of 16 amino acids) completely abolished the production of inositol phosphates, while the cAMP signalling of the porcine receptor remained unaffected (Nussenzveig *et al.*, 1994). In contrast, residues in the first intracellular loop of the murine GnRH receptor, which are critical for cAMP signalling, were found not to be essential for $G_{q/11}$ signalling (Arora *et al.*, 1998).

For the EP_3 prostanoid receptor, the C-terminal tail seems to be the critical determinant in the coupling to G proteins. The EP_3 receptor comprises 4 splice variants which differ only at their C-terminal tails (Namba *et al.*, 1993). EP_{3A} activates the G_i family, while both EP_{3B} and EP_{3C} activate G_s, and EP_{3D} couples to G_i, G_s, and the G_q families.

1.3.2 Structural features of the G protein important for coupling

The most important region within the α subunit for coupling to the receptor appears to be the extreme C-terminus. ADP-ribosylation of $G_{i\alpha}$ on a cysteine residue close to the C-terminus was shown to uncouple the G protein from the receptor (West *et al.*, 1985). A proline to arginine mutation at the sixth amino acid from the C-terminus of $G_{s\alpha}$ abolished adenylyl cyclase activation upon receptor stimulation (Sullivan *et al.*, 1987).

The development of chimeric G proteins further highlighted the role of the extreme C-terminus of G_α in receptor coupling. Replacement of the native C-terminal sequence of $G_{q\alpha}$ with the corresponding residues of $G_{i\alpha}$ created a chimera that mediated stimulation of phospholipase C by receptors otherwise coupled exclusively to G_i (Conklin *et al.*, 1993). Moreover, antibodies directed against the extreme C-terminus of G_α subunits were found to be capable of inhibiting receptor-mediated activation of G proteins (Simonds *et al.*, 1989).

1.3.3 Diversity in signalling

GPCRs can couple to more than one G_α subunit and hence activate multiple effectors. Studies have shown that mutations can abolish the signalling output through one class of G protein while the coupling to other families remains unaffected, thus highlighting the fact GPCRs selectively interact with G proteins at distinct sites within their structure.

In human thyroid cells, activated TSH receptors can signal through all the four classes of G protein (Laugwitz *et al.*, 1996). Substitution of a tyrosine residue in TM V (Tyr^{605}) resulted in a loss of agonist-induced inositol phosphate production, yet unchanged cAMP generation (Biebermann *et al.*, 1998) therefore demonstrating the role of this tyrosine residue in the coupling to $G_{q/11}$.

In the case of the G_s- and $G_{q/11}$-coupling luteinising-hormone receptor, point mutations in Asp^{583} in the third intracellular loop decreased cAMP formation whereas agonist binding and inositol phosphate hydrolysis remained unaltered (Gilchrist *et al.*, 1996).

For the β_2-AR, coupling can switch from G_s to G_i upon receptor phosphorylation. Agonist-induced phosphorylation by cAMP-dependent protein kinase (PKA), subsequently allowed the recruitment of G_i which appears to be involved in initiating MAP kinase signalling by the receptor (Daaka *et al.*, 1997).

1.4 Adenylyl Cyclases

1.4.1 Introduction

Despite the discovery of numerous second messengers since Sutherland and Rall (Rall *et al.*, 1957; Sutherland and Rall, 1958) discovered the role of cAMP in hormone signalling, the adenylyl cyclases have continued to play a pivotal role in signal transduction. Principally, adenylyl cyclases catalyse the conversion of ATP to cAMP (Table 1.1). This enzyme family consists of 9 isoforms of ~120 kDa with increased diversity produced by splice variants of some of the isoforms (Taussig and Gilman,

1995). Krupinski and coworkers (1989) were able to purify the first adenylyl cyclase (AC) isoform (AC I) using a forskolin affinity matrix. From the deduced cDNA sequence of the full length protein, PCR reaction and low affinity hybridisation techniques allowed a further 6 full length isoforms to be isolated (AC II-VI, and VIII) (Feinstein *et al.*, 1991; Bakalyar and Reed, 1990; Gao and Gilman, 1991; Katsushika *et al.*, 1992; Premont *et al.*, 1992a; Yoshimura and Cooper, 1992; Cali *et al.*, 1994). AC VII was isolated as a partial sequence of novel isoforms (Krupinski *et al.*, 1992).

1.4.2 Structure of adenylyl cyclases

The nine cloned isoforms share a common structure comprising a short cytoplasmic amino terminus followed by a transmembrane domain (C_1) of six α helices (M_1) then a large cytoplasmic domain (C_1) which is followed by a further six transmembrane spanning region (M_2) and another cytoplasmic domain (C_2) (Hurley, 1999; Taussig and Gilman, 1995, Figure 1.4). Within the AC family, it is the cytoplasmic domains which are the most highly conserved (up to 93% homology). The C_1 and C_2 domains are further subdivided into C_{1a}, C_{1b}, and C_{2a}, C_{2b}. It is these regions which are responsible for the catalytic site of the enzyme. The catalytic activity of the enzyme depends on the heterodimerisation of C_{1a} and C_2. The substrate binding site is formed by ionic interactions between C_2 and the purine ring of ATP. The C_1 domain plays a more supporting role in substrate binding (Liu *et al.*, 1997). The ATP binding site is surrounded by hydrophobic residues (contributed by C_2) that pack the purine ring and ionic interactions contributed by both C_1 and C_2 stabilise the phosphate groups (Liu *et al.*, 1997).

1.4.3 Activation and regulation of adenylyl cyclases

All mammalian adenylyl cyclases are activated by the diterpene forskolin except type IX. Forskolin binds the catalytic core and activates the enzyme by "gluing together" the two domains C_1 and C_2 using hydrophobic and hydrogen bond interactions (Zhang *et al.*, 1997). Type IX is non-responsive to forskolin due to differences in amino acid sequence in the binding pocket, unlike types I-VIII where this sequence is conserved.

Figure 1.4

Diagrammatical representation of the structure of membrane adenylyl cyclase isoforms.

The putative adenylyl cyclase structure has been deduced from sequence analysis implying 12 transmembrane helices. Functional studies have revealed the catalytic and regulatory sites within the intracellular regions of the enzyme (adapted from Taussig and Gilman, 1995).

Table 1.1

Differential regulation of the adenylyl cyclase isoforms.

Summary of the biochemical characteristics of each AC isoform.

Figure 1.4

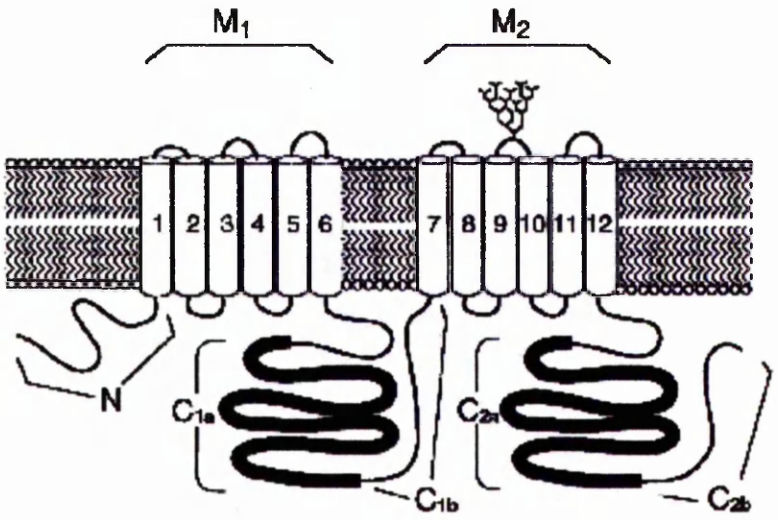

N, amino-terminal domain; M_1, first set of membrane-spanning regions; C_{1a} and C_{1b}, the first large intracellular cytoplasmic domain; M_2, second set of transmembrane spanning regions; and C_{2a} and C_{2b}, second large intracellular domain.

Table 1.1

	Response to cAMP signalling					
AC Isoform	**$G_{s\alpha}$**	**$G_{i\alpha}$**	**$G_{\beta\gamma}$**	**Forskolin**	**Ca^{2+}**	**Protein Kinases**
1	↑	↓ (CAM or Forskolin-stimulated)	↓	↑	↑ (CAM) ↓ (CAM Kinase IV)	↑ PKC (weak) ↓ CAM Kinase IV
2	↑	→	↑ (when stimulated by $G_{s\alpha}$)	↑		↑ PKC
3	↑	↓		↑	↑ (CAM, *in vitro*) ↓ (CAM Kinase II)	↑ PKC (weak) ↓ CAM Kinase II
4	↑		↑	↑		↑ PKC
5	↑	↓	↓ ($\beta_1\gamma_2$)	↑	↓ (<1μM)	↓ PKA ↑PKC
6	↑	↓	↓ ($\beta_1\gamma_2$)	↑	↓ (<1μM)	↓ PKA, PKC
7	↑		↑	↑		↑ PKC
8	↑	↓ (Ca^{2+} rises)		↑	↑ (CAM)	→ PKC
9	↑	↓		↑ (weak)	↓ (calcineurin)	

↑, positive response; ↓, negative response; →, neutral response

All cyclase isoforms are activated by GTP-bound $G_{s\alpha}$. GTP-$G_{s\alpha}$ binds to a crevice on the outside of C_2 and the N-terminal portion of C_1. GTP-$G_{s\alpha}$ can activate cyclase by the same mechanism as forskolin but it can also stimulate catalysis by inducing a conformational change in the enzyme to allosterically regulate it (Yan *et al*, 1997).

$G_{i\alpha}$ selectively inhibits AC V and VII. Mutational analysis suggests that $G_{i\alpha}$ binds to the catalytic core on a groove similar to the $G_{s\alpha}$ binding groove (Yan *et al.*, 1997). In association with $G_{s\alpha}$, $\beta\gamma$ subunits can bind to AC isoforms and regulate them. The binding site of $\beta\gamma$ is adjacent to the $G_{s\alpha}$ site, consistent with the observation that type II is activated by $G_{\beta\gamma}$ when $G_{s\alpha}$ is bound (Chen *et al.*, 1995).

Changes in the intracellular Ca^{2+} ion concentration can profoundly affect types I and VIII. These isoforms are activated by nanomolar concentrations of Ca^{2+}/calmodulin. At higher concentrations of Ca^{2+} (100-1000μM) inhibition occurs as a result of competition with Mg^{2+} ions in the active site, which are essential for catalysis (Hurley, 1999).

The possibility for PKA-mediated phosphorylation being a negative feedback on adenylyl cyclase activity has been investigated but evidence for such a mechanism remains flimsy (Premont *et al.*, 1992b). However, regulation by phosphorylation of AC isoforms has been demonstrated by PKC. PKC activates AC type II by phosphorylation on Thr^{1057} (Bol *et al.*, 1997). Jacobowitz and coworkers (1993) observed moderate phosphorylation of AC V by PKC *in vivo*.

1.5 GPCR Desensitisation

1.5.1 Introduction

Agonist activation of GPCRs initiates a series of reactions which result in the "turn off" of the GPCR signal. This process is known as desensitisation and is characterised by the waning of a stimulated response in the presence of continuous agonist exposure. This attenuation of GPCR responsiveness to agonist represents an important mechanism that protects against both acute and chronic receptor stimulation.

The phenomenon of desensitisation can be subdivided into agonist-specific (homologous) and agonist-non-specific (heterologous) events. Homologous desensitisation refers to the situation whereby only the activated GPCRs desensitise, while heterologous desensitisation refers to the situation whereby activation of one GPCR leads to the desensitisation of responses initiated by another, heterologous GPCR. Homologous desensitisation occurs as a consequence of G protein uncoupling in response to phosphorylation by GRKs and second messenger kinases. GPCR phosphorylation promotes the binding of β-arrestins, which not only uncouple receptors from heterotrimeric G proteins but also target GPCRs for internalisation in clathrin coated vesicles (Ferguson and Caron, 1998; Figure 1.5). Prolonged agonist exposure can also result in downregulation of receptor levels as a result of reduced receptor mRNA and protein synthesis, as well as both the lysosomal and plasma membrane degradation of pre-existing receptors (Doss *et al.*, 1981; Hadcock and Malbon, 1988; Valiquette *et al.*, 1990, 1995; Jockers *et al.*, 1999; Pak *et al.*, 1999). These processes occur over time periods ranging from seconds (phosphorylation) to minutes (endocytosis) and hours (downregulation).

The level of desensitisation varies from complete termination of receptor signalling, as observed in the visual and olfactory signals, to the reduction in agonist potency and maximal responsiveness. Desensitisation of the photoreceptor rhodopsin in response to light, and the response to hormone by the β_2-AR, are the best studied systems of this process (Hausdorff *et al.*, 1990; Hargrave and McDowell, 1992). In order to perceive continuous light changes, desensitisation of rhodopsin was found to occur in less than 1 second following light stimulation, thereby preventing a flash of light as being seen as continuous illumination (Schleicher *et al*, 1989). For the β_2-AR, within a few minutes of agonist exposure, cAMP accumulation was observed to plateau or return to basal levels (Shear *et al.*, 1976; Su *et al.*, 1979; Sibley *et al.*, 1987). For the β_2-AR, this desensitisation was demonstrated to be induced by a distinct effect on the receptor and not the G protein since isolated desensitised β_2-ARs were unable to stimulate adenylyl cyclase in reconstituted systems (Strulovici *et al.*, 1984).

Figure 1.5

Schematic representation of GPCR desensitisation.

For GPCRs including the β_2-AR, receptor activation leads to receptor phosphorylation by GRKs facilitating the translocation and binding of β-arrestins to the receptor thereby uncoupling GPCR/G protein interactions. β-Arrestins then target receptors for endocytosis via clathrin coated pits. Figure adapted from Ferguson and Caron, 1998.

Figure 1.5

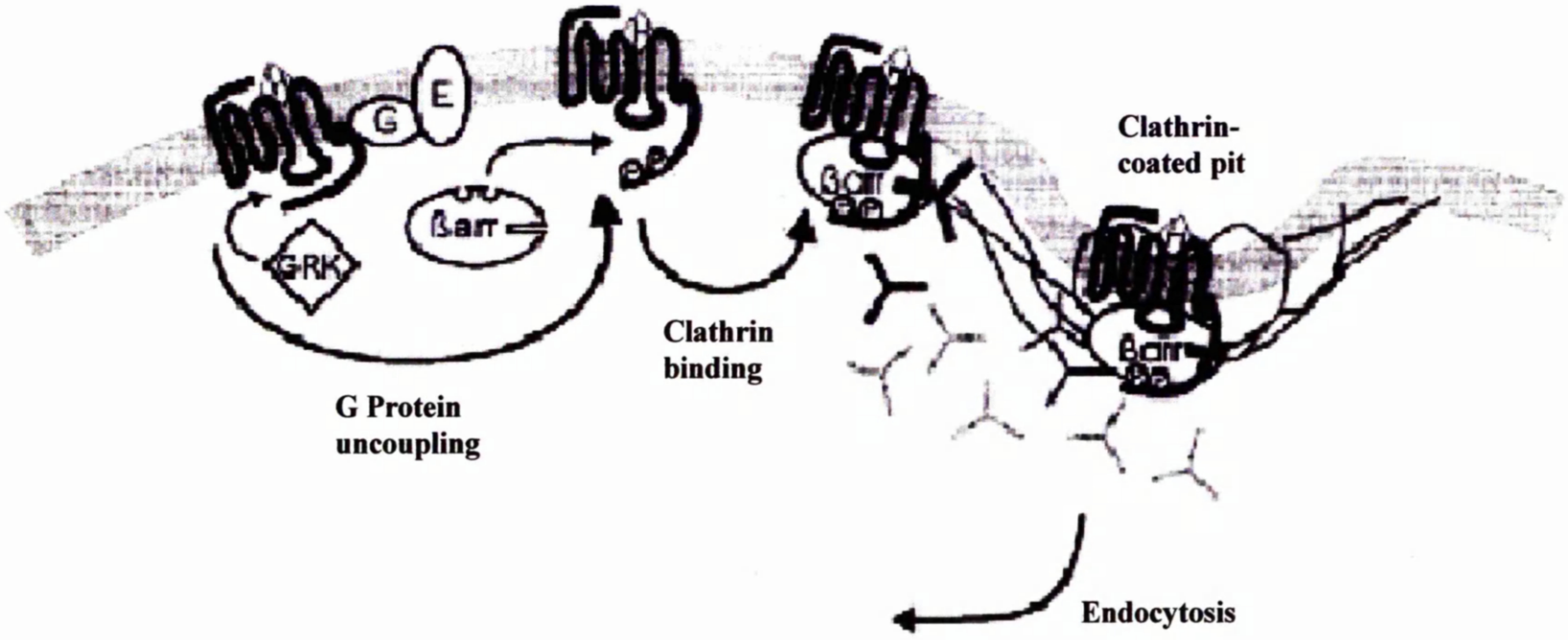

βarr, β-arrestin; E, effector enzyme; G, heterotrimeric G protein; GRK, G protein-coupled receptor kinase; H, hormone; P, phosphate group.

1.5.2 Role of phosphorylation in GPCR desensitisation

The discovery of light-dependent phosphorylation of the rhodopsin *in vivo* correlated well with the loss of cGMP phosphodiesterase activity (Bownds *et al.*, 1972). The kinase responsible was identified as rhodopsin kinase (or GRK 1) which phosphorylates the light activated receptors at multiple serine and threonine residues (Bownds *et al.*, 1972). The subsequent cloning of rhodopsin kinase showed that it is predominantly expressed in the retinal cones and rods (Lorenz *et al.*, 1991). Studies *in vivo* mapped the phosphorylation sites of rhodopsin to residues in the C-terminal region, namely Ser^{334}, Ser^{338}, and Ser^{343} (Ohguro *et al.*, 1995). The role of phosphorylation in inactivating rhodopsin was further demonstrated using transgenic mice expressing a C-terminally truncated mutant of rhodopsin. In such mice, abnormally long responses were detected in the retinal rods (Chen *et al.*, 1995).

The role of phosphorylation in β_2-AR desensitisation was originally suggested upon notice that the kinetics of β_2-AR phosphorylation mimicked those of desensitisation (Stadel *et al.*, 1983a). GRKs were first implicated in agonist-specific phosphorylation when it was observed that desensitisation of the β_2-AR still occurred in kin^- S49 lymphoma cells (which lack PKA) (Green and Clark, 1981). A partially purified preparation of a kinase from the supernatant of kin^- S49 cells was capable of phosphorylating β_2-AR *in vitro* (Benovic *et al.*, 1986). Subsequent cDNA cloning of the kinase identified it as a novel GRK termed β-adrenergic receptor kinase, βARK (or GRK 2) (Benovic *et al.*, 1989). Further studies identified Ser^{369}, Ser^{401}, and Ser^{407} and Thr^{384} as the sites of βARK phosphorylation of the human β_2-AR (Fredericks *et al.*, 1996).

1.5.3 G protein-coupled receptor kinase family

βARK and rhodopsin kinase were found to be part of a GRK family when βARK 2 (GRK 3) and GRKs 4-7 were cloned from cDNA libraries (Benovic *et al.*, 1991; Ambrose *et al*, 1992; Kunapuli and Benovic, 1993; Benovic and Gomez, 1993; Weiss *et al.*, 1998). GRKs are 62-80 kDa proteins that are members of the large family of serine/threonine kinases. Like GRK 1, expression of GRK 4 and GRK 7 are tissue-

specific (testis and retinal rods respectively) while the other GRKs are more ubiquitously expressed. The GRKs share similar structural features with each possessing a central catalytic domain, an amino-terminal domain which contains an RGS-like domain thought to be important for substrate recognition, and a carboxyl-terminal domain that is required for targeting of the kinase to the plasma membrane (Figure 1.6 and Table 1.2).

1.5.4 GRK targeting and regulation

It has emerged that lipid modification or interactions may be important for membrane localisation and activity of GRKs. Upon agonist activation of GPCRs, cytosolic GRKs 1-3 translocate to the membrane-bound receptors. For GRK 1, plasma membrane association is facilitated by post-translational farnesylation on it its C-terminus (Inglese *et al.*, 1992). For GRKs 2 and 3, plasma membrane targeting is aided by phosphatidylinositol 4,5-bisphosphate binding to their carboxyl-terminal pleckstrin homology domains (Pitcher *et al.*, 1995a). In unstimulated cells GRKs 4, 5, and 6 all exhibit substantial membrane localisation. Both GRKs 4 and 6 are palmitoylated (Stoffel *et al.*, 1994; Premont *et al.*, 1996; Stoffel *et al.*, 1998) which seems to be essential for their localisation to the plasma membrane. GRK 5 forms electrostatic interactions between 46 basic residues in the carboxyl terminus of the protein and the phospholipids from the bilayer (Kunapuli *et al.*, 1994)

Apart from lipid modification, other factors regulate GRK activity. GRK 1 activity can be inhibited by the Ca^{2+}-binding protein recoverin (Iacovelli *et al.*, 1999), while GRKs 2, 5, and 6 appear to be negatively regulated by Ca^{2+}/calmodulin (Pronin *et al.*, 1997) with the inhibitory effects being most significant with GRK 5. A calmodulin-binding domain has been located within the N-terminal domain of GRK 5 (Pronin *et al.*, 1997). Studies have demonstrated that an important regulator of GRKs 2 and 3 are the $G_{\beta\gamma}$ subunits (Daaka *et al.*, 1997; Pitcher *et al.*, 1992). The binding site for the $\beta\gamma$ proteins to the kinase was localised to the pleckstrin homology domain within the C-terminus (Koch *et al.*, 1993). It may be that $G_{\beta\gamma}$ provides a signal for the docking of GRK 2 and 3 to the membrane. GRKs 2 and 5 are also substrates for phosphorylation by PKC

Figure 1.6

Diagrammatical representation of the structure of GRKs 1-7.

The amino terminal domain of the GPCR-binding domain of each GRK contains a conserved RGS domain. The carboxyl terminal domains of the GRKs mediate their targeting to the plasma membrane. GRKs 1 and 7 are farnesylated at "CAAX" motifs in their carboxyl termini. GRKs 2 and 3 contain βγ-subunit binding that exhibits sequence homology to a pleckstrin homology domain. GRK5 contains a stretch of 46 basic amino acids that mediate interactions with the phospholipids in the plasma membrane. GRKs 4 and 6 are palmitoylated at cysteine residues.

Table 1.2

Molecular properties of the GRKs.

Overview of the characteristics and biochemical regulation of the GRKs.

Figure 1.6

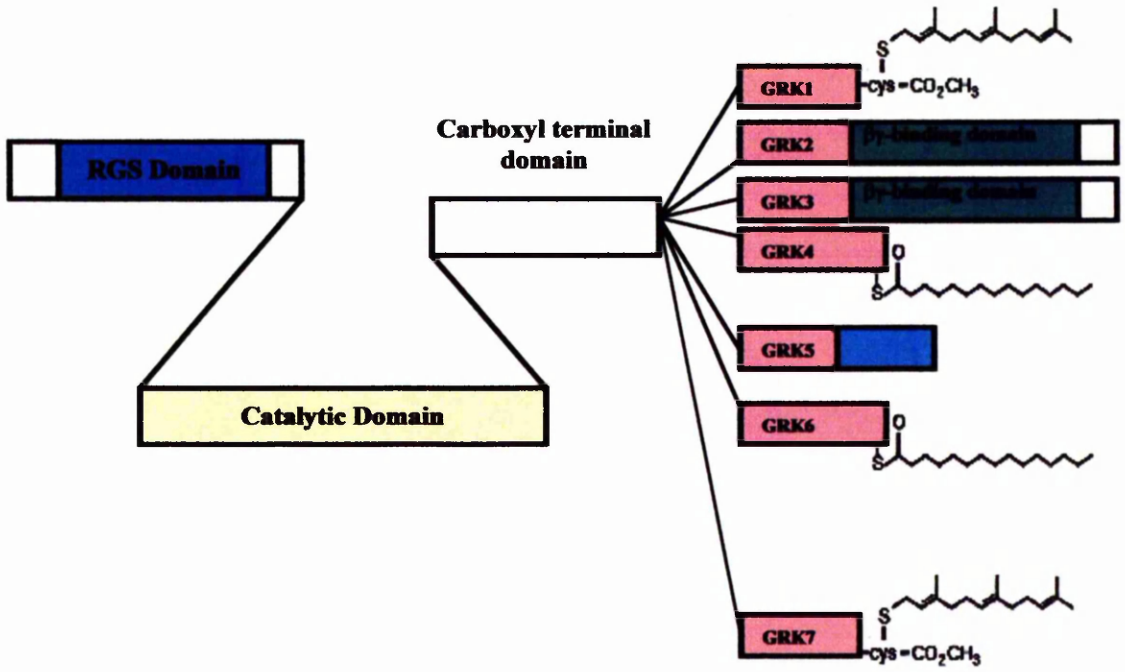

Table 1.2

GRK	Size (kDa)	Polypeptide Variants	Covalent Modification	Activators	Inactivators
1	63	ND	Farnesylation	Polycations	Recoverin
2	79	ND	ND	$G_{\beta\gamma}$, PIP_2, PKC, c-Src	MAPK
3	80	ND	ND	$G_{\beta\gamma}$, PIP_2	ND
4	66	4	Palmitoylation	ND	ND
5	68	ND	ND	Polycations, PIP_2	PKC, calmodulin
6	66	Yes	Palmitoylation	Polycations	ND
7	62	ND	Farnesylation	ND	ND

ND, not determined

(Chuang *et al.*, 1995; Pronin and Benovic, 1997). For GRK 2, PKC phosphorylation activates the enzyme, whereas PKC reduces GRK 5 activity.

1.5.5 Role of GRKs in GPCR desensitisation

There is an abundance of evidence to suggest that desensitisation of GPCRs is associated with GRK phosphorylation. Coexpression of GRKs with GPCRs in cells resulted in augmented desensitisation of receptors including the β_2-adrenergic (Pippig *et al.*, 1993), β_1-adrenergic (Freedman *et al.*, 1995), α_{1B}-adrenergic (Diviani *et al.*, 1996), α_2-adrenergic (Jewell-Motz and Liggett, 1996), angiotensin II_{1A} (AT_{1A}) (Opperman *et al.*, 1996), A3 adenosine (Palmer *et al.*, 1995), m2 muscarinic (Schlador and Nathanson, 1997), histamine H2 (Shayo *et al.*, 2001) and m3 muscarinic (Willets *et al.*, 2001) receptors.

A few GPCRs show preference for phosphorylation by a particular GRK, such as the endothelin receptors which are phosphorylated only by GRK 2 in HEK293 cells (Freedman *et al.*, 1997) while thrombin receptors (Ishii *et al.*, 1994) are specifically phosphorylated by GRK 3. Conversely, there are GPCRs which can be phosphorylated by several GRKs, including the AT_{1A} (Opperman *et al.*, 1996), β_2-adrenergic (Premont *et al.*, 1995), and muscarinic m2 and m3 (Richardson *et al.*, 1993; Debburman *et al.*, 1995) receptors.

Deletions or mutations in putative phosphorylation sites in GPCR cytoplasmic domains have been shown to reduce desensitisation due to the loss of receptor phosphorylation, a phenomenon which has been observed for GPCRs including the α_{2A}-adrenergic (Liggett *et al.*, 1992), thrombin (Ishii *et al.*, 1994), m2 muscarinic (Pals-Rylaarsdam *et al.*, 1995), β_2-adrenergic (Bouvier *et al.*, 1988), and the α_{1B}-adrenergic (Lattion *et al.*, 1994) receptors. Similarly, coexpression of dominant negative GRK mutants (which lack kinase activity) with GPCRs was found to inhibit desensitisation of the m2 muscarinic (Pals-Rylaarsdam *et al.*, 1995), AT_{1A} (Opperman *et al.*, 1996), β_2-adrenergic (Kong *et al.*, 1994), β_1-adrenergic (Freedman *et al.*, 1995), α_{1B}-adrenergic (Diviani *et al.*, 1996), δ-opioid (Pei *et al.*, 1995) and A2 adenosine (Mundell *et al.*, 1997) receptors.

In vivo studies using transgenic mice have also given some insight into GRK activity in different tissues. Mice engineered to overexpress GRK 2 in cardiac myocytes displayed a reduction in their responsiveness to β-AR agonists and angiotensin II, while mice overexpressing the C-terminal portion of GRK 2 (consequently inhibiting GRK 2 by sequestering the $G_{\beta\gamma}$ pool) exhibited increased sensitivity to such agonists (Koch *et al.*, 1995; Rockman *et al.*, 1996). Similarly, long term exposure with β-AR agonists or antagonists in mice induced GRK 2 upregulation and downregulation respectively (Iaccarino *et al.*, 1998).

1.5.6 Other kinases which phosphorylate GPCRs

GPCRs are also substrates for phosphorylation by other kinases apart from GRKs and/or second messenger kinases. Studies have revealed that casein kinase 1α can phosphorylate the m3 muscarinic receptor on the third intracellular loop (Tobin *et al.*, 1997) although receptor mutants lacking the potential casein kinase 1α phosphorylation sites still underwent agonist-mediated desensitisation (Budd *et al.*, 2000). The phosphorylation of TRH receptor on its C-terminal tail by casein kinase II (Hanyaloglu *et al.*, 2001) was deemed to be important for receptor internalisation but not desensitisation. Tyrosine phosphorylation of agonist-occupied μ-opioid receptors (Pak *et al.*, 1999) has been suggested to be an important signal for downregulation of the receptor. For the bradykinin B_2 receptor, tyrosine kinase inhibitors blocked bradykinin-mediated prostaglandin E_2 production, indicating that tyrosine kinase phosphorylation of the receptor is critical for its signal transduction (Jong *et al.*, 1993).

1.5.7 The role of visual arrestin in rhodopsin desensitisation

Phosphorylation by GRKs of rhodopsin has been shown to be insufficient to promote complete desensitisation of the receptor. It was observed that full inactivation of the receptors required an additional interaction with an "arresting" protein. The identification of arrestin was first made in the rod photoreceptor cells where a 48 kDa protein, originally called S-antigen, was demonstrated to regulate rhodopsin signal transduction (thus it is now known as visual arrestin) (Pfister *et al.*, 1985).

Visual arrestin was shown to translocate from the cytoplasm to the membrane following light activation of rhodopsin (Kuhn *et al.*, 1984) and the protein was subsequently purified from the retinal rod membranes via its light-dependent binding to phosphorylated rhodopsin (Wilden *et al.*, 1986a). The cDNA sequence of visual arrestin revealed it to encode a 404-amino acid protein (Shinohara *et al.*, 1987) and that its expression was localised to the retinal tissue (Lohse *et al.*, 1990a). More recently, another retinal-specific arrestin was cloned and found to share ~50% sequence homology with visual arrestin. With expression being primarily localised to the cone photoreceptors, the protein was named cone arrestin (Craft *et al.*, 1994; Murakami *et al.*, 1993).

Receptor activation and phosphorylation is an absolute requirement for the binding of visual arrestin to rhodopsin. *In vitro* studies revealed that there was a 10-12- fold increase in the binding of visual arrestin to rhodopsin when the receptor was phosphorylated and light-activated, compared to when it was phosphorylated dark rhodopsin or light-activated (non-phosphorylated) rhodopsin (Gurevich and Benovic, 1992).

The complete quenching of the cGMP phosphodiesterase activity of activated rhodopsin receptors occurred only when visual arrestin bound to the receptor, indicating that phosphorylation alone is not sufficient to produce full desensitisation (Wilden *et al.*, 1986b). Phosphorylation alone reduced coupling to transducin by 30-50% (Krupnick *et al.*, 1997). Visual arrestin produces full quenching of the signal by acting as a physical barrier to prevent transducin coupling to the phosphorylated activated receptors. Binding studies using purified arrestin and transducin have demonstrated that the two proteins compete for binding to phosphorylated light-activated rhodopsin (Krupnick *et al.*, 1997).

1.5.8 The role of non-visual arrestins in GPCR desensitisation

Evidence for the existence of other arrestin proteins involved in the desensitisation of other GPCRs besides rhodopsin originated from the observation that a partially purified βARK preparation inhibited up to 80% of β-AR signally *in vitro*, whereas a more highly

purified βARK only inhibited signalling modestly (Benovic *et al.*, 1987). This cofactor in the βARK preparation was subsequently cloned and termed β-arrestin (Lohse *et al.*, 1990a, Table 1.3). β-Arrestin was found to be a 418 amino acid protein which shares a 59% sequence homology to visual arrestin. Another non-visual arrestin, called β-arrestin 2 was cloned (Attramadal *et al.*, 1992) and encodes a 409 amino acid protein. The expression of the β-arrestins is ubiquitous, but they are predominantly localised in the neuronal tissues and in the spleen (Attramadal *et al.*, 1992). A third class of arrestins has been identified, namely D- and E-arrestin (Craft *et al.*, 1994). Although the mRNAs for D- and E-arrestin are expressed in many tissues, it is unclear whether such proteins exist and if they are functional (Craft *et al.*, 1994).

As with visual arrestin, *in vitro* studies with the β-arrestin proteins has greatly enhanced the understanding of their interactions with GPCRs. Translated β-arrestin 1 was found to bind to the m2 muscarinic receptor in a phosphorylation-dependent manner, with the highest binding occurring with an agonist-activated phosphorylated form of the receptor (Gurevich *et al.*, 1993). Furthermore, purified β-arrestin 1 was observed to bind preferentially to ligand-activated, phosphorylated β_2-ARs, with a K_d of ~2nM and a stoichiometry of 1 β-arrestin molecule per receptor (Sohlemann *et al.*, 1995). However, unlike visual arrestin, substantial binding of the β-arrestins to phosphorylated non-activated forms of the m2 muscarinic receptor and β_2-AR, as well as agonist-activated non-phosphorylated forms of the receptors was detected (Gurevich *et al.*, 1995). Furthermore, *in vitro* studies with the β_2-AR showed that β-arrestin 1 works in concert with βARK to effect agonist-specific desensitisation of the receptor. It was observed that βARK phosphorylation, but not PKA phosphorylation, greatly enhanced β_2-AR desensitisation (Lohse *et al.*, 1992), an observation which was in accord with the finding that β-arrestins preferentially bind GRK-phosphorylated as opposed to second messenger kinase-phosphorylated receptors (Lohse *et al.*, 1990a, 1992).

The role of β-arrestins in desensitisation *in vivo* has been studied for an array of GPCRs. In cells expressing receptors such as the β_2-adrenergic, β_1-adrenergic, α_{1B}-adrenergic and m2 muscarinic receptors, coexpression of β-arrestin 1 or β-arrestin 2 was found to

increase desensitisation (Pippig *et al.*, 1993; Freedman *et al.*, 1995; Diviani *et al.*, 1996; Schlador and Nathanson).

1.5.9 Structure and function of the arrestin proteins

Alternative splice variants have been identified for visual arrestin and the β-arrestins. Bovine visual arrestin is expressed as a 404 amino acid residue protein, as well as p44 (for which the last 35 amino acids are replaced by alanine) and another that lacks residues encoded by exon 13 (Yamaki *et al.*, 1990; Smith *et al.*, 1994). The p44 splice variant is specifically localised to the rod outer segment and is more potent at inhibiting rhodopsin signalling than the full length form, thus demonstrating that the carboxyl terminal domain of arrestin is not essential for binding to rhodopsin. Like visual arrestin, the β-arrestins express at least two alternative spliced forms. The variant form of β-arrestin 1 has an eight amino acid insertion between residues 333 and 334 (Parruti *et al.*, 1993) and the alternate β-arrestin 2 has an eleven amino acid insert between residues 362 and 363 (Sterne-Marr *et al.*, 1993). No differences in activity of the β-arrestin splice variants have been reported.

The observation that arrestins preferentially bind to phosphorylated, ligand-activated receptors suggests that there is a domain(s) that makes specific contacts with GPCRs in the active state (Figure 1.7). Initial investigations to locate the activation-recognition region suggested that it was present in the N-terminal half of the protein (residues 1-191) as a truncated visual arrestin containing residues 1-191 retained its ability to bind light-activated state of rhodopsin (Gurevich and Benovic, 1992). Moreover, it had been previously shown that the p44 visual arrestin mutant binds with high affinity to rhodopsin (Palczewski *et al.*, 1994). Further mutagenesis studies mapped the phosphorylation-recognition site to a discrete region within the N-terminus. Arrestin truncated at residue 185 bound to phosphorylated light-activated rhodopsin and phosphorylated dark rhodopsin, while arrestin truncated at residue 158 exhibited a reduction in its ability to detect the phosphorylated form of the receptor, thus focusing the location of the phosphorylation-recognition region to between residues 158 and 185 (Gurevich and Benovic, 1993). Mutagenesis of individual residues within region 158-185 of arrestin identified several basic residues, namely Arg^{171}, Arg^{175}, and Lys^{176},

Figure 1.7

Structure of the arrestin proteins.

Crystallographic and mutagenesis studies have identified that the arrestin proteins comprise an amino regulatory domain (residues 1-24), a receptor activation domain (residues 24-180), a phosphate sensor domain (163-182), a secondary receptor-binding domain (residues 180-330), and a carboxyl terminal domain (residues 330-404). The black box highlights the clathrin- and β-adaptin-binding domains that are conserved among non-visual arrestins.

Table 1.3

Characteristics of the arrestin proteins.

Summary of the molecular properties of the members of the arrestin family.

Figure 1.7

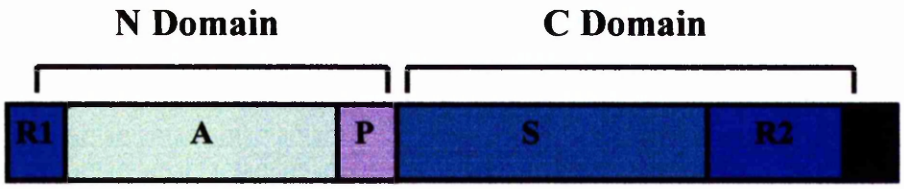

R1, amino regulatory domain; A, receptor activation domain; P, phosphate sensor domain; S, secondary receptor-binding domain; R2, carboxyl terminal regulatory domain

Table 1.3

Name	Size (residues)	Polypeptide Variant (residues)	Substrate	Phosphorylation	Function
Visual arrestin, *bovine*	404	390, 370 (p44)	rhodopsin > β_2-AR > m2 muscarinic receptor	PKC Ca^{2+}-camodulin	Desensitisation
Cone arrestin, *human*	388	ND	ND	ND	Desensitisation
β-arrestin 1, *rat*	418	410	β_2-AR > m2 muscarinic receptor >> rhodopsin	MAPK	Desensitisation, Endocytosis, Signalling
β-arrestin 2, *rat*	410	399	β_2-AR > m2 muscarinic receptor >> rhodopsin	Casein kinase II	Desensitisation, Endocytosis, Signalling

ND, not determined

which were crucial for phosphate binding (Gurevich and Benovic, 1995). Furthermore, Arg^{175} was suggested to function as a phosphorylation-sensitive trigger, since mutation of this residue to a neutral or acidic amino acid resulted in constitutive binding of arrestin to non-phosphorylated light-activated rhodopsin (Gurevich and Benovic, 1995). The N-terminal segment of the β-arrestins also retained the ability to recognise agonist-activated receptors, indicating that the activation-recognition region of all arrestins was contained within the N-terminal half (Gurevich *et al.*, 1995).

Visual arrestin undergoes a conformational change upon its binding to light-activated phosphorylated rhodopsin. This was first implied when it was noticed that the arrestin molecule became more sensitive to limited proteolysis when bound to activated rhodopsin (Palczewski *et al.*, 1991). Further studies confirmed that the conformational change was driven by the primary interactions of the activation-recognition and phosphorylation-recognition regions with corresponding contact sites on the receptor. These interactions lead to a conformational change that exposes a secondary hydrophobic binding site (between residues 191 and 365) for high affinity binding (Gurevich and Benovic, 1993). The involvement of hydrophobic interactions in high affinity binding of the arrestin to the receptor was further demonstrated from the observation that salt promoted the interaction of arrestin with the activated receptor (Gurevich and Benovic, 1993).

The selectivity of visual arrestin for binding to phosphorylated light activated receptors is mediated by an intramolecular interaction between the basic N-terminus and acidic C-terminus (Gurevich *et al.*, 1993; 1995). The rigid structure of the arrestin C-terminus is maintained until the receptor is activated and the intramolecular arrestin interactions are replaced by contacts with the receptor. The lack of discrimination of C-terminal truncated arrestin mutants for phosphorylated light-activated rhodopsin therefore indicated that such mutants were unable to form a rigid structure leading to an increased availability of the hydrophobic region to the receptor for binding (Gurevich *et al.*, 1994).

Visual arrestin/β-arrestin chimeras have been important tools used in the discovery of the regions of arrestins which are critical for determining GPCR binding specificity.

Two large central domains in visual arrestin (residues 48-365) and β-arrestin (residues 45-367) have been identified as being important for determining specificity of GPCR binding (Gurevich *et al.*, 1995). Switching the N- and C-terminal domains of visual arrestin with the complementary β-arrestin domains did not prevent the binding of the chimeric arrestin to activated rhodopsin. Similarly, a chimeric β-arrestin, which possessed the N- and C- terminal regions of visual arrestin, was still able to bind to agonist-occupied, phosphorylated m2 muscarinic and β_2-ARs (Gurevich *et al.*, 1995). Such observations were consistent with the assumed roles of the N- and C-termini of the arrestins in regulation of their conformation.

More recently, the resolution of visual arrestin crystal structure has provided further understanding of arrestin/rhodopsin interactions (Granzin *et al.*, 1998). The solution of the visual arrestin structure confirmed the presence of the different arrestin domains which had already been identified in mutagenesis studies: a receptor activation domain (residues 24-180), a secondary receptor binding domain (residues 180-330), a phosphate sensor domain (163-182), an N-terminal regulatory domain (residues 1-24) and a carboxyl regulatory domain (residues 330-404) (Granzin *et al.*, 1998; Hirsch *et al.*, 1999). Taken together, the crystallographic and mutagenesis studies of arrestin have demonstrated that its molecular structure is designed to resist agonist- and phosphorylation-independent interactions with receptors.

1.6 GPCR internalisation

1.6.1 Introduction

An important aspect of GPCR regulation is the internalisation of agonist-activated receptors. Studies have demonstrated that many GPCRs translocate from the cell surface to intracellular membrane compartments upon exposure to agonist.

The discovery of GPCR internalisation originated from the observation that there was a rapid distribution of β_2-ARs from the cell surface upon agonist treatment of bullfrog erythrocytes. It was noticed that the loss of cell surface receptors corresponded with an

increase in intracellular β_2-ARs (Chuang and Costa, 1979). Subsequently, early ligand binding studies were able to distinguish cell surface receptors from internalised β_2-AR binding sites using differential sedimentation on sucrose gradients or by the use of hydrophobic and hydrophilic ligands for the receptor (Harden *et al.*, 1980; Staehelin and Simons, 1982). The internalised receptors were found to be associated with a "light vesicle" fraction that could be separated from a "heavy vesicle" plasma membrane fraction that was associated with the cell surface receptors (Harden *et al.*, 1980). Similarly, the internalised receptors were not accessible to hydrophilic ligands but were accessible to hydrophobic ligands (Staehelin and Simons, 1982). More recently, immunocytochemical staining of epitope-tagged β_2-ARs, as well as the use of green fluorescent protein (GFP) tagged β_2-ARs, has permitted the visualisation of receptor trafficking in real time in live cells (von Zastrow and Kobilka, 1992; Barak *et al.*, 1997a).

1.6.2 The role of phosphorylation in GPCR internalisation

Early studies into the role of phosphorylation in receptor endocytosis were inconclusive as β_2-AR mutants lacking sites for both PKA- and GRK-mediated receptor phosphorylation showed no significant difference in internalisation compared to the wild-type β_2-AR (Bouvier *et al.*, 1988; Hausdorff *et al.*, 1989). Similarly, PKA and GRK inhibitors were unable to inhibit internalisation of the β_2-AR in A431 cells (Lohse *et al.*, 1990b).

Despite these original studies with the β_2-AR, evidence was accumulating that phosphorylation might be important for the internalisation of other GPCRs. A Ser/Thr-rich sequence was suggested to be a crucial factor in the sequestration of the m1, m2, and m3 muscarinic receptors (Moro *et al.*, 1993). Mutation of the serine and threonine residues within the third intracellular loop of the m2 muscarinic receptor reduced the rate of internalisation (Moro *et al.*, 1993). Moreover, overexpression of GRK 2 enhanced the rate of m2 muscarinic receptor internalisation, whereas expression of a dominant-negative GRK 2 mutant led to a decrease in receptor phosphorylation and internalisation in COS 7 cells (Tsuga *et al.*, 1994). Further evidence to support the role of phosphorylation in internalisation was highlighted in studies with the thrombin

receptor (Shapiro *et al.*, 1996). Truncation or mutation of the Ser/Thr residues in the C-terminus of the thrombin receptor reduced both agonist-induced phosphorylation and sequestration. In addition, C-terminal deletions or point mutations of Ser/Thr residues in the C-terminus of the δ-opioid receptor significantly reduced its agonist-induced internalisation (Trapaidze *et al.*, 1996).

The direct role of phosphorylation of the β_2-AR in its sequestration was eventually demonstrated using a phosphorylation- and internalisation-defective mutant, β_2-AR-Y326A (Ferguson *et al.*, 1995). Overexpression of GRK 2 enhanced both the phosphorylation and internalisation of the receptor mutant. Likewise, overexpression of GRKs 3-6 also enhanced phosphorylation and sequestration of β_2-AR-Y326A with the agonist-dependent restoration of phosphorylation correlating with the rescue of internalisation (Menard *et al.*, 1996). In addition, the phosphorylation and internalisation of the wild-type β_2-AR in HEK293 cells was reduced by overexpression of a dominant negative GRK 2 mutant (Ferguson *et al.*, 1995). GRK 2 phosphorylation has been shown to mediate internalisation of other GPCRs including the AT_{1a} (Smith *et al.*, 1998), endothelin A (Bremnes *et al.*, 2000), D2 dopamine (Itokawa *et al.*, 1996) and the chemokine receptors CCR-5 (Aramori *et al.*, 1997) and CXCR1 (Barlic *et al.*, 1999).

1.6.3 The role of β-arrestins in GPCR internalisation

GRK-mediated phosphorylation is not an absolute necessity for internalisation (Bouvier *et al.*, 1998; Hausdorff *et al.*, 1989) but instead promotes the interaction of the GPCR with other cellular proteins. It has now become evident that the ability of GRKs to promote GPCR endocytosis is dependent on the binding of β-arrestins to the receptor. In addition to uncoupling receptors from G proteins, β-arrestins act as endocytic adapters targeting GPCRs for internalisation into clathrin-coated vesicles (CCVs) (Zhang *et al.*, 1996). Overexpression of both β-arrestin 1 and β-arrestin 2 alone with the β_2-AR-Y326A mutant augmented receptor sequestration even in the absence of GRKs (Ferguson *et al.*, 1996). Moreover, β-arrestins promoted internalisation of C-terminal tail truncated β_2-ARs and mutants lacking putative GRK phosphorylation sites.

The relationship between GRK-mediated phosphorylation and β-arrestin recruitment is likely dependent upon the receptor subtype and the cell type in which it is expressed. Different GPCR subtypes have different requirements for internalisation. For example, internalisation of the chemokine receptors CCR-5 and CXCR1 in HEK293 cells required overexpression of both GRKs and β-arrestins (Aramori *et al.*, 1997; Barlic *et al.*, 1999). For the m2 muscarinic receptor, internalisation required GRK phosphorylation but not β-arrestin, depending on the cellular environment in which it was expressed (Tsuga *et al.*, 1994; Schlador and Nathanson, 1997; Werbonat *et al.*, 2000). Studies of β_2-AR sequestration have shown that there is significant correlation between the endogenous complement of GRKs and β-arrestins in the cell types and the kinetics of β_2-AR agonist-induced internalisation in such cells (Menard *et al.*, 1997). Similarly, for the CXCR1 receptor, sequestration could be detected in the GRK- and β-arrestin-rich RBL-2H3 cells, but not in HEK293 cells in which expression of these proteins is lower (Barlic *et al.*, 1999).

1.6.4 β-Arrestin interactions with clathrin in GPCR endocytosis

The first evidence that β-arrestins direct GPCRs for endocytosis into CCVs originated from the study of the effects of β-arrestin and dynamin dominant-negative mutants on β_2-AR and $AT_{1A}R$ internalisation (Zhang *et al.*, 1996). The large GTPase dynamin is involved in the pinching off of CCVs from the plasma membrane (Damke *et al.*, 1994). The expression of a GTPase-deficient dynamin mutant (K44A) effectively inhibited both β_2-AR and $AT_{1A}R$ sequestration (Zhang *et al.*, 1996). Furthermore, immunofluorescence analysis by Goodman *et al.* (1996) demonstrated that β_2-ARs and β-arrestin colocalise with clathrin in coated pits.

Recent studies have shown that β-arrestins directly interact with components of the endocytic machinery involved in the formation of clathrin-coated pits (Goodman *et al.*, 1996; Laporte *et al.*, 1999, 2000, Figure 1.7). β-Arrestins bind to both the clathrin heavy chain and the β2-adaptin subunit of the heterotetrameric AP-2 adapter complex (Goodman *et al.*, 1997; Laporte *et al.*, 1999, 2000). The clathrin β-arrestin binding domain lies between residues 89-100 of the amino-terminal globular region in the

terminal domain of the clathrin heavy chain which is located at the distal portion of each clathrin triskelion (Goodman *et al.*, 1997). Amino acid residues 373-377 in the carboxyl terminus of β-arrestin 2 are involved in clathrin binding (Krupnick *et al.*, 1997). The β-arrestin domain responsible for binding to the β2-adaptin subunit of the AP-2 adapter complex is also localised to the C-termini of the β-arrestin proteins (Laporte *et al.*, 1999). More specifically, *in vitro* studies have revealed that residues Arg^{394} and Arg^{396} in β-arrestin 2 are required for β2-adaptin binding (Laporte *et al.*, 2000). The interaction of β-arrestins with the AP-2 adapter, rather than clathrin, is essential for the initial translocation of receptors to coated pits (Laporte *et al.*, 2000). Immunocytochemical studies demonstrated that β-arrestin mutants lacking the β-arrestin clathrin binding site motif retained the ability to redistribute with the β_2-AR to coated pits whereas mutation of the β-arrestin β2-adaptin binding site blocked the targeting of receptors to CCVs (Laporte *et al.*, 2000).

1.6.5 β-Arrestin regulation and signalling

The use of GFP-tagged β-arrestins has shown that cytosolic β-arrestin translocates to the plasma membrane upon GPCR activation and subsequently associates with the receptors in clathrin-coated pits (Barak *et al.*, 1997b). The underlying mechanism of this receptor-mediated response remains undetermined. However, feedback regulation of β-arrestins has been demonstrated. β_2-AR activation leads to phosphorylation of β-arrestin 1 on serine residue 412 by extracellular signal-regulated kinases (ERKs) (Lin *et al.*, 1998, 1999). β-Arrestin 1 appears to be dephosphorylated upon its recruitment to the plasma membrane-bound receptors, while cytoplasmic β-arrestin 1 is primarily in the phosphorylated form (Lin *et al.*, 1998). Hence, a S412D β-arrestin 1 mutant was found to function as a dominant negative of β_2-AR endocytosis. However, the mutant had no apparent affect on receptor desensitisation (Lin *et al.*, 1998). The dephosphorylation of β-arrestin-1 does not seem to be a prerequisite for the redistribution of β-arrestin 1 to the membrane (Oakley *et al.*, 2000). It has been suggested that ERK-mediated phosphorylation contributes to the regulation of β-arrestin 1/β-adaptin interactions (Lin *et al.*, 1999). For β-arrestin 2, there is no conserved serine residue for phosphorylation.

Therefore, ERK-mediated phosphorylation either occurs at a different site or β-arrestin 2 regulation is mediated by an alternative mechanism.

β-Arrestin activity is also regulated by phosphoinositides, particularly IP_6 (Gaidarov and Keen, 1999; Gaidarov *et al.*, 1999). Residues 233-251 of β-arrestin 2 form the phosphoinositide-binding site. Mutation of residues within this domain produced a β-arrestin mutant defective in stimulating β_2-AR internalisation in COS 1 cells. Furthermore, the mutant did not localise to clathrin coated pits. Thus, these observations suggest that phosphoinositide binding may be involved in the routing of receptor/β-arrestin complexes to the clathrin-coated pits.

As well as functioning as adapter proteins regulating GPCR desensitisation and internalisation, β-arrestins have recently been shown to play important roles in the localisation of signalling proteins to agonist-activated GPCRs (Miller and Lefkowitz, 2001). It has been revealed that the interaction of β-arrestins with molecules such as Src, Raf, and JNK3 appears to regulate signalling pathways which result in the activation of MAP kinases. For the β_2-AR, the recruitment of Src was found to be essential for both receptor-mediated activation of the ERK cascade and receptor internalisation. Src-induced phosphorylation of components of the endocytic machinery, such as dynamin and clathrin, appear to be critical for the internalisation process (Miller *et al.*, 2000; Ahn *et al.*, 1999).

1.6.6 Alternative GPCR endocytic pathways

It is now recognised that not all GPCRs internalise via a β-arrestin- and clathrin-dependent route. This was first suggested from experiments of $AT_{1A}R$ internalisation in COS 7 cells and HEK293 cells (Zhang *et al.*, 1996). In COS 7 cells, in which the endogenous level of GRKs and β-arrestin is relatively low, the maximal extent of receptor internalisation was the same as in HEK293 cells which express much higher levels of the proteins. In contrast, β_2-AR internalisation was markedly reduced in COS 7 cells (Zhang *et al.*, 1996). Other experiments have shown that the effects of dominant negative mutants of β-arrestin and dynamin on GPCR endocytosis varies depending on the receptor studied (Zhang *et al.*, 1996; Vogler *et al.*, 1999). For the AT_{1A} and m2

muscarinic receptors, coexpression of either dominant-negative β-arrestin or dynamin mutants did not inhibit agonist-stimulated internalisation (Zhang *et al.*, 1996; Vogler *et al.*, 1999), whereas β-arrestin-mediated sequestration of the $AT_{1A}R$ was blocked completely by the expression of a dominant-negative dynamin mutant (Zhang *et al.*, 1996). Taken together, these observations suggest that the internalisation of some GPCRs, at least in the presence of dominant-negative inhibitors of clathrin-mediated endocytosis, use an alternative endocytic mechanism. This idea may be of significance since the overexpression of dynamin mutants is reported to stimulate an increase in activity of alternative internalisation pathways, such as pinocytosis (Damke *et al.*, 1995).

The likelihood of a clathrin-dependent pathway being involved in the normal sequestration of the AT_{1A} and m2 muscarinic receptors is supported by the observation that a dynamin dominant-negative mutant exhibiting mutations of all three dynamin GTPase domains abolished internalisation of both receptors (Werbonat *et al.*, 2000). Furthermore, the K44A-dynamin mutant trapped $AT_{1A}R$/β-arrestin complexes in coated pits and prevented the co-internalisation of β-arrestin with the receptor into endosomes (Anborgh *et al.*, 2000). However, these observations do not rule out the possibility of alternative pathways for GPCR internalisation.

Internalisation of GPCRs in non-coated vesicles has also been reported as an alternative pathway for endocytosis. The internalisation of the β_2-AR in A431 cells is believed to be in association with small microdomains of plasma membrane rich in cholesterol and glycosphingolipids known as caveolae. Electron microscopy of A431 cells showed that β_2-ARs internalised via microdomains with the caveolae marker protein caveolin-1 (Raposo *et al.*, 1989). A clathrin-dependent pathway for internalisation was shown to be functional in these cells since transferrin receptors were endocytosed in clathrin coated pits (Daukas and Zigmond, 1985). The identification of the β_2-AR's caveolin-binding motif was unexpectedly localised to residues within the extracellular portion of the seventh transmembrane domain (Raposo *et al.*, 1989; Watson and Arkinstall, 1994; Couet *et al.*, 1997). Such findings indicated that the receptor's caveolin binding motif was inaccessible to caveolin and therefore was unlikely to be involved in the internalisation of the β_2-AR. Caveolae have also been implicated in the internalisation

of the endothelin A receptor in transfected COS cells (Chun *et al.*, 1994) and in the sequestration of muscarinic receptors in human fibroblasts (Raposo *et al.*, 1987). The putative caveolin-binding motifs in the muscarinic receptor family (Watson and Arkinstall, 1994) and endothelin A receptor (Watson and Arkinstall, 1994; Bremnes *et al.*, 2000) were also found to be in receptor domains that are inaccessible to caveolin thus ruling out the interaction of caveolin with such domains.

1.6.7 Receptor determinants for endocytosis

Multiple receptor domains appear to contribute to the internalisation properties of GPCRs. For many GPCRs the second and third intracellular loop domains are functionally important in GPCR internalisation. For the m2 muscarinic receptor, the determinants for internalisation are found within a serine/threonine rich domain of the receptor's third intracellular loop (Moro *et al.*, 1993). Presumably, these residues are the sites of GRK phosphorylation that are critical for inducing receptor endocytosis (Tsuga *et al.*, 1998). As well as the third intracellular loop, the conserved DRYXXV/IXXPL sequence of the second intracellular loop domain is also involved in the internalisation of some GPCRs including the m1 muscarinic and GnRH receptors. Specifically, mutation of the motif's leucine residue led to a reduction in internalisation of both receptors (Moro *et al.*, 1994, Arora *et al.*, 1995).

Many investigators have examined the role of GPCR C-terminal tails and putative GRK phosphorylation sites in regulating agonist-stimulated GPCR internalisation. Although the internalisation of the β_2-AR is β-arrestin-dependent, neither the truncation of the β_2-AR carboxyl tail nor the mutation of potential GRK phosphorylation sites was found to inhibit β_2-AR internalisation (Hausdorff *et al.*, 1989; Ferguson *et al.*, 1995). Conversely, truncation of the C-tail or mutation of putative GRK sites of the $AT_{1A}R$ blocked its internalisation (Thomas *et al.*, 1995; Zhang *et al.*, 1996; Smith *et al.*, 1998). Both positive and negative regulators of agonist-stimulated internalisation have been identified within the GPCR carboxyl terminal tail. A dileucine motif within the C-tail of the β_2-AR is involved in receptor internalisation (Gabilondo *et al.*, 1997) whereas a carboxyl-terminal tail dileucine motif negatively regulates lutropin/choriogonadotropin

receptor sequestration since mutation of the motif was revealed to increase agonist stimulated receptor internalisation (Nakamura and Ascoli, 1999).

1.6.8 The role of internalisation in receptor desensitisation

GPCR internalisation was originally thought to be the principal mediator of receptor desensitisation due to the physical separation of the receptor from its effectors (Sibley and Lefkowitz, 1985). However further studies showed that receptor desensitisation occurs more rapidly than receptor endocytosis and the majority of sequestered receptors are phosphorylated and thus already desensitised. Furthermore, treatments such as hypertonic sucrose and concanavalin A that inhibit GPCR internalisation were demonstrated not to affect the β_2-AR's ability to desensitise (Pippig *et al.*, 1995). In analysis of truncated C-tail receptors and phosphorylation-deficient mutants, many studies have reported that desensitisation and internalisation are distinct processes. This has been demonstrated for receptors including the AT_{1A} (Thomas *et al.*, 1995), D1 dopamine (Ng *et al.*, 1995), m2 muscarinic (Pals-Rylaarsdam *et al.*, 1995) and H2 histamine (Fukushima *et al.*, 1997) receptors.

1.6.9 The role of internalisation in resensitisation

Although GPCR internalisation may not a play a critical role in agonist-induced desensitisation, recent studies have highlighted the importance of internalisation in the recovery from desensitisation (a process also known as resensitisation). The mechanisms of GPCR resensitisation are thought to involve the internalisation of agonist-activated receptors into endosomal compartments which contain a GPCR-specific phosphatase. Endosomal acidification promotes the association of the receptor with the GPCR phosphatase and dephosphorylation of the receptor. Dephosphorylated GPCRs are subsequently recycled back to the cell surface where they can be again activated by agonist (Figure 1.8).

The role of internalisation in resensitisation was first observed in studies of the β_2-AR. Following agonist exposure, β_2-ARs were found to endocytose and subsequently recycle back to the plasma membrane (Staehelin and Simons, 1982; Morrison *et al.*,

Figure 1.8

Schematic representation of GPCR resensitisation.

GPCR resensitisation is achieved by the dephosphorylation of internalised receptors by a receptor phosphatase and subsequent recycling of receptors back to the cell surface. Alternatively, sequestered receptors are retained intracellularly and/or targetted for downregulation in lysosomes. In this instance, resensitisation is mediated by the mobilisation of an intracellular pool of naïve receptors and/or *de novo* receptor synthesis. Figure adapted from Ferguson and Caron, 1998.

Figure 1.8

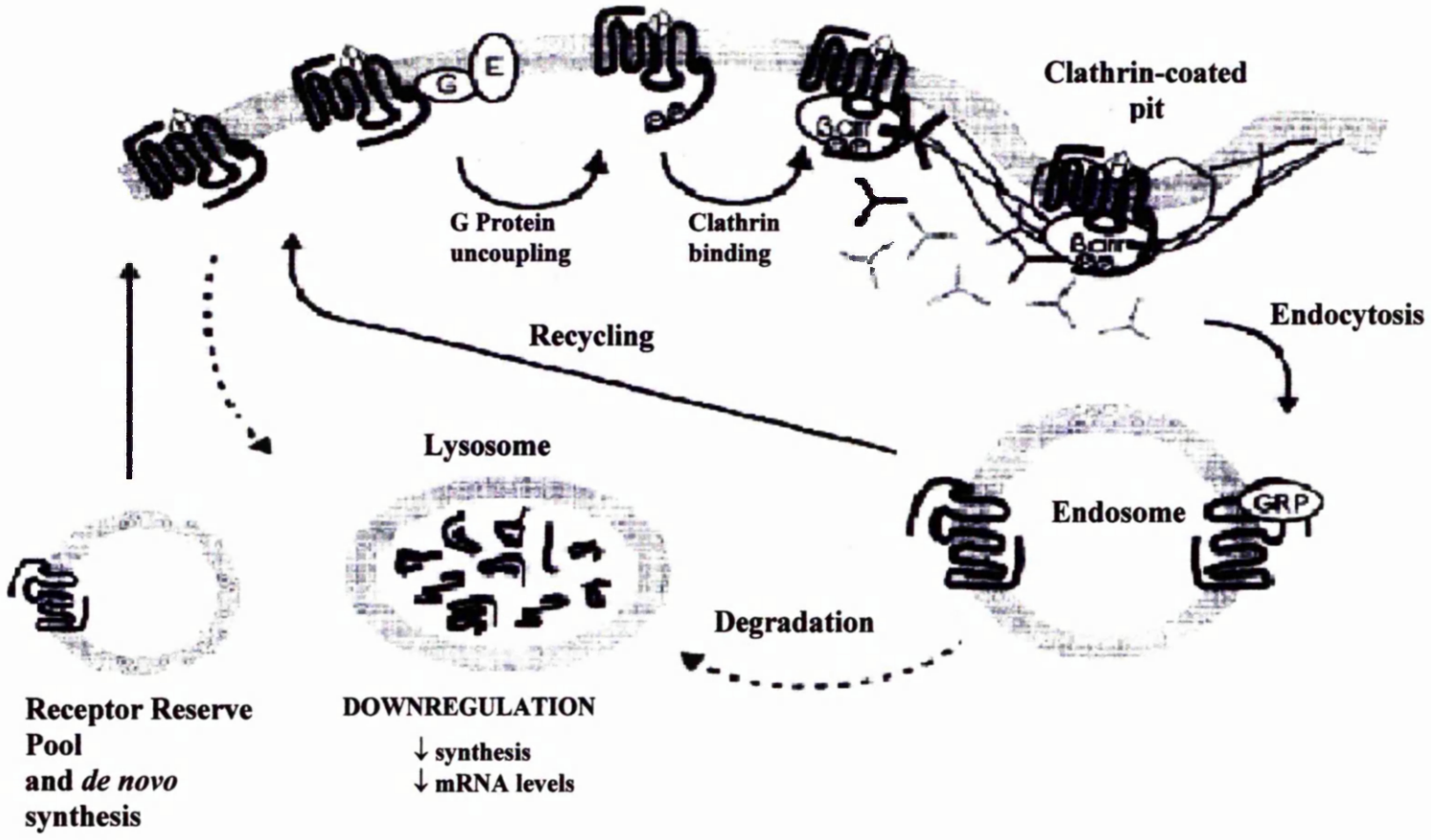

βarr, β-arrestin; E, effector enzyme; G, heterotrimeric G protein; GRP, G protein-coupled receptor phosphatase; H, hormone; P, phosphate group.

1996). Furthermore, sequestered β_2-ARs were capable of stimulating adenylyl cyclase in reconstituted systems (Stadel *et al.*, 1983b; Strulovici *et al.*, 1983). The use of internalisation inhibitors such as sucrose and concanavalin A also blocked β_2-AR resensitisation while G-protein coupling and desensitisation were unaffected (Pippig *et al.*, 1995; Yu and Lefkowitz, 1993). It was subsequently proposed that dephosphorylation of internalised receptors in the endosomes followed by recycling back to the cell surface was responsible for restoring β_2-AR function (Pippig *et al.*, 1995). This model was actually intimated in earlier studies when it was noticed that sequestered β_2-ARs exhibited a reduced phosphorylated state (~0.75 mol/mol stoichiometry) compared to the whole cellular pool of β_2-ARs (~2.1 mol/mol stoichiometry), and that the "light vesicular" fractions (endosomes) were enriched with a GPCR-specific phosphatase (Sibley *et al.*, 1986; Pitcher *et al.*, 1995a). The critical importance of both phosphatase activity and receptor recycling in β_2-AR resensitisation was further demonstrated by the ability of calyculin A, an inhibitor of protein phosphatases, and monesin, an inhibitor of intracellular trafficking, to block receptor resensitisation (Pippig *et al.*, 1995). Sequestration has been reported to be critical for the resensitisation of many other GPCRs including the m3 muscarinic (Edwardson and Szekeres, 1999), neurokinin 1 (Garland *et al.*, 1996), δ-opioid (Hasbi *et al.*, 2000), and endothelin A (Bremnes *et al.*, 2000) receptors.

1.6.10 Receptor downregulation

Receptor downregulation involves a loss in the total cellular complement of a particular GPCR in response to prolonged or repeated agonist stimulation. Downregulation occurs as a consequence of both increased lysosomal degradation of pre-existing receptors and reduced mRNA and protein synthesis. Initial studies with the β_2-AR revealed that long term exposure of cells to agonist resulted in a form of the β_2-AR that was undetectable by radioligand binding but, nonetheless, retained its primary amino acid structure. The undetectable receptors appeared to be retained until agonist was removed, whereupon they became detectable by radioligand binding within a $t_{1/2}$ of about 36 hours in the presence of cycloheximide (Doss *et al.*, 1981). Incubation of DDT1 MF-2 hamster vas deferens cells with β-adrenergic agonists resulted in a time- and concentration-dependent decrease in β-adrenergic receptor mRNA. In downregulated cells, the

addition of an antagonist was able to restore receptor mRNA levels to 90% of the control value within 12 hours. Full recovery of steady-state β_2-AR mRNA was achieved within 60 hrs (Hadcock and Malbon, 1988). Significant levels of mRNA downregulation could also be observed in cells treated with cell permeable analogues of cAMP or by activators of adenylyl cyclase (Bouvier *et al.*, 1989).

Mutational analysis of the human β_2-AR highlighted residues Tyr^{350} and Tyr^{354} as being important in receptor downregulation. This mutation dramatically decreased the ability of the β_2-AR to undergo agonist-induced downregulation. However, the substitution of Tyr^{350} and Tyr^{354} did not affect agonist-induced sequestration of the receptor (Valiquette *et al.*, 1990) suggesting that sequestration is not linked to downregulation. Blocking β_2-AR endocytosis with chemical treatments or by expressing a dominant negative mutant of dynamin could not prevent receptor downregulation indicating that this process may occur at the plasma membrane (Jockers *et al.*, 1999).

Contrary to this, some studies have shown that β_2-AR downregulation is linked with sequestration. Using immunocytochemical techniques to label epitope-tagged β_2-ARs, agonist treatment induced redistribution of the receptors in punctate accumulations within the cells. While the majority of internalised receptors were recycled back to the plasma membrane, a small fraction of the internalised receptors were sorted in endosomes for degradation in lysosomes (von Zastrow and Kobilka, 1992). The development of a β_2-AR conjugated with green fluorescent protein (β_2-AR-GFP) provided the opportunity for more extensive optical analysis of β_2-AR sequestration, downregulation and recycling in cells. Time-dependent colocalisation of β_2-AR-GFP with rhodamine-labeled transferrin and rhodamine-labeled dextran following agonist exposure demonstrated receptor distribution to early endosomes (sequestration) and lysosomes (downregulation) respectively (Kallal *et al.*, 1998). In HEK293 cells, the dynamin-K44A mutant profoundly inhibited agonist-induced internalisation and downregulation of the β_2-AR, suggesting that receptor internalisation was critical for downregulation in these cells. Moreover, a dominant-negative mutant of β-arrestin, β-arrestin-(319-418), also inhibited both agonist-induced receptor internalisation and downregulation illustrating that downregulation of the β_2-AR is in part due to trafficking of the receptor via clathrin coated pits (Gagnon *et al.*, 1998). More recently,

immunofluorescence microscopy has been used to directly visualise the localisation of β_2-ARs with the lysosomal protease cathepsin D following prolonged agonist exposure (Moore *et al.*, 1999).

1.7 Prostaglandin Receptors

1.7.1 Prostaglandins

Prostaglandins (PGs) were initially discovered in the 1930s when von Euler (1934) and others identified a smooth muscle-contracting and vasodepressor activity in seminal fluid as a lipid soluble acid. They called the substance "prostaglandin" because it was believed, erroneously, that it came only from the prostate gland. It was not for a further 20 years before technical advances allowed the purification of the first PGs, PGE_1 and $PGF_{1\alpha}$ (Bergström and Sjövall, 1957) which demonstrated that PGs were in fact a family of lipid compounds of unique structure. Further research showed that the PG's were part of a diverse family, being named alphabetically from PGA_2 to PGH_2, of which PGA_2, PGB_2, and PGC_2 are prone to extraction artefacts (Schneider *et al.*, 1966). PGG_2 and PGH_2 are unstable intermediates in the synthesis of other members of the family (Hamberg and Samuelsson, 1973). PGs are biosynthesised from three fatty acid precursors namely dihomo-γ-linolenic acid, arachidonic acid, and eicosapentaenoic acid, which generate 1-, 2-, and 3-series PGs respectively (van Dorp *et al.*, 1964); the numerals referring to the number of carbon double bonds present. In animals, arachidonic acid is the main precursor and therefore the 2-series PGs are the most abundant. The synthesis of second-series PGs from arichidonate is catalysed by cyclooxygenases which convert arachidonate to PGH_2. In turn, PGH_2 serves as a substrate for cell-specific isomerases and synthases to generate five primary bioactive prostanoids: PGE_2, $PGF_{2\alpha}$, PGD_2, PGI_2, and thromboxane A_2 (TXA_2). By the late 1970s it was becoming evident that prostanoids are capable of mediating a broad array of physiological responses and were becoming under increased scrutiny as possible therapeutic agents and drug targets (Figure 1.9).

Figure 1.9

Diagrammatical representation of the prostanoids.

The chemical structure of the five primary bioactive prostanoid metabolites: PGE_2, PGD_2, $PGF_{2\alpha}$, TXA_2 and PGI_2.

Figure 1.9

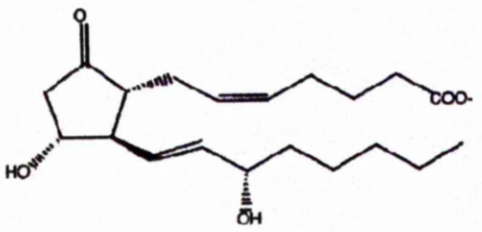

PGE_2

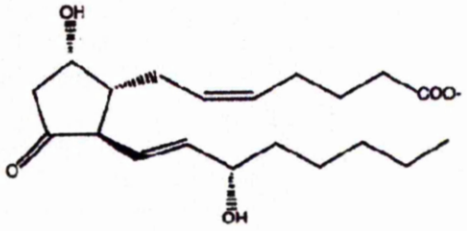

PGD_2

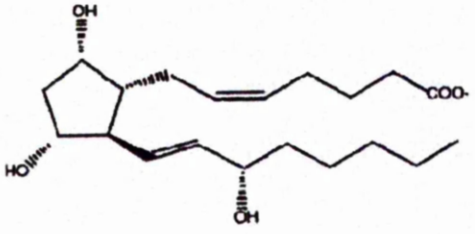

$PGF_{2\alpha}$

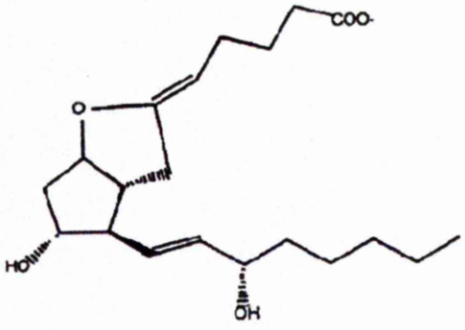

PGI_2

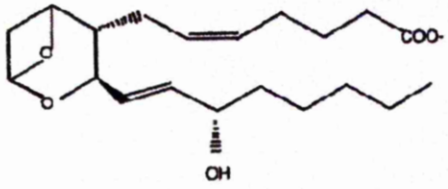

TXA_2

1.7.2 Prostaglandin Receptors

By virtue of their lipid nature, PGs were originally thought to mediate their actions by diffusion across the cell membranes. However, despite this, in the 1970s work began to identify and classify prostanoid receptors in an attempt to rationalise the many and varied actions of prostanoids. Preliminary research demonstrated that both natural and synthetic prostanoids showed different rank orders of agonist activity over a wide range of isolated smooth muscle preparations (Andersen and Ramwell, 1974; Andersen *et al.*, 1980; Gardiner and Collier, 1980). In 1982, on the basis of functional studies with both natural and synthetic agonists, and some antagonists, Kennedy and coworkers outlined a comprehensive classification of receptors (Kennedy *et al.*, 1982; Coleman *et al.*, 1984). The receptors were classified into the DP, EP, FP, IP, and TP receptors which were specific for the five primary prostanoids, PGs D_2, E_2, F_2, I_2, and TXA_2 respectively. From the functional data it was evident that at each receptor, one of the natural ligands was at least one order of magnitude more potent than any of the other four. Further diversity in the prostanoid receptor family has since been uncovered with the discovery of subdivision within the EP receptor family. Four EP receptor subtypes have been identified, termed EP_1, EP_2, EP_3, and EP_4.

The prostanoid receptors belong to the family of GPCRs which include receptors for autacrine, paracrine, and endocrine factors such as tripeptides, pituitary hormones, glycoprotein hormones, opioids and platelet-activating factor. The family overall shares a 20-30% sequence identity, with 65 amino acid residues conserved among the family. Of these residues, 34 are identical across the prostanoid receptor family. Most of these conserved residues lie within the transmembrane regions, although a considerable number of the conserved amino acids is present in the second extracellular loop (Audoly and Breyer, 1997a). Functional analysis has demonstrated that these domains are important in ligand binding. Another characteristic of the prostanoid receptor family is the existence of alternatively spliced variants of the TP, FP, EP_1, and EP_3 receptors. In each instance, the alternative splicing sites are found within the intracellular carboxyl tail of the receptor.

1.7.3 TP receptor

Thromboxane is a potent agonist at the TP receptor mediating platelet aggregation as well as proliferation of smooth muscle cells and vasoconstriction. Upregulation of thromboxane biosynthesis has been suggested in cardiovascular diseases including acute myocardial ischaemia (Oates *et al.*, 1988), heart failure (Castellani *et al.*, 1997), and renal disorders (Spurney *et al.*, 1992). Thus, antagonists of thromboxane have potential therapeutic benefits.

The thromboxane receptor, TP, was the first eicosanoid receptor to be cloned and was found to encode a 343 amino acid protein (Hirata *et al.*, 1994). Two alternatively spliced variants of the TP receptor have since been identified and named TPα and TPβ (Raychowdhury *et al.*, 1994). The original TP receptor cloned was termed TPα and the subsequent 407 amino acid variant, which possesses a longer intracellular tail, was designated TPβ.

Mutational analysis of the TP receptor indicated that Trp^{299} in TMVII was a critical determinant of ligand binding selectivity. A W299L receptor mutant bound the synthetic agonists I-BOP and U-46619 but was unable to bind the antagonist SQ29548 (Funk *et al.*, 1993). Ligand binding and receptor signalling were abolished by mutation of the universally conserved Arg^{295} in TMVII (Funk *et al.*, 1993), an observation that has been reported for other members of the prostanoid family (Audoly and Breyer, 1997b). The extracellular loops have also been implicated in ligand binding as mutation of cysteine residues in these regions impaired ligand interaction with the receptor, suggesting that there are essential disulphide bonds in the receptor structure (D'Angelo *et al.*, 1996).

Thromboxane receptors couple primarily to the G_q class of G proteins, activating the Ca^{2+}/DAG effector signalling. More recently it has been shown that the receptor can also activate the G_{11}, G_{12}, and G_{13} proteins (Kinsella *et al.*, 1997; Becker *et al.*, 1999; Offermanns *et al.*, 1994). Although both splice variants can bind ligands and couple to G proteins equally well, the TPβ variant has been shown to exhibit an increased ability to internalise compared to the α variant (Parent *et al.*, 1999). In HEK293 cells, the TPβ

receptor was observed to traffic via a β-arrestin-, GRK- and dynamin-dependent pathway (Parent *et al.*, 1999) suggesting that the longer tail of the TPβ receptor is a target for phosphorylation and arrestin binding, and thus acts as a regulator of internalisation. The TPα splice variant, but not TPβ, can undergo prostacyclin-activated PKA phosphorylation, indicating that the TPα variant may be of importance in the maintenance of thromboxane/prostacyclin-mediated vascular homeostasis (Walsh *et al.*, 2000).

1.7.4 FP receptor

$PGF_{2\alpha}$ receptor cDNA was cloned from a human kidney cDNA library (Abramovitz *et al.*, 1994) and it encodes a 359 amino acid protein. Alternative spliced variants of the ovine FP receptor were identified which differ only at their C-terminal tails. The FP_A receptor has an additional 46 amino acid residues after the splice site, whereas the FP_B receptor has only one residue distal to the splice junction. Mutation of His^{81} in TMII of the rat FP receptor was shown to abrogate ligand binding. It was suggested that an interaction between His^{81} and the conserved Arg residue in TMVII is responsible for ligand binding (Rehwald *et al.*, 1999).

FP receptor expression in corpora lutea has been shown to be crucial in parturition (Sugimoto *et al.*, 1997) as determined with knockout mice lacking FP receptor expression. The human FP receptor, when expressed in oocytes, was found to elicit a Ca^{2+}-dependent Cl^- ion current, thus demonstrating that FP receptor signalling mediates increases in intracellular Ca^{2+} concentration (Abramovitz *et al.*, 1994). Ovine FP receptors have also been observed to effect phosphoinositide turnover and Rho activation (Pierce *et al.*, 1999). The different splice variants of the ovine FP receptor exhibit different levels of agonist-mediated phosphorylation. The longer form has multiple PKC phosphorylation sites, and has been observed to undergo PKC-mediated phosphorylation in cell culture (Fujino *et al.*, 2000). Differential phosphorylation of the FP receptor variants has been suggested to induce desensitisation of the longer form but not of the FP_B variant.

1.7.5 EP_1 receptor

A 402 amino acid protein is encoded by the cloned human EP_1 receptor cDNA (Funk *et al.*, 1993). An alternative variant of the rat EP_1 receptor has been reported which comprises an alternative 49 amino acids from the middle of TMVI to the carboxyl terminus (Okuda-Ashitaka *et al.*, 1996). The human receptor signals via the $G_{q/11}$ class of G protein, stimulating IP_3 generation and increasing the concentration of intracellular Ca^{2+} ions. The variant rat EP_1 receptor does not appear to signal although it is still capable of binding ligand (Okuda-Ashitaka *et al.*, 1996). It has been suggested that the short EP_1 variant may inhibit the signalling of the rat EP_1 receptor as Ca^{2+} mobilisation induced by the longer EP_1 receptor was attenuated by the shorter variant when they were coexpressed in cells. Antagonists of the EP_1 receptor appear to have analgesic properties. Therefore agents which block EP_1 receptor activation would provide pain relief without producing the side effects which are associated with cyclooxygenase inhibitor drugs (Hallinan *et al.*, 1994).

1.7.6 EP_2 receptor

The human EP_2 receptor cDNA encodes a 358 amino acid polypeptide which couples to G_s. (Regan *et al.*, 1994a). EP_2 receptor expression in the uterus has been linked to embryonic implantation (Hizaki *et al.*, 1999) and in the lung it is suggested to play an important role in bronchodilation (Pavord *et al.*, 1991).

The EP_2 receptor shares the greatest sequence homology with the DP and IP receptor subtypes. Mutagenesis studies of the receptor revealed that Leu^{384} in TMVII is critical in ligand binding selectivity as a L384Y receptor mutant gained the ability to bind the IP selective agonist, iloprost (Kedzie *et al.*, 1998). Ligand binding was abolished by mutation of an adjacent conserved arginine residue, Arg^{302}, further highlighting the importance of this region in ligand binding for the prostanoid receptor family. Pharmacological analysis of the receptor demonstrated its inability to undergo short-term agonist induced desensitisation. It was suggested the short C-tail of the EP_2 receptor is a poor substrate for kinase phosphorylation thereby reducing that rate of receptor desensitisation (Nishigaki *et al.*, 1996).

1.7.7 EP_3 receptor

A unique feature of this prostanoid receptor family member is the existence of multiple alternative spliced forms which differ at their carboxyl tails (Schmid *et al.*, 1995). The splice variants encode proteins of between 40 and 45 kDa (Regan *et al.*, 1994b) which bind PGE_2 with similar affinity. Mutagenesis studies on the conserved arginine, Arg^{329}, in the EP_3 receptor have proposed that there is a non-ionic interaction between the C-1 carboxylate of the prostanoid and the conserved residue (Audoly and Breyer, 1997a,b). The conserved sequence in the second extracellular loop has also been shown to be important in ligand binding properties of the EP_3 receptor. A P200S substitution in this region led to a reduction in the binding selectivity for prostanoid agonists (Audoly and Breyer, 1997a).

The EP_3 splice variants exhibit differences in receptor phosphorylation and desensitisation, intracellular trafficking, and G protein coupling. The variants generally inhibit cAMP production through coupling to G_i, though signalling through G_s and Ca^{2+} release has also been observed and appears to be mediated by the different C-tails (Namba *et al.*, 1993). Rho activation via the EP_3 receptors has also been suggested recently. Activation of the bovine EP_3 in PC12 cells caused neurite retraction which could be blocked by tyrosine kinase inhibitors upstream and downstream of Rho (Aoki *et al.*, 1999).

1.7.8 EP_4 receptor

The human EP_4 receptor cDNA encodes a 488 amino acid polypeptide (Bastien *et al.*, 1994). As with the EP_2 receptor, the EP_4 couples to G_s. The EP_4 receptor is widely expressed and its activation has been reported to be important in inducing vasodilation of blood vessels (Coleman *et al.*, 1994). It has also been suggested to function in the closure of the pulmonary ductus arteriosus in new-borns as demonstrated by studies of knockout mice lacking EP_4 receptor gene expression (Segi *et al.*, 1998).

Unlike the EP_2 receptor, the EP_4 receptor has a long (156 amino acids) C-tail which contains 38 serine and threonine sites which are potential phosphorylation targets. As mentioned above, the EP_2 receptor, which has a short C-tail, is insensitive to agonist

mediated desensitisation whereas the EP_4 receptor rapidly undergoes phosphorylation and G protein uncoupling (Nishigaki *et al.*, 1996). Deletion studies identified a stretch of six serines in the tail which are thought to be sites of kinase action and thus be important in receptor desensitisation (Bastepe and Ashby, 1999). The two receptors G_s-coupled EP receptors, EP_2 and EP_4, may therefore mediate different physiological responses in the presence of agonist.

1.7.9 DP receptor

The human DP receptor is the most recent prostanoid receptor to be cloned and it encodes a 359 amino acid protein that binds PGD_2 with high affinity (Boie *et al.*, 1995). PGD_2 is involved in hypersensitivity reactions, being the major prostanoid released from mast cells after IgE challenge (Lewis *et al.*, 1982). It has also been shown to be an important regulator of the sleep-wake cycle (it induces sleep) and body temperature (it produces hypothermia) in rats (Urade and Hayaishi, 1999; Sri Kantha *et al.*, 1994). In peripheral tissues, PGD_2 has been show to affect vascular tone, as well as inhibiting platelet aggregation (Giles *et al.*, 1989). The receptor couples to G_s, stimulating adenylyl cyclase. It shares the most sequence homology with the IP receptor. DP/IP receptor chimeras in which the first and second intracellular loops of the IP receptor containing the third transmembrane domain were replaced with the corresponding regions of the DP receptor gained the ability to bind PGD_2, thus highlighting the role of the TMIII domain in conferring the selective binding of PGD_2 to the DP receptor (Kobayashi *et al.*, 2000).

1.7.10 IP receptor

The human IP (prostacyclin) receptor, which is the focus of this study, was cloned in 1994 (Boie *et al.*, 1994) and encodes a 386 amino acid protein with a predicted molecular weight of 41 kDa (Figure 1.10). IP receptor mRNA is predominantly expressed in neurons of the dorsal root ganglia and vascular tissue including aorta, pulmonary artery, and renal afferent arterioles (Oida *et al.*, 1995).

Ligand binding studies of the IP receptor using stable analogues of PGI_2 have shown that the most selective agonist of the IP receptor is iloprost. Displacement binding

Figure 1.10

The human prostacyclin receptor.

The primary structure of the human IP receptor and its predicted configuration in the membrane. Figure adapted from Smyth *et al.*, 1996.

Figure 1.10

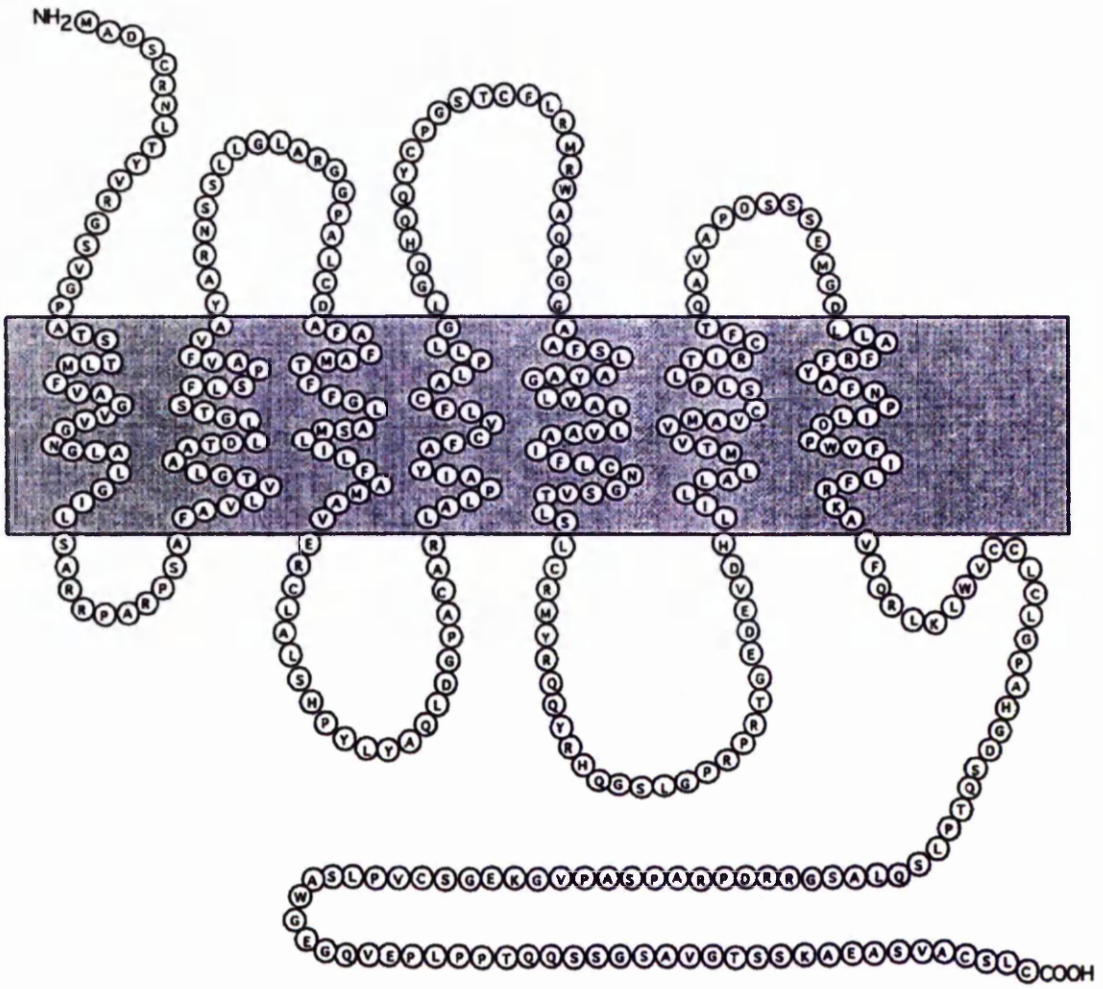

studies have produced a rank order of agonist potencies at the IP receptor as iloprost ≥ cicaprost > carbacyclin > PGE_2 > > $PGF_{2\alpha}$, PGD_2. Of the prostanoid receptor family, the IP receptor is the least discriminating in terms of ligand binding selectivity, being capable of binding PGE_1 analogues with high affinity. The receptor, however, binds PGE_2 analogues with much lower affinity. Using IP/DP receptor chimeras in which IP receptor residues spanning from TMVI to the carboxyl terminus were replaced with the corresponding domains of the DP receptor, an increased PGE_2 binding was observed while the binding of iloprost and PGE_1 remained unaltered. Thus, TM regions VI and VII determine the specificity of PGE_1 binding over PGE_2 (Kobayashi *et al.* 2000). The generation of further IP/DP receptor chimeras identified the IP receptor's TMI and first extracellular loop as important determinants in the binding selectivity of the prostanoid ring between the two receptors (Kobayashi *et al.* 2000).

Most studies suggest that the activated IP receptor signals through increased cAMP. Coexpression of the cloned IP receptor in *Xenopus* oocytes with the cystic fibrosis transmembrane conductance regulator (cAMP-activated Cl^- ion channel) and subsequent challenge with iloprost induced a specific inward Cl^- ion current, demonstrating that the receptor couples to cAMP production (Boie *et al.*, 1994). IP receptors couple to adenylyl cyclase via G_s as originally demonstrated in mouse mastocytoma P-815 cells where the dissociation of bound [^{3}H] iloprost from the cell membranes was specifically enhanced by guanine nucleotides. Furthermore, iloprost dose-dependently enhanced the activity of adenylyl cyclase in a GTP-dependent manner (Hashimoto *et al.*, 1990). Many other functional studies of the IP receptor have confirmed its ability to activate G_s (Nilius *et al.*, 2000; Lawler *et al.*, 2001; Smyth *et al.*, 1996, 1998, 2000; Hayes *et al.*, 1999).

At relatively high concentrations of agonist, the IP receptor has been shown to stimulate phosphoinositide turnover (Namba *et al.*, 1994) in transfected CHO cells. A 10,000-fold higher agonist concentration was required to stimulate PIP_2 hydrolysis in the cells compared to the concentrations required to activate adenylyl cyclase. PGI_2 analogues have also been shown to evoke smooth muscle contraction via increases in intracellular Ca^{2+} ion concentrations (Lawrence *et al.*, 1992). Furthermore, iloprost-stimulated increases in intracellular Ca^{2+} ion concentration in the human erythroleukaemia cell line

were mediated by a pertussis-toxin sensitive G protein (Schwaner *et al.*, 1992). HEK293 cells stably expressing IP receptors also exhibited substantial agonist-mediated inositol phosphate production (Smyth *et al.*, 1996, 1998, 2000) but this may be an artefact of the transfection system. More recently, it has been reported that murine IP receptors can switch their coupling from G_s to G_i and G_q upon agonist-induced PKA phosphorylation of the receptor (Lawler *et al.*, 2001).

A feature of the IP receptor that may be unique among GPCRs is that it is isoprenylated (Hayes *et al.*, 1999). Isoprenylation occurs as a post-translational lipid modification to the first cysteine residue in the CSLC motif at the C-terminal sequence of the receptor. Disruption of this motif resulted in a receptor with defects in coupling to adenylyl cyclase and phospholipase C, indicating that lipid modification of the receptor is crucial for efficient signal transduction. In addition, a number of studies have confirmed that the IP receptor undergoes agonist induced phosphorylation, internalisation and downregulation in human platelets, NG108-15 neuronal cells, and HEK293 cell lines (Smyth *et al.*, 1998, 2000; Leigh and MacDermot, 1985; Krane *et al.*, 1994; Giovanazzi *et al.*, 1997).

Prostacyclin plays a key role in many physiological processes and pathological states. Prostacyclin is mainly produced by the vascular endothelium where it acts as a potent inhibitor of platelet aggregation and as a vasodilator (Vane *et al.*, 1995). Thus, prostacyclin causes relaxation of arterial smooth muscle and inhibition of platelet aggregation, degranulation and shape change and is, therefore, thought to be important in maintaining vascular homeostasis. In unstable angina, prostacyclin synthesis is increased during ischaemic attack to function as a homeostatic regulator of platelet-vascular interactions in atherosclerotic plaque ruptures. Prostacyclin has also been reported to confer a cytoprotective effect against tissue injury during acute myocardial ischaemia or in response to hypoxia (Sakai *et al.*, 1990). The actions of prostacyclin generally counteract those of TXA_2 and thus the relative levels of these two prostanoids in the circulation are important in the local control of vascular homeostasis. Imbalances in TXA_2 or prostacyclin levels have been reported to be a major contributing factor in the development of a number of cardiovascular disorders including thrombosis, myocardial infarction, unstable angina, stroke, and atherosclerosis (Vane *et al.*, 1995; Lefer *et al.*, 1990; Rasmanis *et al.*, 1995). In addition to its central role in the

cardiovascular system, prostacyclin may be important in the regulation of renal blood flow (Negishi et al., 1995); it also acts as a negative feedback regulator of histamine release from mast cells (Holgate *et al.*, 1980) and as a lipolytic agent in adipocytes (Chatzipanteli *et al.*, 1992). Moreover, transgenic mice lacking IP receptor expression exhibited reduced pain perception, thus establishing prostacyclin as a mediator of nociception (Murata *et al.*, 1997). The development of selective PGI_2 mimetics or antagonists may therefore serve as possible therapeutic agents in certain disease states.

1.8 Research Objectives

The aims of this project were to study the functional significance of the carboxyl terminal domain of the prostacyclin receptor in the following processes:

- Sequestration
- Desensitisation
- Resensitisation

Receptor chimera models were used to investigate these events.

Chapter 2

Materials and Methods

2.1 Materials

All reagents used were of the highest grade possible and were obtained from the following suppliers.

2.1.1 General reagents

BDH, Lutterworth, Leicestershire, UK

Sodium di-hydrogen orthophosphate, potassium hydroxide, potassium chloride, glacial acetic acid, trichloroacetic acid, ethanol, methanol, isopropanol, chloroform, microscope slides, 22mm coverslips.

Calbiochem, CN Biosciences UK, Nottingham, UK

H89, GF109203X, geneticin sulphate (G418).

Duchefa, Haarlem, The Netherlands

Yeast extract, tryptone, agar.

Fisher Scientific UK Ltd, Loughborough, Leicestershire, UK

Ammonium sulphate, glycine, HEPES, sucrose, SDS, potassium acetate, potassium di-hydrogen orthophosphate, calcium chloride, HCl, sodium bicarbonate, manganese chloride, mercaptoethanol.

Interactiva, Ulm, Germany

Oligonucleotides for PCR reactions.

Invitrogen BV, Groningen, The Netherlands

NuPage® Novex pre-cast bis-tris gels, XCell Surelock™ mini-cell gel tank, XCell II™ blot module, MOPS running buffer, MES running buffer.

Konica Europe, Hohenbrunn, Germany

X-ray film

Molecular Probes, Eugene, Oregon, USA

Texas Red® transferrin

Pierce, Perbio Science UK Ltd., Tattenhall, Cheshire, UK

Supersignal® west pico chemiluminescent substrate, EZ-Link™ Biotin-LC-Hydrazide, Streptavidin-HRP conjugate.

Promega UK Ltd., Southampton, UK

Restriction endonucleases, pfu polymerase, calf intestinal alkaline phosphatase, DNA purification kits- Wizard™ Plus SV Minipreps and Wizard™ Plus SV Maxipreps systems.

Quiagen, Crawley West Sussex, UK

QIAquick gel extraction kit.

Roche Diagnostics Ltd., Lewes, East Sussex, UK

Complete™ mini-protease inhibitor cocktail tablets, 1kb DNA ladder, T4 DNA ligase, bovine serum albumin (fraction V).

Sigma-Aldrich Company Ltd., Poole, Dorset, UK

Alumina, agarose, gelatin (porcine, type A), magnesium chloride, sodium chloride, sodium hydroxide, sodium acetate, DTT, di-sodium pyrophosphate, di-sodium orthophosphate, tris, Dowex-50W, EDTA, bromophenol blue, deoxycholic acid, rubidium chloride, imidazole, Triton X-100, DMSO, glycerol, Tween 20, ethylene glycol, paraformaldehyde, ampicillin, DMEM (powder), Protein G-Sepharose, ethidium bromide, ATP, cAMP, IBMX, concanavalin A, PMA, gelatin (bovine, 2% solution), bovine albumin (essentially globulin-free), MOPS, Ponceau S, forskolin, mineral oil, sodium tartrate, sodium m-periodate.

Whatman International Ltd., Maidstone, UK

3mm-filter paper, chromatography paper, GF/C Glass fibre filters

2.1.2 Tissue culture plastic ware & reagents

American Tissue Culture Collection, Rockville, USA

HEK293 cells

Bibby Sterilin Ltd., Stone, Staffordshire, UK.

15ml and 50ml centrifuge tubes

Costar, Cambridge, MA., USA

5ml, 10ml, and 25ml pipettes, 75cm^2 tissue culture flasks, 25cm^2 tissue culture flasks, 60mm and 100mm dishes, 6, 12, 24, and 96 well plates, cryovials, cell scrapers.

Gibco BRL, Life Technologies Ltd., Paisley, UK

Lipofectamine™ transfection reagent, OPTIMEM-1, L-glutamine (200mM), NBCS, DMEM without sodium pyruvate.

Sigma-Aldrich Company Ltd., Poole, Dorset, UK

DMEM, 0.25% Trypsin-EDTA, Poly-D-Lysine.

2.1.3 Radiochemicals

Amersham Pharmacia Biotech UK Ltd., Little Chalfont, Buckinghamshire, UK

[2-^{3}H] Adenine (25 Ci/mmol)

[^{3}H] Iloprost (17 Ci/mmol) (supplied with 2mg unlabelled compound)

NEN™ Life Science Products, Hounslow, UK

[^{32}P] Orthophosphoric acid (285.5Ci/mg, 10mCi/ml)

2.1.4 Antisera

Amersham Pharmacia Biotech UK Ltd., Little Chalfont, Buckinghamshire, UK

Goat anti-mouse IgG-HRP conjugate

Donkey anti-rabbit IgG-HRP conjugate

Donkey anti-sheep IgG-HRP conjugate

Molecular Probes, Eugene, Oregon, USA

Alexa® 594 goat anti-mouse IgG conjugate

Anti-β-arrestin 1 monoclonal mouse IgG

Roche Diagnostics Ltd., Lewes, East Sussex, UK

12CA5 monoclonal mouse IgG, binds to haemagglutinin (HA) epitope-tagged proteins.

Sigma-Aldrich Company Ltd., Poole, Dorset, UK

Anti-Flag® M2 monoclonal mouse IgG, binds to proteins which contain a FLAG epitope.

A sheep polyclonal anti-GFP antibody, which recognises proteins that are GFP-tagged, was generated in house.

2.2 Buffers

2.2.1 General buffers

Phosphate Buffered Saline (10x)

137mM NaCl, 2.7mM KCl, 1.5 mM KH_2PO_4, 10.2mM Na_2HPO_4, pH 7.4

This was diluted 1:10 to make a 1x stock which was stored at 4°C.

Tris-EDTA (TE) Buffer

10mM Tris, 0.1mM EDTA, pH 7.5

This was stored at room temperature.

Laemmli Buffer (2x)

0.4M DTT, 0.17M SDS, 50mM Tris, 5M Urea, 0.01%(w/v) Bromophenol Blue.

This was stored in aliquots at -20°C.

2.2.2 Molecular Biology Solutions

TAE buffer (50x)

For 500mls:

40mM Tris	121g
1mM EDTA	50mls of 0.5M (pH 8) stock
Glacial acetic acid	28.55ml

This was diluted 1:50 prior to use.

DNA Loading Buffer

For 10ml:

Bromophenol Blue (2%)	1.25ml
Sucrose	4g

This was dissolved in water and stored in aliquots at -20°C.

Liquid Broth (LB)

For 1 litre:

Yeast Extract	5g
Tryptone	10g
NaCl	10g

This was dissolved in deionised water, pH adjusted to 7, and then sterilised by autoclaving at 126°C.

2.3 Molecular Biology Protocols

2.3.1 LB ampicillin agar plates

This has the same composition as LB but with 1.5% (w/v) agar added. After autoclaving, it was left to cool before ampicillin was added to a final concentration of 50μg/ml. The liquid agar was poured into 10cm diameter petri dishes, and allowed to solidify before storing at 4°C. LB agar plates can be stored for up to 3 weeks without any loss of antibiotic activity.

2.3.2 Preparation of competent bacteria

The uptake and expression of foreign DNA into *E. Coli* is known as transformation. Before transformation can take place, the *E. Coli* strain, which in this case was DH5α, has to be made receptive, or competent, for the uptake and expression of the pcDNA3.1 (+) vector containing a particular cDNA insert. Competent *E.Coli* cells are made using the following procedure.

Solution 1 (for 100ml)

1M Potassium acetate	3ml
1M $RbCl_2$	1ml
1M $CaCl_2$	1ml
1M $MnCl_2$	5ml
80% (w/v) glycerol	18.75ml

This was pH adjusted to 5.8 with 100mM acetic acid and made up to a final volume of 100ml with deionised water. The solution was filter-sterilised and stored at 4°C.

Solution 2 (for 40ml)

100mM MOPS pH 6.5	4ml
1M $CaCl_2$	3ml
1M $RuCl_2$	0.4ml
80% (w/v) glycerol	7.5ml

This was pH adjusted to 6.5 with HCl and made up to a final volume of 40ml with deionised water. The solution was filter-sterilised and stored at 4°C.

DH5α cells were streaked out on a minimal agar plate (no antibiotics) and grown overnight at 37°C. A single colony from the plate was chosen and cultured overnight in 5ml of LB at 37°C. The 5ml culture was then added to 100ml fresh LB and grown until the OD_{550} was 0.48. The culture was chilled on ice for 5 min and then spun at 3000rpm for 10 min at 4°C in 50ml sterile tubes. The pellets were resuspended in 20ml of solution 1, then chilled on ice for 5 min and spun as before. The pellets were then resuspended in 2ml of solution 2 and chilled on ice for a further 15 min. Cells were aliquoted and stored at -80°C.

2.3.3 Transformation of competent bacterial cells with plasmid DNA

Between 10-50ng of plasmid DNA was incubated with 50µl of competent bacterial cells on ice for 20 min. The mix was then heat shocked for 90 seconds at 42°C and placed back on ice for a further 2 min. 1ml of LB was added and the cells were allowed to recover by incubation at 37°C for 1 hour in a shaking incubator. 200µl of this mix was spread out on a LB agar ampicillin plate. Plates were then incubated overnight at 37°C. Colonies picked from the plates were cultured in 5ml LB containing 50µg/ml ampicillin.

2.3.4 Plasmid DNA preparation

Plasmid DNA was purified from bacterial cultures using the Promega Wizard™ Plus SV Minipreps and Wizard™ Plus SV Maxipreps systems. For minipreps, a 5ml culture of transformed bacterial cell was first set up. 3ml of the culture was spun down and the cell pellet was resuspended in resuspension solution (50mM Tris-HCl pH 7.5, 10mM EDTA, 100ug/ml RNase A), followed by lysis with lysis solution (0.2M NaOH, 1% SDS). Neutralising solution (4.09M guanidine hydrochloride, 0.76M potassium acetate, 2.12M glacial acetic acid, pH 4.2) was added to the lysate to precipitate the bacterial chromosomal DNA. This was spun down and the resulting supernatant was transferred to a DNA purification column. The column was washed twice with column wash (60mM potassium acetate, 10mM Tris-HCl pH 7.5, 60% ethanol) and the DNA was eluted from the column with sterile water. From each column a 100µl plasmid DNA solution with a concentration of 0.1-0.4µg/µl was yielded. For maxipreps, a similar method of purification was used but on a much larger scale. 500ml cultures were used to generate approximately 1ml of plasmid DNA at a concentration between 0.5-2µg/µl.

2.3.5 Quantification of DNA

The concentration of plasmid DNA generated from maxipreps and minipreps was determined by measurement of the absorbance at 260nm of a 1:50 dilution of the DNA sample. An A_{260} value of 1 unit was assumed to be equivalent to 50µg/ml of double stranded DNA. The A_{280} value of the solution was also measured to assess the purity of the DNA solution. A DNA solution with an A_{260}/A_{280} ratio of between 1.7 and 2.0 was considered pure enough for use.

2.3.6 Digestion of DNA with restriction endonucleases

Restriction digests of DNA were carried out for the subcloning of DNA fragments into plasmid vectors. The digests were set up using the conditions recommended by the manufacturer. In brief, 1μg of DNA was digested in 10μl of a buffered solution containing 1 unit of the appropriate enzyme for a minimum of 2 hours at 37°C.

2.3.7 DNA gel electrophoresis

Digested DNA fragments were separated and analysed using agarose gel electrophoresis. Samples were mixed with 6x loading buffer to make a final 1x concentration. DNA fragments between 0.4 and 5kb were separated using 1% (w/v) agarose gels containing TAE buffer and 2.5mg/ml ethidium bromide. The gels were run at 75mA in horizontal gel tanks containing TAE buffer. Ultraviolet light was used to analyse the separated DNA fragments on the gels. The size of each DNA fragment was calculated by comparison with a 1kb ladder.

2.3.8 DNA purification from agarose gels

Purification of DNA fragments from agarose gels was carried out using the Quiagen QIAquick gel extraction kit. DNA fragments were excised from the gel using a sterile razorblade and dissolved in QIAquick buffer QG. One volume of isopropanol was then added and the solution was loaded onto a QIAquick column. The column was then washed with an ethanol solution (PE) and the DNA was eluted from the column using sterile water.

2.3.9 Alkaline phosphatase treatment of plasmid vectors

Alkaline phosphatase treatment of cut plasmid vectors was carried out to minimise re-ligation of the vector with itself. The 5′ phosphate group was removed by incubation of 200ng of digested vector with 2 units of the enzyme in the appropriate buffered conditions for 2 hours at 37°C. The plasmid was isolated from the reaction mixture by agarose gel electrophoresis and gel extraction as described previously.

2.3.10 DNA ligations

Ligations of vector DNA with a desired cDNA insert(s) were performed using T4 DNA ligase. For each ligation, a vector:insert ratio of 1:2 was used. Reactions were performed

in a total volume of 10µl containing enzyme buffer with 1 unit of T4 ligase and incubated at 4°C for at least 16 hours. Ligation mixtures were used for transformation reactions as described in 2.3.2.

2.3.11 Polymerase chain reaction

PCR reactions were carried out in a total volume of 50µl containing 20ng of DNA template, 0.2mM dNTPs (dATP, dCTP, dGTP, dTTP), 25pmol of sense and antisense oligonucleotide primers, 1x thermophilic buffer, and 2 units of Pfu polymerase. Samples were overlaid with mineral oil to prevent evaporation and the reactions were carried out on a Hybaid Omnigene thermal cycler. The enzyme was added after the reaction mixtures were given an initial heat to 95°C for 5 min.

PCR Cycles:

Denaturation	Annealing	Extension	Cycles
95°C, 1 min	50-60°C, 1 min	72°C, 2 min	30
95°C, 1 min	50-60°C, 1 min	72°C, 5 min	1

The annealing temperatures were empirically determined and were set at 50, 55, or 60°C.

2.4 Construction of chimeric GPCR fusion cDNA

2.4.1 FLAG-IP-GFP

A *Bam*HI-FLAG-IP-GFP-*Eco*RI cDNA had been generated previously in the laboratory and was used as template to synthesise the N terminal-TMVII DNA fragment for construction of the chimeric receptor fusions.

2.4.2 FLAG-IP-TRH-GFP

FLAG-IP-GFP in pcDNA3 was amplified from the N-terminal FLAG region to the end of the seventh transmembrane encoding region (N-TMVII). This was done using the following primers:

Sense 5′-AAGGATCCGCCACCATG(GACTACAAGGACGACGATGATAAG)-GCGGATTCGTGCAGGAACC-3′, where the *Bam*HI site is underlined and the FLAG epitope, which was inserted after the initiating methionine, is in parenthesis.

Antisense 5′-ATAGAATTCCCTTGCGGAAAAGGATGAAGACC-3′, where the *Eco*RI site is underlined.

Wild type TRH-GFP, which had been generated previously in the laboratory, was used a template to PCR the sequence encoding the tail of TRH receptor with GFP linked at the carboxyl terminus. The primers used were:

Sense 5′-AGGGAATTCTATACAACCTCATGTCTCAGAAGTTTC-3′, where the *Eco*RI site is underlined.

Antisense 5′-GCTATCTAGAG(TCA)AAGCTTCTCCTGTTTGGCAGTCAAA-3′, where the *Xba*I site is underlined, followed by the stop codon in parenthesis.

The *Bam*HI-FLAG-IP (N-TMVII)-*Eco*RI PCR product and the *Eco*RI-TRH (C-tail)-GFP-*Xba*I fragment were digested with the appropriate restriction enzymes and ligated into pcDNA3.1(+) to generate FLAG-IP-TRH-GFP.

2.4.3 FLAG-IP-β_2-GFP

The N-TMVII fragment of IP-GFP was generated in the same way as in the construction of FLAG-IP-TRH-GFP.

Wild type β_2-AR-GFP, which was a kind gift from GlaxoSmithKline, Stevenage, was used a template to PCR the sequence encoding the β_2-AR tail linked to GFP. The primers used were:

Sense 5′-AGGGAATTCTATACAACCTCATGTCTCAGAAGTTTC-3′, where the *Eco*RI site is underlined.

Antisense 5’-GCTCTAGAG(TTA)CTTGTACAGCTC-3′, where the *Xba*I site is underlined, followed by the stop codon in parenthesis.

The *Bam*HI-FLAG-IP (N-TMVII)-*Eco*RI PCR product and the *Eco*RI-β_2-AR (C-tail)-GFP-*Xba*I fragment were digested with the appropriate restriction enzymes and ligated into pcDNA3.1 (+) to generate FLAG-IP-β_2-GFP.

2.4.4 HA-IP

FLAG-IP-GFP was used as a template to generate a full-length IP receptor construct with an HA epitope tag at the amino terminus. The primers used were:

Sense 5′-TTGGATCCAAAATG(TATCCCTACGACGTCCCCGATTATGCG)G-CGGATTCGTGCAGG-3′, where the *Bam*HI site is underlined and the HA epitope, which follows the initiating methionine, is in parenthesis.

Antisense 5′-GCTCTAGAT(TCA)GCAGAGGGAGCAGGCGACGCTGGC-3′, where the *Xba*I site is underlined, followed by the stop codon in parenthesis. The fragment was digested with the restriction enzymes and subcloned into pcDNA3.1 (+).

2.4.5 HA-IP-TRH

FLAG-IP-TRH-GFP in pcDNA3.1 (+) was used as a template to amplify the region encoding the amino terminus to the end of the TRH carboxyl tail. The sense primer, which was used to change the amino tag from FLAG to HA, was the same as used in the construction of the HA-IP sequence. The antisense primer introduced a stop codon at the end of the TRH tail coding sequence followed by a *Xba*I site.

Antisense 5′-GCTCTAGAGC(TCA)TATTTTCTCCTGTTTGGCAGTCAAAGA-ATAT-3′, where the *Xba*I site is underlined, followed by the stop codon in parenthesis. The fragment was digested with *Bam*HI and *Xba*I restriction enzymes and subcloned into pcDNA3.1 (+).

2.4.6 HA-IP-β_2

FLAG-IP-β_2-GFP in pcDNA3.1 (+) was used as a template to generate the fragment encoding the sequence from the amino terminus to the last residue of the β_2-AR carboxyl tail. The sense primer that was used to change the epitope tag from FLAG to HA was the same as used in the HA-IP and HA-IP-TRH PCR reactions. The antisense primer created a stop codon at the end of the β_2-AR tail coding sequence with a *Xba*I site following it.

Antisense 5′-CGTCTAGAT(TTA)CAGCAGTGAGTCATTTGTACTACAATTC-3′, where the *Xba*I site is underlined and the stop codon in parenthesis. The PCR fragment was digested with *Bam*HI and *Xba*I restriction enzymes and subcloned into pcDNA3.1 (+).

The Department of Genetics, University of Glasgow, sequenced all constructs generated before they were used for experimental analysis.

2.5 Routine Cell Culture

2.5.1 Cell growth

The primary cell line used in this study was Human Embryonic Kidney (HEK293) cells. It was grown in monolayers in 75cm^2 flasks in Dulbecco's Modified Eagle Medium (DMEM) supplemented with 2mM L-glutamine and 10% Newborn Calf Serum (NBCS). The flasks were incubated in a humidified atmosphere of 95% air/5% CO_2 at 37°C.

2.5.2 Passage of cells

Confluent flasks of cells were passaged using a sterile 0.25% trypsin-EDTA solution. Growth medium was removed from the cells and 2ml of the trypsin solution was added. After all the cells had detached from the surface of the flask, 8ml of fresh medium was added and gently mixed to resuspend the cells. The cell suspension was split into flasks and dishes as required.

2.5.3 Coating plates with poly-D-lysine

50mg of poly-D-lysine was diluted with 50ml of sterile water to make a 1mg/ml stock solution. Tissue culture plates and coverslips were coated with a 1:10 dilution of the stock solution for 10 min. The solution was then removed and plates were left to dry for 20 min before cells were added.

2.5.4 Transient transfections

Transfection of plasmid DNA into HEK293 cells was performed using Lipofectamine™ according to manufacturer's instructions.

For transfection of 10cm dishes, cells were grown to 60-80% confluency and 10μg of DNA was used for each dish. A typical transfection was as follows:

	Tube 1	Tube 2
DNA	10μg	-
Optimem-1	200μl	190μl
Lipofectamine™	-	10μl

The DNA mix was incubated with the Lipofectamine™ mix for 30 min at room temperature and then 5ml of Optimem-1 was added to the complex. The cells were washed twice with Optimem-1 and the complex was added gently to the cells. Following an incubation period of 4-5 hours, 10ml of DMEM containing 10% NBCS was added and left overnight. The following day, the medium on the dish was replaced with fresh DMEM/NBCS and incubated for a further 24 or 48 hours before the cells were harvested or assayed.

For transfection of cells on coverslips in 6 well plates, the same protocol was followed except the amount of DNA used for each transfection was 1μg/well. For transfection of one coverslip the following mixes were prepared:

	Tube 1	Tube 2
DNA	1μg	-
Optimem-1	35μl	60μl
Lipofectamine™	-	3.5μl

The two tubes were mixed and incubated as described previously. 1ml of Optimem-1 was added to the incubation and then added to the appropriate well. After 4-5 hours, 2ml of DMEM/NBCS was added to the well and left overnight. The next day the medium was removed and replaced by 2ml fresh NBCS/DMEM. The cells were incubated for a further 24 hours before they were fixed and viewed using confocal microscopy.

2.5.5 Generation and maintenance of stable cell lines

The generation of stable cell lines involved selecting isolated colonies of cells (clones) which had incorporated the transfected DNA into their chromosomes. The plasmids used for transfection contained an antibiotic resistance gene which conferred resistance to plasmid-expressing cells in the presence of the antibiotic whereas non-expressing cells were killed.

The transfection protocol used was the same for that of transfection in 10cm dishes. 24 hours after transfection the cells were split 1:3 into 10cm dishes. At the same time, a 10cm plate of untransfected parental HEK293 was split to use as a negative control to determine the rate of cell death. The following day the medium was changed for

medium containing the antibiotic selection marker G418 at a concentration of 2mg/ml. The medium was changed every three days to maintain selection of resistant clones.

After 7-10 days, when all the cells in the control dish were dead, isolated clones in the transfected plates were picked. Approximately 40 clones were picked from each transfection. The clones were transferred to 24 well plates and grown in medium containing 1mg/ml G418. The medium was renewed every 3 days and once the clones were confluent they were split to 6 well dishes then 25cm^2 flasks and then finally into 75cm^2 flasks. Each of the selected clones was then assayed for expression of the transfected constructs. As all the stable lines generated in this study expressed GFP-tagged constructs, positive clones were selected by visualisation of their fluorescence under a fluorescent microscope.

2.5.6 Preservation of stable cell lines

Stable cell lines were preserved in the earliest passage possible. Cells were grown in 75cm^2 flasks before trypsinisation as described in 2.5.2. After the addition of 8ml of medium to the cells, the suspension was added to a 15ml centrifuge tube and spun at 1000*g* for 5 min. The cell pellet was resuspended in 1ml of NBCS containing 10% DMSO (as a cryo-protectant). This was then transferred to a cryovial and wrapped in cotton wool before being frozen overnight at -80°C and then placed in liquid nitrogen the following day.

Cells were regenerated by warming the cryovials at 37°C and resuspending the thawed cells in 10ml of growth medium. After centrifugation for 5 min at 1000*g* to remove the DMSO, the pellet was resuspended in 10ml of medium and transferred to a 75cm^2 flask.

2.5.7 Cell harvesting

Cells were harvested by first removal of the growth medium and rinsing twice with cold PBS. Using a cell scraper, the cells were dislodged from the bottom of the flask/dish in 5ml of PBS. The cell suspension was collected into tubes and spun at 1000*g* at 4°C for 5 min. The cell pellets were then frozen at -80°C until required.

2.6 Protein Biochemistry

2.6.1 BCA assay to determine protein concentration

Protein concentration in cell lysates and membrane preparations was determined using bincinhoninic acid (BCA) and copper sulphate solutions. Proteins reduce Cu(II) ions to Cu(I) in a concentration-dependent manner. BCA forms a complex with Cu(I) ions to form a purple coloured solution with an absorbance maximum at 562nm. The A_{562} value of the solution is directly proportional to the protein concentration. The protein concentration was determined using known concentrations of BSA solutions as standards (0.1-2mg/ml).

Reagent A	Reagent B
1% (w/v) BCA	4% $CuSO_4$
2% (w/c) Na_2CO_3	
0.16% (w/v) sodium tartrate	
0.4% NaOH	
0.95% $NaHCO_3$	
pH 11.25	

One part reagent B was added to 49 parts reagent A, and 200µl of the working solution was added to 10µl of each protein sample/standard in a 96 well plate. After incubation at 37°C for 30 min, the absorbance was read.

2.6.2 Preparation of cell membranes

Harvested cell pellets were thawed and resuspended in TE buffer. The cells were ruptured with 50 strokes of a glass on Teflon homogeniser. Unbroken cells and nuclei were removed by spinning at 1000rpm for 5 min in a refrigerated centrifuge. The supernatant fraction was then passed through a 25 gauge syringe needle 20 times and then centrifuged at 75 000rpm for 30 min in a Beckman Optima TLX Ultracentrifuge (Palo Alto, CA) with a TLA 100.2 rotor. The pellets were resuspended in TE buffer to a final concentration of 1-3mg/ml and stored at -80°C until use.

2.6.3 Sample preparation for SDS-PAGE gel electrophoresis

a) Membrane protein samples

Membrane protein samples (10-30μg) were diluted 1:1 in Laemmli buffer and boiled for 5 min prior to loading onto SDS-PAGE gels.

b) Immunoprecipitation of samples

Cells from 60mm dishes or 6 well plates were washed 3 times with ice cold PBS and then lysed using 500μl radio-immune precipitation (RIPA) buffer (50mM HEPES, pH 7.5, 150mM NaCl, 1% (v/v) Triton X-100, 0.5% deoxycholic acid, 0.1% SDS, 5mM EDTA, 10mM NaF, 5% (v/v) ethylene glycol) containing 1x Complete™ mini-protease inhibitor cocktail solution. After incubation on a rotating wheel for 1 hour at 4°C, insoluble material was removed by centrifugation (14 000rpm, 10 min, 4°C). Extracts were then equalised by protein assay as described in 2.6.1 and precleared of non-specific binding proteins by incubation with 20μl of protein G-Sepharose in the presence of 0.2% (w/v) globulin-free BSA for 1 hour at 4°C. Receptors were then immunoprecipitated from each precleared supernatant by incubation with 20μl of protein G-Sepharose and the appropriate antibody (2μg anti-GFP, 4μg anti-FLAG M2, or 1μg 12CA5) for at least 2 hours at 4°C. The immune complexes were isolated by centrifugation at 14 000rpm for 1 min, washed twice with 1ml RIPA buffer supplemented with 0.2M ammonium sulphate and once with 1ml RIPA alone. The proteins were eluted from the protein-G Sepharose by the addition of 30-50μl Laemmli buffer and incubation at 37°C for 1 hour. The eluates were then loaded onto SDS-PAGE gels.

2.6.4 SDS-PAGE gel electrophoresis and Western blotting

Samples were resolved on NuPage® Novex pre-cast bis-tris gels from Invitrogen BV. The NuPage® system is based upon a bis-tris-HCl buffered (pH 6.4) polyacrylamide gel, with a separating gel that operates at pH 7.0. Gels with a 4-12% acrylamide concentration were used to achieve the best separation of the proteins of interest. NuPage® MOPS SDS and MES SDS buffers were used for running the gels. The gels were run at 200V, ~100mA, using the XCell Surelock™ mini-cell gel tank (Invitrogen BV).

Following SDS-PAGE, the proteins were electrophoretically transferred onto nitrocellulose using the XCell II™ blot module (Invitrogen BV). Gels were transferred at 30V, ~140mA, for 1 hour in transfer buffer (0.2M glycine, 25mM tris, and 20% (v/v) methanol). The transfer of proteins onto the nitrocellulose was checked using Ponceau stain (0.1% (w/v) Ponceau S, 3% (w/v) trichloroacetic acid). Membranes were then blocked with 5% (w/v) fat-free milk in PBS/0.1%(v/v) Tween 20 (PBS-T) for 1 hour at room temperature. After a brief wash in PBS-T, membranes were incubated with the appropriate primary antibody in blocking buffer for 1 hour at room temperature. After extensive washing with PBS-T, blots were treated with the required HRP-conjugated secondary antibody in blocking buffer for 1 hour at room temperature. After further washing in PBS-T, the reactive proteins were visualised by enhanced chemiluminescence. For Western blot analysis the following antibody incubations were used:

1° Antibody	Dilution	2° Antibody	Dilution
Anti-FLAG M2	1:2000	Anti-mouse IgG	1:10 000
Anti-GFP	1:20 000	Anti-sheep IgG	1:10 000
12CA5	1:1000	Anti-mouse IgG	1:10 000

2.7 Assays

2.7.1 [^{3}H] Iloprost radioligand binding in membrane preparations

The expression of the IP prostanoid receptor constructs in stable cell lines was assessed using [^{3}H] iloprost membrane binding studies. These were performed in borosilicate glass tubes in triplicates, containing the following mix:

Membrane protein (1mg/ml)		40µl
Assay buffer (50mM Tris, pH 7.5, 5mM $MgCl_2$)		40µl
[^{3}H] Iloprost (~20nM)		10µl
Iloprost (100µM) or assay buffer		10µl
	Total Volume:	**100µl**

Reactions were incubated for 30 min at 30°C. Binding was stopped by vacuum filtration through GF/C filters. The filters were washed 3 times with ice cold wash buffer (50mM tris, pH 7.5, 0.25mM EDTA) to remove unbound radioligand from the membrane. Filters were inserted in vials containing 5ml liquid scintillant. The vials were then counted in a Beckman LS6500 scintillation counter using the [^{3}H] counting channel. Specific binding was determined by subtracting the counts produced in the absence of unlabelled iloprost (total counts) from those with unlabelled ligand present (non-specific counts). Receptor expression levels (fmol/mg protein) were calculated from the known specific activity of [^{3}H] iloprost (17 Ci/mmol) and the amount of protein used per tube.

The maximal binding (B_{max}) and the equilibrium dissociation constant (K_d) for iloprost at the various GFP-tagged prostacyclin receptor constructs was assessed using increasing concentrations of [^{3}H] iloprost (0.1-100nM) in the absence or presence of 20μM iloprost (to measure non-specific binding). Membrane binding was also assayed using homologous competitive binding experiments in which increasing concentrations of iloprost (10^{-12} – 10^{-4}M) were used to displace the binding of a single concentration (~20nM) of the trititiated ligand.

Data were analysed using GraphPad Prism Software (San Diego, CA). Saturation binding data were fitted to non-linear regression curves using both one and two site binding models. Data were also converted to Scatchard plots to determine the B_{max} and K_d values of the binding sites. Data from homologous displacement binding curves were fitted to one site competition curves.

2.7.2 Whole cell radioligand binding with [^{3}H] iloprost

The binding of [^{3}H] iloprost to plasma membrane receptors in transiently transfected cells was assessed using homologous displacement binding experiments. As for membrane binding, cells were incubated with a single concentration of [^{3}H] iloprost (~20nM). Non-specific binding was determined by incubation with excess of the unlabelled drug (10^{-4}M). 0.4M sucrose was used in the reactions to prevent agonist-mediated internalisation of the receptors. The reactions were performed in borosilicate glass tubes in triplicates, containing the following:

Intact cells ($5x10^6 - 6x10^6$) in assay buffer/0.4M sucrose		80µl
[^{3}H] Iloprost (~20nM)		10µl
Iloprost (10^{-4}M) or buffer/sucrose		10µl
	Total Volume:	**100µl**

Reactions were carried out as described for membrane binding experiments. A haemocytometer was used to determine the number of cells/µl of suspension. Receptor number was calculated by the converting of the number of fmoles of [^{3}H] iloprost bound/cell to receptors/cell using Avagadro's constant.

2.7.3 Intact cell adenylyl cyclase assay

Whole cell adenylyl cyclase activity was determined by measuring the production of [^{3}H] cAMP in cells which had been pre-treated with [^{3}H] adenine to label the intracellular adenine nucleotides. [^{3}H] cAMP was separated from the other [^{3}H] adenine nucleotides using column chromatography.

a) Column preparation

Dowex: For 100 columns, 200g of Dowex-50W was washed once with 1 litre of 1M HCl, once with 1 litre of 1M NaOH and then several times with distilled water until the residual wash was pH 7. The washed Dowex was then made up to 200ml with water and 2ml of the solution was added to a glass wool stoppered column. The columns were washed with 2ml of 1M HCl and 10ml of water prior to use. Columns were stored in water after use.

Alumina: For alumina columns, 0.5g of dry alumina was added to each glass wool stoppered column and washed once with 12ml of 1M imidazole (pH 7.3), followed by 15ml of 0.1M imidazole (pH 7.3). Prior to use, the columns were washed with 10ml of 0.1M imidazole (pH 7.3). After use they were stored in water.

b) Adenylyl cyclase dose response assays

Cells were seeded onto poly-D-lysine coated 24 well plates and incubated in medium containing [^{3}H] adenine (0.5µCi/well) for 16-24 hours. The [^{3}H] adenine was then removed and the cells were washed once with 1ml of HEPES/DMEM assay medium (1x DMEM supplemented with 20mM HEPES, pH 7.4, 2mM L-glutamine, and 1mM

IBMX). Cells were incubated with 0.25ml assay medium containing increasing concentrations of iloprost (10^{-12} – 10^{-6}M) for 30 minutes at 37°C. At the end of the incubation, the medium was aspirated and the reactions were stopped by the addition of 0.5ml ice cold stop solution (5% (w/v) TCA, 1mM ATP, 1mM cAMP) to each well. After 30 minutes, the supernatant was removed from the cells and applied to the pre-washed Dowex columns over scintillation vials containing 4ml of scintillant. 3ml of water was applied to each Dowex column to elute the non-cyclic [^{3}H] adenine nucleotides. The Dowex columns were then placed over the alumina columns and 10ml of water was applied to wash the [^{3}H] cAMP onto the alumina columns. The [^{3}H] cAMP was eluted with 6ml of 0.1M imidazole and collected in scintillation vials containing 8ml of scintillant, which had been placed over the alumina columns.

c) Adenylyl cyclase desensitisation/resensitisation/kinase inhibition assays

For desensitisation experiments, cells were pre-incubated with assay medium containing 1μM iloprost for periods of 10-60 min at 37°C. Cells were then washed 3 times with medium and re-exposed to increasing concentrations of iloprost (10^{-12} – 10^{-6}M) for 30 min at 37°C. [^{3}H] cAMP accumulation in the cells was assayed as described before. The net amount of [^{3}H] cAMP generated in desensitisation experiments was determined by subtracting the [^{3}H] cAMP accumulation in cells not re-challenged with agonist from the total [^{3}H] cAMP generated (after re-exposure).

In resensitisation assays, cells were pre-exposed to 1μM iloprost for 60 min at 37°C and then washed 3 times in medium and left to recover at 37°C for 30-60 min before re-exposure to increasing concentrations of agonist. The net accumulation of [^{3}H] cAMP in the cells was calculated as described for desensitisation experiments.

To assay the effects of kinase inhibitors, cells were pre-treated with 10μM H89 or 5μM GF109203X for 30 min at 37°C. Cells were then challenged with 1μM agonist for periods ranging from 0-30 min in the presence of the inhibitors and assayed for [^{3}H] cAMP generation as described previously.

2.7.4 *In vivo* phosphorylation assays

Agonist-mediated phosphorylation of the IP receptors was assessed using *in vivo* phosphorylation assays. HEK293 cells stably expressing the IP receptor constructs were plated onto 6 well plates at a density of approximately 10^6 cells/well and cultured

overnight. The next day the cells were washed twice with phosphate-free DMEM and incubated in the same medium supplemented with 0.2mCi/ml [^{32}P] orthophosphate for 90 min. Cells were then treated with 1μM iloprost for periods ranging from 30 sec to 10 min, or with 5μM forskolin or 5μM PMA for 10 min. To assay kinase inhibition, cells were pre-treated with 10μM H89 or 5μM GF109203X for 30 min prior to agonist exposure. The reactions were terminated by placing the cells on ice and washing 3 times with ice cold PBS. Cells were then solubilised for receptor immunoprecipitation with an anti-GFP antibody as described in 2.6.3b. After fractionation of immunoprecipitated receptors by SDS-PAGE, gels were dried and analysed by autoradiography. Observed bands were quantified by densitometric scanning of the X-ray films.

2.7.5 Receptor internalisation assay

IP receptor-expressing HEK293 cells were plated onto 6 well plates at a density of 10^6 cells/well. The next day, the cells were washed, and 1ml/well medium was applied. Cells were treated with 1μM iloprost for timepoints ranging from 0-60 min, or with 5μM forskolin or 5μM PMA for 1 hour. Inhibitors of internalisation were added 30 min prior to stimulation with agonist. The reactions were terminated by placing the plates on ice and washing the cells 3 times with ice cold PBS. The alcohol groups on the cell-surface glycoproteins were oxidised to aldehydes by a 30 min incubation with 10mM sodium m-periodate. After the removal of the periodate, cells were washed once with PBS and twice with 0.1M sodium acetate, pH 5.5, and incubated in the same buffer supplemented with 1mM biotin-LC-hydrazide. This reacts with the newly formed aldehyde groups, thereby labelling all cell surface glycoproteins with biotin. Labelling was terminated by removal of the biotin solution and washing the cells three times with PBS. Cells were then solubilised for receptor immunoprecipitation with the anti-GFP or 12CA5 antibody as described in 2.6.3b. After SDS-PAGE and the transfer of the proteins onto nitrocellulose membranes, cell surface biotin-labelled receptors were identified by incubation of the membranes with 1μg/ml HRP-conjugated streptavidin in 5% (w/v) non-fat milk/PBS-T for 1 hour at room temperature. After several washes with PBS-T, reactive proteins were visualised by enhanced chemiluminescence. Agonist-mediated loss of cell surface receptors was quantified by densitometric scanning of blots.

2.7.6 Confocal laser scanning microscopy

For all microscopic analysis in this study, fixed cell work was used. Cells were observed using a laser scanning confocal microscope (Ziess Axiovert 100:Zeiss Oberkochen, Germany) with a Ziess Plan-Apo 63 x 1.40 NA oil immersion objective, pinhole of 20, and electric zoom of 2-3. Typically, 10-12 optical sections were taken at 1μM intervals through the cells. Mid-cellular sections were acquired and averaged over 64 scans/frame. The GFP was excited using a 488nm argon/krypton laser and detected with a 515-540nm band pass filter. Red fluorescent protein (RFP) and the Alexa® 594 label were excited using a 543nm argon/krypton laser and detected with a 590nm long pass filter.

a) Visualisation of receptor internalisation

Receptor-GFP: Cells stably or transiently expressing the GFP-tagged IP receptor constructs were split onto poly-D-lysine coated coverslips and incubated overnight. The following day, the cells were treated with or without 1μM iloprost for 0-2 hours at 37°C and then placed on ice to terminate the reactions. Cells were then washed 3 times with ice cold PBS and fixed for 15 min at room temperature using 4% paraformaldehyde in PBS. After 2 further washes with PBS, the coverslips were mounted onto microscope slides with 40% glycerol in PBS.

HA-tagged receptor: HEK293 cells which had been transiently transfected with the HA-tagged IP receptor constructs were immunostained using an Alexa® 594-labelled goat anti-mouse secondary antibody to detect receptors which had been labelled with the 12CA5 antibody. In brief, transfected cells were plated onto poly-D-lysine coated coverslips and incubated overnight. The following day the medium was changed for DMEM supplemented with 4μg/ml 12CA5 antibody for 1 hour at 37°C. Where required, 1μM iloprost was added and incubated for up to 2 hours at 37°C. Coverslips were then washed twice with PBS and fixed with 4% paraformaldehyde as described previously. Cells were then permeabilised with 0.15% Triton-X-100/3% (w/v) non-fat milk/PBS (TM buffer) for 10 min at room temperature. The coverslips were subsequently incubated with Alexa® 594-labelled goat anti-mouse secondary antibody at a dilution of 5μg/ml for 1 hour at room temperature and then washed twice with TM buffer and once with PBS. The coverslips were mounted onto microscope slides with 40% glycerol in PBS.

b) Receptor/arrestin colocalisation experiments

GFP-tagged receptors trafficking with β-arrestin 1 and β-arrestin 2-RFP: Cells stably expressing the GFP-tagged IP receptors were transfected with either β-arrestin 1 or β-arrestin 2-RFP and split onto poly-D-lysine coated coverslips. 24 hours later, cells were treated with agonist for various timepoints and then fixed. For β-arrestin 2-RFP experiments, no immunostaining of the cells was necessary. β-Arrestin 1 was visualised by permeabilising the cells and incubating with an anti-β-arrestin 1 antibody (1:200 dilution) for 1 hour at room temperature. The cells were subsequently incubated with an Alexa® 594-labelled goat anti-mouse secondary antibody as described before and then mounted onto microscope slides.

HA-tagged receptors trafficking with β-arrestin 1-GFP and β-arrestin 2-GFP: HEK293 cells were co-transfected with the HA-tagged receptor constructs and β-arrestin-GFP cDNAs and then split onto coverslips. The next day, cells were stimulated with or without agonist and fixed. The cells were immunostained for the HA-tagged receptors as described in 2.7.6a before coverslips were mounted onto microscope slides.

c) Labelling with Texas Red® transferrin

Cells grown on coverslips were labelled with medium containing Texas Red® transferrin (25μg/ml) for 30 min at 37°C in 5% CO_2. Cells were then washed twice with medium before being treated with or without agonist for 30 min at 37°C. The cells were subsequently fixed and mounted onto microscope slides.

Chapter 3

Analysis of the Pharmacology and Trafficking of GFP- and HA-tagged forms of the Prostacyclin Receptor in Conjunction with Receptor Chimeras possessing the Carboxyl Termini of the β_2-adrenergic and TRH receptors

Chapter 3

3.1 Introduction

Prostacyclin is an important mediator of physiological processes in a variety of tissues, including platelets, neuronal cells, and vascular smooth muscle. Prostacyclin acts as a potent mediator of vasodilation and inhibitor of platelet activation. Thus, prostacyclin induces smooth muscle relaxation in arterial beds as well as inhibition of platelet aggregation, and is, therefore, thought to be an important regulator of vascular homeostasis (Vane *et al.*, 1995). Other possible roles of prostacyclin are not well established but include regulation of renal blood flow, hyper-immune responses, and lipolysis (Negishi *et al.*, 1995; Holgate *et al.*, 1980; Chatzipanteli *et al.*, 1992). In common with other prostaglandins, prostacyclin also evokes inflammatory responses such as hyperaemia, oedema, hyperanalgesia, and pyrexia primarily through its role as a vasodilator (Murata *et al.*, 1997; Bley *et al.*, 1998). Prostacyclin exerts its effects by activating the IP prostanoid receptor. The IP receptor couples to G_s and G_q as suggested by stimulation of both cAMP and IP_3/DAG production (Boie *et al.*, 1994; Namba *et al.*, 1994). However, stimulation of G_q in all investigated cell types occurs only at high concentrations of agonist.

In general, GPCRs tend to be tightly regulated by desensitisation, a phenomenon by which a receptor's response to ligand is attenuated. The β_2-AR has served as a prototype for the molecular events responsible for desensitisation (Ferguson and Caron, 1998). The general model for GPCR regulation involves three key mechanisms. The first and most rapid phase of desensitisation occurs within seconds after exposure to agonist and is due to receptor phosphorylation mediated by second messenger kinases and/or GRKs. Phosphorylation by GRKs promotes the binding of arrestins, which triggers desensitisation by uncoupling the receptor from its G protein. This is followed by sequestration of receptors away from the cell surface via clathrin coated pits by an arrestin-dependent process. Finally, more prolonged receptor stimulation leads to the redirection of internalised receptors to a lysosomal compartment with subsequent downregulation.

It is likely that similar mechanisms govern IP receptor regulation. *In vitro* studies of the IP receptor, expressed in HEK293 cells, revealed that agonist stimulation leads to rapid receptor desensitisation, a process which seems to coincide with receptor phosphorylation (Smyth *et al.*, 1996, 1998). Internalisation of the IP receptor in response to agonist treatment has been observed in transfected HEK293 cells and in cell lines which endogenously express the receptor (Smyth *et al.*, 2000; Giovanazzi *et al.*, 1997; Leigh and MacDermot, 1985; Krane *et al.*, 1994). Furthermore, downregulation of native IP receptors has been demonstrated in NG108-15 cells and platelets in response to sustained prostacyclin challenge (Giovanazzi *et al.*, 1997; Krane *et al.*, 1994)

Clathrin-mediated endocytosis of GPCRs requires the interaction of specific receptor domains with components of the endocytic machinery. Data from GPCR sequestration studies have identified several receptor domains that are involved in regulating internalisation. However, a common endocytic motif has not been identified. It seems that the determinants for endocytosis are located within multiple receptor regions which regulate the rate and extent of receptor sequestration in response to agonist exposure. For many GPCRs, the endocytic domains are found within the intracellular C-terminal tail. The C-tails of many GPCRs are rich in serine and threonine residues which serve as substrates for kinase phosphorylation, and subsequently act as sites for arrestin docking leading to receptor desensitisation and internalisation.

In studies of the thromboxane receptor splice variants, TPα and TPβ (which differ only at their C-terminal tails), the longer TPβ isoform was shown to be sensitive to kinase phosphorylation and internalised rapidly in response to agonist whereas the shorter TPα splice variant did not (Parent *et al.*, 1999). Similarly, the EP_2 receptor, which possesses a comparatively short C-terminal tail, was found to be resistant to agonist-induced internalisation (Nishigaki *et al.*, 1996). Studies of the mammalian GnRH-R, which is unique among the GPCR family in that it does not possess a C-terminal tail, revealed that the receptor displayed exceptionally slow kinetics of receptor desensitisation and internalisation as compared to non-mammalian forms of the receptor which possess a carboxyl terminal domain (Heding *et al.*, 1998).

Numerous GPCR studies have investigated the role of the C-terminal tail in regulating internalisation using receptor mutants exhibiting point mutations and/or truncations within this region. In such investigations it has been frequently shown that the tail of the receptor plays an important role in internalisation and/or desensitisation.

For the histamine H2 receptor, a series of C-tail truncations identified a region between Glu^{314} and Asn^{320} (ETSLRSN) as important in regulating internalisation. Furthermore, mutation of Thr^{315} to alanine, but not that at Ser^{316}, abolished internalisation, thus identifying a key threonine residue of functional significance for receptor endocytosis (Fukushima *et al.*, 1997).

In the parathyroid hormone receptor C-tail, 91 of the 127 residues could be deleted without affecting internalisation. However, further truncation of residues 475 to 494 resulted in a 50-60% decrease in ligand internalisation. A mutant with an internal deletion of these 20 amino acids showed a similar reduction in internalisation, confirming the presence of a positive endocytic signal. Further truncations of the membrane-proximal region of the tail exhibited no further loss in receptor internalisation, indicating the presence of only one endocytic signal within the tail (Huang *et al.*, 1995).

In investigations of somatostatin receptor type 5 internalisation, 60% of cell surface receptors were shown to internalise after 1 hour's agonist treatment. Truncation of the C-tail to 318, 328, and 338 residues reduced this to 46, 46, and 23%, respectively. Deletion to 347 residues slightly improved internalisation (72%), demonstrating the presence of both positive and negative regulators of internalisation within the domain (Hukovic *et al.*, 1998).

In cells expressing C-tail mutants of the δ-opioid receptor, those lacking the distal 15 amino acid residues of the carboxyl terminus displayed a substantially slower rate of internalisation. In addition, cells expressing receptors with point mutations of any of the Ser/Thr residues between Ser^{344} and Ser^{363} in the C-terminal tail exhibited a significant reduction in their internalisation rate (Trapaidze *et al.*, 1996).

Tyrosine-containing endocytic motifs have been identified in many single transmembrane receptors (Sorkin and Carpenter, 1993). Equivalent motifs in the C-tails of GPCRs have also been implicated in their sequestration. For the neurokinin-1 receptor, mutation of conserved tyrosine residues (positions 331, 341 and 349) impaired agonist-induced endocytosis without substantially affecting agonist binding or signalling (Bohm *et al.*, 1997). Tyrosine-containing motifs in the C-terminal domain of the $AT_{1A}R$ are also important for internalisation, with a 2.5 fold decrease in internalisation noted in cells expressing a Y318A receptor mutant (Thomas *et al.*, 1995). In contrast, mutation of tyrosine residues in the cytoplasmic tail of the β_2-AR ($Tyr^{350, 354}$) has been shown to have no affect on receptor sequestration (Valiquette *et al.*, 1990). For the β_2-AR, additional structural elements within the C-tail such as dileucine repeats that bind AP-1 and AP-2 adapter proteins associated with clathrin coated pits seem to be critical for internalisation (Gabilondo *et al.*, 1997).

Interpretation of sequestration data from GPCR substitution/deletion studies must be made with caution. Since receptors exist as three-dimensional entities, the possibility of non-specific conformational effects have to be taken into account. Mutations of specific residues that are not themselves directly required for internalisation may interfere with conformational changes in domains that are essential for endocytosis. For instance, in sequestration studies of the EP_4 receptor, truncations after amino acid residue 369 were demonstrated to markedly attenuate internalisation, whereas a receptor exhibiting mutations of all serine and threonine residues between residues 350 and 383 was found to internalise to the same extent as the wild type receptor (Desai *et al.*, 2000). Additionally, modifications of the carboxyl termini of GPCRs have been shown not only alter the rate and extent of receptor internalisation, but also the mechanism. In investigations of adenosine A_{2B} receptor sequestration it was shown that a receptor mutant truncated at Ser^{326} was unable to undergo arrestin/clathrin-dependent internalisation, whereas the S326A point mutant displayed an arrestin/clathrin-dependent internalisation phenotype identical to the wild type receptor (Matharu *et al.*, 2001).

An alternative approach to deletion and substitution experiments is the creation of receptor chimeras. This strategy offers advantages for analysis of structure and function

in that the expected outcome is the alteration or addition, rather than the loss of receptor function. Chimeric receptors have been generated to study the internalisation patterns of several GPCRs.

The chimeric strategy has been used to investigate the trafficking of the thrombin (PAR1) receptor (Trejo and Coughlin, 1999). Wild type PAR1-R is activated by an irreversible proteolytic mechanism in which thrombin binds to and cleaves the amino-terminal exodomain of the receptor. Receptor cleavage results in the generation of a new amino terminus that functions as a tethered ligand. Unlike most GPCRs, the activated PAR1-R is sorted predominantly to the lysosomes after internalisation. To identify the domain(s) that specifies sorting to the lysosomes of activated PAR1 receptors, chimeras between the PAR1-R and the substance P receptor were generated. Exchanging of the carboxyl tails of the PAR1-R and the substance P receptor switched their trafficking behaviours after activation. The substance P chimera with the PAR1-R tail internalised upon activation and sorted to the lysosomes like the wild type PAR1-R. Conversely, the PAR1-R bearing the cytoplasmic tail of the substance P receptor internalised upon activation but recycled back to the membrane thus allowing for 'resignalling' of the proteolytically activated chimeric receptor even after the removal of thrombin.

Chimeric receptors have also been used to study the role of the carboxyl terminus in bombesin receptor regulation. In such studies the C-tail was switched for those of the m3 muscarinic (BMC) and cholecystokinin A (BCC) receptors. In CHO cells, ligand internalisation of the chimeric receptors generally assumed the properties of the donor receptors. Thus, BCC receptors internalised ligand to a similar extent as wild-type CCK whereas BMC receptors showed reduced ligand internalisation, like wild type m3 muscarinic receptors (Tseng *et al.*, 1995).

The desensitisation and internalisation kinetics of the tail-less mammalian GnRH receptor have also been examined using receptor chimeras. To investigate the role of a cytoplasmic tail in these events, a chimeric receptor was constructed where the intracellular tail of the TRH-R was fused to the C-terminus of the GnRH-R. The study demonstrated that the addition of a functional intracellular tail to the GnRH-R

accelerated receptor desensitisation and increased internalisation rates (Heding *et al.*, 1998).

In this chapter, chimeric GPCRs were generated to examine the function of the IP prostanoid receptor C-terminal tail in its internalisation in response to agonist treatment. Chimeric receptors possessing the carboxyl terminal domains of the human β_2-adrenergic and rat TRH-1 receptors were created. Initially, C-terminally GFP-tagged forms of the receptor proteins were used to directly monitor receptor trafficking using confocal microscopy. Experiments were then repeated using the equivalent non-GFP tagged forms of the receptors. Functional characterisation of the receptor constructs was performed at first. Receptor expression in transfected HEK293 cells was confirmed using radioligand binding assays, and for the GFP-tagged receptors, confocal microscopy was also used to visualise expression. Intact cell adenylyl cyclase assays were utilised to test the receptors' coupling capacity to G_s. More extensive pharmacological analysis was carried out with stable cell lines expressing the GFP-tagged IP receptor constructs. Finally, the agonist-mediated internalisation properties of receptors were analysed visually by confocal microscopy and quantified by immuno-detection of biotin-labelled cell surface receptors.

3.2 Construction and expression of chimeric IP prostanoid receptor-green fluorescent protein fusion proteins.

PCR was used to link cDNAs encoding GFP-tagged versions of both the rat TRH-1-R and human β_2-AR intracellular carboxyl terminal tails to the distal end of TMVII of the IP receptor. A PCR strategy was also used to insert a FLAG (Asp-Tyr-Lys-Asp-Asp-Asp-Asp-Lys) epitope at the N-terminus of the protein after the initiating methionine residue. A full length IP receptor linked C-terminally to GFP and tagged at the amino terminus with a FLAG epitope, which was also used in this study, was constructed previously in the laboratory. Figure 3.1a is a diagrammatic representation of the GFP-tagged receptors which were used in this investigation. Figure 3.1b shows the amino acid composition of the different C-tails of the prostacyclin receptor proteins.

These cDNA constructs were transiently transfected into HEK293 cells and their expression was initially investigated by Western blot analysis. Immuno-detection of the receptors' N-terminal FLAG epitope and C-terminal GFP moiety confirmed the expression of full-length proteins post transfection (Figure 3.2). Immunoblotting of transiently transfected membranes with both the anti-FLAG and anti-GFP antibodies detected broad immuno-reactive bands of molecular mass ~60-100 kDa which were not present in mock transfected membranes. Since the predicted molecular weight of each construct is approximately 68 kDa, it is therefore likely that the higher molecular weight bands corresponded to differentially glycosylated forms of the receptors.

The expression of the receptor constructs at the plasma membrane was further assessed by the binding of ~20nM [^{3}H] iloprost to transfected whole cells (Figure 3.3). From these experiments it was evident that the transient expression of each construct at the plasma membrane was exceptionally low (IP-GFP 42 ± 9.8 fmol/10^6 cells, IP-TRH-GFP 72 ± 8.8 fmol/10^6 cells, and IP-β_2-GFP 39 ± 13.7 fmol/10^6 cells). Expression levels were not augmented by transfection of more receptor cDNA.

The G_s coupling capacity of each of the IP receptor constructs was determined by measurement of agonist-induced cAMP accumulation in transiently transfected cells (Figure 3.4). After 15 min incubation with agonist, the [^{3}H] cAMP generated in

response to 1μM iloprost exposure was at best 2-3 fold higher than basal levels, which was further indicative of low receptor expression in the transfection assays. Direct activation of adenylyl cyclase with 50μM forskolin resulted in substantial second messenger production in the cells. In addition, a synergistic effect was observed in cells treated with both iloprost and forskolin.

Confocal analysis was used to visualise the GFP-tagged receptors in transiently transfected HEK293 cells. Figure 3.5 illustrates the confocal images generated for both unstimulated and agonist treated cells. In each case, it was evident that the expression of the receptors was predominantly localised to intracellular membranous compartments, thus making it impossible to detect agonist-mediated internalisation of plasma membrane receptors. Improper targeting of GPCRs is a commonly observed problem in transient expression systems. Therefore, stable cell lines of each of the chimeric receptors were generated in an attempt to overcome this.

Once stable cell lines expressing IP-TRH-GFP and IP-β_2-GFP receptors were established in HEK293 cells, single clones of each were selected for study in conjunction with a stable cell line expressing IP-GFP receptors which had been generated previously in the laboratory. Screening for positive clones was carried out using fluorescence microscopy. Only a small number of clones generated were autofluorescent. Approximately 25% of the putative IP-TRH-GFP clones selected were positive whereas only ~10% of the IP-β_2-GFP clones selected fluoresced. Positive clones were initially analysed using radioligand binding and adenylyl cyclase assays. Figure 3.6 gives an approximate indication of expression levels of each clone from the binding of a single concentration of [^{3}H] iloprost. The coupling efficiency of each clone was then assessed by measurement of cAMP generation in cells after 15 min challenge with 1μM iloprost (Figure 3.7). From these experiments it could be seen that second messenger output in each clone correlated well with the receptor expression level. All positive clones were further examined using confocal microscopy to visualise receptor distribution within the cells (Figure 3.8). Although all clones showed significantly more plasma membrane expression as compared to transient systems, for many of the clones substantial amounts of the GFP-derived autofluorescence was present in intracellular compartments. As one of the main objectives of this study was to use GFP to directly

visualise the trafficking of the IP receptor constructs, the clones with mainly plasma membrane delineated fluorescence were selected for further investigation. Of the IP-TRH-GFP clones, clone 19 was selected and of the IP-β_2-GFP clones, clone 17 was chosen.

3.3 Pharmacological characterisation of stable cell lines expressing the GFP-tagged IP receptor proteins.

To determine more accurately the receptor expression level of each of the selected clones, saturation binding experiments were performed by incubation of isolated membrane fractions with concentrations of [^{3}H] iloprost ranging from 0-100nM. The non-specific binding of [^{3}H] iloprost was determined by incubation with 20μM unlabelled iloprost (Figure 3.9 a, c, e). Saturation binding curves were converted to Scatchard plots (Figure 3.9 b, d, f) which revealed the presence of two binding sites (one high affinity and one low affinity) for each of the receptor constructs. For the IP-GFP receptor, a high affinity binding site with dissociation constant (K_d) of 2.6 ± 0.25nM and maximum receptor level (B_{max}) of 696 ± 53.4 fmol/mg membrane protein was observed. The K_d value for the low affinity binding site was 66.9 ± 5.3nM with a B_{max} of 4806 ± 106 fmol/mg. For the IP-TRH-GFP receptor, the high and low affinity binding sites exhibited dissociation constants of 2.9 ± 0.5nM (B_{max} of 682 ± 83.7 fmol/mg) and 33.5 ± 4.6nM (B_{max} of 1591 ± 157 fmol/mg) respectively. For the IP-β_2-GFP receptor, [^{3}H] iloprost bound at two binding sites with K_d values of 1.12 ± 0.28nM (B_{max} 168 ± 48.5 fmol/mg) and 81.6 ± 25.6nM (B_{max} 1780 ± 145 fmol/mg).

Practical concentrations of [^{3}H] iloprost used in saturation binding assays were restricted to 100nM at most. Consequently, the K_d values for the low affinity binding sites could not be calculated accurately from such experiments. Further ligand binding analysis of the receptor constructs was therefore carried out using homologous displacement binding assays (Figure 3.10). However, an intrinsic feature of competitive binding curves is that they are invariably unable to detect two classes of binding site when the same compound serves as radioligand and competitor. It is impossible to detect two classes of site in such experiments when the density of the low affinity site is less than or equal to that of the high affinity sites. Even when the low affinity site is in

abundance, it is only possible to detect two sites when the concentration of radioligand is appropriate: small enough so that a reasonable fraction of the binding is to the high affinity site, and large enough so that some binds to the low affinity site. Increasing concentrations of iloprost displaced the binding of 20 nM [^{3}H] iloprost from IP-GFP, IP-TRH-GFP, and IP-β_2-GFP membranes with IC_{50} values of 87.7 ± 7.5nM, 52 ± 4nM, and 61 ± 7nM respectively. Applying the formalisms of De Blasi and coworkers (1989), this produced K_d values of 67.6 ± 7.5nM for IP-GFP, 32 ± 4nM for IP-TRH-GFP, and 42 ± 7nM for IP-β_2-GFP receptors. The Hill slope coefficient for each binding curve suggested the presence of a heterogeneous population of receptors i.e. the receptors did not all bind the drug with the same affinity.

The dose-dependent effect of iloprost on adenylyl cyclase activity was studied for IP-GFP, IP-TRH-GFP, and IP-β_2-GFP cells (Figure 3.11). After labelling overnight with [^{3}H] adenine, cells were challenged with iloprost concentrations ranging from 1pM to 1μM for 30 min. Iloprost was most potent at stimulating adenylyl cyclase in IP-GFP cells (EC_{50} of 0.096 ± 0.022nM), whereas agonist potency at the chimeric receptors was significantly lower (EC_{50} values of 0.41 ± 0.07nM for IP-TRH-GFP and 0.36 ± 0.05nM for IP-β_2-GFP). IP-GFP and IP-β_2-GFP cells displayed similar maximum levels of [^{3}H] cAMP production (24.8 ± 3% and 23.5 ± 1.1% of total intracellular adenine pool respectively). By comparison, the maximal level of second messenger production in IP-TRH-GFP cells was markedly lower (13.6 ± 1.2%).

3.4 Internalisation studies of stable cell lines expressing the GFP-tagged IP receptor proteins.

The sequestration of the GFP-tagged receptors in the stable cell clones was initially monitored by direct visualisation of GFP redistribution in response to agonist treatment. Cells grown on glass coverslips were incubated with 1μM iloprost for timepoints ranging from 0-60 min and then fixed before examination by confocal microscopy. Receptors in IP-GFP cells displayed predominantly plasma membrane expression in the unstimulated state. Upon exposure to agonist, receptors could be seen to translocate to intracellular compartments. After 30 min incubation, a significant proportion of the receptor population appeared to be intracellular, which became more pronounced at the

1 hour timepoint (Figure 3.12). IP-TRH-GFP cells exhibited a more rapid time-dependent internalisation of receptors into discrete intracellular vesicles, with considerable sequestration detectable within 5 min of agonist treatment (Figure 3.13). After a further 15 min, the bulk of receptors appeared to have been lost from the plasmalemmal surface. In the IP-β_2-GFP cells, receptors were found to be equally distributed between the cell surface and intracellular membranes in the unstimulated state (Figure 3.14). After incubation with iloprost, more noticeable fluorescence could be detected inside the cells within 30 min.

Confocal analysis of the stable cell clones (particularly in the case of IP-β_2-GFP cells) confirmed that in the unstimulated state significant receptor expression was localised intracellularly, thus making visualisation of receptor trafficking troublesome. Immunocytochemical experiments were undertaken to try and overcome this problem (Figure 3.15). Since each of the constructs possessed an amino-terminal FLAG epitope, live cells were incubated with an anti-FLAG antibody to label the cell surface receptors before treatment with agonist. Cells were then fixed and permeabilised prior to incubation with an Alexa^{594}-conjugated secondary antibody to detect the FLAG antibody-labelled receptors at the cell surface and those which had internalised in response to agonist. It was anticipated that this technique could be used to highlight only the intracellular receptor pool which had sequestered in response to agonist. Initial experiments with IP-GFP cells were promising as the anti-FLAG antibody successfully decorated the cells (Figure 3.15a). Surprisingly, this was not the case with the chimeric IP receptor constructs as no specific labelling of the receptors could be seen (Figure 3.15 b, and c). The anti-FLAG antibody had previously been shown to detect the epitope in membrane preparations from cells expressing the IP-TRH-GFP and IP-β_2-GFP constructs (Figure 3.2a) thus confirming its incorporation into the protein. The possibility that receptors were not being expressed at the cell surface, making them inaccessible to the antibody, was ruled out by assaying the binding of radioligand to cell surface receptors in intact cells (data not shown). It is possible that the anti-FLAG antibody used was ineffective at detecting the epitope in immunocytochemical experiments. It is also possible that switching of the IP receptor C-tail altered the conformation of the protein, resulting in changes in the interaction of the N-terminal

segment with components of the extracellular matrix thus preventing epitope recognition by the antibody.

The confocal images of receptor internalisation suggested that each of the receptor constructs exhibited different rates of endocytosis over a 60 min agonist time course (Figures 3.12, 3.13, 3.14). To accurately determine the time courses of agonist-mediated internalisation, receptor biotin labelling experiments were used. After treatment of cells with or without 1μM iloprost for timepoints up to 1 hour, cells were placed on ice (to prevent further internalisation) and the cell surface glycoproteins were labelled with a membrane-impermeable derivative of biotin. Receptors were extracted from the cells by immunoprecipitation using an anti-GFP antibody. After fractionation of immunoprecipitated receptors by SDS-PAGE, followed by transfer to nitrocellulose membranes, biotinylated proteins were detected by HRP-conjugated streptavidin. Agonist-induced loss of the cell surface receptor population was quantified by densitometric scanning of the blots. For IP-GFP cells, agonist treatment induced an initial rapid loss of cell surface receptors in the first 5 min of agonist treatment which was followed by a more steady reduction in the level of cell surface receptors for the remainder of the time course. With cell surface receptor level in unstimulated cells set at 100%, after 1 hour iloprost stimulation, 59 ± 7% of the biotin labelled receptors were detected at the plasma membrane (Figure 3.16). The IP-TRH-GFP construct internalised more rapidly and to a greater extent than the IP-GFP receptor (Figure 3.17). After 5 min agonist exposure, almost half of the total cell surface receptors had endocytosed (58 ± 6% at cell surface). After 15 min, the rate of internalisation decreased until it plateaued after 1 hour of agonist treatment (36 ± 4% at cell surface). The IP-β_2-GFP construct internalised to a similar extent as the IP-GFP receptor. Over the 60 min time course, the internalisation rate appeared to be constant. After 1 hour iloprost stimulation, 59 ± 7% of the labelled receptors were present at the cell surface (Figure 3.18). In agreement with the confocal data, the biotin labelling assays confirmed that the IP-TRH-GFP receptor internalised the most rapidly whereas the IP-GFP and IP-β_2-GFP receptors behaved similarly, exhibiting slower kinetics of internalisation (Figure 3.19). In order to assess the effects, if any, of GFP on the internalisation rate of the receptors, the equivalent cDNA constructs were generated without GFP. These constructs were subsequently used in assays for receptor internalisation.

3.5 Construction and pharmacological characterisation of HA-tagged IP prostanoid receptor fusion proteins.

A PCR based strategy was used to construct the equivalent non-GFP tagged IP receptor cDNAs in which the FLAG epitope tag was also removed and replaced with a sequence encoding an HA tag (Tyr-Pro-Tyr-Asp-Val-Pro-Asp-Tyr-Ala) (Figure 3.20).

The constructs were transiently transfected into HEK293 cells and their expression was detected by immunoblotting using the anti-HA antibody 12CA5 (Figure 3.21). Western blot analysis of membrane preparations from transfected cells detected broad immuno-reactive bands of ~35-60 kDa. The predicted molecular weight of each of the IP receptor proteins is 41 kDa, which would suggest that the slower migrating bands indicated the presence of glycosylated forms of the receptors. A non-specific reactive species of ~50 kDa, as detected in mock transfected cells, obscured the region of specific antibody binding in receptor-transfected cells.

Receptors were further characterised in transient transfections by radioligand binding and adenylyl cyclase assays. The plasma membrane expression of receptors was determined by binding of [^{3}H] iloprost to transfected whole cells (Figure 3.22). As highlighted previously in binding experiments with the GFP-tagged constructs, low levels of binding were detected in cells expressing the HA-tagged IP receptors, indicating poor transfection efficiency (HA-IP 94 ± 18.6 fmol/10^6 cells, HA-IP-TRH 86 ± 24 fmol/10^6 cells, and HA-IP-β_2 126 ± 40 fmol/10^6 cells). Furthermore, cAMP production in response to agonist challenge in transiently transfected cells was exceptionally low (Figure 3.23). When treated with forskolin, to directly stimulate adenylyl cyclase, significant second messenger production was detected. Adenylyl cyclase activity was further enhanced when cells were treated with both iloprost and forskolin, thus confirming the expression and G protein coupling of the HA-tagged IP receptor constructs in HEK293 cells.

3.6 Analysis of receptor internalisation in HEK293 cells transiently transfected with HA-tagged IP prostanoid receptor constructs.

An immunocytochemical approach was used to observe the trafficking of the HA-tagged IP receptors in cells. In contrast to earlier immunostaining analysis with the anti-FLAG antibody (Figure 3.15), the 12CA5 antibody effectively labelled each of the transiently expressed HA-receptor constructs in live HEK293 cells. Therefore, agonist-mediated internalisation of the HA-receptors was studied using confocal microscopy. In cells expressing the HA-IP construct, a 60 min time course of 1μM iloprost treatment promoted the translocation of antibody labelled receptors from the cell surface to intracellular compartments (Figure 3.24). Within 15 min of agonist exposure, a significant portion of the fluorescent signal could be detected inside the cells, and at the 1 hour timepoint, the plasma membrane appeared less defined due to the loss of fluorescence from the surface. For HA-IP-TRH transfected cells, most of the cells' fluorescence seemed to be cytoplasmic within the first 5 min of agonist treatment (Figure 3.25). Prolonged exposure to agonist resulted in further loss of receptors from the cell surface as illustrated by the intracellular concentration of the fluorescent signal. In HA-IP-β_2 expressing cells, the localisation of antibody labelled receptors inside the cells could be detected within 5 min of agonist treatment and steadily increased during the 60 min time course (Figure 3.26). From these experiments it could be seen that all three of the IP receptor constructs endocytosed in response to treatment with iloprost. Although such data could not be used to accurately determine the internalisation rates of each receptor construct, the images generated from immunocytochemical analysis suggested that the HA-IP-TRH receptor sequestered more quickly in response to agonist than the other IP receptor proteins.

Quantification of agonist-mediated internalisation for each of the constructs was carried out using receptor biotin labelling experiments as essentially described in section 3.4, except that receptors were immunoprecipitated from cell lysates using the 12CA5 antibody. Densitometric analysis of blots from biotin labelling experiments with the HA-IP construct indicated that there was an initial rapid loss of receptors from the cell surface within the first 5 min of agonist (87 ± 2.9% receptors at the cell surface). Receptor internalisation continued over the rest of the time course but at a much slower

rate (Figure 3.27). In HA-IP-TRH expressing cells, approximately 40% of the cell surface receptors had internalised within 5 min of iloprost treatment (Figure 3.28). Only a further ~10% loss in receptor cell surface expression was detected over the 60 min period. For the HA-IP-β_2 receptor, a continuous and steady reduction in the cell surface expression of receptors occurred with 51 ± 5.3% receptors remaining at the plasma membrane after 1 hour's agonist treatment (Figure 3.29). In summary, the results suggest that the HA-IP-TRH receptor internalised rapidly in response to agonist while the HA-IP and HA-IP-β_2 receptors displayed much slower and essentially similar internalisation rates (Figure 3.30).

Figure 3.1

a) Schematic representation of the receptor-GFP constructs used in this study.

The IP-GFP cDNA (1) was constructed previously in the laboratory. The IP-TRH-GFP (2) and IP-β_2-GFP (3) constructs were generated by PCR as described in section 2.4.

b) Primary structure of the receptor carboxyl terminal sequences.

The amino acid composition of the carboxyl terminal domains of the prostacyclin receptor constructs.

Figure 3.2

Western blot analysis of membranes transiently transfected with the receptor-GFP constructs.

20μg of membrane preparations from HEK293 cells transiently transfected with the IP-GFP (1), IP-TRH-GFP (2), IP-β_2-GFP (3) constructs, and empty vector (4) were resolved on SDS-PAGE gels then transferred onto nitrocellulose membranes and blotted with a) anti-FLAG™ and b) anti-GFP antibodies. Two further experiments produced similar results.

Fig. 3.1a

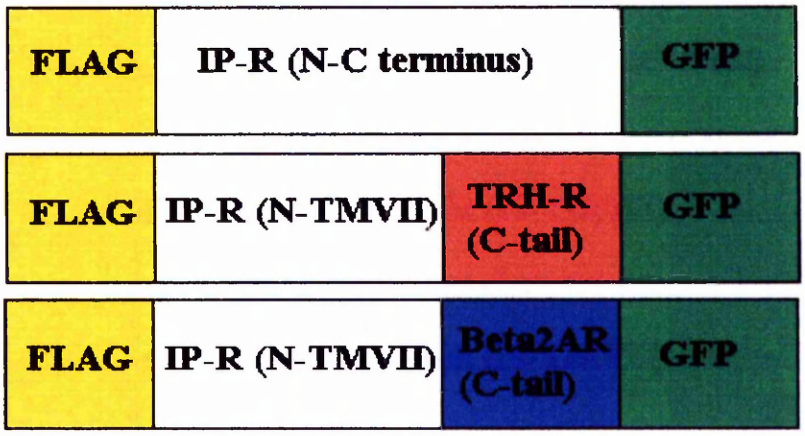

Fig. 3.1b

IP-R

VFQRLKLWVCCLCLGPAHGDSQTPLSQLASGRRDPRAPSAPVGKEGSCVPLSAW
GEGQVEPLPPTQQSSGSAVGTSSKAEASVACSLC

TRH-R

YNLMSQKFRAAFRKLCNCKQKPTEKAANYSVALNYSVIKESDRFSTELDDITVT
DTYVSTTKVSFDDTCLASEKNGPSSCTYGYSLTAKQEKL

β_2-AR

CRSPDFRIAFQELLCLRRSSLKAYGNGYSSNGNTGEQSGYHVEQEKENKLLCEDL
PGTEDFVGHQGTVPSDNIDSQGRNCSTNDSLL

Fig. 3.2

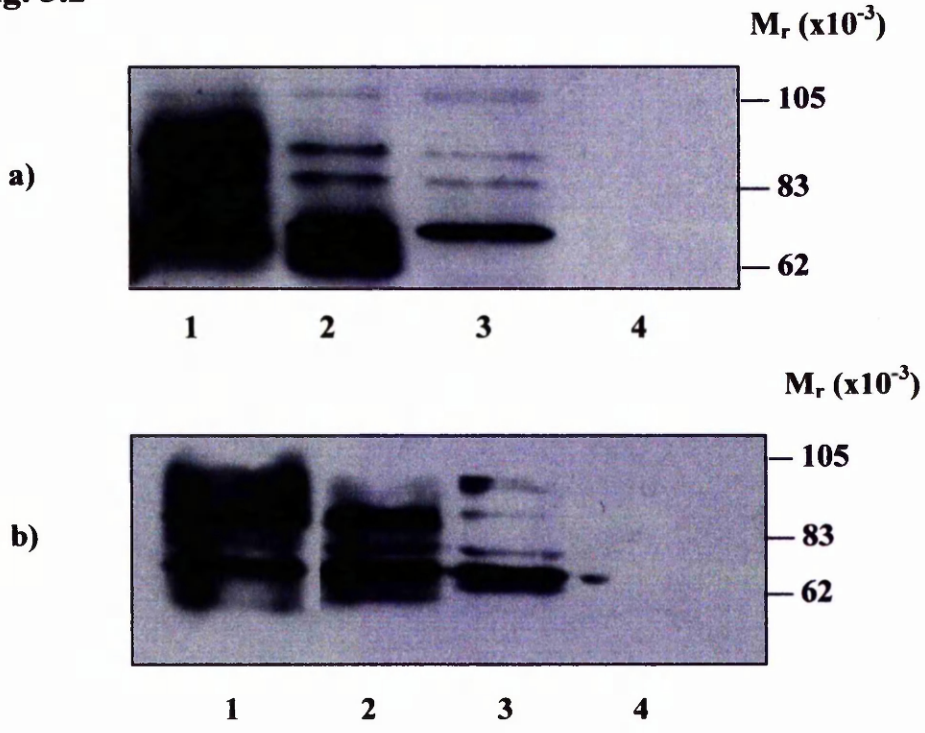

Figure 3.3

One-point [^{3}H] iloprost binding in intact HEK293 cells transiently transfected the receptor-GFP constructs.

The specific binding of [^{3}H] iloprost in cells transiently transfected with the receptor-GFP constructs was determined by incubation with 20nM [^{3}H] iloprost as essentially described in section 2.7.2. Data shown are presented as specific fmol bound/10^6 cells and are means ± S.E.M., n=3.

Figure 3.4

Adenylyl cyclase activity in cells transiently expressing the receptor-GFP constructs.

The G_s coupling of the receptor-GFP constructs was assessed by stimulation of cells for 15 min with 1μM iloprost. Cells were also challenged with adenylyl cyclase activator forskolin (50μM), or both iloprost and forskolin. The cAMP accumulation in the cells is expressed as a percentage of the total adenine nucleotide intracellular pool. The data shown represent means ± S.E.M. from a single assay performed in triplicate. A further two experiments produced similar results.

Fig. 3.3

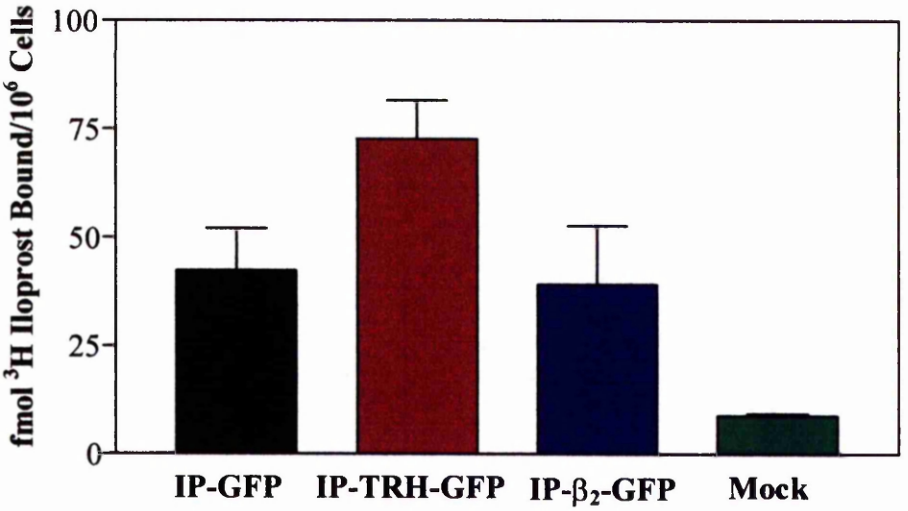
fmol ^{3}H Iloprost Bound/10^6 Cells
100
75
50
25
0
IP-GFP
IP-TRH-GFP
IP-β_2-GFP
Mock

Fig. 3.4

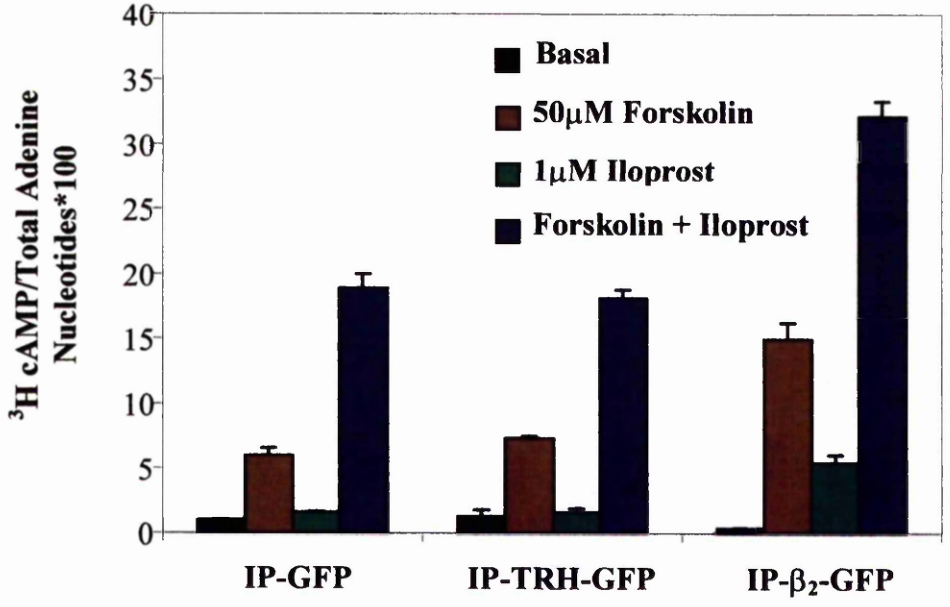
^{3}H cAMP/Total Adenine Nucleotides*100
40
35
30
25
20
15
10
5
0
Basal
50μM Forskolin
1μM Iloprost
Forskolin + Iloprost
IP-GFP
IP-TRH-GFP
IP-β_2-GFP

Figure 3.5

The receptor-GFP constructs exhibit a diffuse pattern of expression in transiently transfected HEK293 cells.

Cells grown on coverslips were transfected with IP-GFP (a, b), IP-TRH-GFP (c, d) and IP-β_2-GFP (e, f) constructs. 48 hours post transfection, cells were treated with vehicle (a, c, e) or 1μM iloprost (b, d, f) for 30 min, before being fixed and mounted onto coverslips as described in section 2.7.6. The confocal images shown are representative from three individual experiments. Scale bar = 2.5μM.

Fig. 3.5

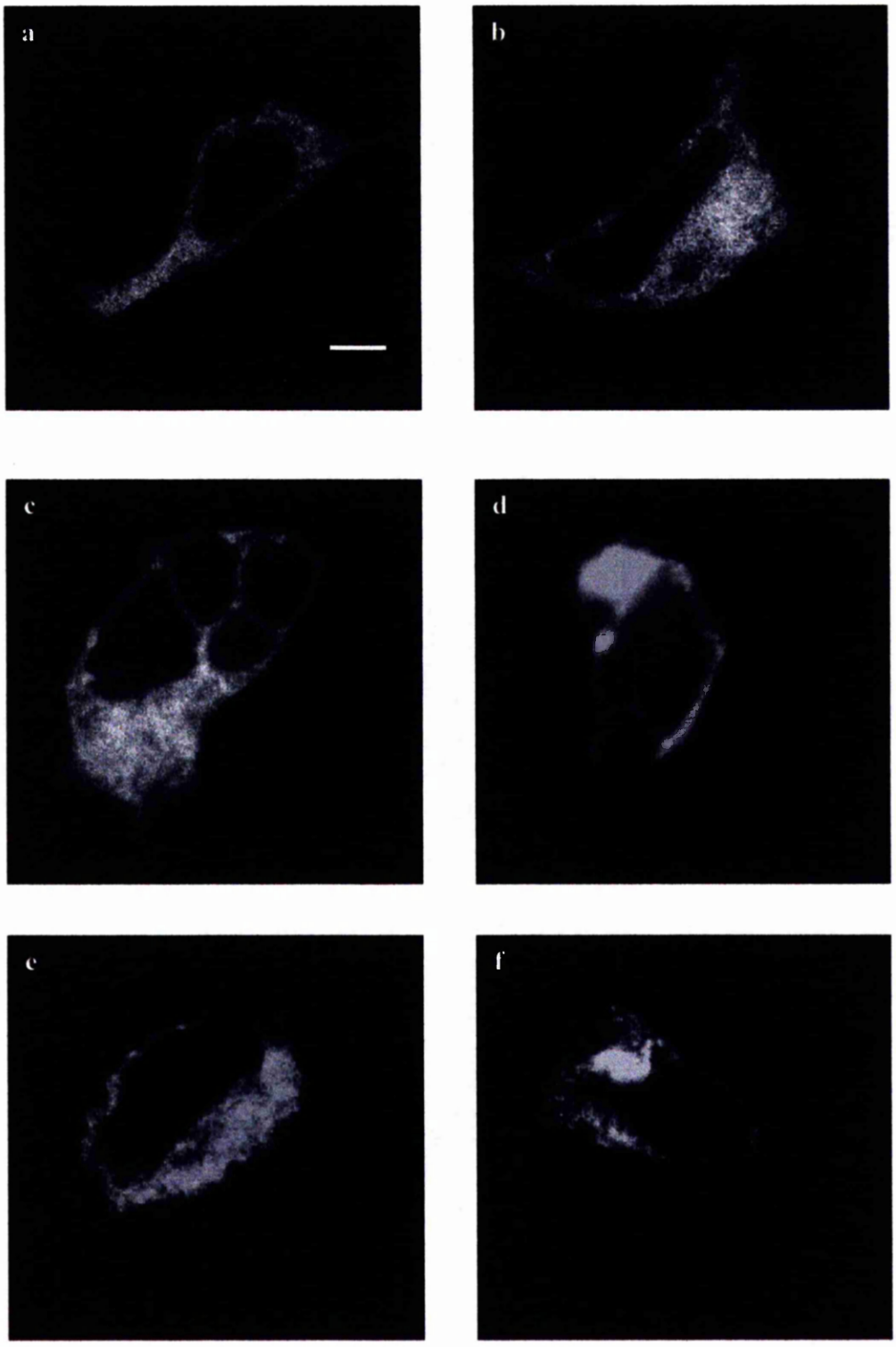

Figure 3.6

One-point [^{3}H] iloprost binding of the stable cell clones.

An indication of the receptor expression level in each of the positive stable cell clones generated for this study was determined by incubation of 40μg of membranes with ~20nM [^{3}H] iloprost as described in section 2.7.1. Data are means ± S.E.M. from a single experiment.

Figure 3.7

Whole-cell adenylyl cyclase activity of the stable cell clones.

The capacity of each of the positive stable clones to couple to G_s was assessed by stimulation of cells with 1μM iloprost for 15 min. Data are means ± S.E.M. from a single experiment.

Fig. 3.6

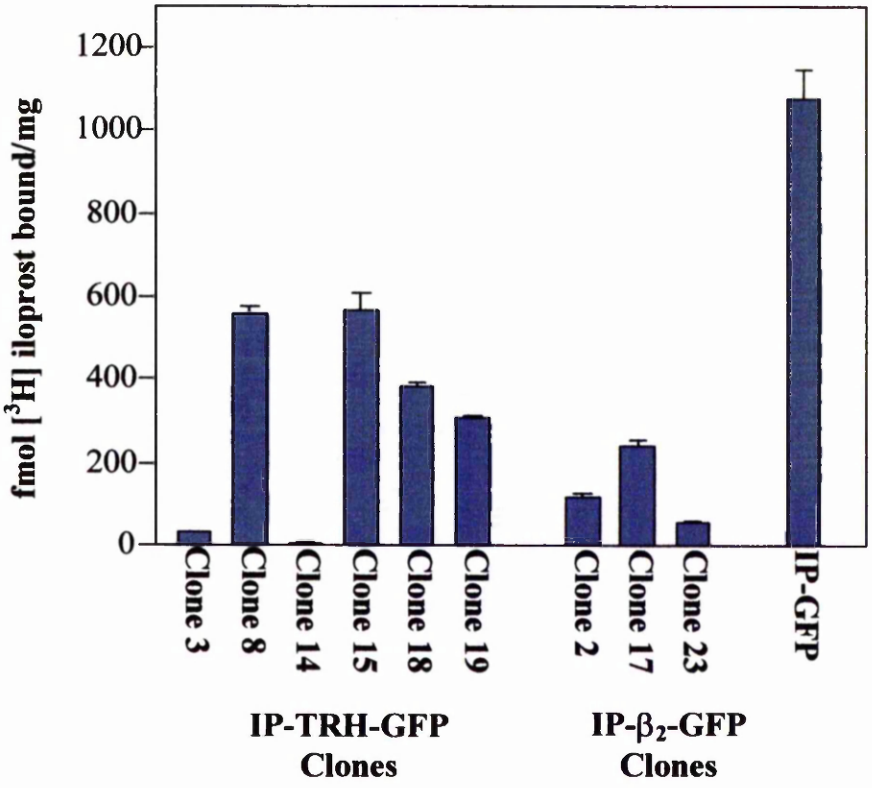
fmol [3H] iloprost bound/mg
1200
1000
800
600
400
200
0
Clone 3
Clone 8
Clone 14
Clone 15
Clone 18
Clone 19
Clone 2
Clone 17
Clone 23
IP-GFP
IP-TRH-GFP Clones
IP-β2-GFP Clones

Fig. 3.7

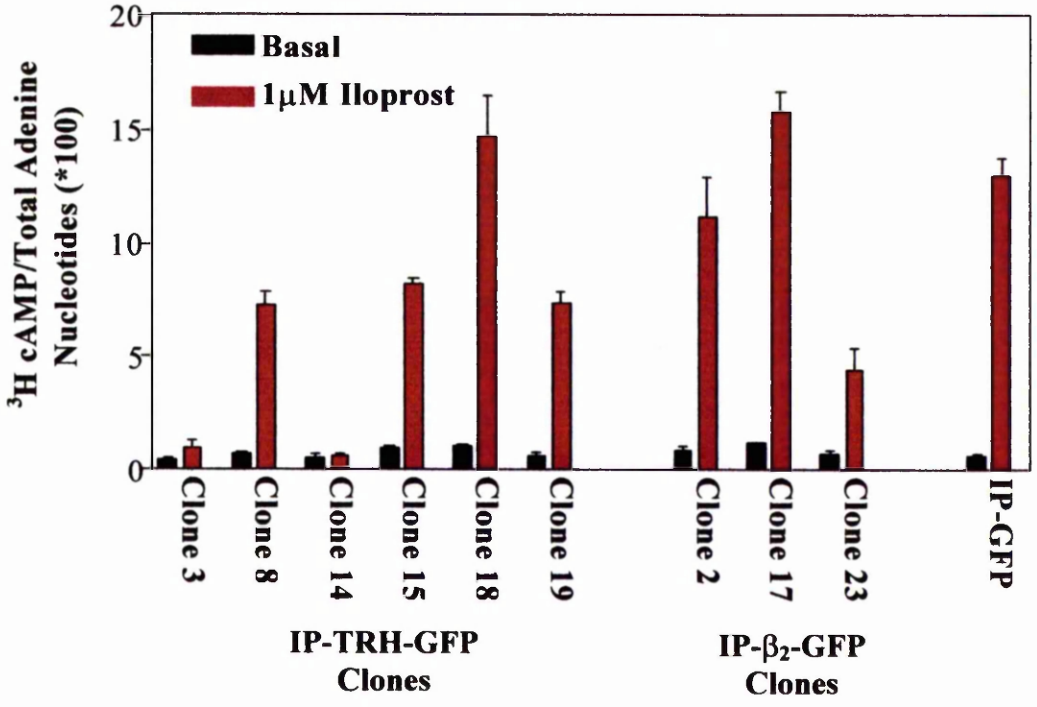
3H cAMP/Total Adenine Nucleotides (*100)
20
15
10
5
0
Basal
1μM Iloprost
Clone 3
Clone 8
Clone 14
Clone 15
Clone 18
Clone 19
Clone 2
Clone 17
Clone 23
IP-GFP
IP-TRH-GFP Clones
IP-β2-GFP Clones

Figure 3.8

a) Confocal analysis of the IP-TRH-GFP stable cell clones.

All the positive stable clones were imaged by confocal microscopy to determine the distribution of the receptors in the HEK293 cells. Each clone exhibited notable intracellular expression in the unstimulated state. Scale bar = 10μM.

b) Imaging of the IP-β_2-GFP stable cell clones.

The GFP autofluorescence of the clones was found at the cells' plasma membrane but a large portion of receptor was also localised intracellularly. Scale bar = 10μM.

Fig 3.8a

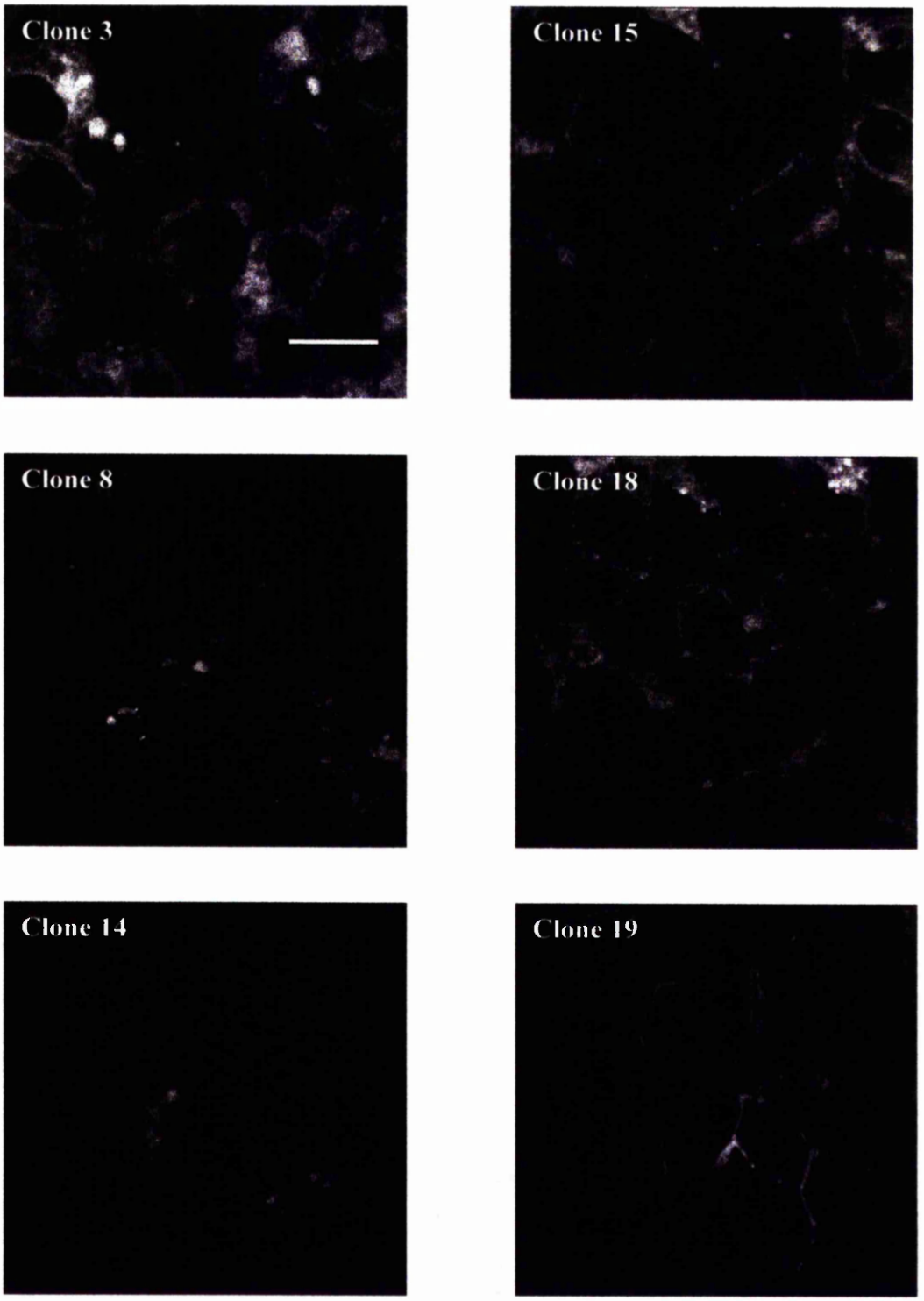

Fig. 3.8b

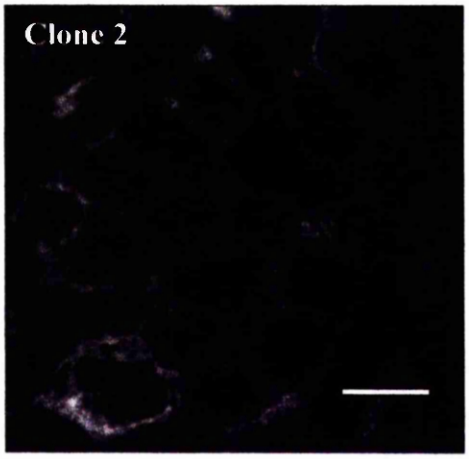

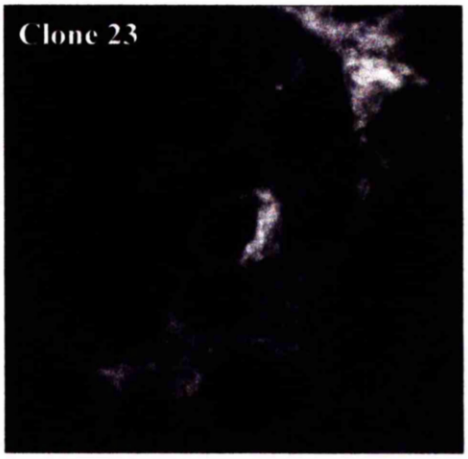

Figure 3.9

Saturation [^{3}H] iloprost binding of the receptor-GFP constructs in the selected stably expressing clones.

a) Membranes from the IP-GFP stable clone were incubated with increasing concentrations of [^{3}H] iloprost as detailed in section 2.7.1. Specific binding (fmol/mg) was calculated by incubation with 20μM unlabelled iloprost. The data shown is representative of a single experiment (means ± S.E.M) which was performed three times with similar results. Non-specific binding at 10nM [^{3}H] iloprost was 33% of the total binding. Non-specific binding at 50nM [^{3}H] iloprost was 46%.

b) Transformation of the non-linear curve into a Scatchard plot. Estimations of the K_d values from the three experiments were 2.6 ± 0.25nM (B_{max} of 696 ± 53.4 fmol/mg) and 66.9 ± 5.3nM (B_{max} of 4806 ± 106 fmol/mg).

c) IP-TRH-GFP cell membranes were incubated with varying concentrations of [^{3}H] iloprost. A saturation curve from a single experiment is shown. The experiment was repeated twice with similar results. Non-specific binding at 10nM [^{3}H] iloprost was 36% of the total binding. Non-specific binding at 50nM [^{3}H] iloprost was 49%.

d) Scatchard plot of the data from the saturation curve in c). The estimated dissociation constants from the three experiments were 2.9 ± 0.5nM (B_{max} of 682 ± 83.7 fmol/mg) and 33.5 ± 4.6nM (B_{max} of 1591 ± 157 fmol/mg).

e) Saturation binding studies of IP-β_2-GFP membranes were performed to determine receptor expression level and ligand binding affinity. The data shown are from a single experiment. Two further experiments were performed with similar results. Non-specific binding at 10nM [^{3}H] iloprost was 37% of the total binding. Non-specific binding at 50nM [^{3}H] iloprost was 54%.

f) Transformation of the data in e) into a Scatchard plot. The predicted K_d values from the experiments were 1.12 ± 0.28nM (B_{max} 168 ± 48.5 fmol/mg) and 81.6 ± 25.6nM (B_{max} 1780 ± 145 fmol/mg).

Fig. 3.9

a)

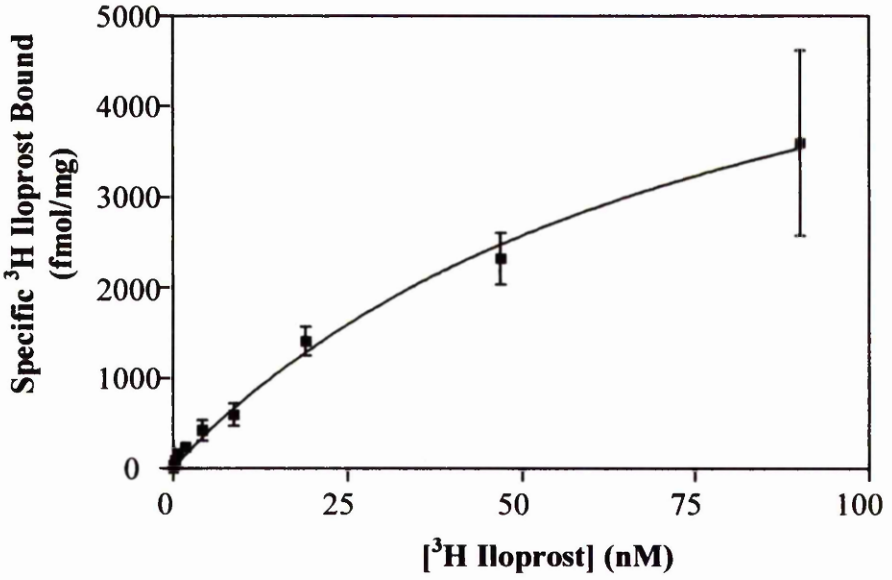
Specific ^{3}H Iloprost Bound (fmol/mg)
5000
4000
3000
2000
1000
0
0
25
50
75
100
[^{3}H Iloprost] (nM)

b)

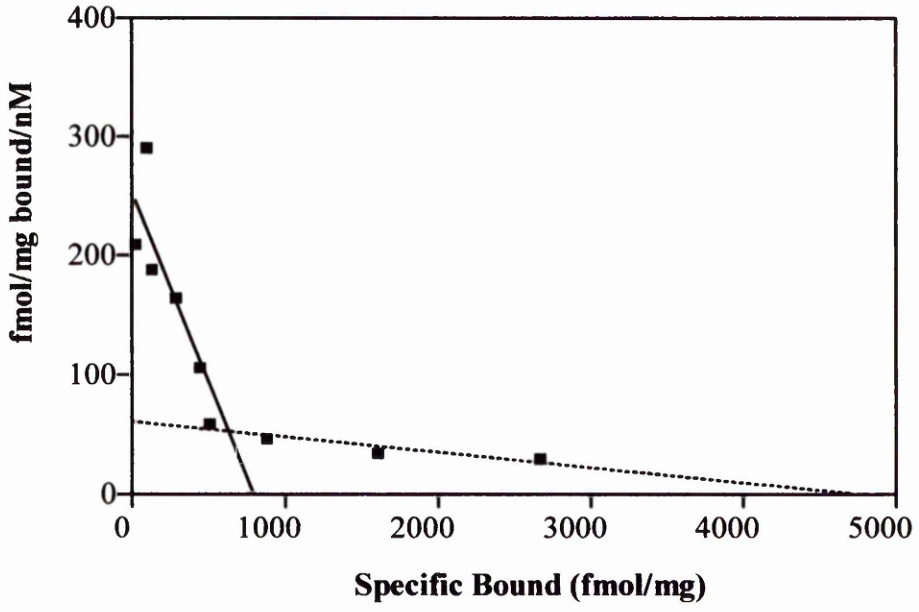
fmol/mg bound/nM
400
300
200
100
0
0
1000
2000
3000
4000
5000
Specific Bound (fmol/mg)

c)

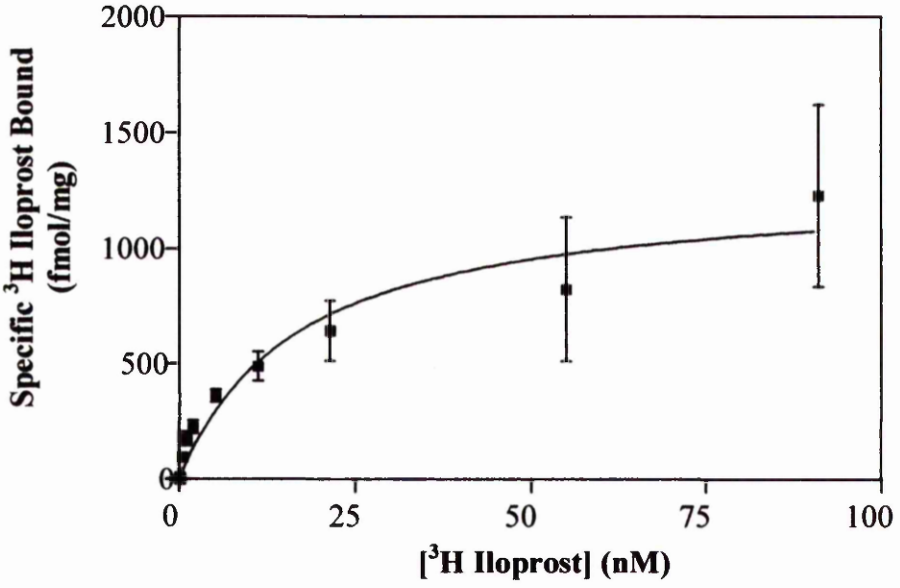
2000
1500
1000
500
0
Specific ^{3}H Iloprost Bound (fmol/mg)
0
25
50
75
100
[^{3}H Iloprost] (nM)

d)

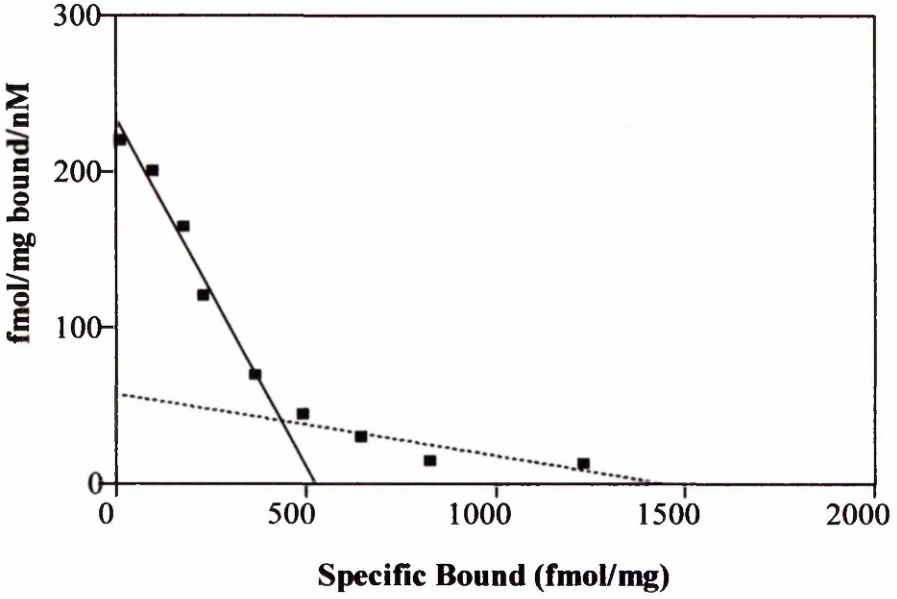
300
200
100
0
fmol/mg bound/nM
0
500
1000
1500
2000
Specific Bound (fmol/mg)

e)

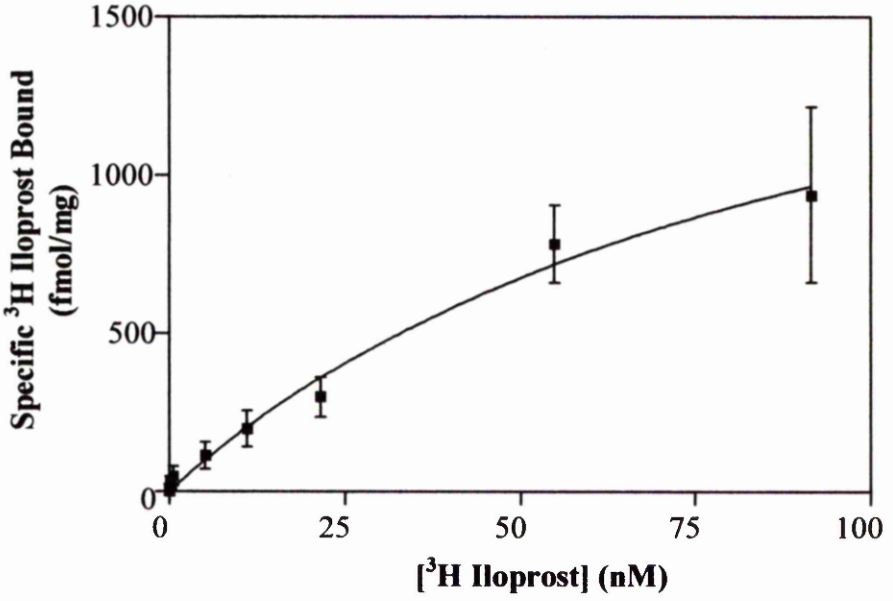
Specific ^{3}H Iloprost Bound (fmol/mg)
1500
1000
500
0
0
25
50
75
100
[^{3}H Iloprost] (nM)

f)

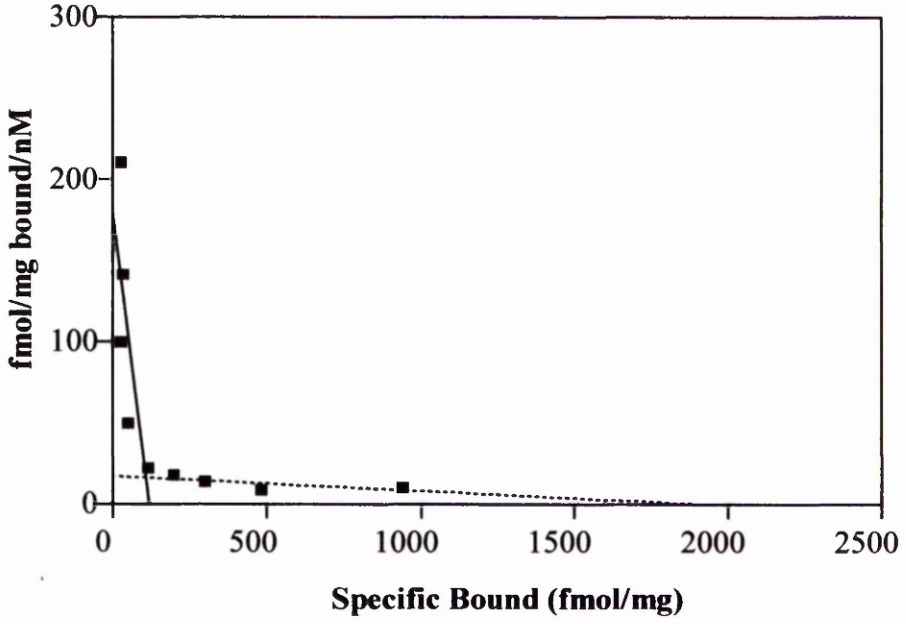
fmol/mg bound/nM
300
200
100
0
0
500
1000
1500
2000
2500
Specific Bound (fmol/mg)

Figure 3.10

Homologous displacement binding of [^{3}H] iloprost to the receptor-GFP stable cell membranes.

The binding of 20nM [^{3}H] iloprost to 40μg membrane preparations of the IP-GFP, IP-TRH-GFP, and IP-β_2-GFP stable cell clones was displaced by increasing concentrations of the unlabelled drug. The specific [^{3}H] iloprost binding (fmol/mg) is expressed as a percentage of the binding observed in the absence of unlabelled drug iloprost (set at 100%). The data shown represent means ± S.E.M. from a single assay performed in triplicate. Similar results were obtained from two additional experiments. Applying the formalisms of De Blasi and coworkers (1989), the estimated K_d values were 67.6 ± 7.5nM for IP-GFP, 32 ± 4nM for IP-TRH-GFP, and 42 ± 7nM for IP-β_2-GFP receptors. The Hill slope coefficients for the IP-GFP, IP-TRH-GFP, and IP-β_2-GFP curves shown are -0.9, -1.3, and –0.9 respectively.

Figure 3.10

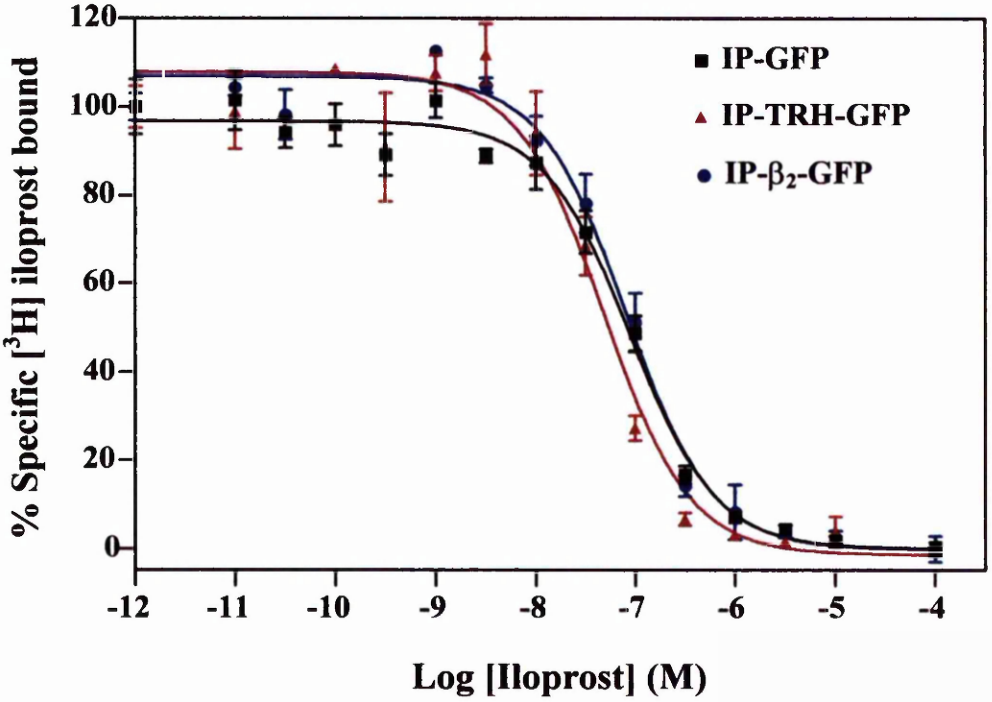
120
100
80
60
40
20
0
% Specific [3H] iloprost bound
-12
-11
-10
-9
-8
-7
-6
-5
-4
Log [Iloprost] (M)
IP-GFP
IP-TRH-GFP
IP-β2-GFP

Figure 3.11

Agonist stimulated adenylyl cyclase stimulation in intact cells stably expressing the receptor-GFP constructs.

Adenylyl cyclase dose response assays were performed as detailed in section 2.7.3. The IP-GFP, IP-TRH-GFP, and IP-β_2-GFP clones were challenged with varying concentrations of iloprost for 30 min and the stimulated cAMP production was determined as described in section 2.7.3. The data shown represent means ± S.E.M. from a single assay performed in triplicate. Similar data were obtained from two further experiments. The average EC_{50} values of agonist potency were 0.096 ± 0.022nM at the IP-GFP receptor, 0.41 ± 0.07nM at the IP-TRH-GFP receptor and 0.36 ± 0.05nM at the IP-β_2-GFP receptor.

Fig. 3.11

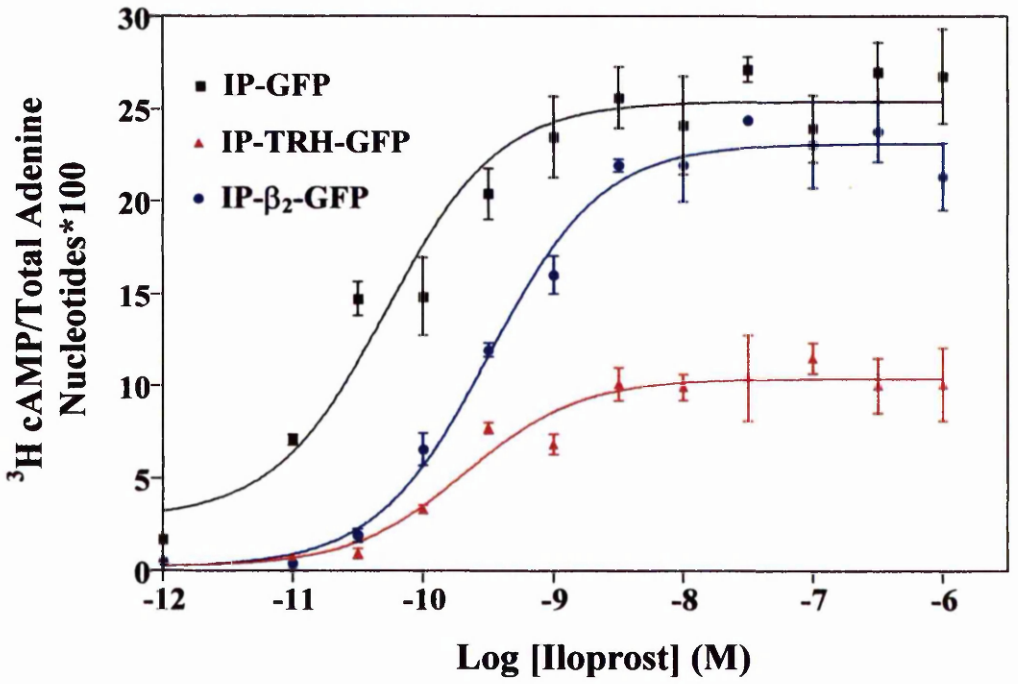
30
25
20
15
10
5
0
-12
-11
-10
-9
-8
-7
-6
IP-GFP
IP-TRH-GFP
IP-β2-GFP
3H cAMP/Total Adenine Nucleotides*100
Log [Iloprost] (M)

Figure 3.12

Internalisation of the IP-GFP receptors.

Confocal microscopy of the IP-GFP stable clone was used to visualise agonist-mediated internalisation of the receptors. Cells were visualised prior to agonist treatment (a) and after the addition of 1μM iloprost for 5 (b), 15 (c), 30 (d) and 60 (e) minutes. The images shown are representative of at least three separate experiments. Scale bar = 10μM.

Fig. 3.12

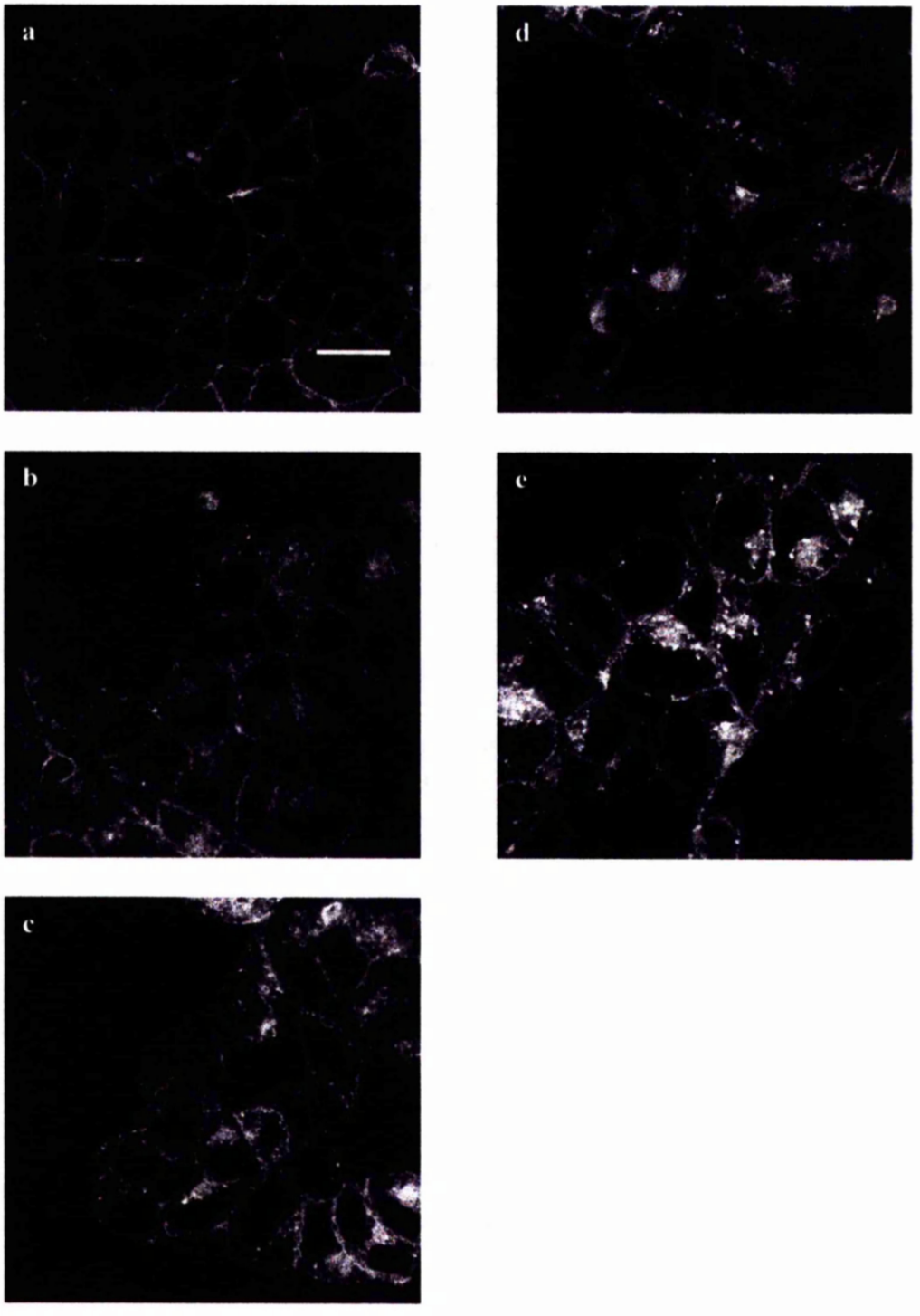

Figure 3.13

Confocal analysis of IP-TRH-GFP sequestration.

The ligand-induced internalisation of the IP-TRH-GFP receptor was visualised by confocal microscopy. Cell images were taken prior to agonist treatment (a) and after the addition of 1μM iloprost for 5 (b), 15 (c), 30 (d) and 60 (e) minutes. The images are representative of at least three further experiments. Scale bar = 10μM.

Fig. 3.13

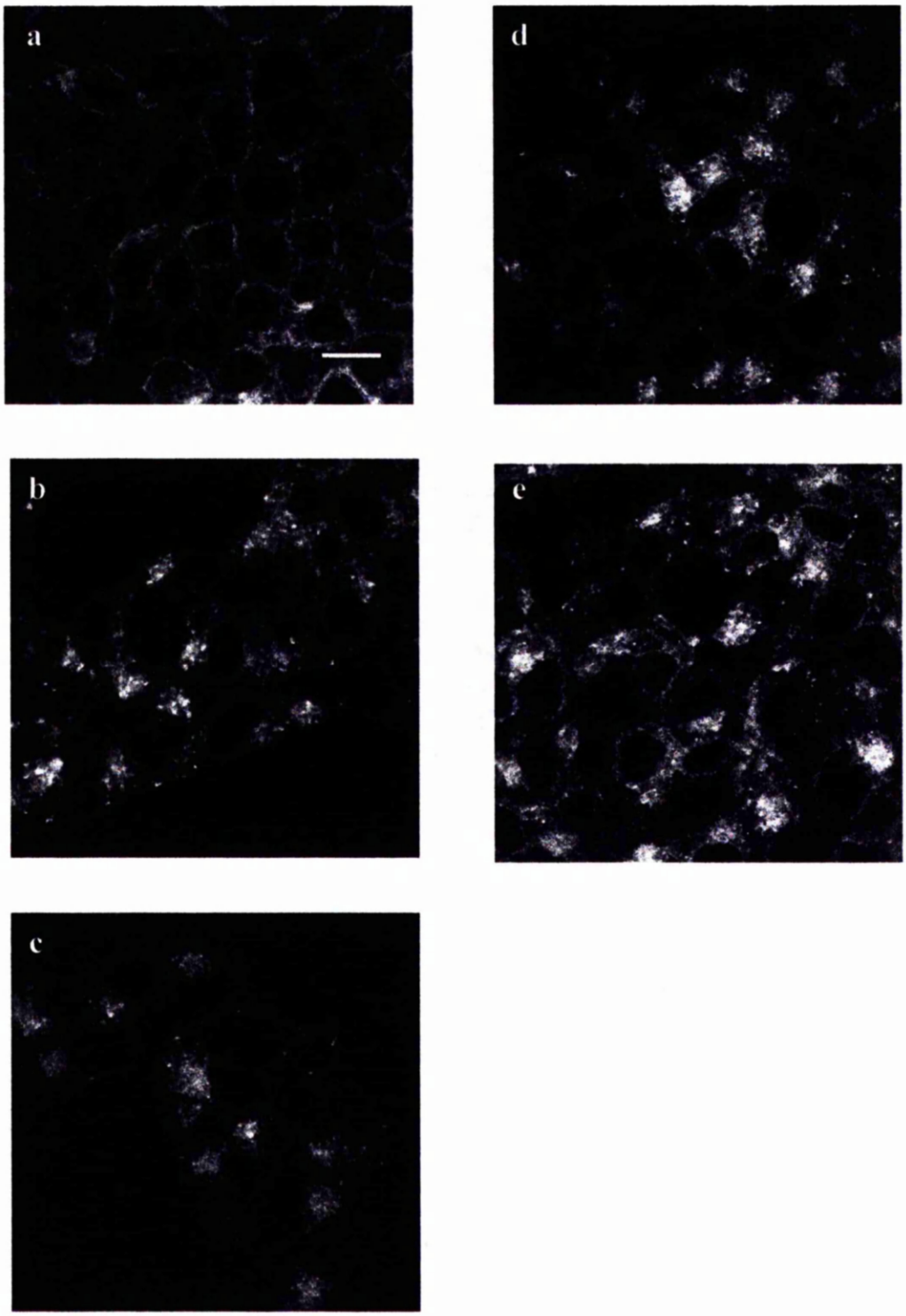

Figure 3.14

Visualisation of IP-β_2-GFP internalisation.

Confocal images of IP-β_2-GFP cells were taken prior to agonist treatment (a) and after the incubation with 1μM iloprost at 5 (b), 15 (c), 30 (d) and 60 (e) minute intervals to visualise receptor sequestration. The images are representative of at least three additional experiments. Scale bar = 10μM.

Fig. 3.14

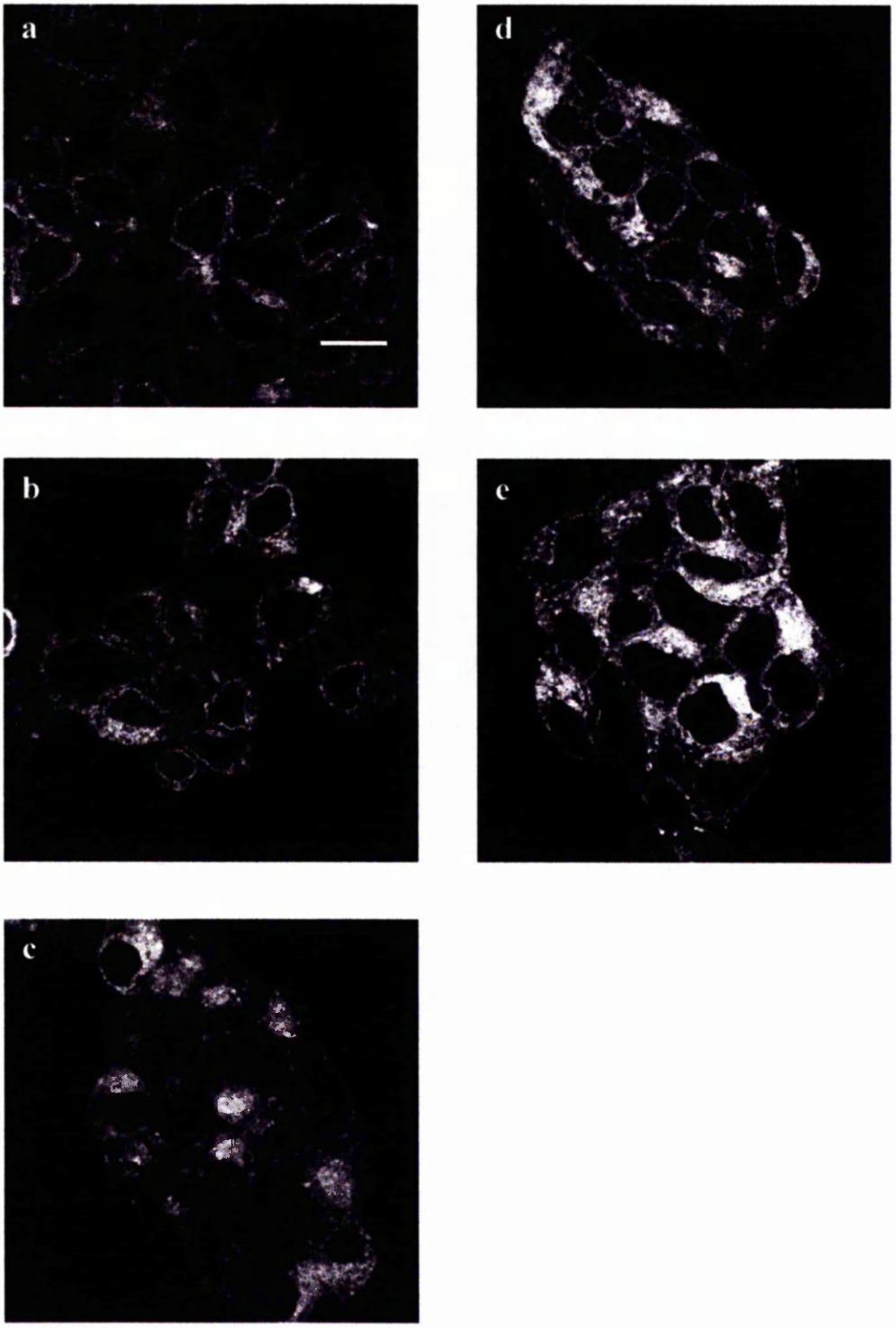

Figure 3.15

Immunocytochemical staining of the receptor-GFP stables using an anti-FLAG™ antibody: non-specific binding of the antibody to receptor-GFP chimeras.

IP-GFP (a), IP-TRH-GFP (b), and IP-β_2-GFP cells were incubated with an antibody against the N-terminal FLAG epitope as described in section 2.7.6 to visualise the cell surface receptor population. In IP-GFP cells, successful decoration of receptors was achieved, however, antibody labelling of the IP-TRH-GFP and IP-β_2-GFP cell lines was non-specific. Scale bar = 10μM.

Figure 3.15

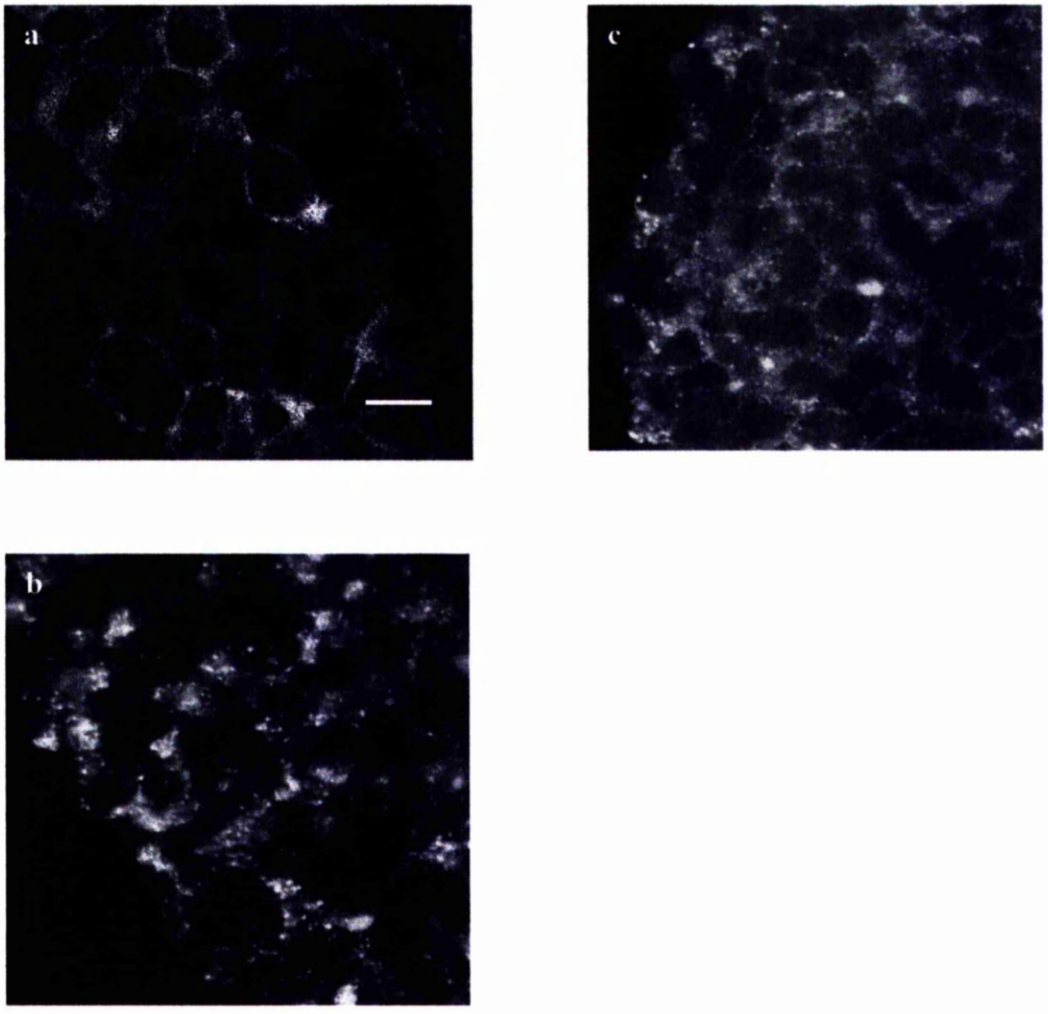

Figure 3.16

Time course of the agonist-mediated internalisation of the IP-GFP receptors.

a) IP-GFP cells were incubated with vehicle (1) or 1μM iloprost for 5 (2), 15 (3), 30 (4), and 60 (5) min at 37°C. Cell surface glycoproteins were labelled with biotin and the receptors were immunoprecipitated and visualised as detailed in section 2.7.5. A representative blot from three individual experiments is shown.

b) Blots were quantified by densitometric scanning. The values shown represent mean ± S.E.M. for three experiments, with the levels of cell surface receptors observed in the absence of agonist set at 100%.

Fig. 3.16

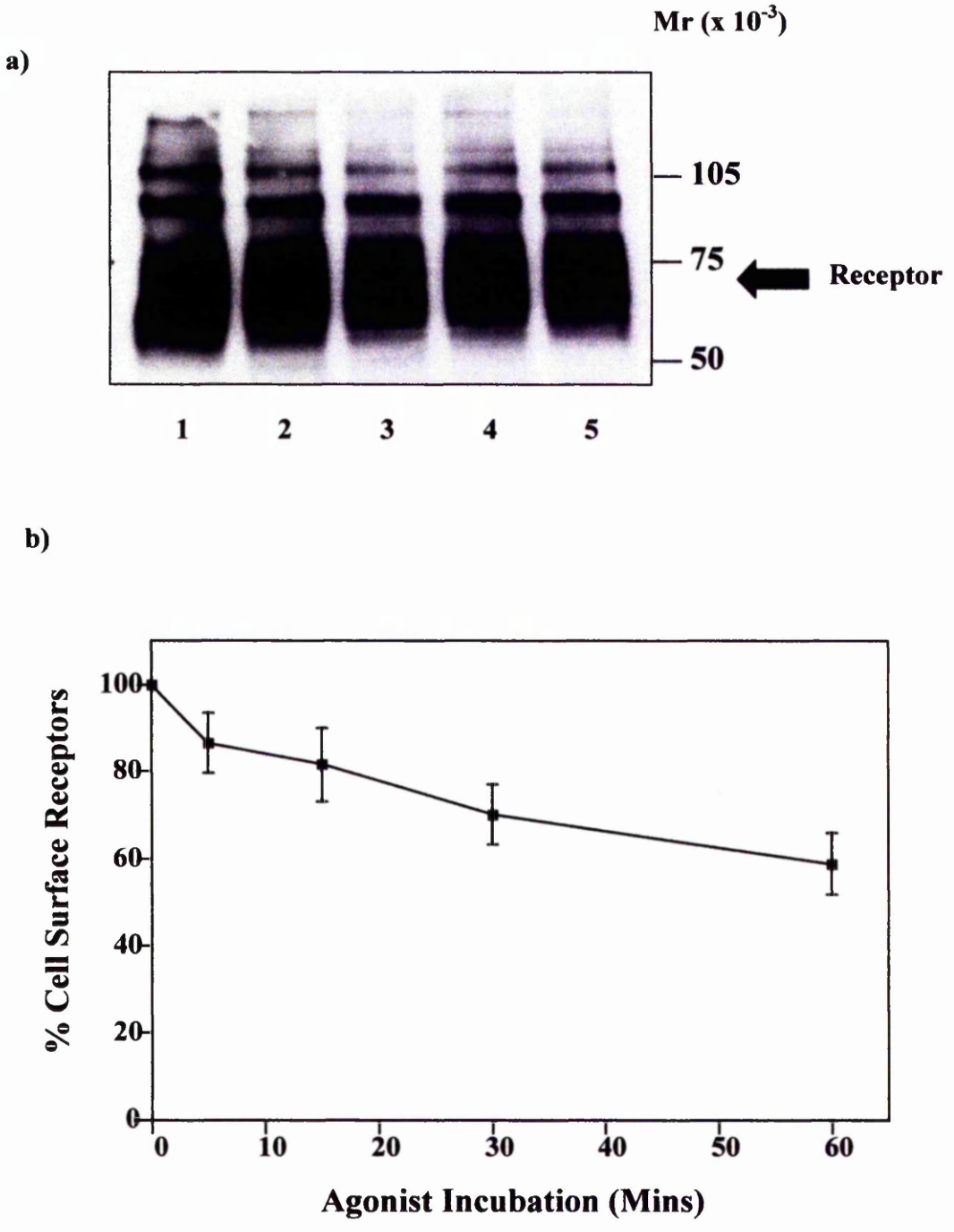
a)
Mr (x 10-3)
105
75
50
Receptor
1
2
3
4
5
b)
% Cell Surface Receptors
100
80
60
40
20
0
0
10
20
30
40
50
60
Agonist Incubation (Mins)

Figure 3.17

Quantification of agonist-mediated internalisation of the IP-TRH-GFP receptors.

a) After incubation with vehicle (1) or 1μM iloprost for 5 (2), 15 (3), 30 (4), and 60 (5) min at 37°C, biotin-labelled cell surface IP-TRH-GFP receptors were immunoprecipitated and visualised. A representative blot from three separate experiments is shown.

b) Quantification of receptor internalisation by densitometric analysis of the biotin blots. The values shown represent mean ± S.E.M. for three experiments, with the levels of cell surface receptors observed in the absence of agonist set at 100%.

Fig. 3.17

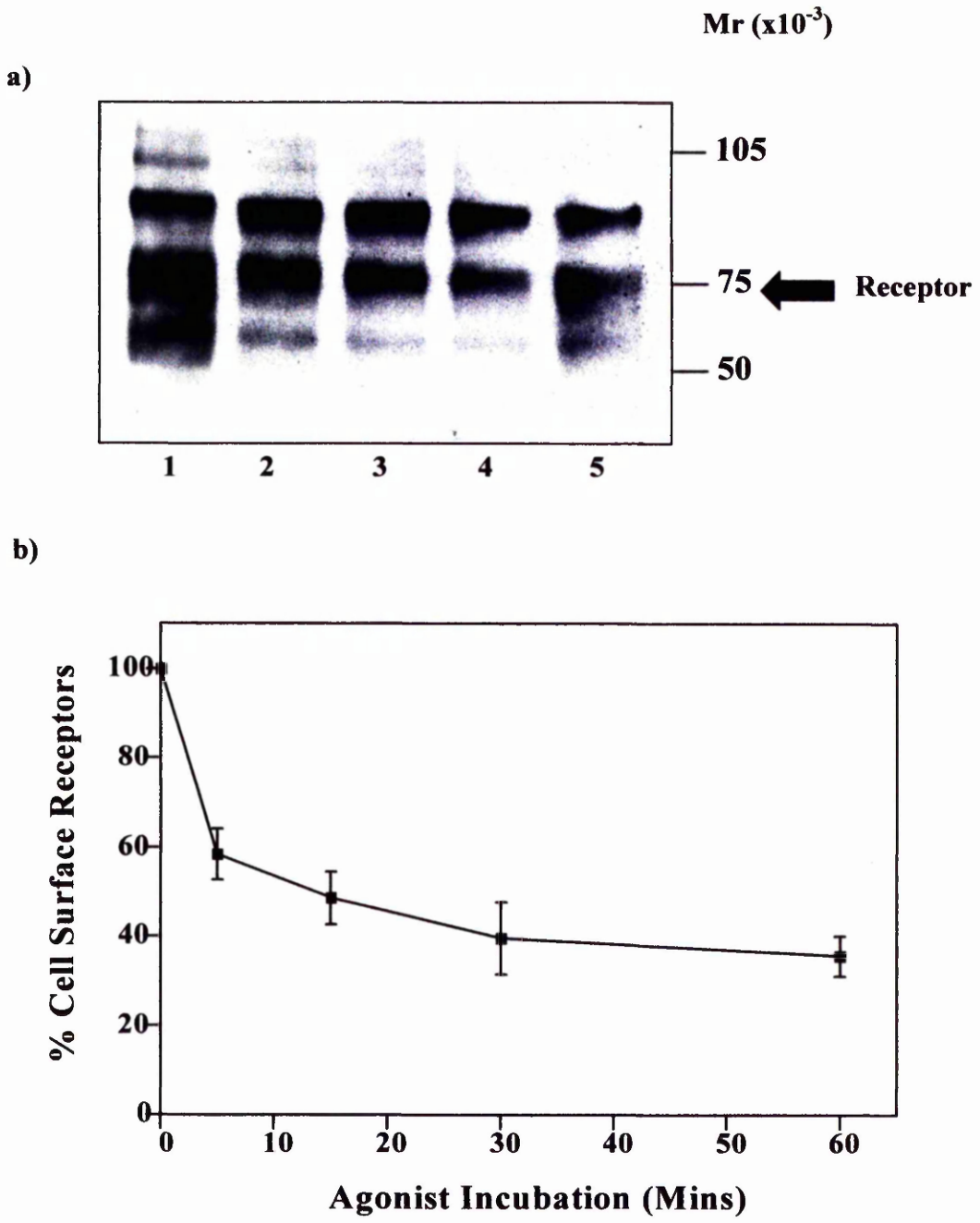
Mr (x10-3)
a)
105
75
Receptor
50
1
2
3
4
5
b)
% Cell Surface Receptors
100
80
60
40
20
0
0
10
20
30
40
50
60
Agonist Incubation (Mins)

Figure 3.18

Quantitative analysis of agonist-stimulated internalisation of the IP-β_2-GFP receptors.

a) Cells were challenged with vehicle (1) or 1μM iloprost for 5 (2), 15 (3), 30 (4), and 60 (5) min at 37°C, prior to biotin-labelling of the plasma membrane receptor population. Receptors were immunoprecipitated and the biotin-labelled receptors were detected in blots. The blot shown is similar to those generated from two further experiments.

b) Densitometric scanning of the biotin blots was used to quantify the levels of cell surface receptors over the time course. The values shown represent mean ± S.E.M. for three experiments, with the levels of cell surface receptors observed in the absence of agonist set at 100%.

Fig. 3.18

a)

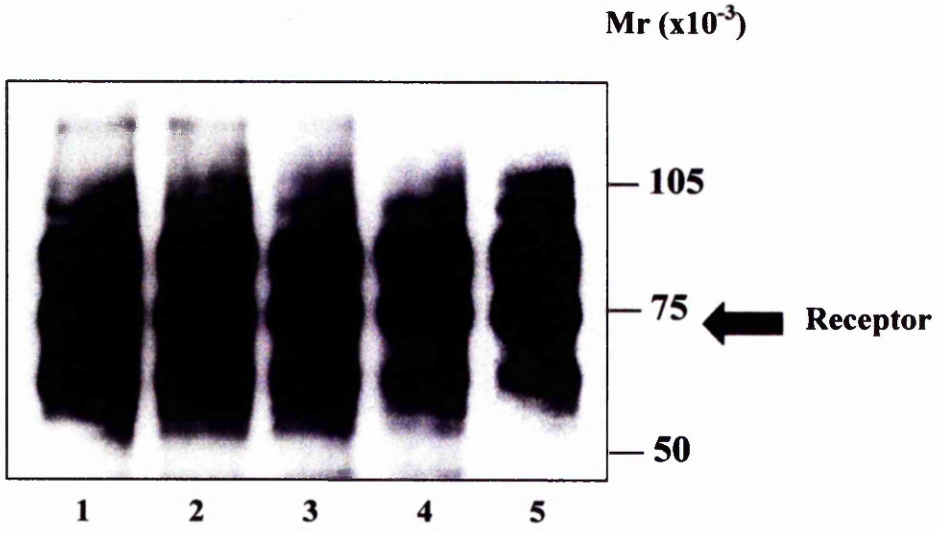
Mr (x10-3)
105
75
Receptor
50
1
2
3
4
5

b)

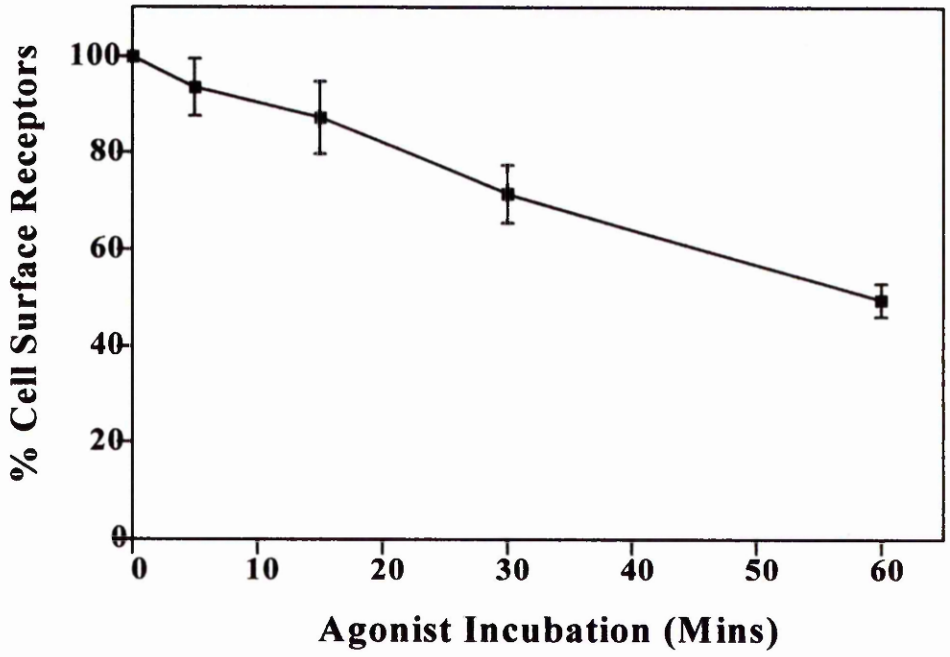
% Cell Surface Receptors
100
80
60
40
20
0
0
10
20
30
40
50
60
Agonist Incubation (Mins)

Figure 3.19

A general overview of the time courses of agonist-mediated internalisation of the receptor-GFP constructs.

Summary of the data shown in figures 3.16, 3.17, and 3.18 to emphasise the different internalisation properties of the full-length and chimeric GFP-tagged prostacyclin receptors.

Fig. 3.19

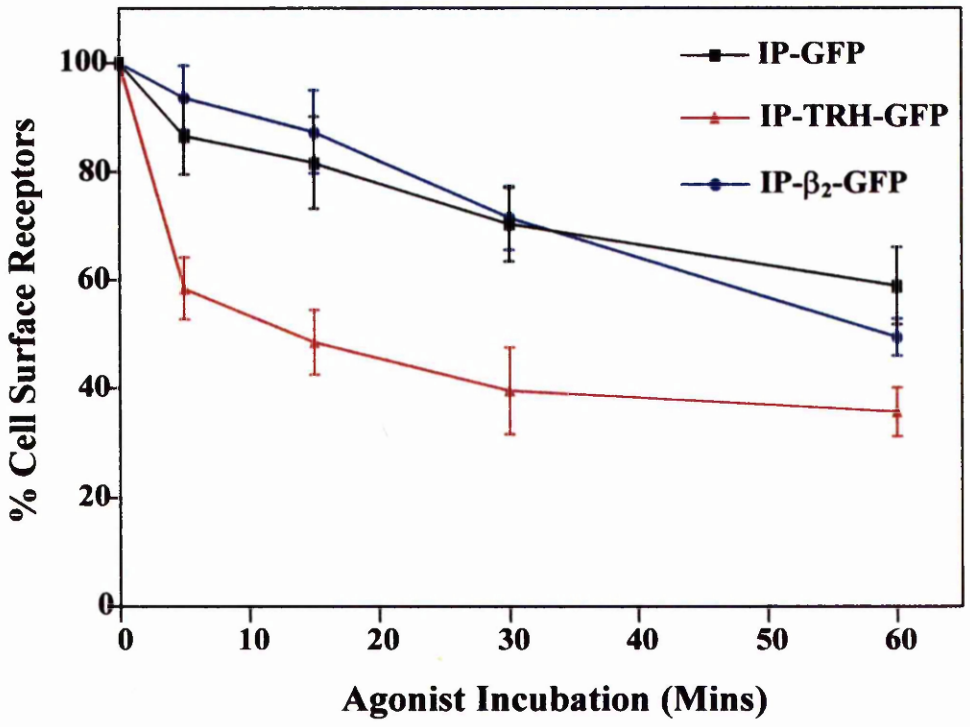
IP-GFP
IP-TRH-GFP
IP-β2-GFP
% Cell Surface Receptors
100
80
60
40
20
0
0
10
20
30
40
50
60
Agonist Incubation (Mins)

Figure 3.20

Diagrammatical representation of the HA-tagged prostacyclin receptor constructs generated for this study.

The HA-IP (a), HA-IP-TRH (b), and HA-IP-β_2 (c) cDNAs were constructed using a PCR-based strategy as described in section 2.4.

Figure 3.21

Western blotting of HEK293 membranes transiently expressing the HA-receptors.

20μg of membrane preparations from HEK293 cells transiently transfected with the HA-IP (1), HA-IP-TRH (2), HA-IP-β_2 (3) cDNAs, and empty vector (4) were resolved on SDS-PAGE gels then transferred onto nitrocellulose membranes and blotted with the 12CA5 antibody. Similar results were obtained from two further experiments.

Fig. 3.20

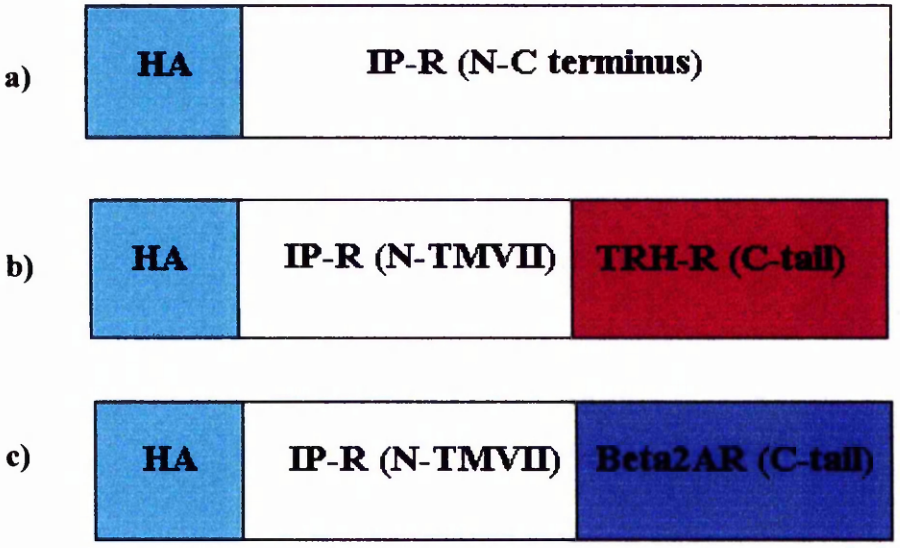

Fig. 3.21

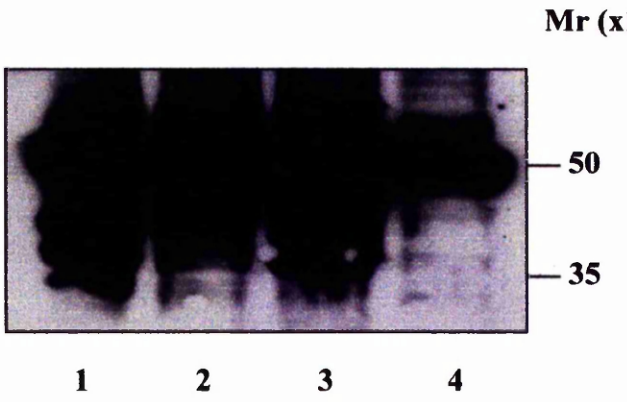

Figure 3.22

One-point [^{3}H] iloprost binding in intact HEK293 cells transiently transfected the HA-tagged receptor constructs.

The specific binding of [^{3}H] iloprost in intact cells transiently transfected with the HA-receptor constructs was determined by incubation with 20nM [^{3}H] iloprost as detailed in section 2.7.2. Data shown are presented as specific fmol bound/10^6 cells and are means ± S.E.M., n=3.

Figure 3.23

Adenylyl cyclase activity in cells transiently transfected with the HA-tagged receptors.

The capacity of the HA-tagged IP receptor proteins to couple to G_s coupling was assessed by stimulation of cells for 15 min with 1μM iloprost. Adenylyl cyclase activity in the cells was also assessed after direct activation of the enzyme with 50μM forskolin, or after both iloprost and forskolin incubation. The cAMP accumulation is expressed as a percentage of the total adenine nucleotide intracellular pool. The data shown represent means ± S.E.M. from a single assay performed in triplicate. A further two experiments produced similar results.

Fig. 3.22

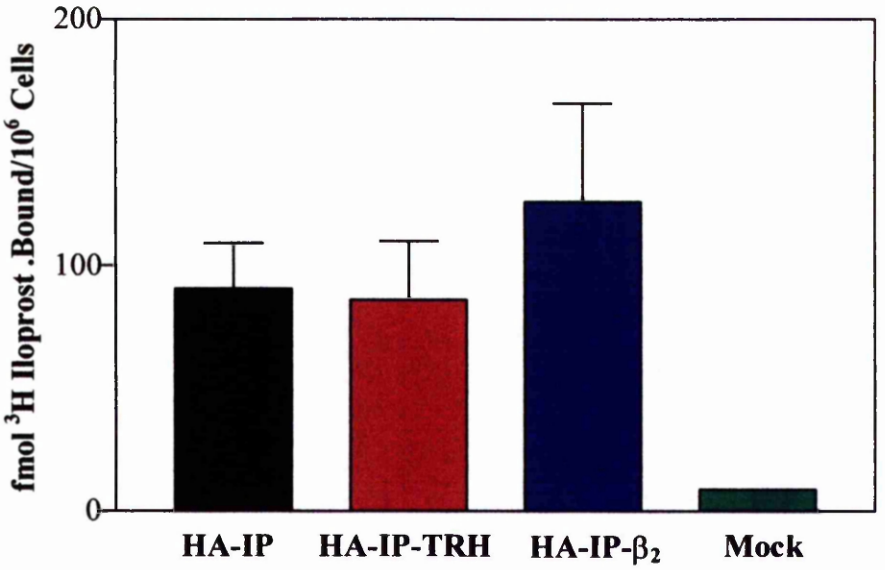

Fig. 3.23

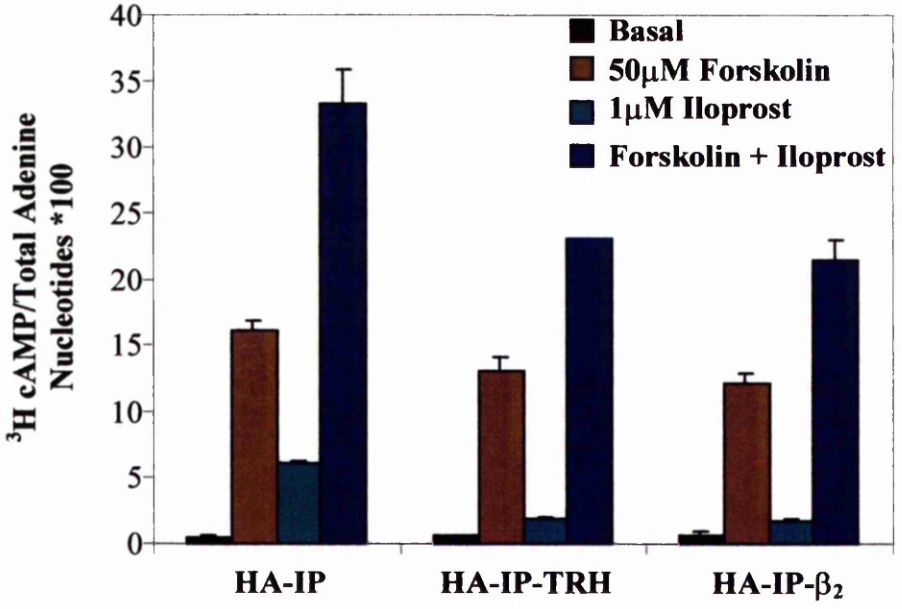

Figure 3.24

Visualisation of agonist-stimulated HA-IP receptor sequestration in transiently transfected HEK293 cells by immunocytochemical staining of receptors.

Cells transfected with the HA-IP receptor construct were immunostained with the 12CA5 antibody to label cell surface HA-IP receptors prior to agonist treatment as detailed in section 2.7.6. Cell images were taken before agonist treatment (a) and after the addition of 1μM iloprost for 5 (b), 15 (c), 30 (d) and 60 (e) minutes. The images are representative of at least two further experiments. Scale bar = 2.5μM.

Fig. 3.24

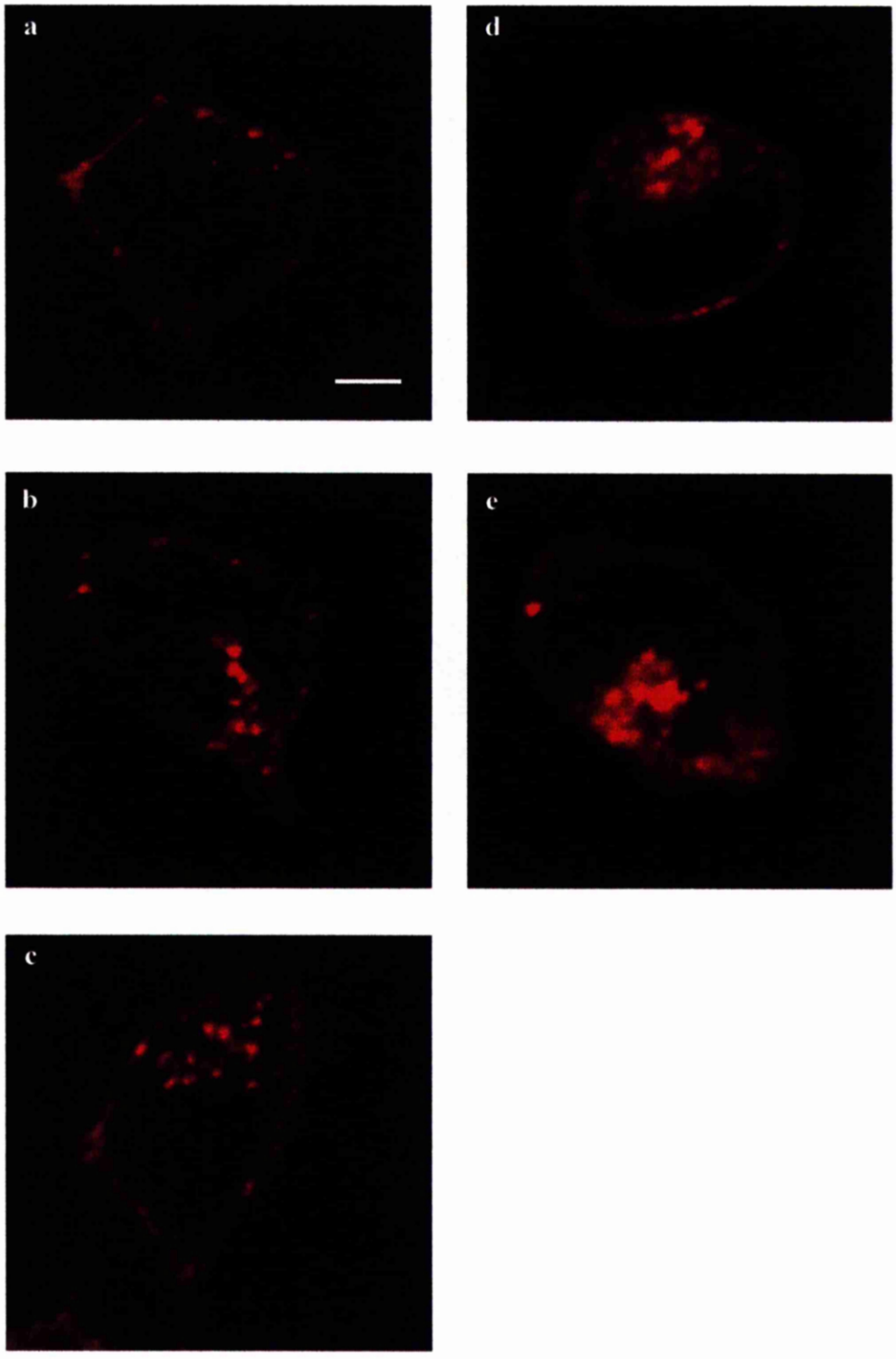

Figure 3.25

Confocal analysis of agonist-stimulated HA-IP-TRH receptor internalisation in transiently transfected HEK293 cells.

Cells transfected with the HA-IP-TRH receptor construct were immunostained using the 12CA5 antibody to label plasma membrane receptors prior to agonist treatment. The confocal images shown are before the addition of agonist (a) and after incubation with 1μM iloprost for 5 (b), 15 (c), 30 (d) and 60 (e) minutes. The images are representative of two further experiments. Scale bar = 2.5μM

Fig. 3.25

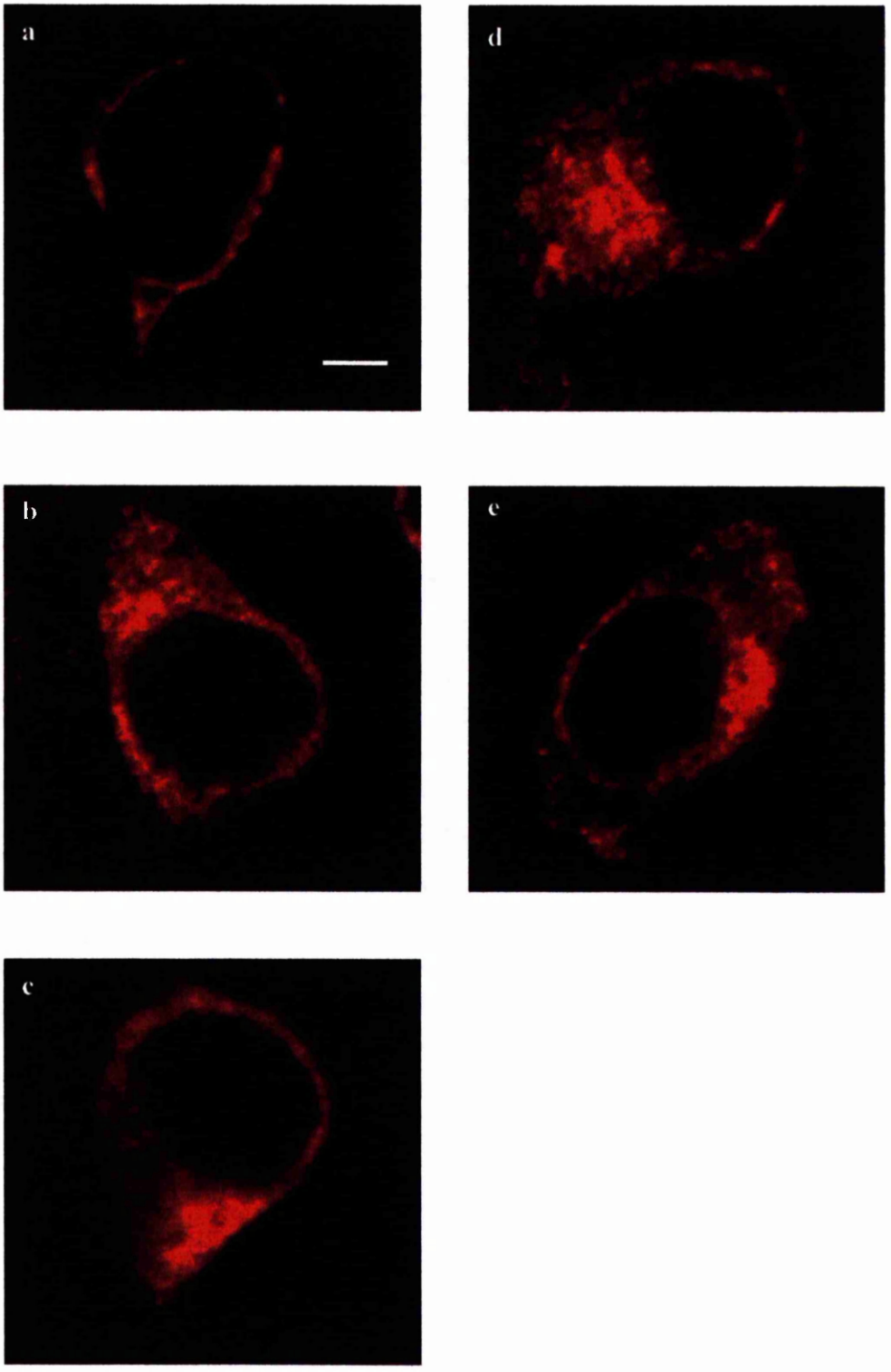

Figure 3.26

Confocal analysis of agonist-stimulated internalisation of the HA-IP-β_2 receptor construct in transiently transfected HEK293 cells.

Cells transfected with the HA-IP-β_2 receptor construct were incubated with the 12CA5 antibody to label the cell surface receptors prior to agonist treatment. The confocal images were taken of cells unstimulated (a) and after treatment with 1μM iloprost for 5 (b), 15 (c), 30 (d) and 60 (e) minutes. The images are representative of two further experiments. Scale bar = 2.5μM.

Fig. 3.26

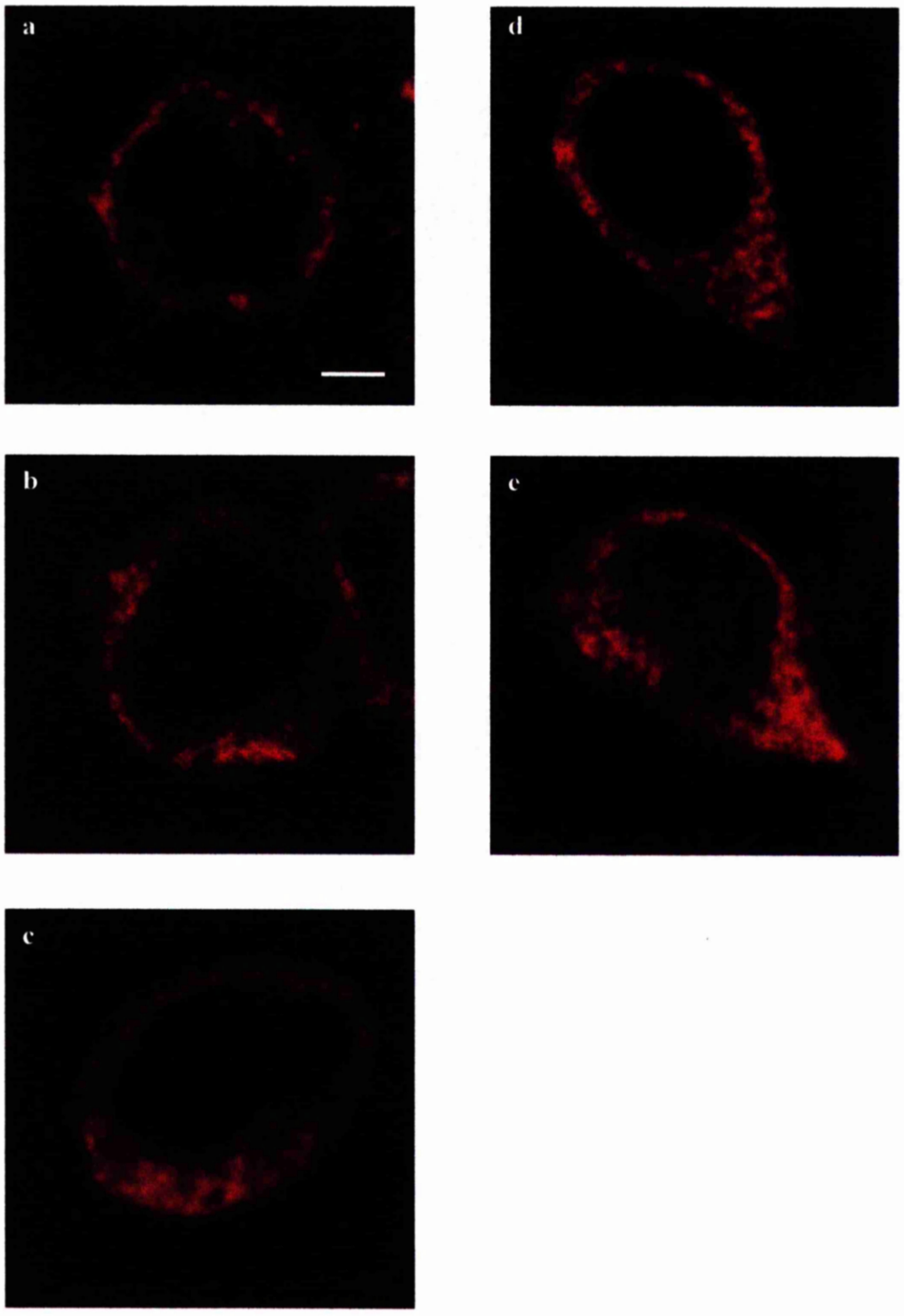

Figure 3.27

Quantification of agonist-mediated internalisation of the HA-IP receptors using biotin labelling receptors.

a) Cells transiently expressing the HA-IP receptor construct were incubated with vehicle (1) or 1μM iloprost for 5 (2), 15 (3), 30 (4), and 60 (5) min at 37°C. Cell surface glycoproteins were labelled with biotin and the receptors were immunoprecipitated and visualised as detailed in section 2.7.5. A representative blot from three individual experiments is shown.

b) Densitometric scanning of the biotin blots was used to quantify the levels of cell surface receptors over the time course. The values shown represent mean ± S.E.M. for three experiments, with the levels of cell surface receptors observed in the absence of agonist set at 100%.

Fig. 3.27

a)

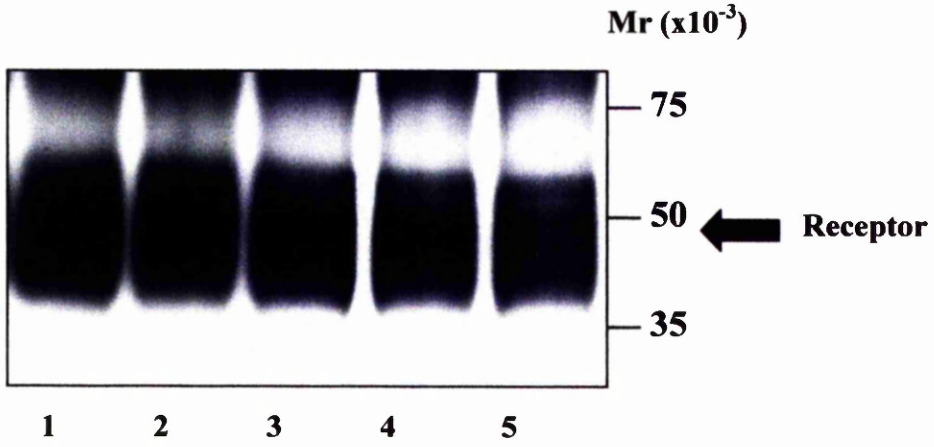
Mr (x10-3)
75
50
35
Receptor
1
2
3
4
5

b)

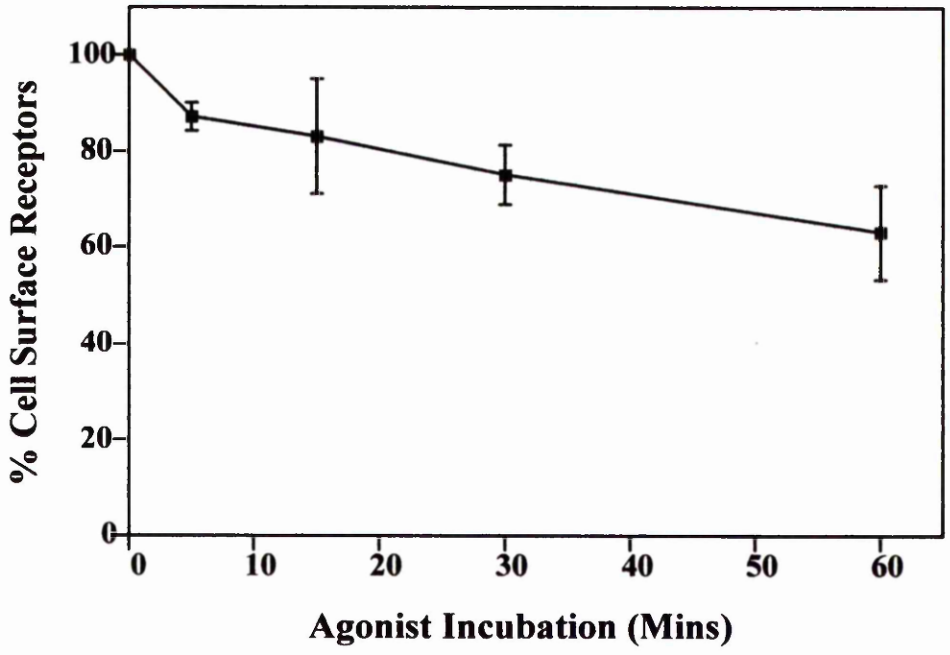
% Cell Surface Receptors
100
80
60
40
20
0
0
10
20
30
40
50
60
Agonist Incubation (Mins)

Figure 3.28

Quantitative analysis of agonist-stimulated internalisation of the HA-IP-TRH receptors.

a) Cells transfected with the HA-IP-TRH constructed were treated with vehicle (1) or 1μM iloprost for 5 (2), 15 (3), 30 (4), and 60 (5) min at 37°C. Cell surface glycoproteins were labelled with biotin and the receptors were immunoprecipitated and visualised as detailed in section 2.7.5. A representative blot from three individual experiments is shown.

b) Blots were quantified by densitometric scanning. The values shown represent mean ± S.E.M. for three experiments, with the levels of cell surface receptors observed in the absence of agonist set at 100%.

Fig. 3.28

a)

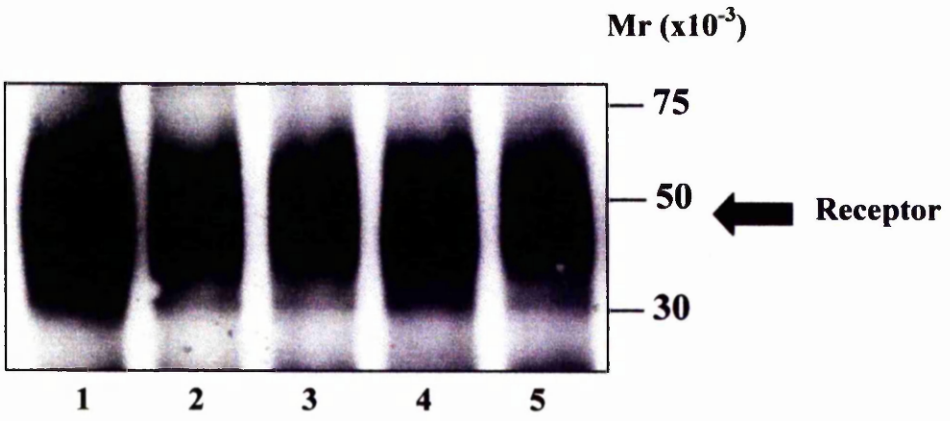
Mr (x10-3)
75
50
30
Receptor
1
2
3
4
5

b)

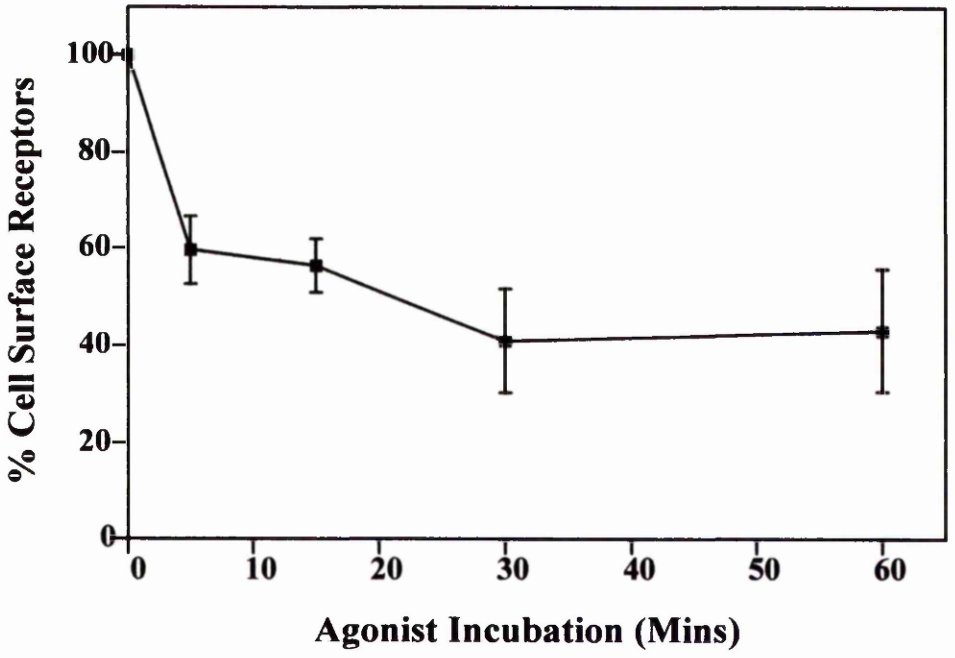
% Cell Surface Receptors
100
80
60
40
20
0
0
10
20
30
40
50
60
Agonist Incubation (Mins)

Figure 3.29

Quantitative analysis of agonist-stimulated internalisation of the HA-IP-β_2 receptors.

a) HEKK293 cells transiently transfected with the HA-IP-β_2 construct were challenged with vehicle (1) or 1μM iloprost for 5 (2), 15 (3), 30 (4), and 60 (5) min at 37°C, prior to biotin-labelling of the plasma membrane receptor population. Receptors were immunoprecipitated and the biotinylated receptors were detected in blots. The blot shown is typical of blots from two further experiments.

b) Receptor internalisation was assessed by densitometric scanning of the blots. The values shown represent mean ± S.E.M. for three experiments, with the levels of cell surface receptors observed in the absence of agonist set at 100%.

Fig. 3.29

a)

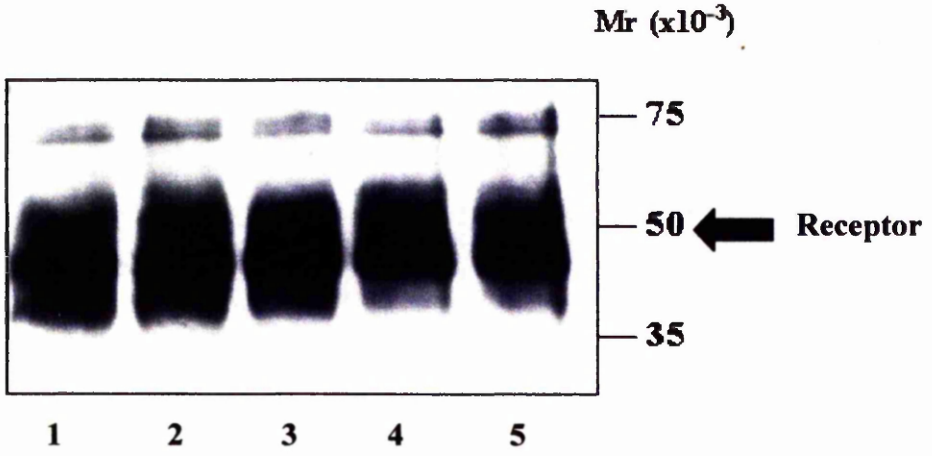
Mr (x10-3)
75
50
Receptor
35
1
2
3
4
5

b)

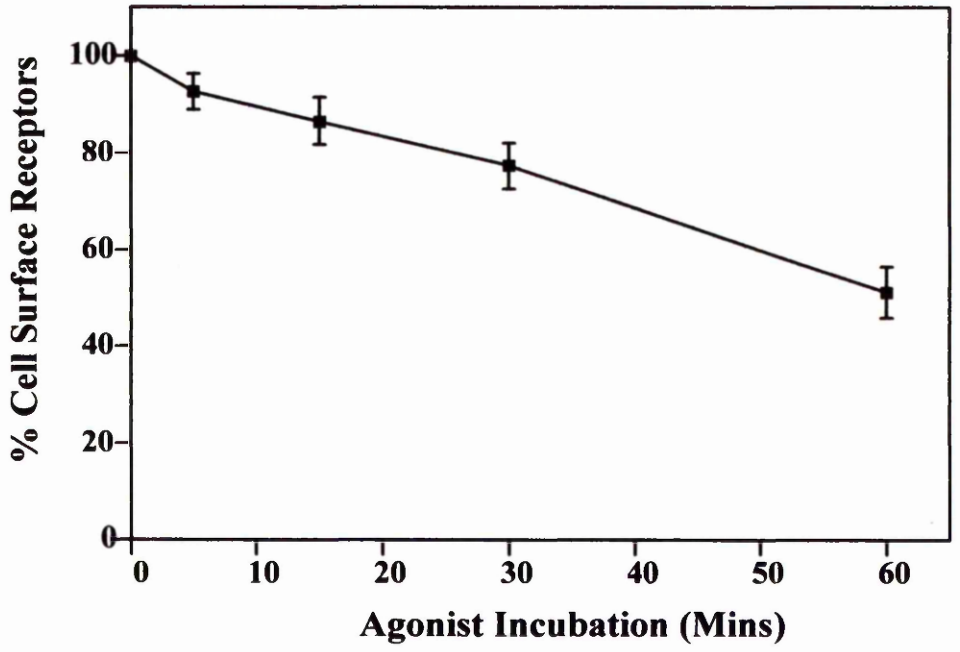
% Cell Surface Receptors
100
80
60
40
20
0
0
10
20
30
40
50
60
Agonist Incubation (Mins)

Figure 3.30

Comparison of the time courses of the agonist-mediated internalisation for each of the HA-receptor constructs.

An overview of the internalisation data in figures 3.27, 3.28, and 3.29. Taken together, the results reveal the differences in agonist-promoted internalisation exhibited by the full-length and chimeric HA-tagged prostacyclin receptors.

Fig. 3.30

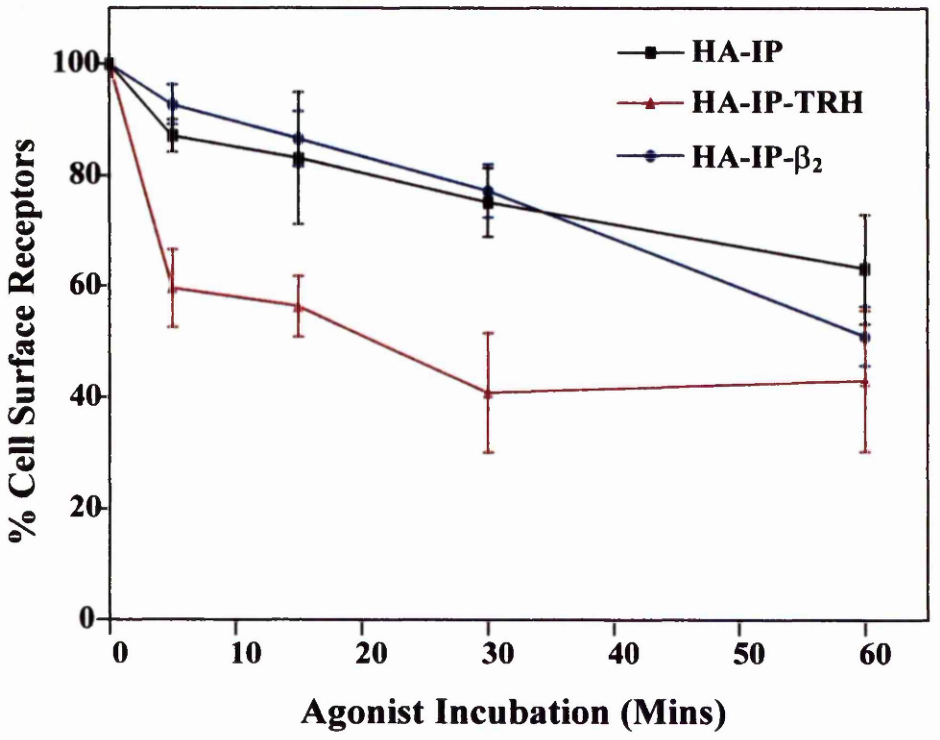
HA-IP
HA-IP-TRH
HA-IP-β2
% Cell Surface Receptors
100
80
60
40
20
0
0
10
20
30
40
50
60
Agonist Incubation (Mins)

3.7 Discussion

The majority of GPCRs undergo agonist-stimulated internalisation and therefore internalisation might be expected to involve a common mechanism. However, thus far, generalised domains and mechanisms for receptor internalisation have been difficult to ascertain. Many domains have been implicated in the internalisation of specific GPCRs. However, these domains have been localised to divergent regions of various receptors and often involve sequences not conserved in other members of the receptor superfamily. Alterations in the carboxyl terminus have been found to influence internalisation in the widest variety of receptors. Many studies have used point mutations and/or truncations of the receptor C-tail to directly study this. A complication of such manipulations is that it has often been difficult to discern whether the alterations were specific or resulted in non-specific conformational changes which indirectly interfered with conformational changes in actual endocytic domains. An alternative to deletion and substitution experiments is the creation of receptor chimeras. The advantage of the chimeric approach is that the predicted outcome is the retention or gain of function, rather than its loss, and it is unlikely that a function would be non-specifically acquired.

The chimeric approach was used to examine the internalisation properties of the IP prostanoid receptor, where the intracellular tail was replaced with a C-tail of similar length from two other GPCRs, namely the rat TRH-1 and human β_2-adrenergic receptors. In addition, receptors C-terminally tagged with a modified form of GFP from the jellyfish *Aequorea victoria* were made, thus providing the means to directly visualise the expression, localisation, and redistribution of the receptors in response to stimuli in intact cells and in real time.

Many GPCRs have been extensively studied in both transient and stable expression cell systems using GFP. An important issue in an approach of this kind is whether the receptor-GFP conjugate maintains the ligand binding and signal transduction properties of the native receptor. There appears to be remarkable retention of normal receptor characteristics when the 27 kDa GFP protein is fused to the C-termini of GPCRs such as the β_2-AR, TRH-R, gastrin-releasing peptide receptor, and the lysophospholipid edg1

receptor (Kallal *et al.*, 1998; Drmota *et al.*, 1998; Slice *et al.*, 1998; Liu *et al.*, 1999). In the early stages of this investigation, experiments were therefore carried out to determine the pharmacological properties of the IP prostanoid receptor constructs and whether GFP and/or the different tails altered receptor pharmacology.

Western blotting of HEK293 cell membranes transfected with the GFP- and HA-tagged constructs demonstrated that the receptors resolved as broad complexes which were not present in mock transfected cells (Figures 3.2 and 3.21). The slower migrating bands, which were of higher molecular weight than the native receptors, suggested that differential glycosylated forms of the receptors were present. It has been previously demonstrated that the IP receptor is expressed as a glycoprotein in HEK293 cells (Smyth *et al.*, 1996). The sites for potential N-linked glycosylation are located within the receptor's N-terminus and first extracellular loop (N^7 and N^{78}). Mutagenesis studies of IP receptor mutants lacking the putative glycosylation sites have highlighted the importance of receptor glycosylation for plasma membrane localisation, ligand binding and signal transduction (Zhang *et al.*, 2001).

One-point [^{3}H] iloprost binding assays in intact cells confirmed the plasmalemmal expression of the HA- and GFP-tagged forms of the receptor constructs, but at relatively low levels (Figures 3.3 and 3.23). Furthermore, the coupling of the cell surface receptors to G_s as shown in assays of adenylyl cyclase activity, demonstrated only moderate agonist-stimulated second messenger production in the transiently transfected cells (Figures 3.4 and 3.24). A common problem with transient transfection of many GPCRs is that when expression is driven by a strong viral promoter, a significant proportion of the protein synthesised appears to be trapped in intracellular compartments like the Golgi membranes and is not effectively trafficked to the plasma membrane. The use of receptor-GFP conjugates has permitted the direct visualisation of this phenomenon. As suggested from the radioligand binding and adenylyl cyclase experiments, the receptor-GFP proteins displayed predominantly intracellular localisation as visualised in confocal microscopy of transiently transfected HEK293 cells (Figure 3.5). Significant intracellular distribution has been described for cell expressing GPCRs such as the α_{2C}-AR (Daunt *et al.*, 1997), α_{1A}-AR (Hirasawa *et al.*,

1997), $5HT_{1B}$ receptor (Langlois *et al.*, 1996), thrombin receptor (Hein *et al.*, 1994), and dopamine D_2 receptor (Prou *et al.*, 2001).

Transient expression of GPCRs certainly overloads secretory intracellular compartments. However, it does not prevent a large portion of receptor pool from being targeted to the plasma membrane in the case of the dopamine D_1 (Prou *et al.*, 2001), β-adrenergic (von Zastrow *et al.*, 1993) or α_{1b}-adrenergic (Fonseca *et al.*, 1995; Hirasawa *et al.*, 1997) receptors. A feasible explanation for the intracellular retention of receptors could be defective glycosylation due to improper folding of the protein in the endoplasmic reticular membranes. As previously noted with the prostacyclin receptor, non/partial glycosylation has been reported to impair the plasma membrane localisation of GPCRs including the EP_{3B}, TXA_2, and calcium receptors (Böer *et al.*, 2000; Walsh *et al.*, 1998; Ray *et al.*, 1998). Constitutively active GPCRs are also known to exhibit predominant intracellular expression of GPCRs. Such a phenomenon has been observed for constitutively active dopamine D_2 receptors where incubation with antibodies against an amino-terminal epitope tag internalised in cells in a clathrin- and dynamin-independent manner (Vickery and von Zastrow, 1999). Spontaneous endocytosis of receptors has also been demonstrated for GFP-tagged CXCR4 receptors (Tarasova *et al.*, 1998)

Confocal analysis of the transiently expressed GFP-tagged prostacyclin receptor constructs posed obvious difficulties for detailed analysis of agonist-stimulated redistribution of the receptors and therefore cell lines stably expressing the GFP-receptors were generated in an attempt to overcome this problem. Previous studies have reported that HEK293 cells stably expressed with a GFP-tagged form of the prostacyclin receptor displayed plasma membrane localisation in the unstimulated state (Smyth *et al.*, 2000). In accordance with such findings, the IP-GFP stable cell line used in this investigation showed a similar cell decoration (Figure 3.12a). Surprisingly, the stable cell clones expressing the receptor chimeras exhibited a more diffuse pattern of expression (Figures 3.13a, 3.14a), thus indicating that modification of the receptor's tail altered its ability to traffic to the cell surface. In investigations with a chimeric prostacyclin receptor possessing the equivalent C-tail region of the DP receptor it was demonstrated that the chimera displayed all the properties of a constitutively active

receptor (Wise, 1999). It could therefore be argued that the loss in plasma membrane localisation of the IP-TRH-GFP and IP-β_2-GFP constructs was due to increased intrinsic activity of the receptors. However, in assays of adenylyl cyclase activity, increased constitutive activity was not detected; the basal level of cAMP accumulation in IP-TRH-GFP and IP-β_2-GFP cells was in fact lower than in the IP-GFP cell line. It is possible that the wild type receptor contains a signal sequence within its carboxyl tail for targeting to the cell surface which is lost when the tail is switched. It is well known that GPCR mutagenesis of the C-tail can often result in poor plasma membrane delivery of the modified protein. In studies with GFP-tagged forms of the vasopressin V_2 receptor it was noted that the wild type receptor appeared to be plasma membrane-delineated while receptors with mutations in a C-tail dileucine motif and an associated upstream glutamate residue (a sequence thought to be important in mediating delivery of receptors to the cell surface) were retained in the endoplasmic reticulum (Schulein *et al.*, 1998). Mutagenesis of basic residues in the membrane proximal domain of the CCR5 receptor carboxyl tail has also been shown to bring about a severe reduction in cell surface expression (Venkatesan *et al.*, 2001).

Scatchard analysis of the IP-GFP stable cell clone revealed the presence of two binding sites, one of high affinity, and one of low affinity (Figure 3.9b). It is well documented that a GPCR coupled to a G protein has a high degree of affinity for agonists whereas the uncoupled form exhibits a lower affinity (Emerit *et al.*, 1990). Thus, the high affinity iloprost binding site is indicative of ligand binding to the prostacyclin receptor construct in its G protein coupled state while iloprost binding to uncoupled receptors would account for the detection of a class of receptors of low affinity. It is also conceivable that the low affinity site is a result of iloprost binding to the EP_1 receptor which is endogenously expressed in HEK293 cells. Previously published data have shown that both the native and recombinant IP receptors exist in two affinity states. Boie and coworkers (1994) demonstrated that in COS cells, [^{3}H] iloprost bound to the native IP receptor with high and low affinity equilibrium dissociation constants of 1 and 44 nM respectively. Similarly, Smyth and coworkers (1996) found that an N-terminal HA-tagged prostacyclin receptor bound [^{3}H] iloprost with similar affinity (high affinity K_d of 0.4 nM and low affinity K_d of 75 nM). The ligand binding properties of the stably expressed IP-GFP receptor were comparable to those already reported for the native and

epitope-tagged forms of the receptor, indicating that neither the FLAG epitope nor the GFP tag altered ligand binding. Furthermore, the binding affinity of [^{3}H] iloprost to the receptor was not significantly affected by the expression of the β_2-AR or the TRH-1-R tails (Figure 3.9d, f); both exhibited two-site binding with high and low affinity dissociation constants similar to those of the IP-GFP receptor. Such data would suggest that the C-tail of the prostacyclin receptor is not a crucial factor in the binding of ligand to the receptor. Indeed, ligand binding studies of the IP receptor using IP/DP receptor chimeras have previously demonstrated that TMs VI and VII and the first extracellular loop region are important in conferring the ligand binding properties of the IP receptor (Kobayashi *et al.*, 1997, 2000).

Functional characterisation of each of the stable cell lines showed that the receptors displayed robust coupling to adenylyl cyclase. Iloprost was most potent at stimulating adenylyl cyclase activity in IP-GFP cells, with an approximate 5-fold reduction in EC_{50} value as compared to the receptor chimeras (Figure 3.11). The potency of iloprost at the IP-GFP receptor was similar to that reported for both HA-tagged and native forms of the receptor (Smyth *et al.*, 1996) thus demonstrating that the fusion of GFP to the C-terminus of the receptor did not affect the receptor's coupling capacity. Both the IP-GFP and IP-β_2-GFP cells displayed similar maximal levels of cAMP production whereas the intrinsic activity of IP-TRH-GFP cells was ~50% lower.

In signalling systems where the effector species is quantitatively the limiting component, it is often observed that elevations in receptor number result in a leftward shift of the dose response curve i.e. decrease the EC_{50} value. Consistent with this, earlier binding analysis demonstrated that the number of ligand binding sites in IP-GFP cells was 2-3 fold higher than in IP-TRH-GFP and IP-β_2-GFP cells. Thus, it could be argued that the increased receptor expression in IP-GFP cells resulted in an increased agonist potency. Similar observations have been reported in other GPCR studies; in functional assays with cell lines expressing β_2- and β_3-adrenoreceptors, the potency of various agonists was found to be proportional to receptor density (Whaley *et al.*, 1994; Wilson *et al.*, 1996). Likewise, it was demonstrated that adenylyl cyclase inhibition by the adenosine A1 receptor exhibited a leftward shift in agonist potency of 2 orders of

magnitude in cells expressing the receptor at relatively high levels as compared to an equivalent cell line in which expression was 16-fold lower (Cordeaux *et al.*, 2000).

Stimulation of adenylyl cyclase, but not phospholipase C, by the IP receptor has been shown to be unaffected by the absence of a C-tail which would suggest that this region of the receptor is redundant in terms of G_s coupling (Smyth *et al.*, 1998). The switching of the IP receptor tail for that of another G_s-coupled GPCR, the β_2-AR, did not alter the maximal response in adenylyl cyclase dose responses whereas the chimera possessing the C-tail region of the $G_{q/11}$-coupled rat TRH-1 receptor exhibited a much lower intrinsic activity. The presence of the TRH-1 tail may have inhibited G_s coupling or brought about conformational changes in the protein which affected its ability to couple efficiently to G_s. The TRH-tailed chimera may have been more effective at stimulating phosphoinositide turnover but this was not investigated in this study.

Earlier research into the agonist-mediated internalisation of the prostacyclin receptor indicated that it displayed relatively slow kinetics of internalisation and desensitisation. In these studies, cell lines which endogenously expressed the receptor (e.g. platelets and NG108-15 cells) were used. Taken together, the data revealed that the time frame of receptor desensitisation was between 3-10 hours which coincided with receptor sequestration and downregulation (Krane *et al.*, 1994; Giovanazzi *et al.*, 1998; Nilius *et al.*, 2000). Whilst in the midst of this present study, further data was published showing that the IP receptor, when overexpressed in HEK293 cells, underwent rapid agonist-induced desensitisation and internalisation, thus conforming to the general paradigm of GPCR regulation (Smyth *et al.*, 1998; 2000). They showed that in HEK293 cells, IP receptor internalisation was evident within 5 min of iloprost treatment (1μM) and plateaued after 30 min with 30-40% loss of cell surface receptors. Confocal analysis of a GFP-tagged form of the receptor seemed to exhibit similar kinetics of internalisation to the wild type, although the rate of internalisation was not quantified in the study (Smyth *et al.*, 2000). In addition, deletion of the carboxyl tail was shown to completely abolish its trafficking in response to iloprost thus confirming its critical role in sequestration.

In this present study, the GFP-tagged IP receptor was shown to translocate from the cell surface and into the intracellular space with 5 min of agonist treatment as demonstrated by both confocal analysis and biotin labelling experiments (Figures 3.12, 3.16). Internalisation was initially rapid, but a more gradual loss of cell surface receptors occurred over the time course with ~40% receptors internalised after 60 min of agonist treatment. Furthermore, similar results were obtained with HEK293 cells transiently expressing an N-terminal HA-tagged version of the prostacyclin receptor (Figures 3.24, 3.27). The internalisation data are in accord with those published for HEK293 cells stably expressing an HA-tagged IP receptor, and add further credence to the opinion that fusing GFP to the receptor's carboxyl tail does not affect its internalisation properties.

The addition of the carboxyl tail of the TRH-1 receptor to the distal end of TMVII of the prostacyclin receptor produced a chimera with enhanced kinetics of internalisation. Confocal analysis of both the GFP- and HA-tagged forms of the receptor chimera showed that the bulk of receptors appeared to be intracellular within 5 min of iloprost incubation (Figures 3.13, 3.25). Biotin labelling experiments confirmed these observations (Figures 3.17, 3.28).

The full length TRH receptor is a GPCR that is internalised quickly in response to agonist. In COS-1 cells, the wild type mouse TRH receptor was shown to be rapidly converted to an acid-resistant (i.e. intracellular) region of the cell upon treatment with TRH (Nussenzveig *et al.*, 1993). After 1 hour agonist exposure, at room temperature, 40% of the TRH bound became acid resistant. This rapid agonist-mediated endocytosis has also been noted in confocal studies of HEK293 cells stably expressing a GFP-tagged form of the rat TRH receptor (Drmota *et al.*, 1998). Initially, the receptor appeared to be localised to the plasma membrane but within 5-10 min of agonist exposure most of receptors appeared to be located in intracellular vesicles.

By a series of C-terminal truncations of the mouse and rat forms of the TRH receptor, the carboxyl tail has been shown to be an important regulator of its sequestration (Nussenzveig *et al.*, 1993; Drmota and Milligan, 2000). In studies of the murine TRH receptor, two domains between residues 335-368 within the intracellular tail were found to be involved in internalisation. First, a domain between residues 360-367 was identified using a mutant truncated at codon 360 which exhibited a 50% reduction in the

level of internalisation to that of the wild type whereas truncation at codon 368 internalised to the same extent as the wild type. A second domain was uncovered by truncations at codons 335 and 338, and the substitutions of the cysteine residues at positions 335 and 337. The C335Stop truncation severely compromised the steady-state level of internalisation whereas lengthening the receptor by the three amino acids partially restored internalisation. The need for the proximal cysteine residues within this domain was demonstrated by their substitution which diminished internalisation by approximately 50% (Nussenzveig *et al.*, 1993). For the rat TRH-1 receptor, truncation studies uncovered a relatively short sequence in the C-tail involved in internalisation of the receptor. Truncation of the 93 amino acid tail to at least 50 amino acids in length had no effect on the agonist-induced internalisation of the receptor. However, further truncation to 45 or 46 amino acids dramatically reduced internalisation to 36% of that of the full length receptor, thus narrowing the region of a key internalisation signal to a four amino acid stretch (Drmota and Milligan, 2000).

From the observations made in studies of wild type TRH receptor sequestration, it could be argued that the addition of the rat TRH-1 receptor carboxyl tail to the IP receptor confers the internalisation properties of the donor to the recipient. Consistent with this hypothesis, in studies of the tail-less mammalian GnRH-R it has been reported that a GnRH/TRH tail chimera exhibited accelerated desensitisation and internalisation kinetics as compared to the wild type GnRH-R (Heding *et al.*, 1998).

Both the HA- and GFP-tagged forms of the IP receptor chimeras possessing the tail of the β_2-AR displayed similar internalisation patterns (Figures 3.18, 3.29), with notable receptor sequestration occurring after 30 min agonist treatment as determined both confocally and quantitatively. These data indicated that the internalisation characteristics of the β_2-AR tailed chimera were more similar to the full-length IP receptor than the IP/TRH tail fusion proteins.

The exact role of the wild type β_2-AR's carboxyl tail in regulating internalisation remains unclear. Neither truncation of the β_2-AR tail nor mutation of putative phosphorylation sites blocked internalisation (Hausdorff *et al.*, 1989; Ferguson *et al.*,

1995, 1996). In contrast, sequestration was markedly inhibited by a mutation of a dileucine motif in the intracellular tail (Gabilondo *et al.*, 1997).

In HEK293 cells, the rate and extent of internalisation of both GFP-conjugated and native β_2-ARs was shown to be similar; both exhibited a rapid loss of receptors from the cell surface, with ~60% of receptors being sequestered within 30 min of agonist exposure (Barak *et al.*, 1997a). The IP chimeras with the β_2-AR tail appended, at best, exhibited a ~30% reduction in cell surface receptor number after 30 min agonist treatment, therefore indicating that the β_2-AR C-tail fusion protein did not acquire the internalisation properties of the donor receptor. In accord with this, chimeric studies with the internalisation-resistant β_3-AR demonstrated that all of the receptor's intracellular domains had to be switched with the equivalent sequences of the β_2-AR in order to establish a sequestration phenotype similar to that of the native β_2-AR (Jockers *et al.*, 1996). It is therefore conceivable that the β_2-AR C-tail alone is insufficient to confer its rapid internalisation properties to the prostacyclin receptor and the substitution of multiple intracellular domains would be required.

In summary, the results show that the introduction of different cytoplasmic tails to the prostacyclin receptor has the capacity to alter the rate and extent of the receptor internalisation and these characteristics are maintained when GFP is added to the C-terminus. In accordance with previously published findings, the data further highlight the crucial role that the intracellular carboxyl tail domain plays in regulating prostacyclin receptor sequestration.

Chapter 4

Examination of the Endocytic Pathways Utilised by the Prostacyclin Receptor Constructs

Chapter 4

4.1 Introduction

An important aspect of GPCR regulation is the sequestration of agonist-occupied receptors from the plasma membrane to intracellular compartments. Intensive investigations into the underlying mechanisms of GPCR internalisation have uncovered multiple pathways of receptor endocytosis for various members of the superfamily.

Phosphorylation of agonist-activated receptors was first suggested as a candidate for inducing internalisation by Sibley and coworkers in 1986 when it was noted that sequestered β_2-ARs exhibited lower stoichiometry of phosphorylation (~0.75 mol/mol), compared to the whole cellular pool of β_2-ARs (~2.1 mol/mol). However, initial experiments with β_2-AR mutants lacking sites for both PKA- and GRK-mediated receptor phosphorylation, did not support this theory (Bouvier *et al.*, 1988; Hausdorff *et al.*, 1989). More recently, the role of phosphorylation in β_2-AR internalisation was confirmed by experiments demonstrating that overexpression of GRKs facilitated the endocytosis of a phosphorylation- and internalisation-defective mutant, β_2-AR-Y326A (Ferguson *et al.*, 1995, Menard *et al.*, 1996).

Internalisation studies of other GPCR subtypes have further highlighted the importance of phosphorylation for endocytosis. Early experiments of m2 muscarinic receptor internalisation demonstrated that sequestration was reduced by mutation of the putative phosphorylation sites within the third intracellular loop of the receptor (Moro *et al.*, 1993). Furthermore, Tsuga and coworkers (1994) were the first to show that, upon overexpression of GRK 2, both the rate and maximal extent of m2 muscarinic receptor sequestration were accelerated, whereas expression of a dominant-negative GRK 2 mutant led to a decrease in receptor phosphorylation and internalisation. Overexpression of GRKs has now been shown to promote internalisation for an array of GPCRs including the endothelin A (Bremnes *et al.*, 2000), follitropin (Lazari *et al.*, 1999), AT_{1A} (Smith *et al.*, 1998) and chemokine CXCR1 (Barlic *et al.*, 1999) receptors.

Some studies have indicated that phosphorylation is not an absolute requirement for internalisation. Indeed, β_2-AR mutants lacking GRK phosphorylation sites were shown to readily internalise in response to agonist (Hausdorff *et al.*, 1989; Bouvier *et al.*, 1988). It has now become evident that GRK phosphorylation promotes the interaction of the receptor with other intracellular components which are directly involved in receptor sequestration. In fact, GRK-mediated phosphorylation of GPCRs increases the affinity of the receptor to bind β-arrestins. β-Arrestins not only uncouple receptors from G proteins but act as adapters for the targeting of GPCRs for internalisation via clathrin coated pits (Zhang *et al.*, 1996; Ferguson *et al.*, 1996). The sequestration of the β_2-AR-Y326A mutant was rescued by overexpression of both β-arrestins 1 and 2, and this effect was enhanced by GRK 2 coexpression (Ferguson *et al.*, 1996). Moreover, β-arrestins facilitated the endocytosis of β_2-AR mutants lacking either carboxyl terminal tails or putative GRK phosphorylation sites (Menard *et al.*, 1997).

Investigations, primarily with the β_2-AR, have delineated a general pathway for receptor internalisation by which GRK-mediated phosphorylation of agonist-activated receptors promotes the recruitment of β-arrestins, uncoupling the receptor-G protein complex and facilitating endocytosis via clathrin coated vesicles (CCVs). However, a large volume of published data would suggest that this pathway is not universally observed.

In some instances, it has been reported that GPCR internalisation can be arrestin-independent. In HEK293 cells, it was shown that internalisation of the m2 muscarinic receptor could proceed via a GRK-dependent, arrestin-independent pathway (Pals-Rylaarsdam *et al.*, 1997). Furthermore, agonist-induced internalisation of the m1, m3, and m4 subtypes was neither altered by overexpression of β-arrestins nor transfection with a dominant negative mutant arrestin (Lee *et al.*, 1998). Similarly, internalisation of agonist-activated $5HT_{2A}$ receptors in HEK293 cells appeared to be insensitive to arrestin dominant negative mutants, although receptor stimulation did promote the translocation of arrestins to the plasma membrane which was accompanied by differential sorting of the arrestins and receptors into distinct intracellular compartments (Bhatnagar *et al.*, 2001). It has also been reported that the maximal extent of AT_{1A} receptor endocytosis in COS7 cells (GRK- and arrestin-deficient) was indistinguishable from that found in HEK293 cells which endogenously express GRKs and arrestins at relatively high levels

(Zhang *et al.*, 1996; Menard *et al.*, 1997). It could be argued that the preferred internalisation pathway of GPCRs is GRK- and β-arrestin-dependent and that the presence of dominant negative inhibitors drives internalisation via alternative endocytic pathways. Indeed, it has been observed that sequestration of the m2 muscarinic and AT_{1A} receptors was augmented by overexpression of GRKs and arrestins (Zhang *et al.*, 1996; Schlador and Nathanson, 1997).

The idea that GPCRs sequester via clathrin coated pits was initially suggested by early investigations of β_2-AR internalisation, in which agents which disrupted clathrin coat assembly (e.g. hypertonicity treatment, cytosolic acidification, intracellular K+ depletion, temperature reduction, and reduced cellular ATP) blocked internalisation (Chuang *et al.*, 1980). This hypothesis was further established with the development of immunocytochemical techniques which revealed the subcellular localisation of agonist-occupied β_2-ARs with the transferrin receptor (von Zastrow and Kobilka, 1992). More recently, the use of GTPase defective dynamin mutants (which inhibit the budding off of CCVs) has proved to be effective in blocking the β-arrestin-dependent internalisation of GPCRs such as the $AT_{1A}R$ and β_2-AR (Zhang *et al.*, 1996). The discovery that β-arrestins possess domains for binding clathrin and the β2-adaptin subunit of the clathrin adapter, AP-2, has provided further evidence for a β-arrestin/clathrin internalisation pathway (Goodman *et al.*, 1997; Laporte *et al.*, 1999, 2000).

Although it seems that the majority of GPCRs use a clathrin pathway for internalisation, which is either dependent or independent of arrestin, some exceptions have been noted. Internalisation of the N-formyl peptide receptor was shown to be independent of arrestin, dynamin, and clathrin in HEK293 cells (Gilbert *et al.*, 2001). Sequestration via non-coated vesicles such as caveolae has also been observed for the endothelin A receptor in transfected COS cells (Chun *et al.*, 1994), the B2 bradykinin receptor in DDT1 MF-2 cells (de Weerd and Leeb-Lundberg, 1997), and for the muscarinic receptors in human fibroblasts (Raposo *et al.*, 1987).

Recent research into β-arrestin dependent internalisation of GPCRs has also revealed striking differences in the ability of the β-arrestin isoforms to bind GPCRs. Initially these findings were observed in *in vitro* binding assays with purified proteins. Studies

with translated visual arrestin protein demonstrated that it bound rhodopsin in preference to the β_2-adrenergic and m2 muscarinic receptors, whereas purified β-arrestins bound the β_2-AR and m2 muscarinic receptor in preference to rhodopsin (Attramadal *et al.*, 1992; Lohse *et al.*, 1992; Gurevich *et al.*, 1993, 1995). Moreover, β-arrestin 1 was shown to exhibit a 2.5-fold greater binding affinity to the β_2-AR than β-arrestin 2, and β-arrestin 2 bound to the m2 muscarinic receptor with a 1.5-fold greater affinity than β-arrestin 1 (Gurevich *et al.*, 1995). More recently, Oakley and coworkers (2000) showed that the specificity in the interactions of arrestins with GPCRs could also be observed in intact cells. They identified two classes of GPCRs, designated A and B, that differed in their affinities for the arrestin isoforms. Class A receptors, such as the β_2-AR, μ-opioid receptor, endothelin A receptor, D1A dopamine receptor, and the α_{1B}-AR, bound β-arrestin 2 with higher affinity than β-arrestin 1, and did not interact with visual arrestin. Conversely, class B receptors ($AT_{1A}R$, neurotensin receptor 1, vasopressin V2 receptor, TRH receptor, and substance P receptor) bound both β-arrestin isoforms with similar high affinities and also interacted with visual arrestin. The different physiological roles of the β-arrestin isoforms were further defined in experiments examining the internalisation of the class A receptor, β_2-AR, and the class B receptor, $AT_{1A}R$, in mouse embryonic cell lines lacking expression of β-arrestin 1, β-arrestin 2, or both (Kohout *et al.*, 2001). Analysis of agonist-stimulated β_2-AR sequestration in the β-arrestin 2 knockout cells was significantly impaired (87% reduction) compared to wild type cells, whereas internalisation in the β-arrestin 1 knockout cells was not compromised. Comparison of the ability of the two β-arrestin proteins to sequester the β_2-AR revealed that β-arrestin 2 bound to the receptor with a 100-fold higher affinity than β-arrestin 1. Investigation of AT_{1A} receptor internalisation showed that β-arrestins 1 and 2 could be substituted for each other in the sequestration of the receptor, and internalisation was only significantly impaired when the receptor was expressed in cells lacking both β-arrestin isoforms (82% reduction).

The binding of β-arrestin isoforms to agonist-activated, GRK-phosphorylated GPCRs is thought to involve the simultaneous interaction of the β-arrestin protein with two regions of the receptor (Gurevich *et al.*, 1993; 1995). The amino-terminal activation recognition domain of β-arrestin recognises the agonist-activated state of GPCRs while

the amino-terminal phosphorylation-recognition domain is thought to interact with the GRK-phosphorylated serine and threonine residues of the intracellular loops and carboxyl termini.

Extensive investigation has identified the carboxyl tail as the main site of β-arrestin binding for many GPCRs, although direct interaction between the third intracellular loop and β-arrestin has been reported for the m2 and m3 muscarinic receptors, the α_{2A}-AR (Wu *et al.*, 1997), and the $5HT_{2A}$ receptor (Gelber *et al.*, 1999). There does not appear to be a universal consensus sequence for β-arrestin binding although the phosphorylation of key serine and threonine residues seems to be an important prerequisite for β-arrestin binding. Mutation or serial truncation of putative phosphorylation sites has been shown to correlate well with loss of β-arrestin association for GPCRs such as the $AT_{1A}R$ (Qian *et al.*, 2001), CCR5 receptor (Kraft *et al.*, 2001), and parathyroid hormone receptor (Vilardaga *et al.*, 2002).

The role of the intracellular tail in β-arrestin-dependent internalisation has been eloquently demonstrated in studies using a GnRH/TRH tail receptor chimera. Agonist-activation of the wild type tail-less GnRH receptor does not induce phosphorylation or interaction with β-arrestin, which seems to account for its exceptionally slow kinetics of desensitisation and internalisation (Vrecl *et al.*, 1998; Heding *et al.*, 1998; Willars *et al.*, 1999). In contrast, the rapid sequestration of the native TRH receptor is β-arrestin sensitive (Groarke *et al.*, 1999; Yu and Hinkle, 1999), and truncation of the receptor's C-tail abolished internalisation (Nussenzveig *et al.*, 1993; Yu and Hinkle, 1999; Drmota and Milligan, 2000), thus highlighting the importance of this domain in the receptor's interaction with β-arrestin. The fusion of the TRH receptor C-tail to the mammalian GnRH receptor was sufficient to switch its internalisation to a β-arrestin-dependent phenotype (Willars *et al.*, 1999; Heding *et al.*, 2000). More recently, the sequence determinants within the TRH receptor tail responsible for β-arrestin binding have been identified as three casein kinase II (CKII) phosphorylation sites. In the GnRH/TRH chimera, mutation of the CKII sites resulted in a loss of β-arrestin binding. Similarly, incubation with a CKII inhibitor produced the same effect (Hanyaloglu *et al.*, 2001).

The carboxyl tails of GPCRs have also been suggested to play a role in the determining the stability of receptor/β-arrestin complexes and the cellular distribution of β-arrestins. In response to agonist stimulation of the β_2-adrenergic, D1A dopamine, and endothelin type A receptors, β-arrestin 2 was observed to translocate to the plasma membrane but did not traffic along with the activated receptors. In contrast, activated AT_{1A} and neurotensin receptors co-internalised with β-arrestin 2 in endocytic vesicles. The switching of the β_2-AR tail for that of the $AT_{1A}R$, and vice versa, was capable of reversing the β-arrestin redistribution pattern of each receptor (Zhang *et al.*, 1999). Moreover, Oakley and coworkers (2000) demonstrated that the differential affinities of visual arrestin and the β-arrestins isoforms for class A and class B GPCRs could be switched by exchanging their carboxyl tails.

In this chapter, experiments were carried out in an effort to determine the molecular mechanisms involved in the agonist-mediated sequestration of both GFP-tagged and non-GFP-tagged forms of the prostacyclin receptor. In addition, the chimeric prostacyclin receptors possessing the tails of the TRH and β_2-adrenergic receptors were used to examine the functional importance of the carboxyl terminal region in regulating the pattern of sequestration. The internalisation pathway of each of the IP receptor constructs was delineated using various biochemical and immunocytochemical techniques.

4.2 The effect of inhibitors of clathrin-mediated endocytosis on agonist-mediated sequestration of the prostacyclin receptor constructs.

Receptor endocytosis via CCVs can be pharmacologically blocked by pre-treatment of cells with concanavalin A and hyperosmolar sucrose. Concanavalin A, a plant lectin, blocks GPCR endocytosis by binding to cell surface glycoproteins and impairing their mobility within the lipid bilayer, without affecting ligand binding or receptor signalling (Pippig *et al.*, 1995; Luttrell *et al.*, 1997). Hypertonic sucrose inhibits clathrin-mediated internalisation by inducing abnormal clathrin polymerisation into empty micro-cages on the membrane (Heuser and Anderson, 1989). The effect of these biochemical agents on iloprost-induced internalisation of the prostacyclin receptor proteins was examined visually by confocal microscopy and quantitatively using biotin labelling experiments. Confocal analysis of the immunostained HA-tagged IP receptors, transiently expressed in HEK293 cells, demonstrated that pre-treatment of cells with 0.4M sucrose or 0.25mg/ml concanavalin A effectively blocked agonist-mediated sequestration of each construct (Figure 4.1). In the stable cell clones expressing the receptor-GFP proteins, the effect of the endocytosis inhibitors was measured quantitatively. Pre-treatment of the stable cell clones with sucrose and concanavalin A prior to 1 hour's challenge with 1μM iloprost, significantly attenuated receptor endocytosis in each clone (Figure 4.2). In IP-GFP cells, agonist alone resulted in a ~40% loss of cell surface receptors after 60 min, whereas the fraction of receptors remaining at the plasma membrane after agonist treatment in cells pre-exposed to 0.4M sucrose and 0.25mg/ml concanavalin A was 91 ± 3% and 80 ± 6% respectively. In the IP-TRH-GFP clone, approximately half of the total cell surface receptors had internalised after incubation with 1μM iloprost alone, whereas in cells pre-treated with sucrose and concanavalin A, the proportion of receptors present at the cell surface was 98 ± 10% and 95 ± 11% respectively. For the IP-β_2-GFP cell line, 70 ± 2% of the plasma membrane receptors remained at the cell surface after 60 min agonist treatment. In cells pre-incubated with sucrose, 99.6 ± 4% of receptors remained at the cell surface after agonist treatment, while after concanavalin A treatment 92 ± 6% of receptors were at the plasmalemmal surface.

4.3 Colocalisation of internalised prostacyclin receptor constructs with transferrin receptors in endosomal compartments.

To further characterise the internalisation pathway of the prostacyclin receptor proteins in HEK293 cells, the receptor-GFP stable cell clones were incubated with Texas Red® labelled transferrin, a well known endosomal marker of clathrin-mediated endocytosis (Woods *et al.*, 1989), to determine whether the agonist-internalised receptors colocalised with vesicles containing transferrin. In the unstimulated state, the GFP-tagged receptors were seen mainly at the cell surface, whereas the transferrin receptors localised predominantly to small punctate intracellular compartments which were indicative of their presence in endosomal membranes (Figure 4.3a). After 30 min incubation with 1μM iloprost, a more pronounced green fluorescent signal could be detected within the cells in each of the clones. The intracellular distribution of the receptors appeared to be similar to those intracellular vesicles which contained transferrin. Dual imaging revealed that many of these vesicles contained both receptor and transferrin as seen by the convergence of the green and red fluorescent signals to produce yellow fluorescence (Figure 4.3b). Such findings therefore suggested that the prostacyclin receptor constructs internalise via clathrin coated pits.

4.4 Association of the β-arrestin isoforms with the GFP-tagged prostacyclin receptor fusion proteins.

In order to determine the functional significance of β-arrestins in the agonist-induced endocytosis of the prostacyclin receptor, the IP-GFP stable cell clone was transfected with native β-arrestin 1 (and subsequently immunostained with an anti-β-arrestin 1 antibody and complementary Alexa^{594}-conjugated secondary antibody) or with a RFP-conjugated form of β-arrestin 2. Confocal microscopy was used to study the interaction of these proteins in the cells at various timepoints in a 60 min time course of agonist stimulation. In addition, the same experiments were performed with the IP-TRH-GFP and IP-β_2-GFP cell lines to determine whether the presence of a different carboxyl terminal tail altered the receptor's affinity for the arrestin proteins.

In IP-GFP cells, both arrestin isoforms were distributed uniformly throughout the cytoplasm in the unstimulated state (Figures 4.4a and 4.5a). However, the RFP moiety which was used to tag β-arrestin 2 displayed a tendency to aggregate, and as a result, red puncta of β-arrestin 2 expression were frequently seen in the cells. Upon the addition of agonist, the receptor translocated from the plasma membrane to intracellular compartments with pronounced cytoplasmic expression after 30 min. The agonist-activation of the IP-GFP receptor did not appear to induce a redistribution of β-arrestin 1 localisation during the time course (Figure 4.4a). Analysis of the separate red and green fluorescent images confirmed this; β-arrestin 1 did not translocate to the plasma membrane or co-internalise with the receptor. It could therefore be argued that β-arrestin 1 is not involved in IP-GFP internalisation in HEK293 cells. Detecting colocalisation of the receptor with β-arrestin 2-RFP was more difficult due to the presence of RFP aggregates in the cells. However, iloprost treatment stimulated the movement of receptors from the cell surface into intracellular vesicles via a pathway which appeared to be independent of β-arrestin 2 (Figure 4.5a). Intracellular vesicles containing agonist-induced receptors were readily observed in the cells but none of these vesicles could be seen to overlap those containing the RFP-tagged arrestin. The possible existence of a β-arrestin 2-specific pathway of IP-GFP internalisation in HEK293 cells therefore seems unlikely. Taken together, the data suggested that an arrestin-independent mechanism is involved in the sequestration of the receptor in HEK293 cells.

In IP-TRH-GFP cells, no change in β-arrestin 1 localisation was detected during the time course of agonist stimulation, whereas the receptors rapidly internalised in endocytic vesicles (Figure 4.4b). The merged images show that the expression patterns of the receptor and arrestin were distinct, indicating that IP-TRH-GFP receptor internalisation is independent of β-arrestin 1. Repeating the experiments with β-arrestin 2-RFP revealed that the agonist-stimulated receptors co-internalised with vesicles containing arrestin (Figure 4.5b). Colocalisation could be seen within 5 min of iloprost treatment and was maintained throughout the time course. The confocal data therefore suggested that IP-TRH-GFP internalisation is β-arrestin 1-independent/β-arrestin 2-dependent.

Analysis of the confocal pictures of IP-β_2-GFP/β-arrestin colocalisation suggested that receptor endocytosis proceeded via a pathway not involving β-arrestin 1 (Figure 4.4c). Agonist stimulation of the cells induced a diffusion of receptors from the cell surface to the cytoplasm while the distribution of β-arrestin 1 expression remained unaffected. In cells transfected with β-arrestin 2-RFP, no obvious translocation of arrestin was detected during the time course. The internalised receptors appeared to be located in vesicles distinct from those containing β-arrestin 2. Accordingly, it would seem that that IP-β_2-GFP receptor sequestration is independent of β-arrestins.

4.5 Interaction of the HA-tagged IP receptor constructs with β-arrestin-GFP conjugates.

The data from the β-arrestin/receptor-GFP colocalisation experiments were somewhat unexpected and it was evident that further analysis was necessary. As previously noted, some of the stable cell clones exhibited significant intracellular receptor expression in the basal state and this may have obscured the espial of any receptor/β-arrestin associations. Additionally, it is possible that the GFP moiety fused to the carboxyl tail of the receptors may have altered their affinities for β-arrestins. In an effort to more accurately analyse receptor/arrestin interactions, HEK293 cells were co-transfected with the N-terminally HA-tagged IP receptors and C-terminally GFP-tagged forms of β-arrestin 1 and 2.

In the absence of agonist, expression of the HA-IP receptor was localised primarily to the plasma membrane (as detected by the 12CA5 antibody and reciprocal Alexa^{594}-labelled secondary antibody) whereas β-arrestin 1-GFP was distributed evenly throughout the cell cytoplasm. Upon agonist addition, large punctate spots of internalised receptor were evident while the scattering of β-arrestin 1-GFP remained unaltered (Figure 4.6a). The decoded images show that agonist treatment did not promote arrestin translocation or stimulate its co-internalisation with the receptor, and when merged, the red and green signals did not overlap. When the experiments were repeated using the β-arrestin 2-GFP construct, no obvious colocalisation could be seen with the receptor and arrestin upon agonist stimulation of the cells. β-Arrestin 2-GFP appeared to remain localised to the cytoplasm and did not traffic with the HA-IP

receptor (Figure 4.7a). Small puncta of green fluorescence could be seen in the cells, but they did not seem to overlay any of the red spots of endocytosed receptor. The requirement of β-arrestin 2 in prostacyclin receptor endocytosis therefore seems dubious. The data, in conjunction with the previous observations from the IP-GFP/arrestin colocalisation experiments, indicated that β-arrestins are not a prerequisite for prostacyclin receptor internalisation in HEK293 cells.

In cells co-expressing β-arrestin 1-GFP and the HA-IP-TRH construct, agonist-mediated internalisation of receptor did not appear to have an effect on the cytoplasmic diffusion of the arrestin isoform (Figure 4.6b). Examination of the separate red and green images revealed that no overlay of the two proteins occurred, thus demonstrating that HA-IP-TRH receptor sequestration is independent of β-arrestin 1. In receptor-expressing cells transfected with β-arrestin 2-GFP, no obvious agonist-induced plasmalemmal localisation of arrestin was observed, but large clusters of green fluorescence could be seen in the cells. The spots of arrestin appeared to associate with those containing receptor, producing a yellow fluorescent signal when the images were merged (Figure 4.7b). It would therefore seem likely that β-arrestin 2 is involved in sequestration of the TRH-tailed chimera.

Agonist-mediated internalisation of the HA-IP-β_2 receptor did not appear to stimulate any noticeable shift in β-arrestin 1-GFP localisation from the cytoplasm to the plasma membrane (Figure 4.6c). Moreover, no obvious receptor/arrestin interactions were observed, therefore suggesting that HA-IP-β_2 receptor sequestration is independent of β-arrestin 1. In receptor cells expressing β-arrestin 2-GFP no obvious movement of the GFP signal was detected in response to iloprost incubation. None of the red spots of internalised receptor appeared to colocalise with the arrestin isoform (Figure 4.7c). It would therefore seem unlikely that β-arrestin 2 plays a role in the sequestration of the prostacyclin receptor chimera with the β_2-AR carboxyl tail. It could therefore be proposed that HA-IP-β_2 receptor endocytosis in HEK293 cells does not require β-arrestins.

4.6 β-Arrestin colocalisation experiments with full-length TRH and β_2-adrenergic receptors.

Control experiments of receptor/arrestin colocalisation were performed using the full-length β_2-adrenergic and TRH receptors; two GPCRs which internalise via an arrestin-dependent pathway. In confocal studies of HEK293 cells transiently expressing a VSV epitope-tagged form of the rat TRH 1 receptor and GFP-conjugated forms of the β-arrestin proteins, significant colocalisation could be seen between the receptor and each of the arrestin isoforms in response to agonist treatment (Figure 4.8). As anticipated, after a 30 min incubation of the cells with 10μM TRH, the receptors sequestered into endocytic vesicles containing β-arrestin. In equivalent experiments with the wild type β_2-AR, a 5 min incubation with 10μM isoproterenol promoted the rapid redistribution of β-arrestins from the cytosol to the receptor at the plasma membrane (Figure 4.9). Previously published observations have demonstrated that the agonist-activated β_2-ARs recruit β-arrestins to the plasma membrane but the receptor/β-arrestin complex dissociates at or near the plasma membrane, and the β-arrestins are excluded from the receptor-containing vesicles (Oakley *et al.*, 1999, 2000; Zhang *et al.*, 1999). In contrast, the TRH receptor forms a stable complex with β-arrestins and traffics with them into early endosomes upon agonist stimulation (Groarke *et al.*, 1999; Oakley *et al.*, 2000).

4.7 Association of β-arrestins with the prostacyclin receptor constructs as determined by co-immunoprecipitation experiments.

The potential physical interaction between β-arrestin and the prostacyclin receptor proteins in HEK293 cells was further assessed in co-immunoprecipitation assays. The HA-tagged forms of the receptor constructs were co-expressed in HEK293 cells with β-arrestin 1-GFP or β-arrestin 2-GFP. Transfected cells were then treated with vehicle or 1μM iloprost for 5 min before being lysed and immunoprecipitated with the anti-GFP antibody. Subsequent immunoblotting with the 12CA5 antibody was performed to detect receptor/arrestin co-precipitations. As shown in Figure 4.10a, the association of both β-arrestin isoforms with the full-length prostacyclin receptor was detected in both unstimulated and agonist treated cells. Somewhat surprisingly, the interaction did not

appear to be enhanced by iloprost treatment. No co-precipitations were detected when the cells were transfected with only vector, receptor, or β-arrestin, thus demonstrating that the immuno-reactivities of the two antibodies were specific. Similar results were produced when the experiments were repeated with the HA-IP-TRH (Figure 4.10b) and HA-IP-β_2 (Figure 4.10c) receptors. No obvious agonist-enhanced association of β-arrestin with receptor was detected with any of the constructs. Any observed variability in the amount of receptor/arrestin co-precipitated seemed merely to reflect the slight differences in protein loading on the gels.

Agonist-specific interactions of β-arrestins with GPCRs in intact cells can be difficult to assess using standard immunoprecipitation techniques but can be readily determined with the use of chemical cross-linking agents which stabilise the complexes prior to immunoprecipitation. This approach has been used successfully in the study of the association of β-arrestins with GPCRs such as the β_2-AR and lutropin receptor (Min *et al.*, 2002; Zhang *et al.*, 1997). In this study, however, chemical cross-linkers did not augment receptor/β-arrestin complex formation in agonist treated cells (data not shown). It therefore seemed likely that the receptor/β-arrestin interactions observed in this investigation were non-specific. To test this, various control experiments were performed. First, the co-immunoprecipitation assays were repeated using less plasmid DNA in the transfections to lower expression of the receptor and β-arrestin constructs in the cells, and therefore reduce the likelihood of the receptor and β-arrestin proteins forming non-specific interactions. An approximate 5-fold reduction in receptor and β-arrestin expression (as detected by Western blot analysis of cell lysates) did not however prevent receptor/arrestin co-precipitation (data not shown). Secondly, co-immunoprecipitation assays were performed using a pooled mixture of receptor-only and β-arrestin-only transfected cells to determine whether the receptor/β-arrestin complexes were forming in the cell lysate. This did not seem to be the case as no co-precipitates were detected in these cells (data not shown) suggesting that the receptor/β-arrestin complexes formed only in intact cells.

4.8 Sequestration of the HA-tagged prostacyclin receptor constructs in COS7 cells.

The extent of agonist-mediated GPCR internalisation can be regulated by the cellular milieu in which it is expressed. For GPCRs which utilise arrestin-dependent mechanisms for internalisation, the rate and extent of internalisation can be affected by the cellular levels of endogenous GRKs and β-arrestins (Menard *et al.*, 1997). For the β_2-AR, sequestration was ablated when expressed in cell lines with relatively low levels of endogenous GRKs and β-arrestins e.g. COS7 cells. Sequestration could be enhanced to levels comparable in HEK293 cells by overexpression of β-arrestin (Menard *et al.*, 1997). Conversely, AT_{1A} receptor sequestration in COS7 cells and HEK293 cells is similar, an observation which suggested that $AT_{1A}R$ internalisation proceeded via an arrestin-independent mechanism (Zhang *et al.*, 1996; Menard *et al.*, 1997).

The HA-tagged prostacyclin constructs were transiently transfected into COS7 cells to determine whether reducing the endogenous complement of GRKs and β-arrestins could impede receptor internalisation. Post transfection, the cells were incubated with the 12CA5 antibody to label the cell surface receptors before being treated with vehicle or 1μM iloprost for 1 hour and then fixed. Confocal analysis of the immunostained cells revealed that the agonist-activated receptors translocated from the cell surface to intracellular membranes (Figure 4.11). After 60 min, sequestration comparable to levels seen in HEK293 cells was observed with each of the constructs, which indicated that GRKs and β-arrestins are not of functional significance in the internalisation of the prostacyclin receptors. The transfection efficiency of the COS7 cells with each of the constructs (as determined visually using confocal microscopy) was exceptionally low which made it impossible to quantify the extent of receptor sequestration in the cells using biotin labelling assays. On the basis of the confocal data, internalisation of the prostacyclin receptor proteins seemed unaltered when expressed in COS7 cells.

4.9 The effect of overexpression of dominant negative dynamin on internalisation of the prostacyclin receptors.

Another important tool which has been used to dissect the pathway of GPCR internalisation is the expression of dominant negative mutant dynamin proteins. GTPase-deficient dynamin mutants such as dynamin-1-K44A have been shown to inhibit clathrin-mediated endocytosis in many systems (Zhang *et al.*, 1996; Lee *et al.*, 1998; Gáborik *et al.*, 2001). To study the potential role of dynamin in internalisation of the prostacyclin receptors, the stable cell clones expressing the GFP-tagged receptor constructs were transfected with a myc epitope-tagged form of the K44E dynamin mutant. The successful expression of the construct in cells was demonstrated by Western blot analysis of cell lysates with an anti-myc antibody (Figure 4.12b). The effect of the mutant dynamin on receptor sequestration was determined using biotin labelling assays; cells transfected with either vector or the mutant dynamin construct were treated with vehicle or 1μM iloprost for 60 min before biotinylation of the cell surface receptors. An inhibitory effect on iloprost-induced sequestration by the dynamin mutant was not demonstrable for any of the receptors as seen in the immunoblots (Figure 4.12a). These data therefore suggested that internalisation of the prostacyclin receptor constructs is dynamin-independent.

Figure 4.1

Visualisation of the HA-tagged prostacyclin receptors in HEK293: the effects of inhibitors of clathrin-mediated transport on receptor sequestration.

Cells were pre-treated with vehicle (a, b), 0.4M sucrose (c), or 0.25mg/ml concanavalin A (d) for 30 min prior to treatment with 1μM iloprost (b, c, d) for 60 min at 37°C. Receptors were visualised by immunostaining with the 12CA5 antibody. The confocal images shown are from a single experiment which was repeated twice. Scale bar = 2.5μM.

Figure 4.1

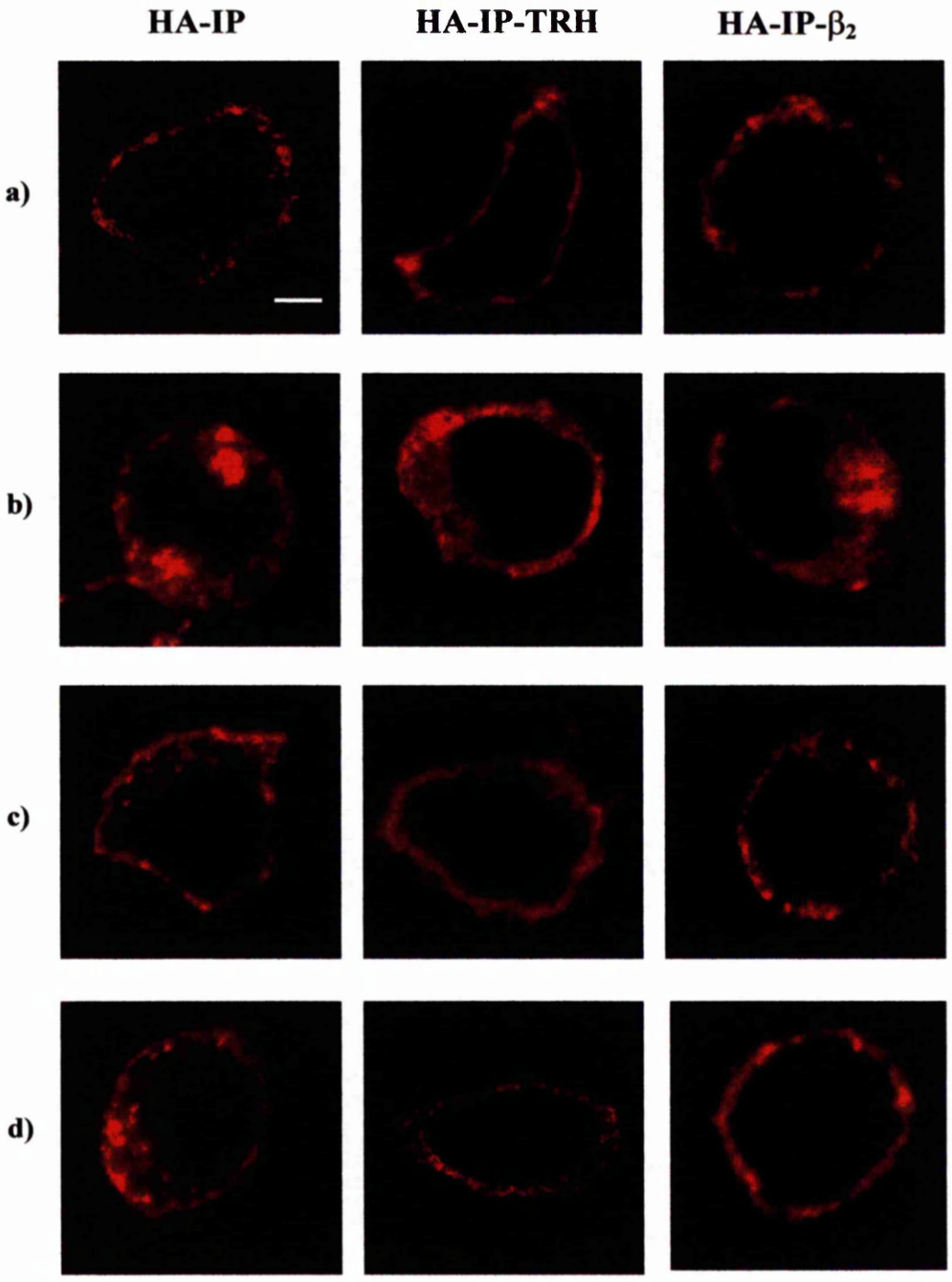

Figure 4.2

Quantification of agonist-mediated internalisation of the GFP-receptor proteins in the presence of hyperosmolar sucrose and concanavalin A.

a) The stable cell clones were pre-incubated with vehicle (1, 2), 0.4M sucrose (3), or 0.25mg/ml concanavalin A (4) prior to 1μM iloprost exposure (2, 3, 4) for 60 min at 37°C. Cell surface glycoproteins were subsequently labelled with biotin and the receptors were immunoprecipitated and visualised as detailed in section 2.7.5. A representative blot from three individual experiments is shown.

b) Densitometric scanning of the biotin blots was used to quantify the levels of cell surface receptors. The values shown represent mean ± S.E.M. for three experiments, with the levels of cell surface receptors observed in the absence of agonist set at 100%.

Figure 4.2

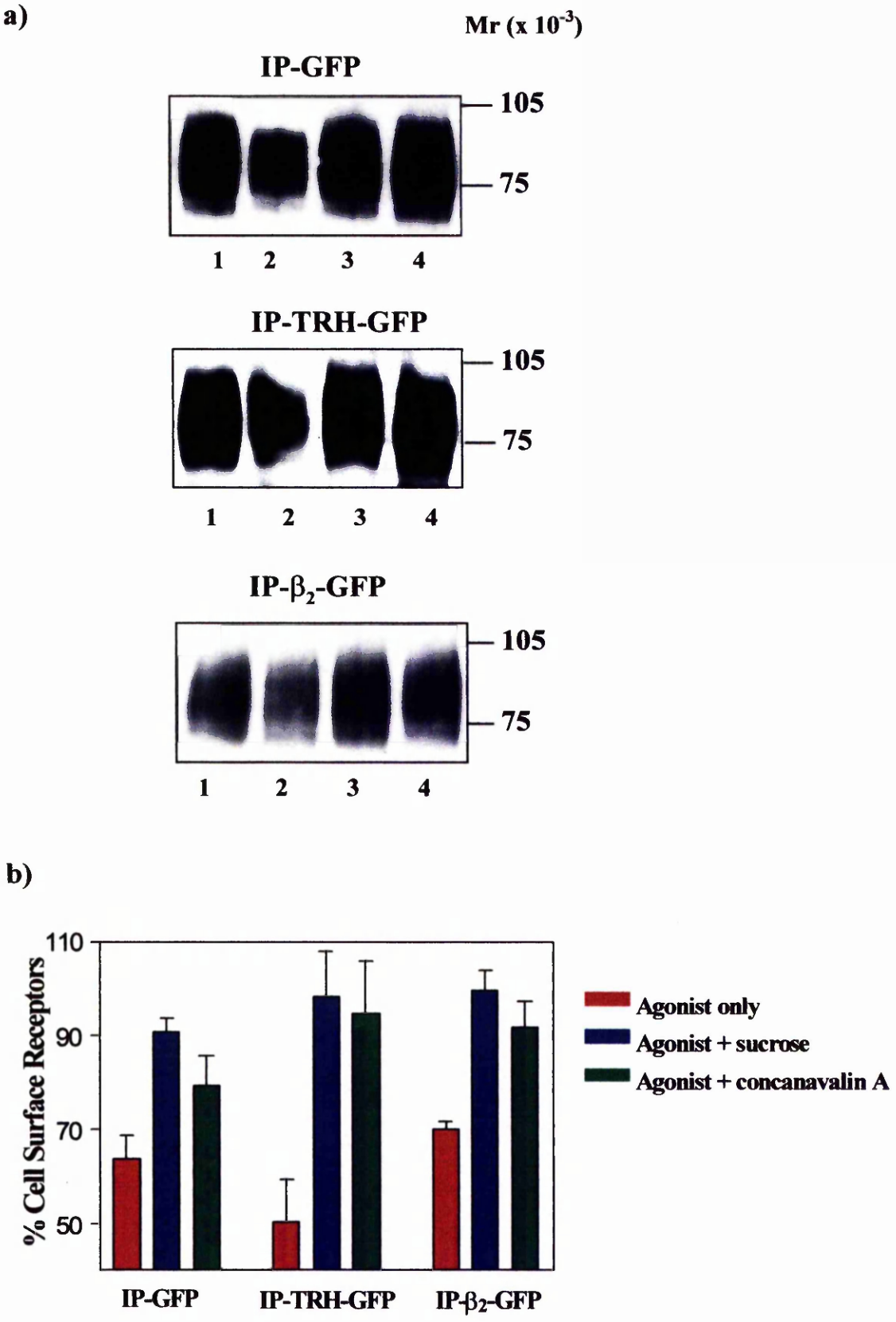
a)
Mr (x 10-3)
IP-GFP
105
75
1 2 3 4
IP-TRH-GFP
105
75
1 2 3 4
IP-β2-GFP
105
75
1 2 3 4
b)
% Cell Surface Receptors
110
90
70
50
IP-GFP
IP-TRH-GFP
IP-β2-GFP
Agonist only
Agonist + sucrose
Agonist + concanavalin A

Figure 4.3

Internalisation of GFP-tagged prostacyclin receptors into vesicles in close apposition to those containing transferrin.

The stable cell clones were pre-labelled with Texas Red® transferrin for 30 min to allow for uptake into transferrin receptor-containing vesicles. After washing, cells were treated with vehicle (a) or 1μM iloprost (b) for 30 min at 37°C. Imaging of each cell clones revealed that the receptor (green) and transferrin (red) signals overlapped after the addition of agonist (observed as yellow). Similar results were obtained from two further experiments. Scale bar = 10μM.

Figure 4.3

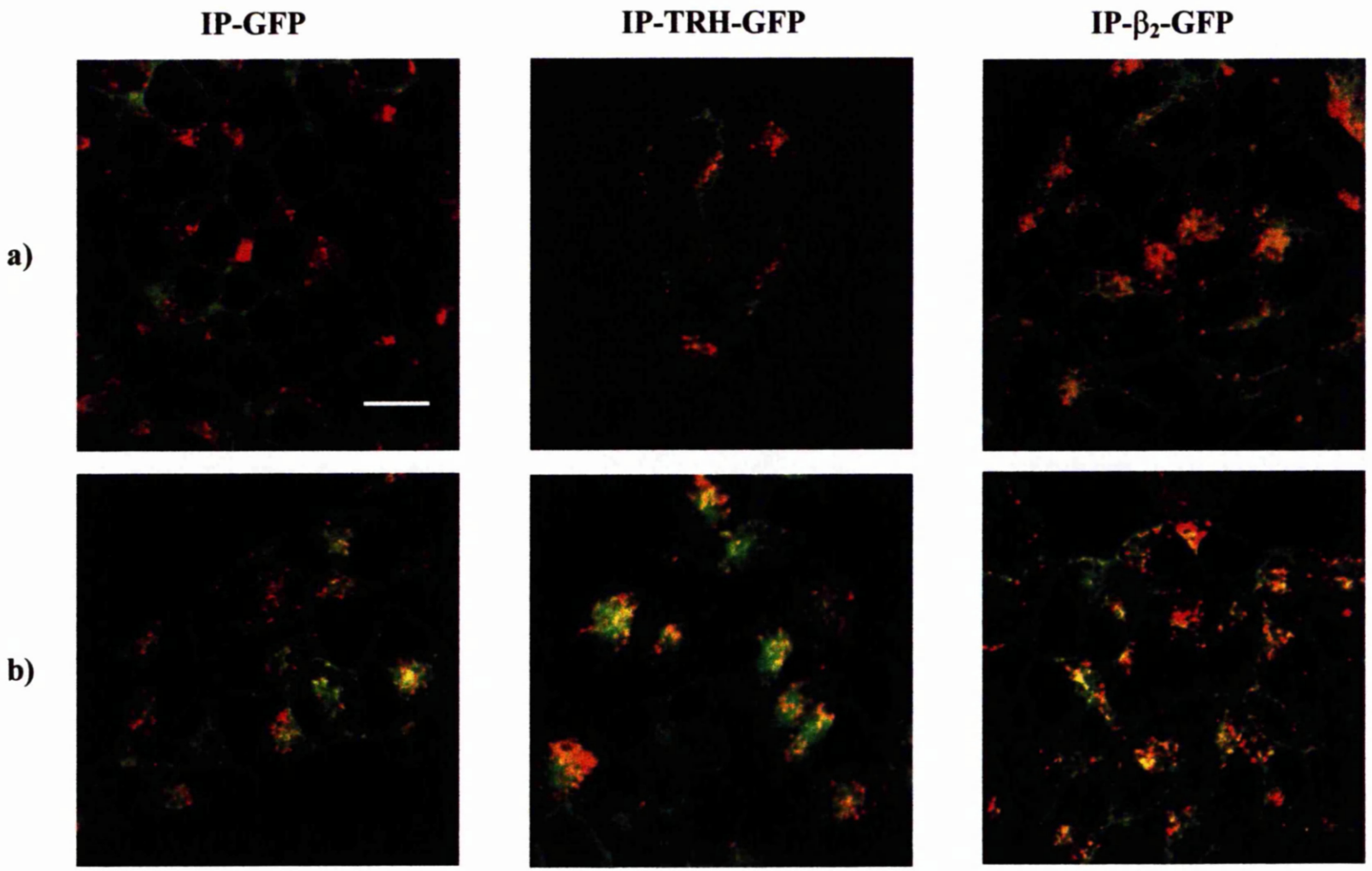

Figure 4.4

Interaction of the stably expressed prostacyclin receptor-GFP fusion proteins with transiently introduced β-arrestin 1 in response to agonist exposure.

a) The trafficking of the IP-GFP receptors (green) over a 60 min time course of agonist treatment was monitored in cells transiently expressing native β-arrestin 1, immunologically stained red. Merging of the fluorescent signals showed that the proteins localised in separate cellular compartments. The confocal images shown are representative of three separate experiments.

b) Examination of the merged confocal images revealed no detectable colocalisation between the sequestered IP-TRH-GFP receptors (green) and the transiently expressed β-arrestin 1 (red) during the time course. Similar results were produced with two further experiments.

c) IP-β_2-GFP receptor (green) sequestration proceeded via a pathway which appeared to be independent of β-arrestin 1 (red). As shown in the confocal images for all the timepoints of iloprost incubation, the red and green signals were differentially located. The images shown were similar to those produced from two further experiments.

Scale bar = 2.5μM.

Figure 4.4

a)

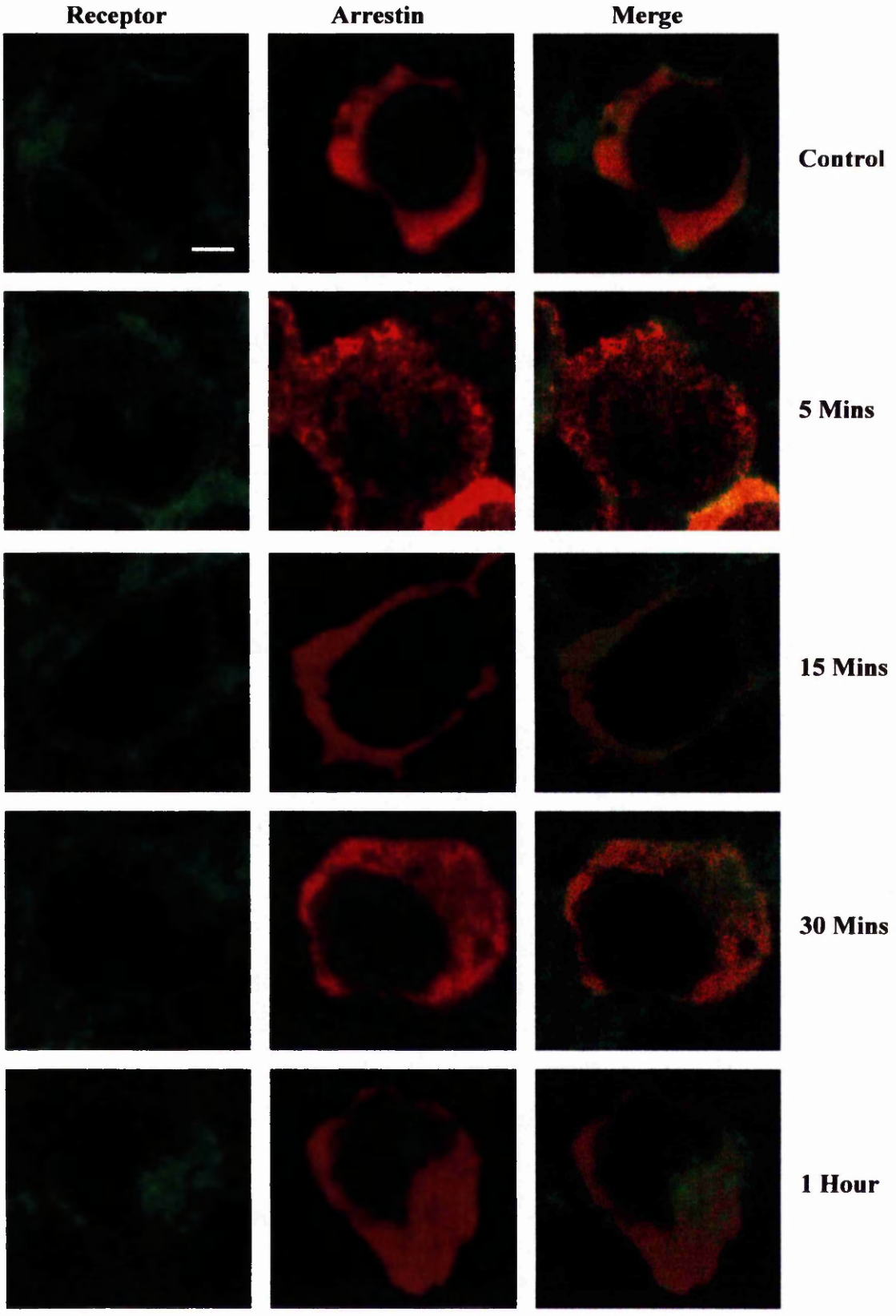
Receptor
Arrestin
Merge
Control
5 Mins
15 Mins
30 Mins
1 Hour

Figure 4.4

b)

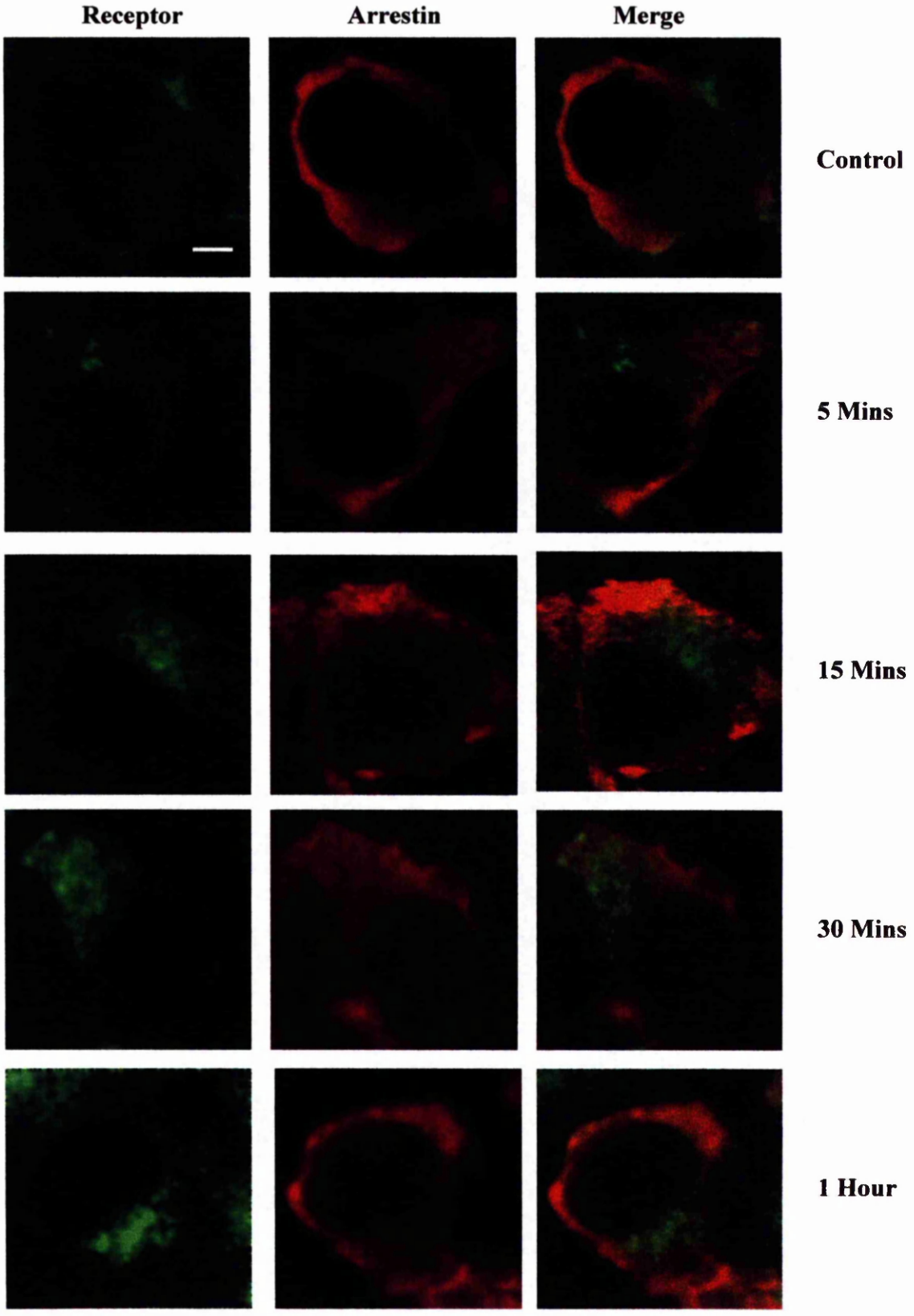
Receptor
Arrestin
Merge
Control
5 Mins
15 Mins
30 Mins
1 Hour

Figure 4.4

c)

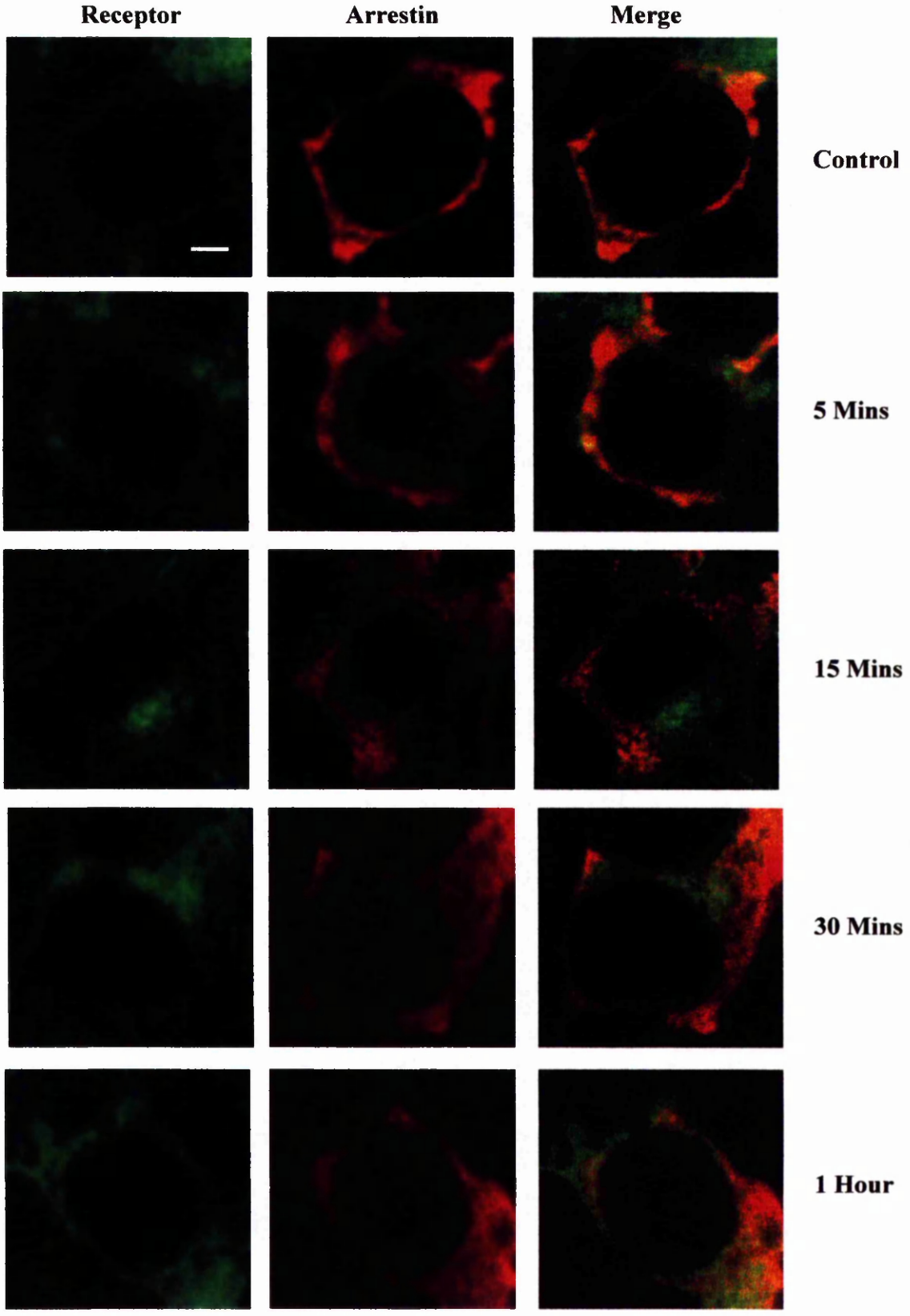
Receptor
Arrestin
Merge
Control
5 Mins
15 Mins
30 Mins
1 Hour

Figure 4.5

Agonist-mediated interactions of the stably expressed prostacyclin receptor-GFP fusion proteins with transiently introduced β-arrestin 2-RFP.

a) Agonist-stimulated trafficking of IP-GFP receptors (green) was observed in cells transiently transfected with β-arrestin 2-RFP (red). No obvious colocalisation of the proteins was observed during the 60 min agonist incubation as determined from analysis of the merged images. Two further experiments produced similar data.

b) Following transient expression of β-arrestin 2-RFP (red) into the IP-TRH-GFP cells (green), colocalisation of the two proteins (yellow) was observed upon the addition of agonist and was maintained for the duration of the time course.

c) Agonist stimulation of the IP-β_2-GFP cells (green) did not seem to induce a redistribution of β-arrestin 2-RFP (red) to the receptors. The merged images reveal that the sequestered receptors were located in vesicles distinct from those which contained the arrestin protein at all timepoints of agonist stimulation. The confocal data shown are representative of three individual experiments.

Scale bar = 2.5μM.

Figure 4.5

a)

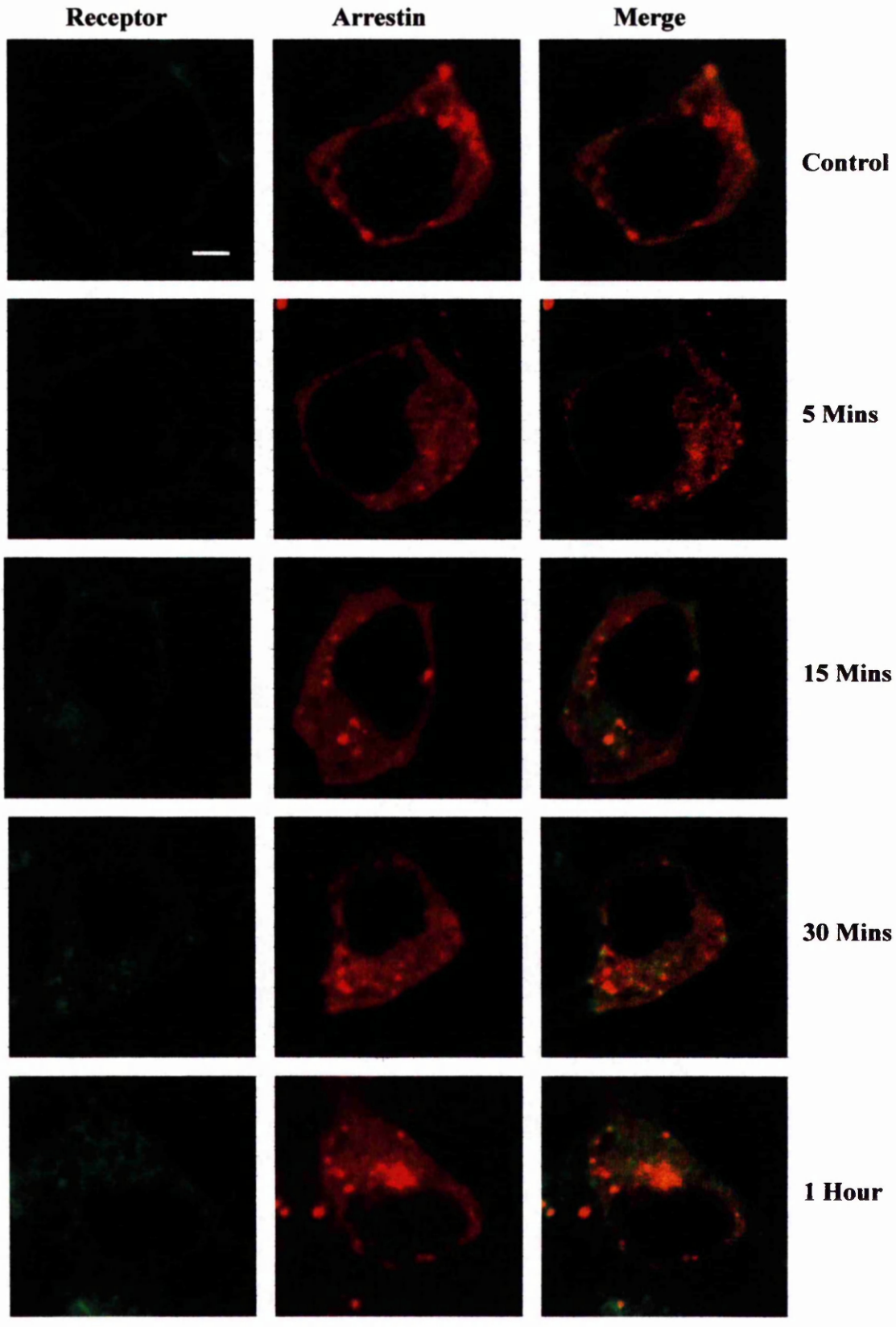
Receptor
Arrestin
Merge
Control
5 Mins
15 Mins
30 Mins
1 Hour

Figure 4.5

b)

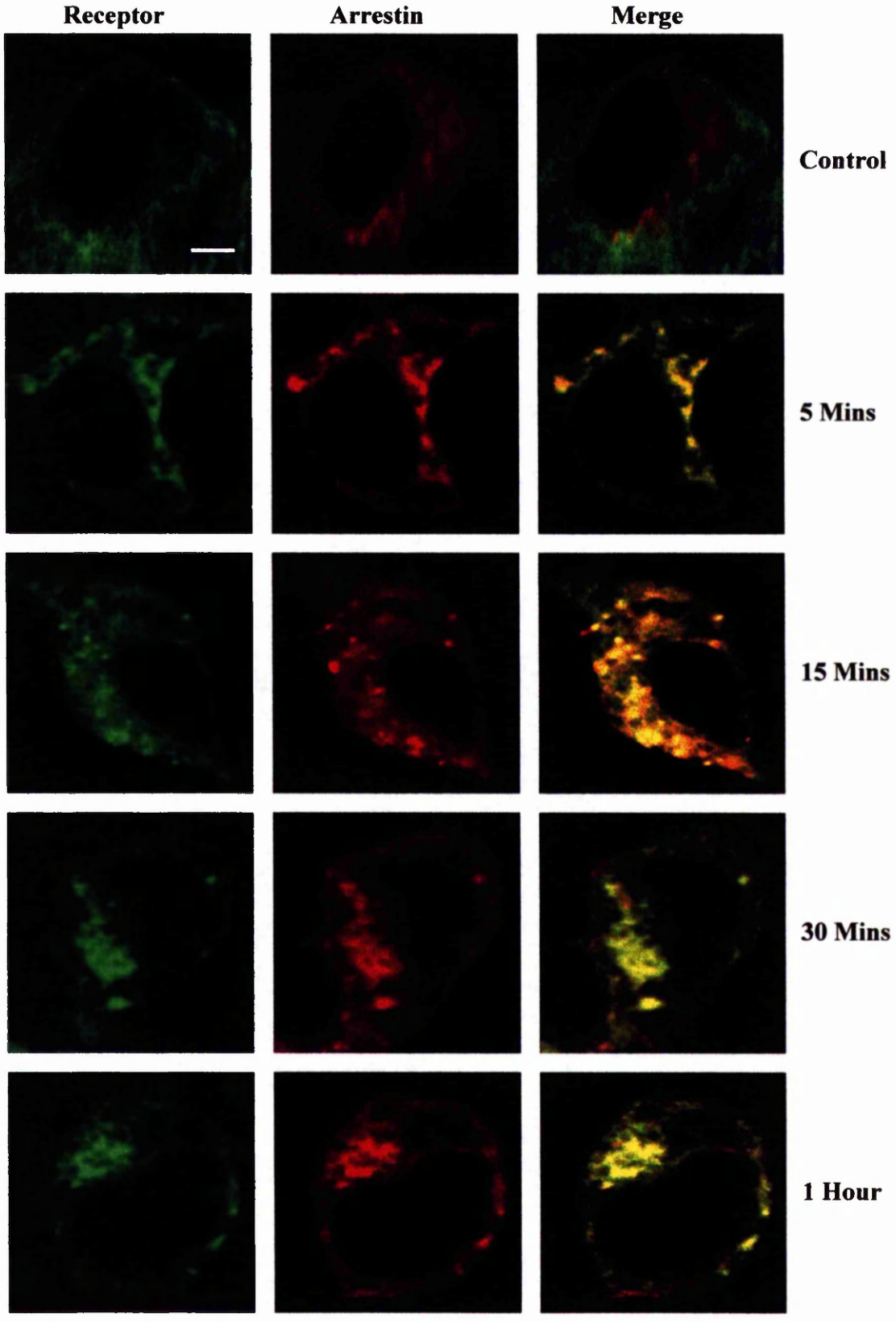
Receptor
Arrestin
Merge
Control
5 Mins
15 Mins
30 Mins
1 Hour

Figure 4.5

c)

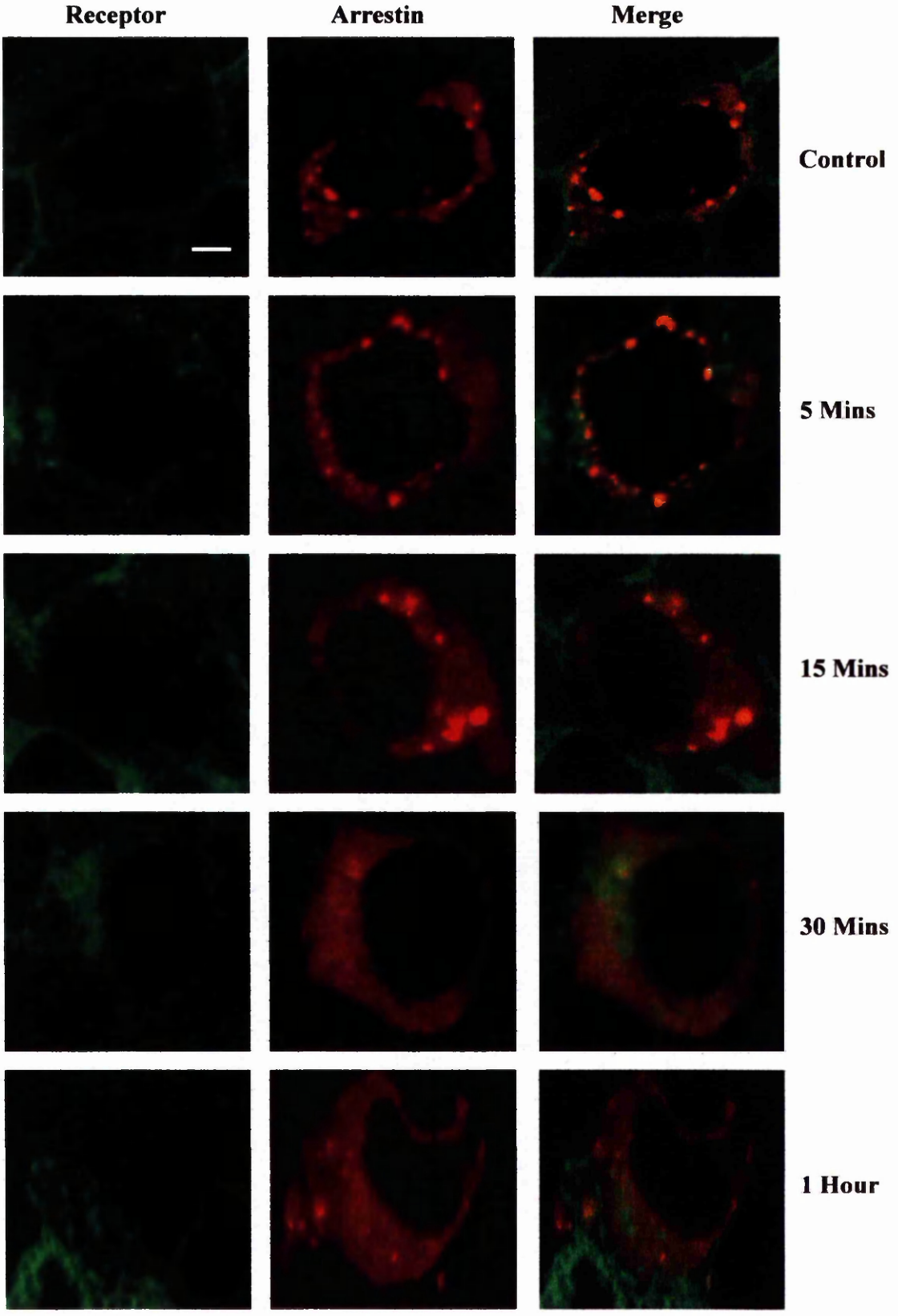
Receptor
Arrestin
Merge
Control
5 Mins
15 Mins
30 Mins
1 Hour

Figure 4.6

Confocal analysis of HEK293 cells transiently expressing the HA-tagged prostacyclin receptor constructs in conjunction with GFP-labelled β-arrestin 1.

a) In cells co-expressing the HA-IP receptor (red) and β-arrestin 1-GFP (green) constructs, agonist-activated receptors sequestered into intracellular compartments distinct from those containing β-arrestin 1-GFP. The images from one 60 min agonist time course is shown. Similar data was produced from two additional experiments.

b) Agonist stimulation of HA-IP-TRH receptors (red) did not trigger the recruitment of β-arrestin 1-GFP (green) to the plasma membrane. The confocal images reveal that the two signal did not overlap during the 60 min time course. Two further experiments produced similar results.

c) Sequestered HA-IP-β_2 receptors (red) did not form any noticeable interaction with the co-transfected β-arrestin 1-GFP construct (green). The merged confocal images of the 60 min agonist incubation demonstrate that the signal localised in differential intracellular structures. The images shown represent one experiment which was performed three times.

Scale bar = 2.5μM.

Figure 4.6

a)

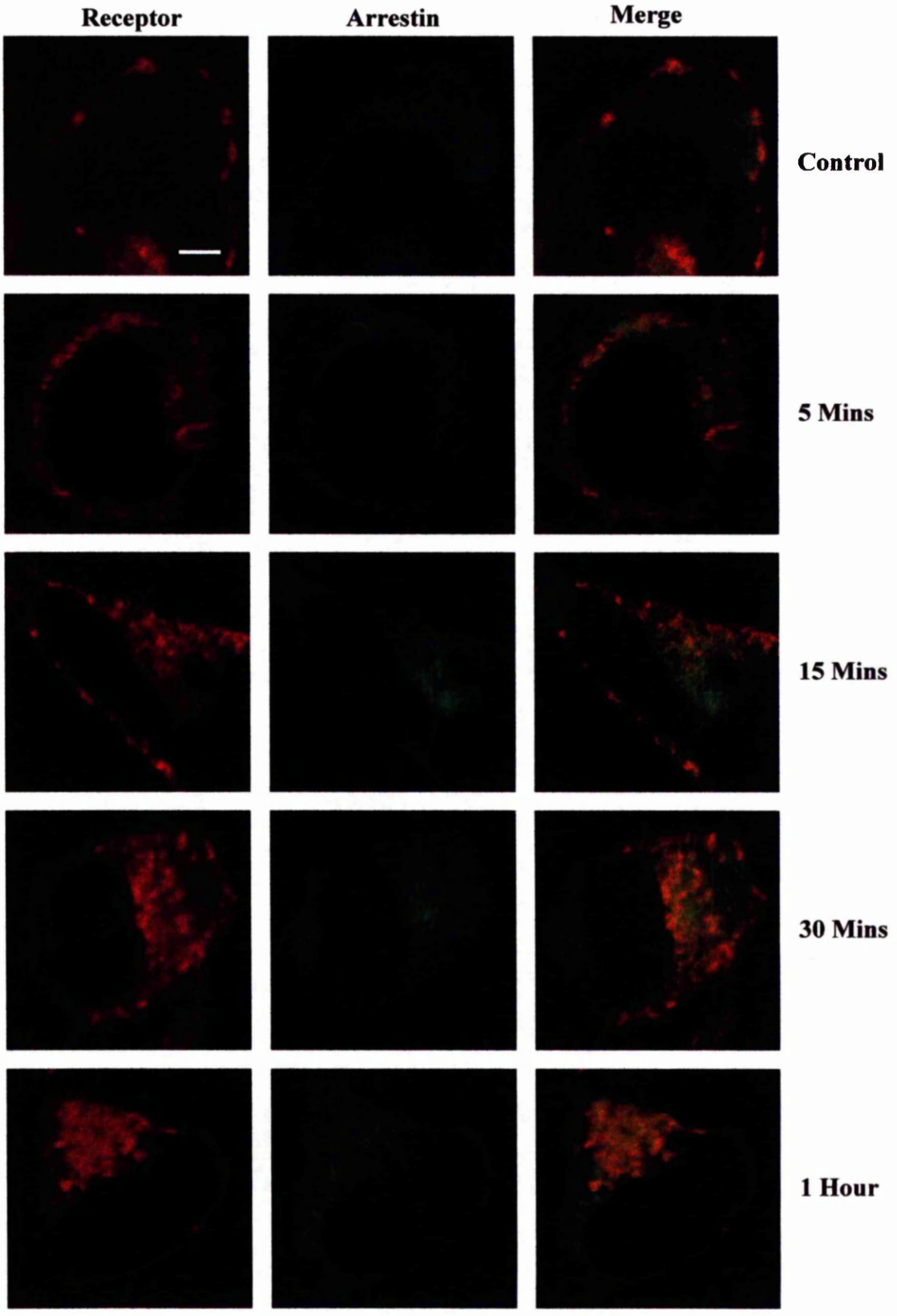
Receptor
Arrestin
Merge
Control
5 Mins
15 Mins
30 Mins
1 Hour

Figure 4.6

b)

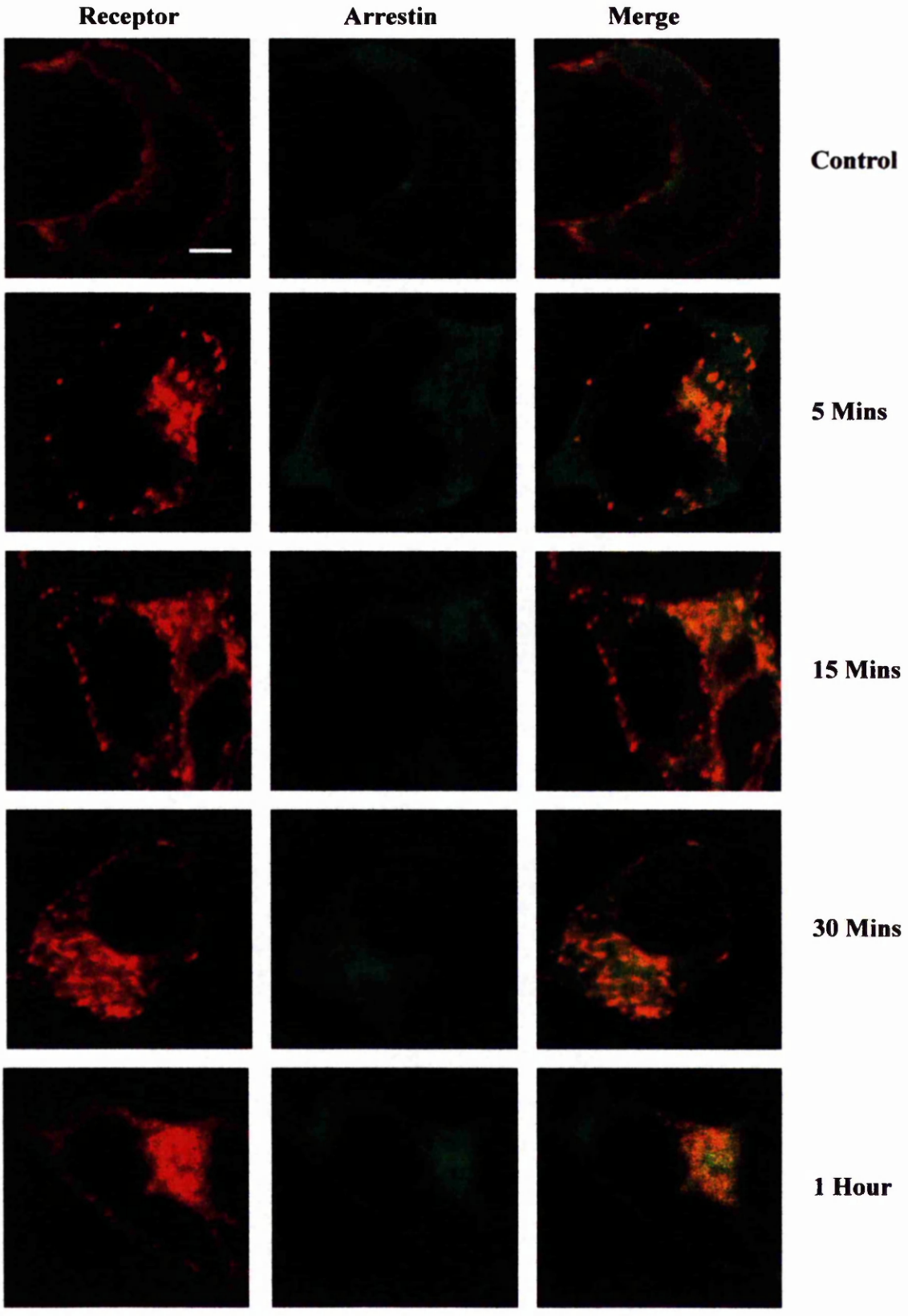
Receptor
Arrestin
Merge
Control
5 Mins
15 Mins
30 Mins
1 Hour

Figure 4.6

c)

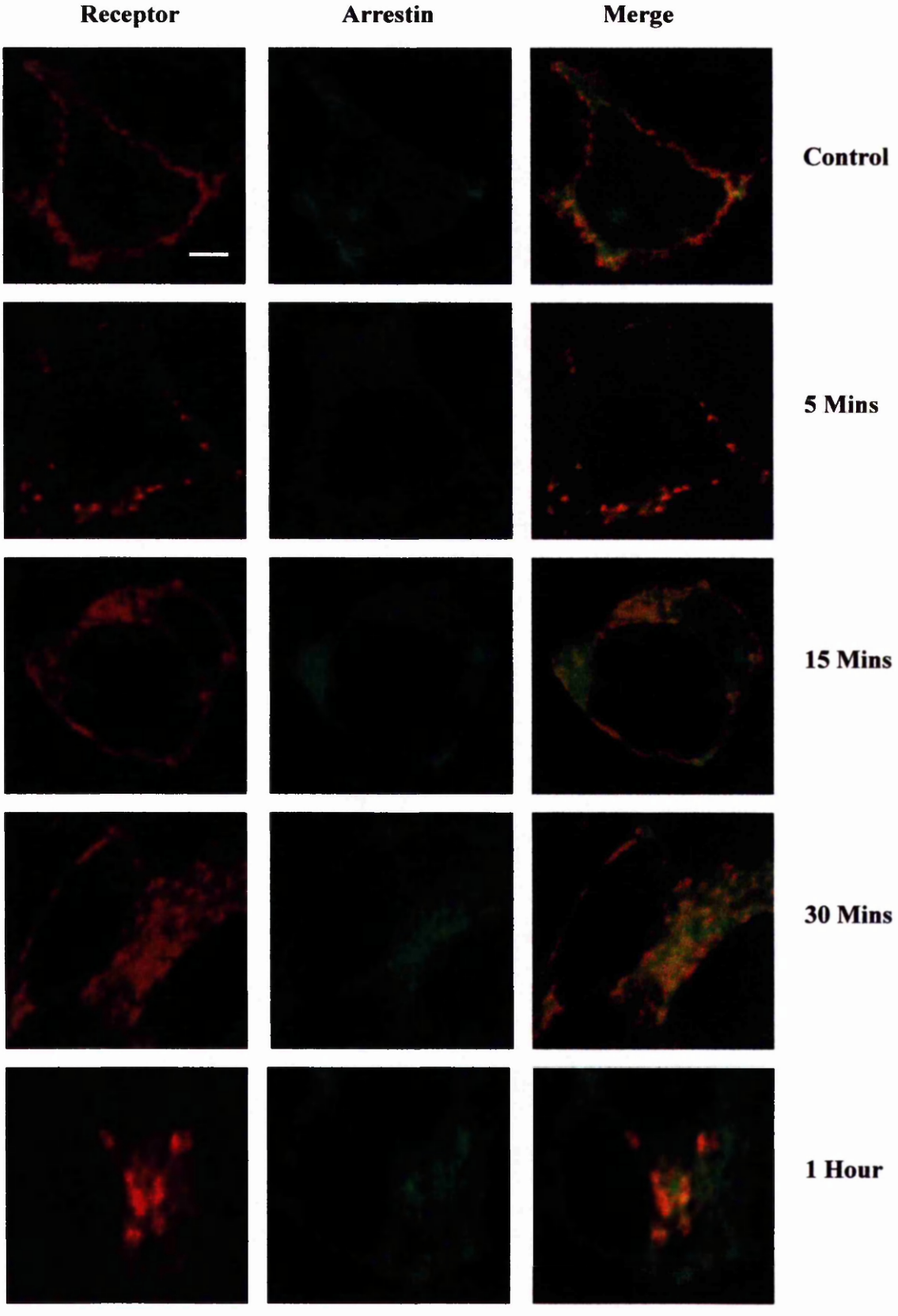
Receptor
Arrestin
Merge
Control
5 Mins
15 Mins
30 Mins
1 Hour

Figure 4.7

Confocal analysis receptor/arrestin interactions in HEK293 cells co-expressing the HA-tagged prostacyclin receptor constructs and β-arrestin 2-GFP.

a) HA-IP receptors (red) showed no obvious colocalisation with β-arrestin 2-GFP (green) upon agonist activation of the receptors. The dual images of the various agonist timepoints reveal that the two proteins did not associate. Similar observations were made with two further experiments.

b) Visualisation of the distribution of agonist-sequestered HA-IP-TRH receptors (red) reveal that receptors co-internalised with β-arrestin 2-GFP (green). Significant colocalisation of the two signals (yellow) can be seen at all timepoints of agonist treatment. The images shown are representative of one experiment which was performed three times.

c) Agonist-mediated internalisation of the HA-IP-β_2 receptors (red) proceeded via a pathway which was independent of β-arrestin 2-GFP (green). Analysis of the confocal images showed that no visible association of the two proteins was evident during the agonist time course. Two further experiments produced similar observations.

Scale bar = 2.5μM.

Figure 4.7

a)

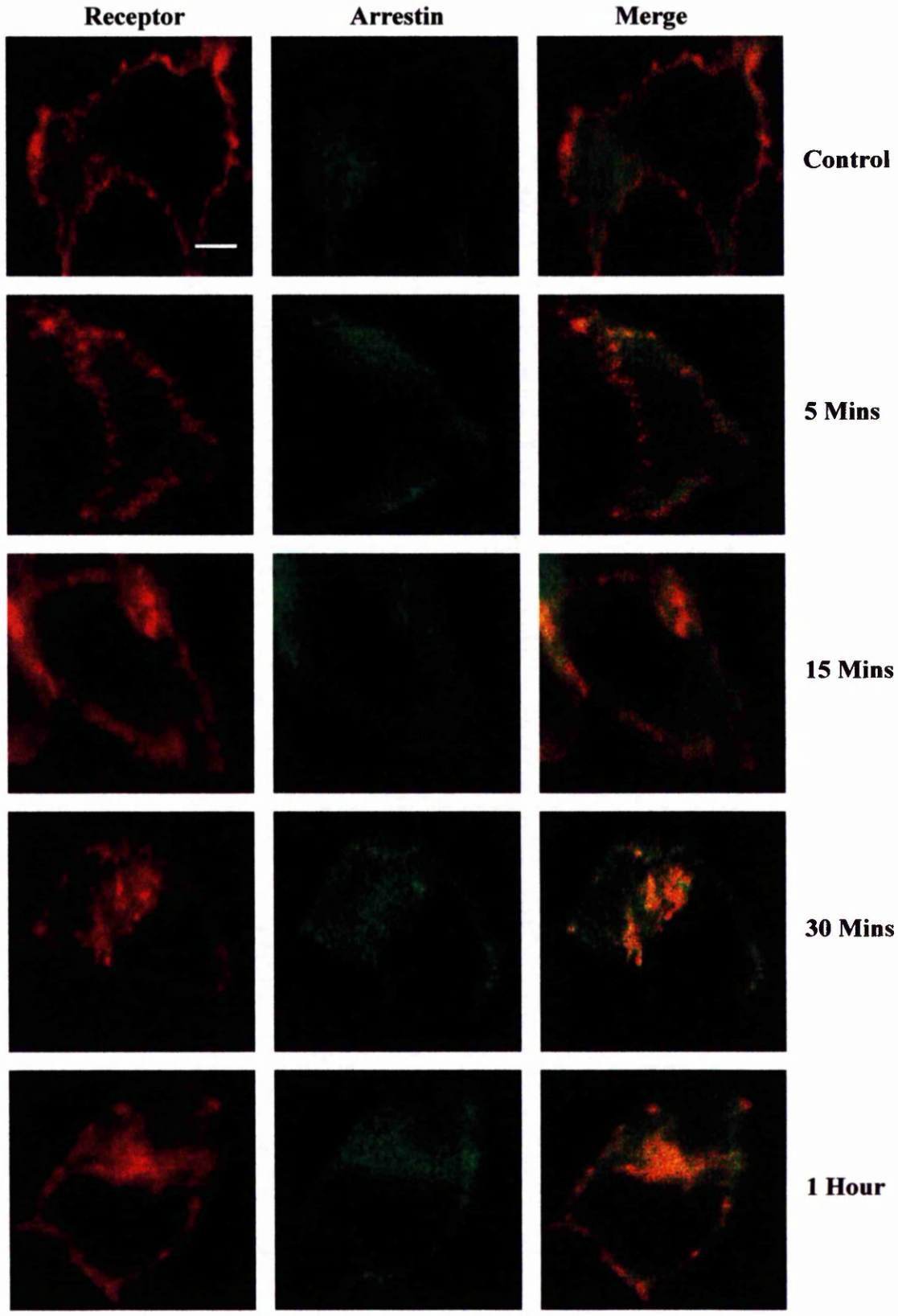
Receptor
Arrestin
Merge
Control
5 Mins
15 Mins
30 Mins
1 Hour

Figure 4.7

b)

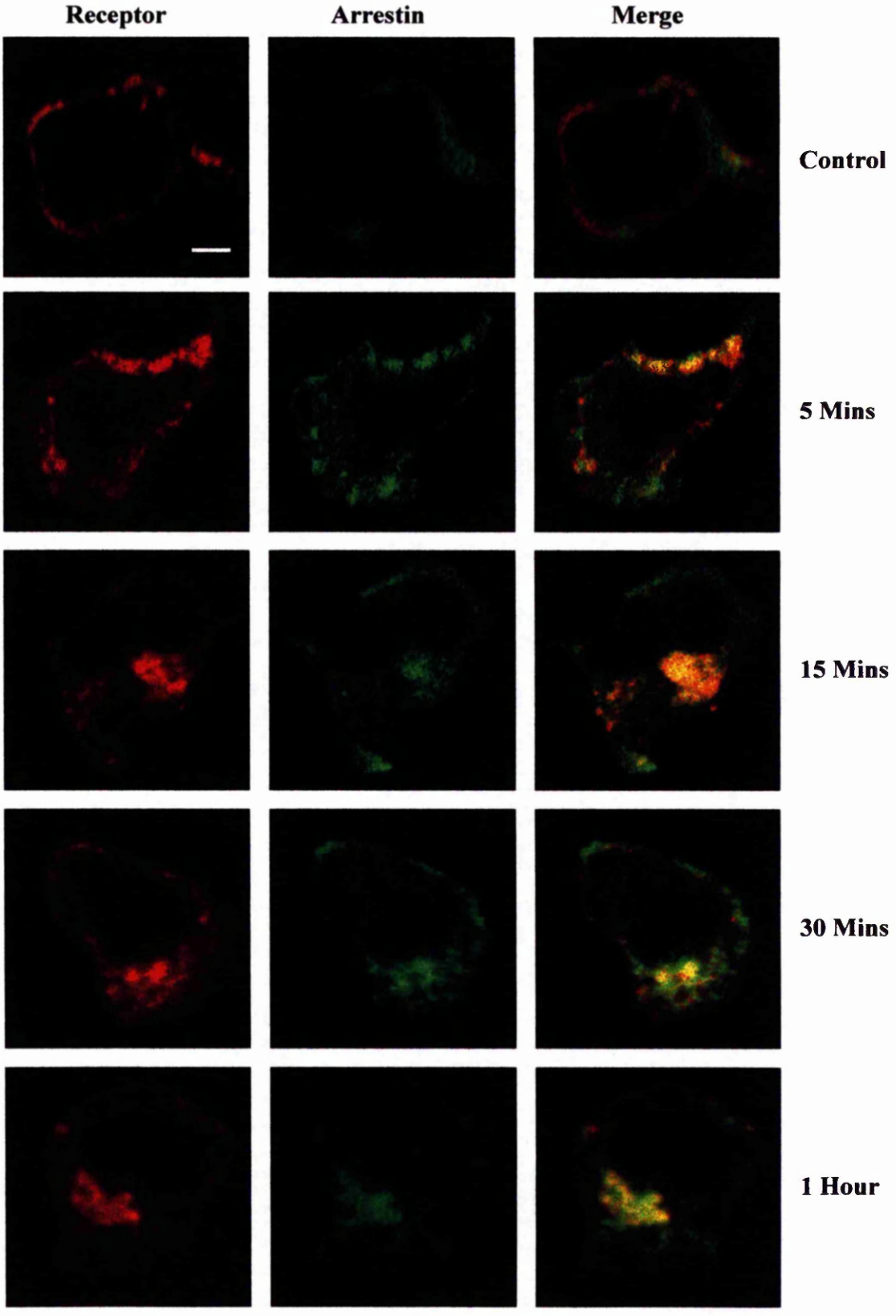
Receptor
Arrestin
Merge
Control
5 Mins
15 Mins
30 Mins
1 Hour

Figure 4.7

c)

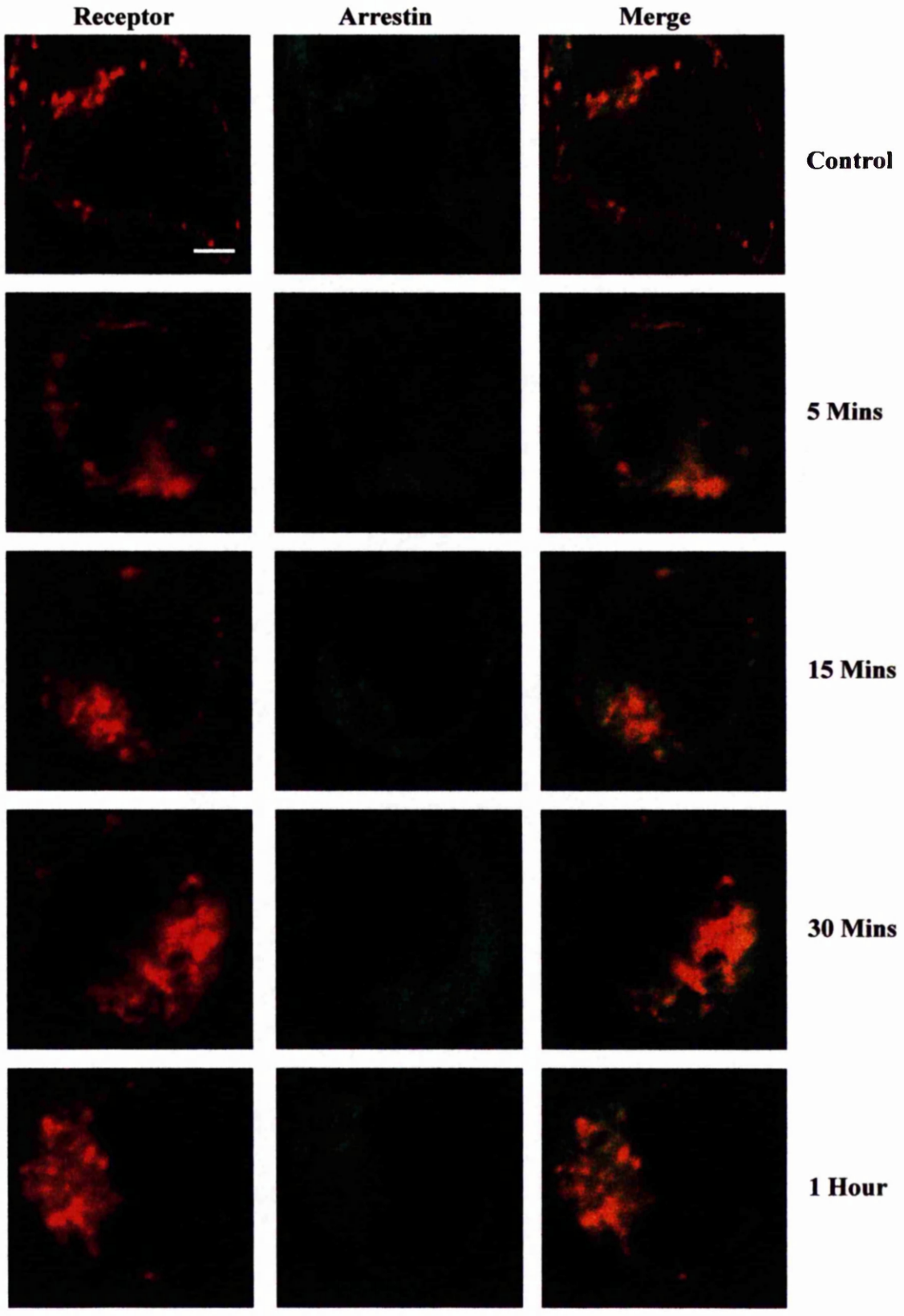
Receptor
Arrestin
Merge
Control
5 Mins
15 Mins
30 Mins
1 Hour

Figure 4.8

Control experiments: Cellular trafficking of the rat TRH-1 receptor with β-arrestins.

a) HEK293 cells were co-transfected with a VSV-tagged TRH receptor (red) and β-arrestin 1-GFP (green). In the unstimulated state, the two signals were differentially localised. After a 30 min exposure to 10μM TRH, the sequestered receptors co-internalised with β-arrestin 1-GFP (yellow). A further experiment produced similar findings.

b) In cells co-expressing the VSV-tagged TRH receptor (red) and β-arrestin 2-GFP (green), significant colocalisation of the two proteins in intracellular vesicles could be seen after 30 min of agonist treatment. Similar observations were made in one further experiment.

Scale bar = 2.5μM.

Figure 4.8

a)

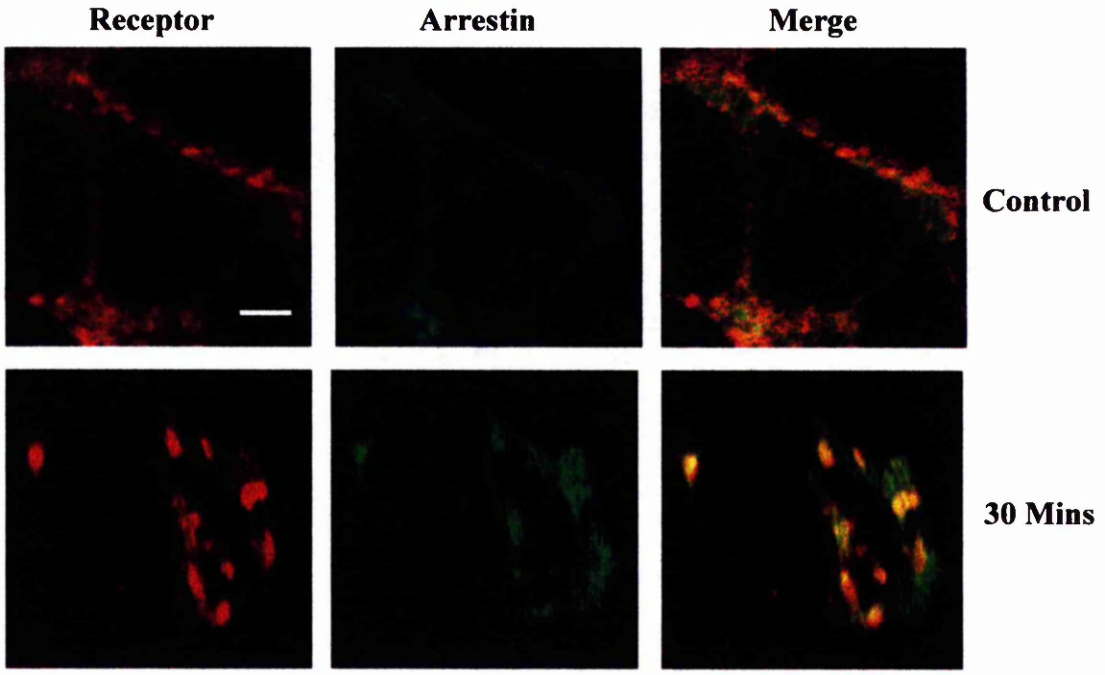
Receptor
Arrestin
Merge
Control
30 Mins

b)

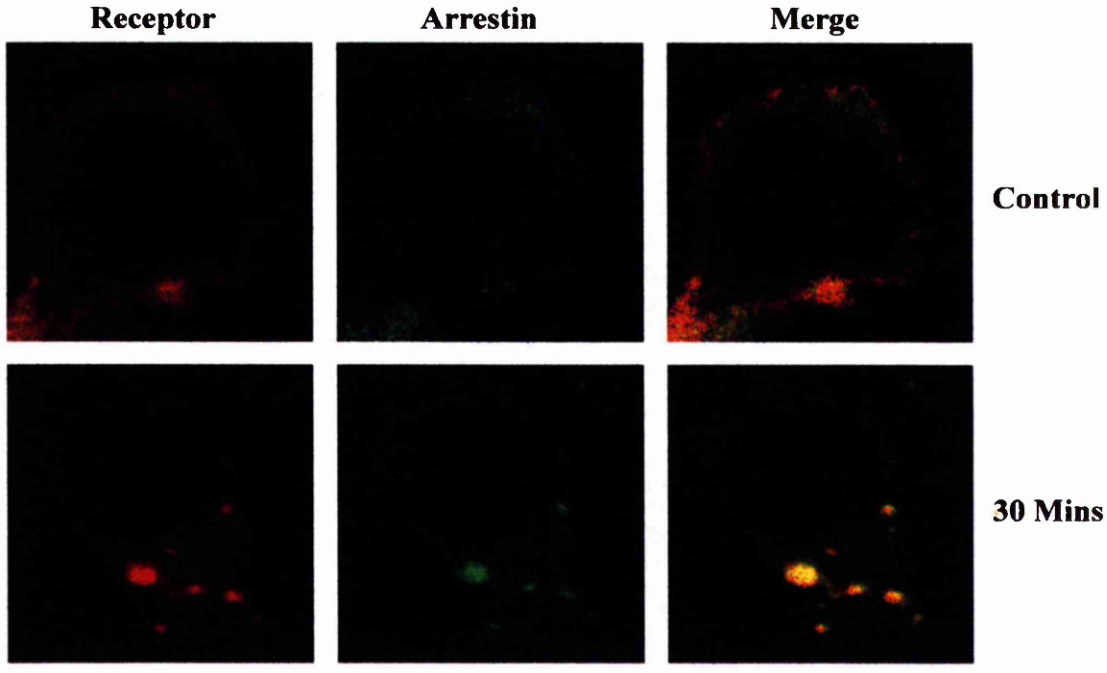
Receptor
Arrestin
Merge
Control
30 Mins

Figure 4.9

Control experiments: Agonist-activation of the β_2-AR promotes translocation of β-arrestins to the plasma membrane.

a) In the basal state, the immunostained β_2-AR (red) was localised at the plasma membrane whereas β-arrestin 1-GFP (green) was distributed diffusely throughout the cytoplasm. Within 5 min of treatment with 10 μM isoproterenol, agonist-activated receptors had triggered the translocation of β-arrestin 1-GFP to the plasmalemmal surface. A similar result was produced when the experiment was repeated.

b) In unstimulated cells the β_2-AR (red) and β-arrestin 2-GFP (green) were differentially located. Agonist stimulation of the β_2-AR induced the redistribution of β-arrestin 2-GFP from the cytoplasm to the agonist-activated receptors within 5 min. One additional experiment produced similar results.

Scale bar = 2.5μM.

Figure 4.9

a)

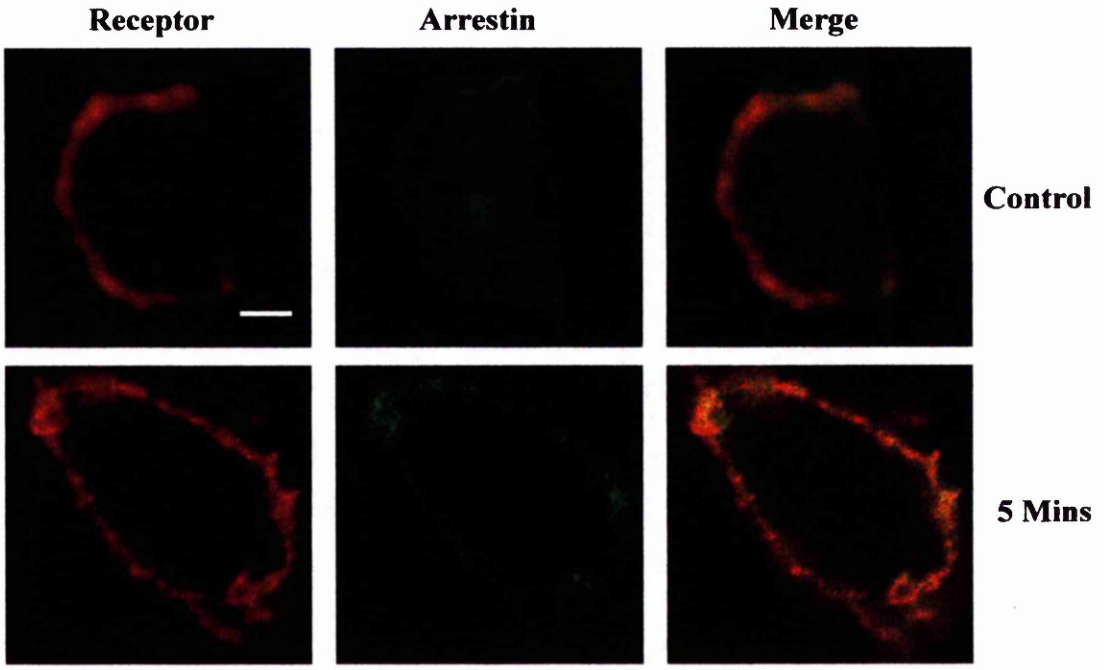
Receptor
Arrestin
Merge
Control
5 Mins

b)

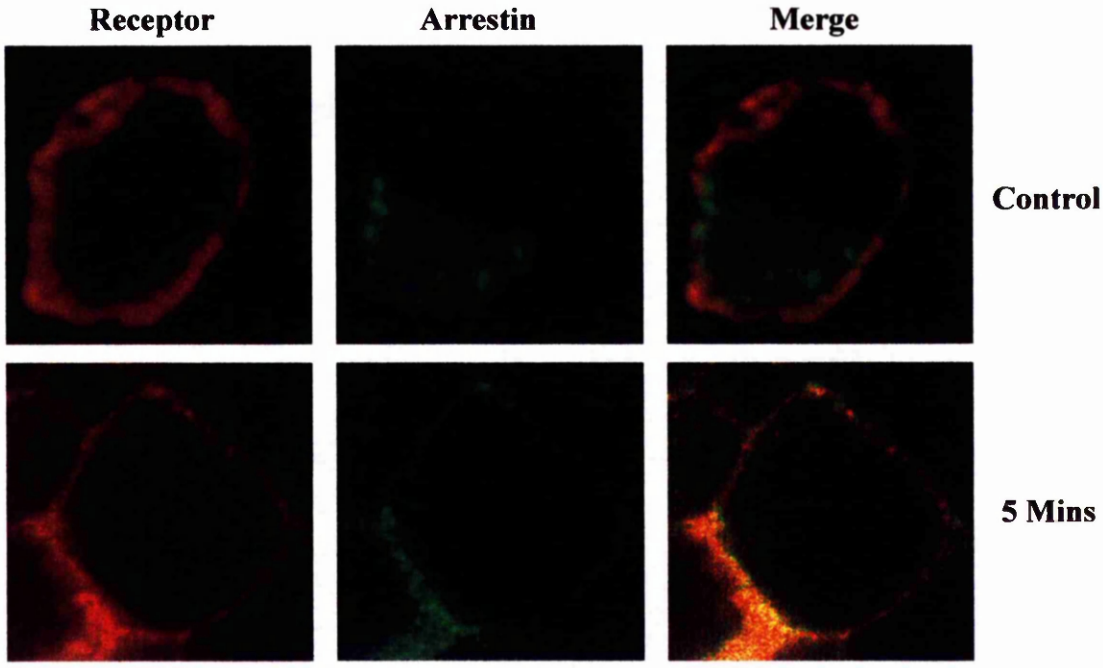
Receptor
Arrestin
Merge
Control
5 Mins

Figure 4.10

Co-immunoprecipitation of the HA-tagged prostacyclin receptors with β-arrestins.

HEK293 cells were transfected with the HA-IP (a), HA-IP-TRH (b), and HA-IP-β_2 (c) receptor constructs in conjunction with either the β-arrestin 1-GFP or β-arrestin 2-GFP plasmids. Cells were incubated with or without 1μM iloprost for 5 min at 37°C. Cells were then lysed and the β-arrestin constructs were immunoprecipitated with the anti-GFP antibody and the presence of receptor in the immunoprecipitates was detected with the 12CA5 antibody following SDS-PAGE and immunoblotting. Co-precipitated receptors were detected as immuno-reactive species of ~40 kDa. No signal was detected in cells transfected with receptor, β-arrestin, or empty vector alone.

Figure 4.10

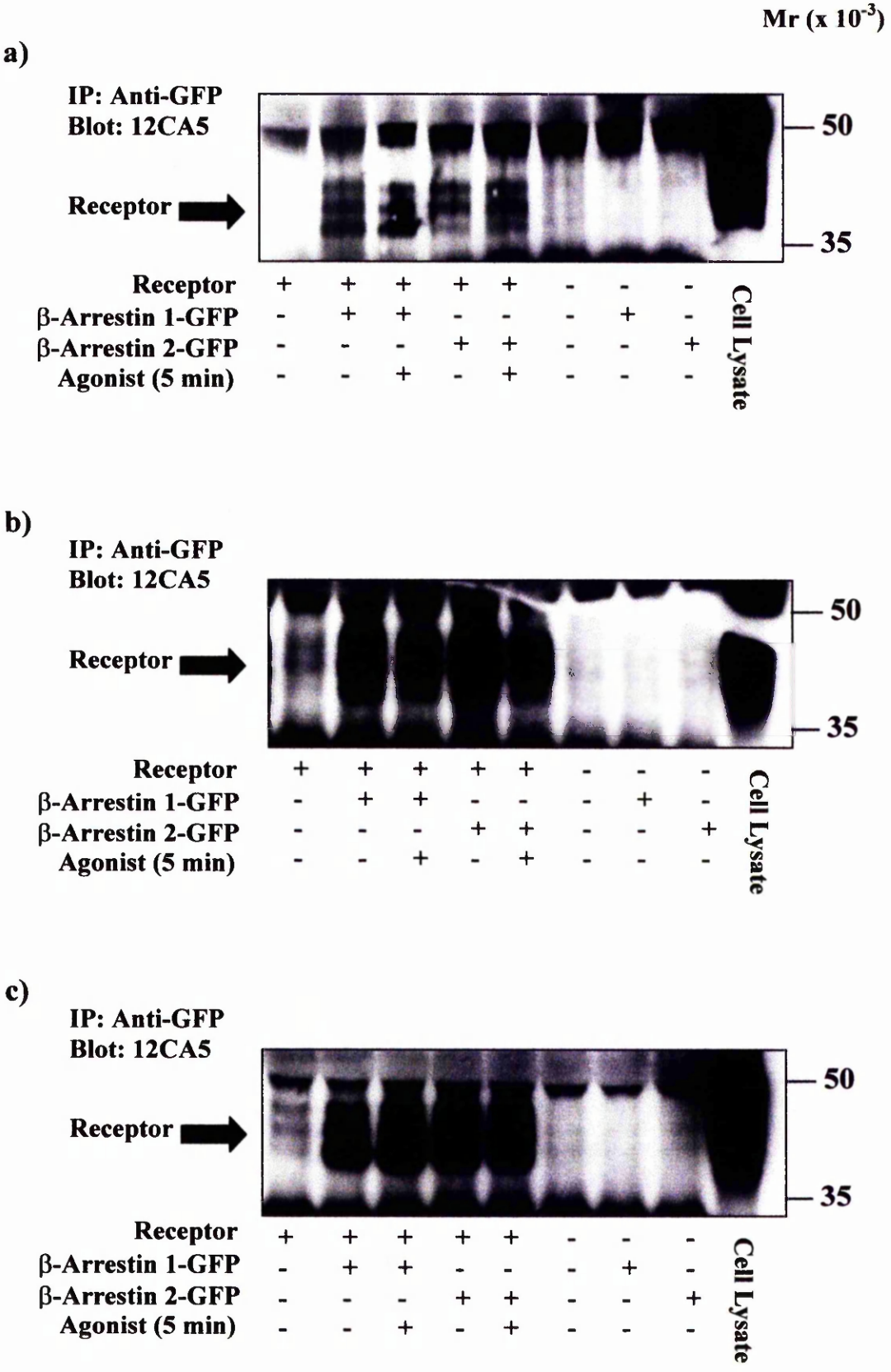
Mr (x 10-3)
a)
IP: Anti-GFP
Blot: 12CA5
Receptor
50
35
Receptor + + + + + - - -
β-Arrestin 1-GFP - + + - - - + -
β-Arrestin 2-GFP - - - + + - - +
Agonist (5 min) - - + - + - - -
Cell Lysate
b)
IP: Anti-GFP
Blot: 12CA5
Receptor
50
35
Receptor + + + + + - - -
β-Arrestin 1-GFP - + + - - - + -
β-Arrestin 2-GFP - - - + + - - +
Agonist (5 min) - - + - + - - -
Cell Lysate
c)
IP: Anti-GFP
Blot: 12CA5
Receptor
50
35
Receptor + + + + + - - -
β-Arrestin 1-GFP - + + - - - + -
β-Arrestin 2-GFP - - - + + - - +
Agonist (5 min) - - + - + - - -
Cell Lysate

Figure 4.11

Agonist-mediated internalisation of the HA-tagged prostacyclin receptors in the GRK- and β-arrestin-deficient COS7 cell line.

COS7 cells were transiently transfected with the HA-IP, HA-IP-TRH, and the HA-IP-β_2 receptor constructs. Cell surface receptors were antibody labelled with the 12CA5 antibody prior to treatment with vehicle or 1μM iloprost for 60 min. Confocal analysis of the immunostained receptors revealed that each of the constructs exhibited significant intracellular localisation in response to agonist. The images shown are from one experiment which was repeated twice with similar results.

Scale bar = 2.5μM.

Figure 4.11

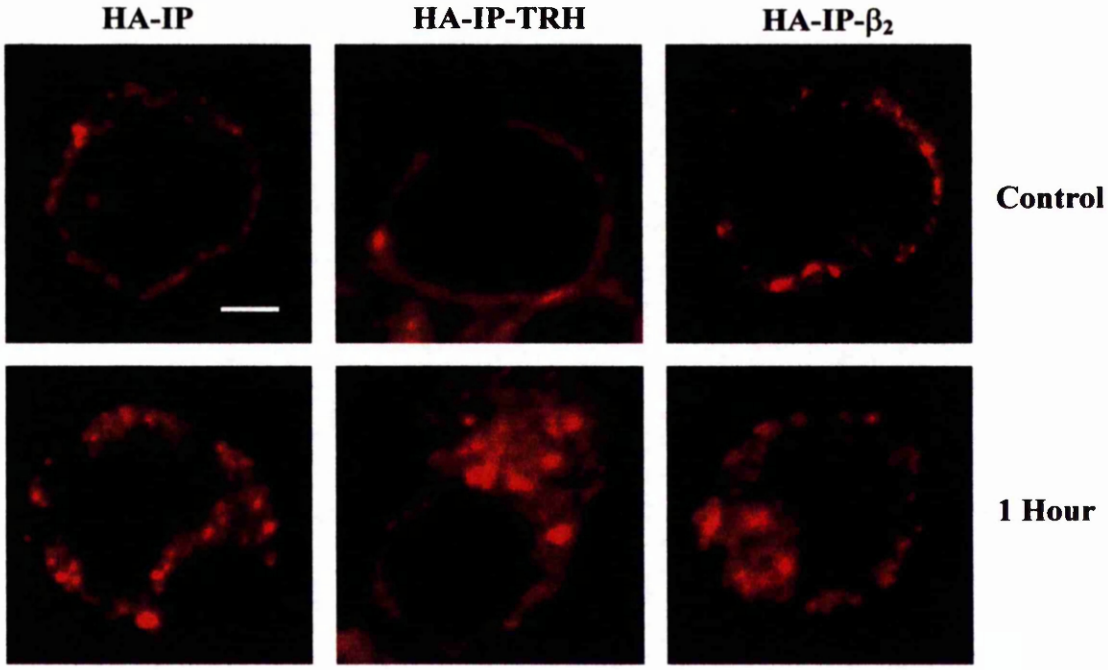

Figure 4.12

Effects of K44E-dynamin overexpression on agonist-induced sequestration of the prostacyclin receptor-GFP fusion proteins.

a) The stable cell lines transiently transfected with empty vector (1, 2) or K44E-dynamin (3) were stimulated with either vehicle (1) or 1μM iloprost (2, 3) for 60 min. The cell surface receptor expression was detected using biotin labelling assays as described in section 2.7.5. The immunoblots shown are representative of two separate experiments.

b) A representative Western blot of lysates from receptor-expressing cells transfected with empty vector (1) or myc-tagged dynamin-K44E (2) and immunoblotted with an anti-myc antibody.

Figure 4.12

a)

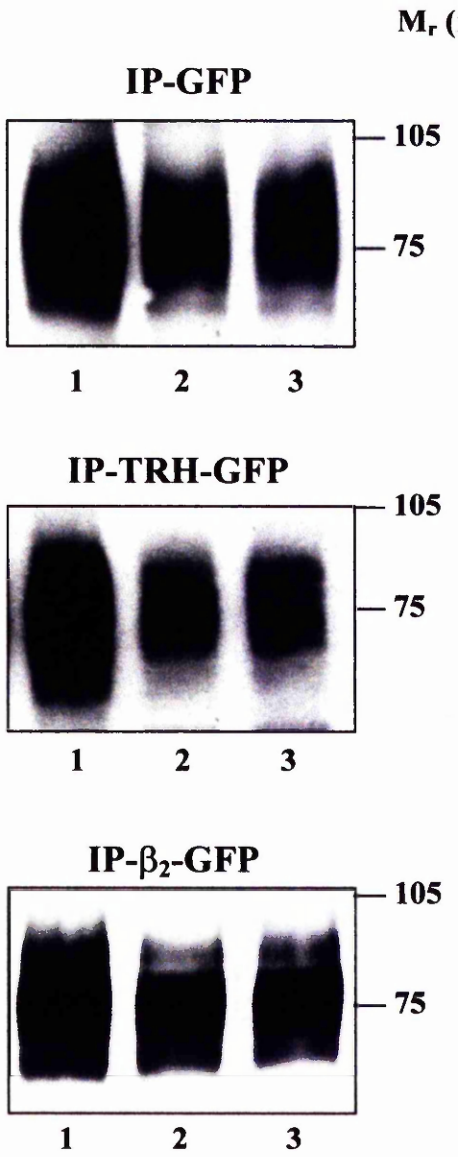

b)

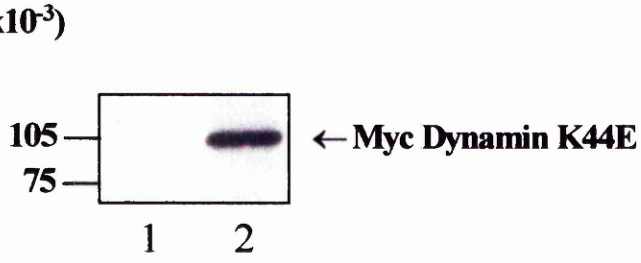

4.10 Discussion

Agonist-induced GPCR internalisation is a multi-step process. In the "classical" pathway of GPCR internalisation, GRK- and/or second messenger kinase-mediated phosphorylation of the receptor facilitates the binding of β-arrestins thereby uncoupling the receptor from G protein and promoting receptor sequestration via clathrin coated vesicles (Ferguson and Caron, 1998). To date, it appears that most GPCRs studied follow this paradigm, but notable exceptions have been observed. Numerous investigations have proposed that the pathway by which a given GPCR internalises is not only governed by receptor structure and activity, but by the cellular environment in which it is expressed. In this investigation, various biochemical assays in concert with immunocytochemical techniques were used to delineate the endocytic pathway used by the prostacyclin receptor, and its chimeric forms, in HEK293 cells. Whilst in the midst of this investigation, Smyth and coworkers (2000) reported that the native prostacyclin receptor exhibited a clathrin-dependent, arrestin-independent internalisation pattern in HEK293 cells. Similar findings are reported in this chapter.

Pharmacological agents such as hyperosmolar sucrose and concanavalin A are known to disrupt receptor internalisation via clathrin coated pits (Heuser and Anderson, 1989; Pippig *et al.*, 1995). Pre-treatment of HEK293 cells transiently expressing the HA-tagged IP receptor constructs with sucrose or concanavalin A significantly reduced agonist-mediated internalisation of the receptors as monitored confocally (Figure 4.1). A similar result was observed with the GFP-tagged forms of the receptors; biotin-labelling experiments showed that receptor internalisation was substantially reduced in the presence of sucrose and concanavalin A (Figure 4.2). To further investigate the nature of the vesicles into which the receptors were internalised, the receptor-GFP stable cell clones were incubated with Texas Red® transferrin. Transferrin is internalised constitutively, along with the transferrin receptor, via clathrin coated pits into early endosomes through a recycling pool and then back to the plasma membrane (Woods *et al.*, 1989; Ghosh *et al.*, 1994). In unstimulated cells the receptors and transferrin were compartmentalised separately. After 30 min of iloprost exposure, an overlap of the red and green signals was evident as demonstrated by the appearance of yellow fluorescence (Figure 4.3) thus indicating the vesicles containing the two proteins

were in close proximity. Taken together, these data suggested that the receptors traffic via a clathrin coated vesicular pathway.

Evidence from numerous GPCR studies has indicated that clathrin-mediated endocytosis of receptors proceeds primarily via an arrestin-dependent pathway. It therefore seemed likely that similar molecular mechanisms were involved in the CCV trafficking of the prostacyclin receptors. Direct monitoring of fluorescently-labelled GPCRs and β-arrestins in intact cells has been used to study the arrestin-dependent sequestration of GPCRs including the β_2-AR, proteinase-activated receptor, TRH receptor, and chemokine CXCR4 receptor (Barak *et al.*, 1997b; Dery *et al.*, 1999; Groarke *et al.*, 1999; Orsini *et al.*, 1999).

A similar approach was used to characterise the endocytic pathway of the prostacyclin receptor; confocal microscopy was used to visualise the interactions of the β-arrestin isoforms with the receptor constructs in intact cells. In colocalisation studies, agonist-mediated internalisation of the full-length GFP- and HA-tagged forms of the receptor did not promote the redistribution of either β-arrestin isoforms in the cells, thus demonstrating that receptor sequestration was primarily arrestin-independent (Figures 4.4a, 4.5a, 4.6a, 4.7a). Smyth and coworkers (2000) reported similar findings; they noted that co-transfection of receptor-expressing HEK293 cells with β-arrestin 1 did not increase iloprost-stimulated sequestration. Moreover, expression of a dominant negative mutant form of β-arrestin 1 did not reduce receptor endocytosis. They concluded from these observations that prostacyclin receptor internalisation is likely arrestin-independent. The group did not, however, investigate the role of β-arrestin 2 in receptor sequestration. Therefore, the data cannot rule out the possible involvement of an arrestin-dependent pathway altogether. Similar to data presented in this chapter, Smyth *et al.* (2000) did report that reagents such as hyperosmotic sucrose or concanavalin A could inhibit endocytosis thus demonstrating that prostacyclin receptor internalisation is clathrin-mediated.

To ascertain the functional importance of the carboxyl terminal domain in conferring arrestin insensitivity to the prostacyclin receptor, arrestin colocalisation studies were performed with the chimeric prostacyclin receptors which possessed the intracellular C-

tail sequences of the rat TRH-1 and human β_2-adrenergic receptors. The agonist-induced internalisation of the native TRH and β_2-adrenergic receptors has been shown to be β-arrestin-mediated (Groarke *et al.*, 1999; Yu and Hinkle, 1999; Zhang *et al.*, 1996; Ferguson *et al.*, 1996). Furthermore, the carboxyl terminal domains of the receptors appear to contribute to the receptor/arrestin interactions (Willars *et al.*, 1999; Heding *et al.*, 2000; Zhang *et al.*, 1999; Oakley *et al.*, 1999, 2000). It is therefore likely that the switching of the carboxyl tail would direct receptor trafficking via an arrestin-dependent pathway.

In the IP-TRH-GFP cells, autofluorescent detection of the receptor and β-arrestin 2 isoform revealed significant colocalisation of the signals upon the addition of agonist to the cells (Figure 4.5b). Similarly, the GFP-tagged form of β-arrestin 2 co-internalised with the HA-tagged receptor in intracellular vesicles after iloprost exposure (Figure 4.7b). However, the chimeric receptor did not appear to exhibit any capacity to interact with the β-arrestin 1 isoform; no visible mobilisation of the cytoplasmic β-arrestin 1 isoform could be seen in the confocal images for the duration of agonist treatment (Figures 4.4b, 4.6b). Taken together, the data were somewhat unexpected. The TRH tail has been shown to confer its β-arrestin sensitivity to the mammalian tail-less GnRH receptor (Willars *et al.*, 1999; Heding *et al.*, 2000). Furthermore, Oakley and coworkers (2000) identified the TRH receptor as a class B GPCR, which bind both β-arrestin isoforms with similar high affinities. Using chimeric receptor models, they also demonstrated that the C-tail played an important role in regulating β-arrestin binding. Contrary to Oakley's model, the TRH-tailed prostacyclin receptor chimeras did not exhibit the TRH receptor's affinity for binding both β-arrestin proteins as readily observed in control experiments with a VSV-tagged form of the TRH receptor (Figure 4.8). Intriguingly, Hanyaloglu and coworkers (2001) reported a similar anomaly with a chimeric form of the mammalian GnRH receptor expressing the C-tail sequence of the β-arrestin-sensitive catfish GnRH receptor. They noted that the sequestration properties of GnRH/catfish-GnRH tail chimera were the same as the wild type mammalian receptor i.e. it internalised independently of β-arrestins. Presumably, the carboxyl terminal domain in conjunction with other intracellular receptor domains determines the GnRH receptor's capacity to bind arrestin. It could therefore be argued that multiple

intracellular domains would have to be swapped in order to switch the endocytic phenotype of the prostacyclin receptor to that of TRH receptor.

The confocal data of the receptor/β-arrestin interactions with the β_2-AR-tailed chimeras demonstrated that there was no apparent agonist-induced redistribution of arrestins to the plasma membrane. Moreover, the internalised receptors were located in endocytic vesicles which were distinct from those containing the arrestins (Figures 4.4c, 4.5c, 4.6c, 4.7c). It could therefore be concluded that the presence of the β_2-AR carboxyl terminal domain failed to confer arrestin binding to the receptor. Confocal analysis of native β_2-AR trafficking has revealed that agonist stimulation triggers the translocation of both β-arrestin isoforms to the plasma membrane. However, the redistributed β-arrestins are confined to the periphery and do not co-internalise with the receptor (Zhang *et al.*, 1999). A similar pattern of receptor/arrestin interactions was observed in the control experiments with the wild type β_2-AR and GFP-tagged β-arrestins in this chapter (Figure 4.9). Using chimeric receptor strategies, some studies have suggested that the β_2-AR C-tail is the critical domain in determining the association and stability of receptor/arrestin complexes (Zhang *et al.*, 1999, Oakley *et al.*, 1999, 2000), whereas several investigators have intimated that β-arrestin interactions with the β_2-AR involve multiple receptor domains including the receptor carboxyl terminus; Jockers *et al.* (1996) showed that several intracellular domains including the first and second intracellular loops and the carboxyl tail of the β_3-AR had to be swapped with the equivalent domains of the β_2-AR to establish a sequestration phenotype of the wild type β_2-AR. Furthermore, β-arrestins have been shown to facilitate the sequestration of β_2-AR mutants lacking the carboxyl tail sequences (Ferguson *et al.*, 1996). The data from the colocalisation experiments would suggest that the β_2-AR C-tail has little functional importance in augmenting the prostacyclin receptor's affinity for β-arrestin. It remains to be seen whether the substitution of further intracellular domains would transform receptor endocytosis to a β_2-AR-like phenotype.

The interpretation of confocal data can be subjective. It therefore seemed appropriate to use an additional method to further analyse arrestin interactions with the prostacyclin receptor constructs. Co-immunoprecipitation assays were carried out to detect the association of the HA-tagged prostacyclin receptors with the arrestin-GFP constructs in

intact cells. This approach has been used successfully to determine the agonist-enhanced binding of β-arrestins to various GPCRs. In this study, each of the IP receptors could be co-precipitated with the arrestins, but somewhat surprisingly, these complexes formed in an agonist-independent manner, which suggested that these formations were merely experimental artefacts (Figure 4.10). Consequently, no significance could be ascertained from the co-immunoprecipitation data. Presumably, a more sensitive technique such as fluorescence resonance energy transfer (FRET) would be needed to monitor the specific interactions of β-arrestins with the prostacyclin receptor proteins. FRET technology is an extremely sensitive method for determining the relative proximity of labelled protein partners. Recently, it has been used to monitor the real-time interaction of β-arrestins with wild type and phosphorylation-deficient chemokine CCR5 receptors in live cells (Kraft *et al.*, 2001).

The cellular complement of β-arrestins and GRKs can significantly affect GPCR internalisation. Menard *et al.* (1997) showed that the extent of β_2-AR internalisation in various cell lines correlated well with the endogenous levels of GRKs and β-arrestins. In COS7 cells which express these proteins at very low levels, β_2-AR sequestration was severely attenuated (Zhang *et al.*, 1996; Menard *et al.*, 1997) thus demonstrating that GRKs and β-arrestins were essential for normal sequestration of the receptor. In this investigation, the sequestration of the prostacyclin receptor constructs was examined in HEK293 cells which have a much higher endogenous complement of GRKs and β-arrestins (Menard *et al.*, 1997). To determine whether receptor sequestration was altered by a reduction in the cellular levels of these endocytic proteins, COS7 cells were transiently transfected with the HA-tagged receptors. Confocal analysis of the immunostained receptors demonstrated that substantial levels of receptor sequestration occurred upon agonist exposure (Figure 4.11). It could therefore be postulated that internalisation of the receptor constructs proceeds via an arrestin-independent mechanism, at least when expressed in a β-arrestin-deficient environment. Whether or not the main endocytic pathway of the prostacyclin receptor proteins is arrestin-independent remains uncertain. The development of cell lines from β-arrestin knockout mice have proved to be better models for studying β-arrestin-mediated GPCR sequestration (Kohout *et al.*, 2001). From earlier studies of $AT_{1A}R$ sequestration, it had been reported that internalisation in COS7 cells was identical to that in HEK293 cells

which suggested that the receptor internalised via an arrestin-independent mechanism (Zhang *et al.*, 1996; Menard *et al.*, 1997). When expressed in the β-arrestin knockout cell lines, $AT_{1A}R$ sequestration was not significantly affected in either the β-arrestin 1-knockout or β-arrestin 2-knockout cell lines. However, internalisation in cells lacking both β-arrestin isoforms was severely impaired (Kohout *et al.*, 2001) thus demonstrating that $AT_{1A}R$ sequestration is primarily via a β-arrestin-dependent pathway, but to a lesser extent, it can internalise independently of β-arrestin. Attempts to use these β-arrestin knockout cell lines to examine prostacyclin receptor sequestration proved to be ineffectual as the cell lines died post transfection.

Clathrin-mediated internalisation of GPCRs requires dynamin. This has been demonstrated most effectively with a GTPase-defective K44A-dynamin mutant which was found to block internalisation of GPCRs including the β_2-AR, $5HT_{2A}R$, and the PAR1-R (Zhang *et al.*, 1996; Bhatnagar *et al.*, 2001; Trejo *et al.*, 2000). Co-expression of a myc-tagged form of K44E-dynamin in the stable cell lines expressing the IP receptor-GFP fusion proteins did not appear to have any noticeable effect on agonist-mediated internalisation of the receptors as determined by biotin labelling experiments (Figure 4.12a). Thus, the data suggested receptor internalisation was dynamin-independent. In a similar investigation, Smyth *et al.* (2000) reported that trafficking of the wild type prostacyclin receptor was only partially reduced by overexpression of the K44A-dynamin mutant, indicating that dynamin-independent pathways may also be involved in prostacyclin receptor sequestration. Using a K44A-dynamin mutant to examine whether GPCR internalisation is dynamin-dependent can, however, be unsuitable: early experiments with the m2 muscarinic and AT_{1A} receptors showed that receptor internalisation proceeded irrespective of K44A-dynamin expression, suggesting that internalisation of these receptors was dynamin-independent (Vogler *et al.*, 1998; Zhang *et al.*, 1996). However, upon further examination of these findings with a N272 mutant dynamin, which lacks the complete GTP-binding domain (residues 1-271), and a K535M mutant which lacks PIP_2-stimulated GTPase activity, it was finally established that both the m2 muscarinic and AT_{1A} receptors internalise via a dynamin-dependent route (Werbonat *et al.*, 2000). More recently, Gáborik and coworkers (2001) revealed that overexpression of the K44A-dynamin mutant could inhibit $AT_{1A}R$ receptor endocytosis at physiological concentrations of agonist, but the effects were reversed at

saturating concentrations of the ligand. In light of these observations, the possible involvement of a dynamin-dependent pathway in prostacyclin receptor sequestration cannot be ruled out. Further analysis with different dominant negative dynamin mutants would be needed to better characterise the endocytic pathways of the prostacyclin receptor and its chimeric forms.

In this chapter, the data presented would suggest that the internalisation of the prostacyclin receptor proceeds primarily via a clathrin-mediated, β-arrestin- and dynamin-independent pathway. Exchanging the carboxyl tail for the equivalent β_2-AR domain did not alter the trafficking properties of the receptor. However, β-arrestin 2 did appear to contribute to the endocytosis of the TRH-tailed chimeras. Taken together, it would seem that the β_2-AR C-tail sequence is not sufficient to confer β-arrestin binding to the prostacyclin receptor whereas the TRH receptor carboxyl tail alone can increase receptor/β-arrestin interactions. The binding of β-arrestins to GPCRs is thought to partly involve an interaction with phosphorylated Ser/Thr residues in the carboxyl termini (Kieselbach *et al.*, 1994). Sequence comparison of the different carboxyl tails has revealed that the TRH tail sequence has 21 potential phosphate acceptor sites whereas the β_2-AR and wild type C-tails have 14 and 16 respectively. Presumably, the TRH-tailed prostacyclin receptors exhibited an increased affinity for β-arrestin due to an increase in phosphorylation of the carboxyl tail. Considering that β-arrestin binding to agonist-activated, phosphorylated GPCRs is thought to involve the simultaneous engagement of the β-arrestin molecule with two distinct regions of the receptor (Gurevich *et al.*, 1995), it could be postulated that additional intracellular domains would have to be exchanged in order for chimeric prostacyclin receptors to assume the endocytic properties of the donor receptors.

Chapter 5

Signal Regulation of the Prostacyclin Receptor and its Chimeric Forms

Chapter 5

5.1 Introduction

Agonist binding to GPCRs not only results in G protein activation, but also initiates signalling cascades which lead to a reduction in GPCR responsiveness. Receptor desensitisation, the waning of GPCR activity in the presence of continuous agonist exposure, is an important negative feedback mechanism which protects against acute and chronic over-stimulation of receptors. The process of desensitisation can be subdivided into homologous and heterologous events. Homologous desensitisation is characterised by the attenuation of receptor responsiveness to agonist only, whereas heterologous desensitisation is characterised by the loss of receptor responsiveness following activation of a heterologous GPCR. The mechanisms of desensitisation include the uncoupling of GPCR/G protein interactions, receptor internalisation and downregulation (Ferguson and Caron, 1998).

The uncoupling of GPCRs from their cognate G proteins occurs within seconds of receptor activation and is mediated through the covalent modification of the receptor's cytosolic domains by protein kinases. The involvement of covalent modification in GPCR desensitisation was initially suggested upon notice of the decreased electrophoretic mobility of desensitised β_2-ARs (Stadel *et al.*, 1982). The modification was later identified as phosphorylation as agonist exposure was shown to increase receptor phosphorylation. Moreover, the kinetics of desensitisation appeared to mimic those of phosphorylation (Stadel *et al.*, 1983a; Strasser *et al.*, 1986). The possible involvement of kinases other than second messenger kinases in homologous desensitisation of the receptor was first suggested when it was revealed that desensitisation of the β_2-AR could still proceed in kin$^-$ S49 lymphoma cells (which lack PKA) (Strasser *et al.*, 1986). The purification of a kinase and the subsequent cloning of the cDNA encoding the protein from kin$^-$ S49 lymphoma cells, revealed an enzyme capable of phosphorylating and desensitising agonist-bound β_2-ARs (Benovic *et al.*, 1986, 1989). The kinase, termed β-adrenergic receptor kinase, was later identified as a member of the GRK family (Pitcher *et al.*, 1998). It has since been well established that second messenger-dependent kinases (e.g. PKA and PKC) and/or GRKs play important

regulatory roles in receptor desensitisation by catalysing the phosphorylation of key serine and threonine residues within the intracellular domains of GPCRs (Ferguson and Caron, 1998).

For most GPCRs, the third intracellular loop and the carboxyl terminal tail domains contain multiple serine and threonine residues which function as substrates for agonist-mediated phosphorylation. Some GPCRs such as the α_2-adrenergic and the m2 muscarinic receptors have relatively short carboxyl tails containing only a few Ser/Thr residues but have enlarged third intracellular loops which are Ser/Thr-enriched. In contrast, some receptors including the β_2-AR and rhodopsin have relatively short third intracellular loops but have long carboxyl tails with many Ser/Thr sites. Numerous investigators have shown that mutation or deletion of these putative phosphorylation sites severely impairs receptor desensitisation, a phenomena which has been reported for an array of GPCRs including the bradykinin B2 (Blaukat *et al.*, 2001), dopamine D1 (Lamey *et al.*, 2002), N-formyl peptide (Maestes *et al.*, 1999) and AT_{1A} (Smith *et al.*, 1998) receptors.

Phosphorylation alone is insufficient to mediate receptor desensitisation (Pfister *et al.*, 1985; Benovic *et al.*, 1987). The arrestin proteins function as co-factors in GPCR desensitisation whereby phosphorylation of agonist-occupied receptors promotes arrestin binding thus sterically hindering receptor/G protein interactions (Benovic *et al.*, 1987; Lohse *et al.*, 1990a, b; Pippig *et al.*, 1993). Arrestins preferentially bind to agonist-activated and GRK-phosphorylated GPCRs as opposed to second messenger kinase-phosphorylated or non-phosphorylated receptors (Lohse *et al.*, 1990a; 1992). For the β_2-AR, GRK phosphorylation within the carboxyl tail promotes β-arrestin binding whereas PKA-phosphorylated receptors do not bind arrestins (Ferguson *et al.*, 1996; Lohse *et al.*, 1990a, 1992).

In addition to uncoupling receptors from heterotrimeric G proteins, the β-arrestins act as endocytic adapter proteins targeting receptors for internalisation. Sequestration was originally thought to be the primary mechanism of GPCR desensitisation as it leads to a reduction in cell surface receptor population and spatial separation of receptors from its effectors (Sibley and Lefkowitz, 1985). However, since desensitisation proceeds more

quickly than receptor endocytosis, sequestration is now thought to play only a minor role in the acute desensitisation of most GPCRs. In A431 cells, β_2-AR sequestration alone was found to contribute to approximately 20-30% of receptor desensitisation while other studies have revealed that blocking receptor internalisation does not affect the β_2-AR's ability to desensitise (Lohse *et al.*, 1992; Yu and Lefkowitz, 1993; Pippig *et al.*, 1995).

Upon prolonged or repeated agonist activation of GPCRs, receptor downregulation occurs. The process is characterised by a reduction in the total cellular complement of receptors thereby mediating long-term desensitisation. The main pathway of downregulation involves the targeting of receptors for degradation via a lysosomal or proteasomal mechanism (von Zastrow, 2001) although receptor number can also be regulated at the level of gene expression and biosynthesis. In β_2-AR downregulation studies, a reduction in gene transcription and mRNA translation has been observed in response to agonist challenge (Collins *et al.*, 1989; Tholanikunnel and Malbon, 1997). In contrast to the processes of G protein uncoupling and sequestration, downregulation proceeds over prolonged time frames ranging from hours to days and is also characterised by slow or partial reversibility after agonist removal.

Following desensitisation, it is necessary for GPCRs to regain responsiveness to extracellular stimuli in order to maintain cellular homeostasis. Receptor internalisation appears to be a prerequisite for resensitisation since pharmacological agents which block internalisation have been shown to inhibit resensitisation without affecting desensitisation (Pippig *et al.*, 1995; Garland *et al.*, 1996; Hasbi *et al.*, 2000). Agonist-internalised receptors are thought to traffic via endosomes enriched with a GPCR-specific phosphatase (Sibley *et al.*, 1986; Pitcher *et al.*, 1995b) which dephosphorylates the receptors prior to their return to the cell surface in the pre-ligand exposed state. In the case of the protease-activated receptor family, internalised receptors are targeted to the lysosomes for degradation. In this instance, receptor resensitisation is mediated by alternative mechanisms including *de novo* synthesis of receptors and the maintenance of an intracellular pool of naïve receptors (Shapiro *et al.*, 1996; Shapiro and Coughlin, 1998).

The recycling rate of resensitised GPCRs varies, with some internalised receptors recycling rapidly to the plasma membrane in a fully sensitised state while others recycle relatively slowly. Dephosphorylation appears to be the critical molecular event governing the recycling rate (Pippig *et al.*, 1995; Garland *et al.*, 1996). An event necessary for dephosphorylation to proceed is the release of bound β-arrestins (Oakley *et al.*, 1999). Recent studies have shown that the ability of β-arrestins to co-internalise with desensitised GPCRs regulates the rate of receptor resensitisation. Receptors which internalise in vesicles without β-arrestin, such as the β_2-AR, were shown to be rapidly dephosphorylated and recycled back to the plasma membrane while receptors which form stable endocytic complexes with β-arrestin, such as the vasopressin V2 receptor, exhibited a slower recycling and resensitisation profile (Zhang *et al.*, 1999; Oakley *et al.*, 1999). Switching of the carboxyl tails of the β_2-AR and the vasopressin V2 receptor reversed their dephosphorylation, recycling, and resensitisation kinetics (Oakley *et al.*, 1999). Moreover, the specific determinants within the carboxyl terminal domains which mediate the association of β-arrestins with endocytosed receptors were identified as clusters of phosphorylated serine residues (Oakley *et al.*, 1999). For the vasopressin V2 receptor, a cluster of three serine residues located in the carboxyl terminus serve as the principle site for GRK-mediated phosphorylation and determine the stability of the receptor/β-arrestin complexes. In the β_2-AR, which forms only transitory interactions with β-arrestin, these putative phosphorylable clusters are notably absent from the carboxyl terminal domain (Oakley *et al.*, 1999).

In this chapter, the regulation of prostacyclin receptor signalling was examined. Assays of G protein coupling and sequestration were used to determine the desensitisation and resensitisation properties of the GFP-tagged form of the receptor. Furthermore, the role of receptor phosphorylation in desensitisation and sequestration was investigated. To assess the role of the receptor's carboxyl terminal tail in these processes, identical experiments were performed with the chimeric prostacyclin receptors possessing the carboxyl tails of the TRH and β_2-adrenergic receptors.

5.2 Agonist-mediated desensitisation of the GFP-tagged prostacyclin receptor constructs.

To examine the agonist-mediated desensitisation properties of the prostacyclin receptor-GFP fusion proteins, the cell lines were pre-exposed to vehicle or 100nM iloprost for 10 min, in the presence of 1mM IBMX, and then re-exposed to increasing concentrations of iloprost for 30 min (Figure 5.1). For the IP-GFP receptor, desensitisation was characterised by an approximate 80% reduction in maximal adenylyl cyclase activity with no observable change in EC_{50} value compared to non-desensitised cells. In the IP-TRH-GFP receptor-expressing cells, after pre-treatment with iloprost, maximal adenylyl cyclase activity decreased by ~40% with no significant shift in EC_{50} value compared to control cells. For the IP-β_2-GFP receptor, modest attenuation of adenylyl cyclase activity was observed after iloprost pre-exposure; agonist pre-treated cells exhibited only a 10-20% reduction in maximal signalling output without any notable rightward shift in the dose response curve.

From these initial experiments it was evident that the IP-GFP receptor rapidly desensitised as demonstrated by the almost complete termination of receptor signalling within 10 min of iloprost pre-treatment. For the chimeric receptor proteins, by comparison, the loss of receptor responsiveness was less substantial. To determine whether the signalling responses of the desensitised receptor chimeras could be further diminished, the cells were pre-exposed to 100nM iloprost for 30 and 60 min intervals prior to assays of adenylyl cyclase activity (Figure 5.2). Indeed, in the IP-TRH-GFP cell line, a more notable reduction in maximal output (~35% of control values) was observed for receptors pre-exposed to iloprost for 30 min. In cells pre-treated with agonist for an additional 30 min, no further receptor desensitisation was achieved. Similarly, for the IP-β_2-GFP receptor, maximal adenylyl cyclase activity was reduced to approximately 50% of control cell values after 30 min pre-treatment with iloprost. A more prolonged period of agonist pre-treatment did not induce further signal attenuation. The data therefore suggested that desensitisation of the receptor chimeras is much slower and less pronounced in comparison to the IP-GFP receptor.

5.3 The effects of second messenger kinase inhibitors on agonist-mediated desensitisation of the prostacyclin receptor-GFP proteins.

The rapid agonist-induced desensitisation of the prostacyclin receptor in HEK293 cells has previously been shown to involve PKC phosphorylation of the carboxyl tail (Smyth *et al.*, 1998). Therefore, the effects of second messenger kinase activation on the desensitisation of the GFP-tagged prostacyclin chimeras were examined using the PKA inhibitor, H89 (Figure 5.3), and the PKC inhibitor, GF109203X (Figure 5.4). Cells, incubated in culture medium containing the phosphodiesterase inhibitor IBMX, were pre-treated with vehicle or kinase inhibitor prior to challenge with 1μM iloprost for various timepoints over a 60 min period. Subsequent measurement of cAMP accumulation in the stable clones was used to monitor receptor desensitisation. Pre-treatment of cells with 10μM H89 for 30 min significantly augmented the cAMP responses elicited by each of the receptors. In IP-GFP cells, cAMP accumulated rapidly within minutes of agonist treatment and reached a plateau after 20 min. In cells pre-treated with H89, intracellular cAMP levels were approximately twice those of non-treated cells after the 60 min period of iloprost incubation. Similarly, in IP-TRH-GFP receptor-expressing cells, H89 treatment induced an approximate twofold increase in cAMP accumulation within 60 min of iloprost challenge compared to non-treated cells. For IP-β_2-GFP cells, a more striking amplification of agonist-mediated cAMP production was demonstrated with H89 incubation. In control cells cAMP accumulation plateaued within 15 min of iloprost exposure whereas in H89-treated cells intracellular cAMP levels continued to rise steadily before reaching a plateau after the 50 min timepoint. Overall, an approximate 3.5-fold increase in cAMP generation was observable in IP-β_2-GFP cells treated with H89 compared to non-treated cells.

In contrast to previous reports of prostacyclin receptor desensitisation (Smyth *et al.*, 1998), PKC inhibition failed to attenuate desensitisation of the IP-GFP receptor. Somewhat surprisingly, pre-treatment of IP-GFP cells with 5μM GF109203X did not alter the agonist-mediated adenylyl cyclase activity of the receptor (Figure 5.4a). Moreover, identical observations were made with the IP-TRH-GFP and IP-β_2-GFP constructs with GF109203X-treated cells eliciting cAMP responses paralleling those of the non-treated cells (Figure 5.4b and Figure 5.4c). Taken together, the data suggested

that receptor phosphorylation by PKA, but not PKC, is involved in the desensitisation of the GFP-tagged prostacyclin receptor constructs.

5.4 The effects of inhibition and activation of PKA and PKC on sequestration of the prostacyclin receptor constructs.

For most GPCRs, phosphorylation is a prerequisite for rapid receptor internalisation (Ferguson and Caron, 1998). To determine whether second messenger kinase phosphorylation is involved in the endocytosis of the prostacyclin receptor proteins, receptor trafficking was monitored in the presence of inhibitors and activators of PKA and PKC. Confocal analysis of the immunostained HA-tagged IP receptors, transiently expressed in HEK293 cells, demonstrated that cells pre-treated with 10μM H89 or 5μM GF109203X exhibited receptor sequestration levels comparable to those in non-treated cells after 60 min of 1μM iloprost exposure (Figure 5.5). Similarly, in the stable cell clones expressing the receptor-GFP constructs, quantitative measurement of receptor internalisation revealed that neither H89 nor GF109203X pre-exposure blocked agonist-stimulated internalisation of the receptors (Figure 5.6).

Heterologous activation of second messenger kinases has been shown to trigger internalisation of GPCRs such as the α_{1B}-AR and δ-opioid receptor in the absence of agonist (Awaji *et al.*, 1998; Xiang *et al.*, 2001). To determine the effects of PKA and PKC activation in promoting sequestration of IP receptor constructs, cells were challenged with 5μM forskolin or 5μM PMA for 60 min (Figures 5.7 and 5.8). Confocal imaging of the antibody-labelled HA-tagged IP receptors, transiently expressed in HEK293 cells, showed that forskolin treatment did not stimulate receptor internalisation whereas each of the constructs exhibited modest levels of endocytosis upon treatment with PMA. Biotin labelling assays which were used to measure sequestration of the GFP-tagged forms of the receptor proteins, revealed that forskolin-treated cells exhibited minimal receptor internalisation; the proportion of IP-GFP receptors remaining at the cell surface after forskolin challenge was 102% ± 3% while for the IP-TRH-GFP and IP-β_2-GFP receptors the cell surface receptor populations were 104% ± 9% and 98% ± 6% respectively. Cells treated with PMA showed considerable levels of receptor internalisation. In IP-GFP cells, 72% ± 5% of the receptor population remained

at the plasmalemmal surface after 60 min of PMA treatment. Similarly, for the IP-TRH-GFP and IP-β_2-GFP cell lines, the fraction of cell surface receptors remaining was 65% ± 3% and 74% ± 6% respectively.

5.5 Phosphorylation of the GFP-conjugated prostacyclin receptor constructs.

The data from sections 5.3 and 5.4 indicated that second messenger kinase activation was of functional importance in the desensitisation and internalisation of the prostacyclin receptor proteins. It therefore seemed appropriate to determine whether the prostacyclin receptor-GFP constructs were phosphorylated upon agonist binding and if second messenger kinases contributed to this process. Earlier investigations by Smyth and coworkers (1996) demonstrated that an HA-tagged form of the native receptor, expressed in HEK293, underwent rapid agonist-mediated phosphorylation. Furthermore, it was shown that the process was, in part, mediated by PKC. Figure 5.9 shows the time course of phosphorylation of the GFP-tagged IP receptor proteins with 1μM iloprost. Each of the receptors underwent rapid phosphorylation in response to agonist. The kinetics of phosphorylation of each construct were similar; significant phosphorylation was detectable within 30 seconds of agonist incubation and was maximal within approximately 5 min. In the absence of agonist, a basal level of phosphorylation was evident for each receptor. Agonist-mediated phosphorylation of the receptors was further examined using inhibitors of PKA and PKC (Figure 5.10). The cells were stimulated with 1μM iloprost for 10 min in the presence of either 10μM H89 or 5μM GF109203X. Both inhibitors were found to modestly decrease the agonist-induced phosphorylation signals of the three receptor constructs thus indicating that agonist-mediated phosphorylation of the receptors may, in part, be mediated by PKA and PKC. Furthermore, receptor-independent activation of PKA by forskolin (5μM) and PKC by PMA (5μM) also induced phosphorylation of the receptors (Figure 5.10). Taken together, the phosphorylation data indicated that each of the prostacyclin receptor-GFP proteins are substrates for PKA and PKC phosphorylation.

5.6 Resensitisation of the prostacyclin receptor-GFP constructs.

The mechanisms responsible for receptor resensitisation are namely recycling of intracellular receptors back to the plasma membrane and/or *de novo* synthesis of receptor protein. Both of these mechanisms have been shown to contribute to the resensitisation of the prostacyclin receptor in various cell lines. While in platelets and HEK293 cells the IP receptor recycles, resensitisation in human fibroblasts and NG108-15 cells requires *de novo* synthesis (Smyth *et al.*, 2000; Fisch *et al.*, 1997; Nilius *et al.*, 2000; Krane *et al.*, 1994). The capacity of the GFP-tagged prostacyclin receptors to resensitise after agonist removal was therefore examined. The receptor-expressing HEK293 cells were treated with vehicle (control) or 100nM iloprost for 30 min and allowed to recover for either 30 or 60 min in agonist-free medium before adenylyl cyclase activity was measured for each condition (Figure 5.11). For the IP-GFP receptor, a rapid restoration of G_s coupling occurred after agonist removal in desensitised cells. After a 30 min recovery period, the maximal adenylyl cyclase stimulation was approximately two thirds of the activity in non-desensitised cells. Further resensitisation was evident in cells which were left to recover for an additional 30 min. After 60 min recovery, the maximal signalling capacity of the receptors was ~80% of control cell values. In contrast, resensitisation of the receptor chimeras was undetectable. In IP-TRH-GFP cells, no obvious restoration of adenylyl cyclase activity was seen within 60 min of agonist removal. The level of agonist responsiveness after 60 min agonist-free conditions was approximately 40% of the maximal activity observed in non-desensitised cells. For the IP-β_2-GFP receptor, agonist withdrawal failed to bring about any amelioration in signalling of the desensitised cells. In fact, a further reduction in adenylyl cyclase activity was apparent. The maximal signalling output after the 60 min recovery period was ~25% of the activity in control cells. Earlier assays had shown that desensitisation of the IP-β_2-GFP receptor was characterised by a ~50% reduction in maximal adenylyl cyclase activity after 30 min of agonist incubation (Figure 5.2).

To assess whether the differential resensitisation responses of the prostacyclin receptor constructs was related to the receptors' recycling efficiency, biotin labelling experiments were used to monitor the return of receptors to the plasma membrane after agonist removal. Cells were incubated with 1μM iloprost for 60 min to promote

receptor internalisation. Agonist was then removed and the return of intracellular receptors to the cell surface was determined after 30 and 60 min intervals (Figure 5.12). Recycling of the IP-GFP receptors was rapid. Setting the level of cell surface receptors in non-treated control cells as 100%, the fraction of receptors at the cell surface after the 30 and 60 min agonist withdrawal periods was 90% ± 7% and 95% ± 9% respectively. By comparison, recycling of internalised receptors back to the cell surface following iloprost treatment was not detected for either of the chimeric constructs. The plasmalemmal expression of IP-TRH-GFP and IP-β_2-GFP receptors after the 60 min recovery period was 45% ± 4% and 68% ± 7% respectively. The results therefore indicated that the differences in ability of the prostacyclin receptor constructs to recycle is a determining factor in their ability to re-establish agonist responsiveness following desensitisation.

The data from the recycling experiments would suggest that the prostacyclin receptor proteins exhibit differential intracellular sorting patterns upon activation by agonist. The failure of the IP-TRH-GFP and IP-β_2-GFP receptors to recycle would indicate that the sequestered proteins are retained within endosomal compartments and possibly targeted for degradation. On this basis, experiments were carried out to assess the receptors' capacity to be downregulated upon prolonged agonist exposure. The stable cell clones were incubated with or without 1μM iloprost for 8 hours and then lysed. The level of receptor protein in the cell lysates was determined by quantitative Western blot analysis (Figure 5.13). In IP-GFP cells, 8 hour's agonist treatment induced a ~30% reduction in receptor protein. For each of the chimeric receptors, a more substantial decrease in receptor protein levels was observable. In iloprost-stimulated IP-TRH-GFP cells an approximate 60% reduction was noted while in IP-β_2-GFP cells, receptor protein levels were diminished by ~70%. Taken together, these findings suggested that the agonist-activated chimeric prostacyclin proteins are predominantly sorted via a pathway which leads to their eventual degradation whereas the full-length receptor is primarily recycled back to the plasma membrane after agonist challenge.

Figure 5.1

Desensitisation of the IP-GFP receptor, and IP-TRH-GFP and IP-β_2-GFP chimeras in intact cells following 10 min agonist pre-exposure.

The IP-GFP (a), IP-TRH-GFP (b) and IP-β_2-GFP (c) stable clones were challenged with vehicle or 100nM iloprost for 10 min at 37°C. Cells were then washed three times with medium and then re-exposed to increasing concentrations of iloprost for 30 min at 37°C. The net cAMP accumulation in desensitised cells was calculated by subtracting the cAMP accumulation (after pre-exposure) measured at zero time. Results for each receptor were normalised to the maximal cAMP accumulation of non-desensitised cells. Maximal cAMP accumulation was designated as 100%. The data represent the mean ± S.E.M. of three independent experiments which were performed in triplicate.

Figure 5.1

a)

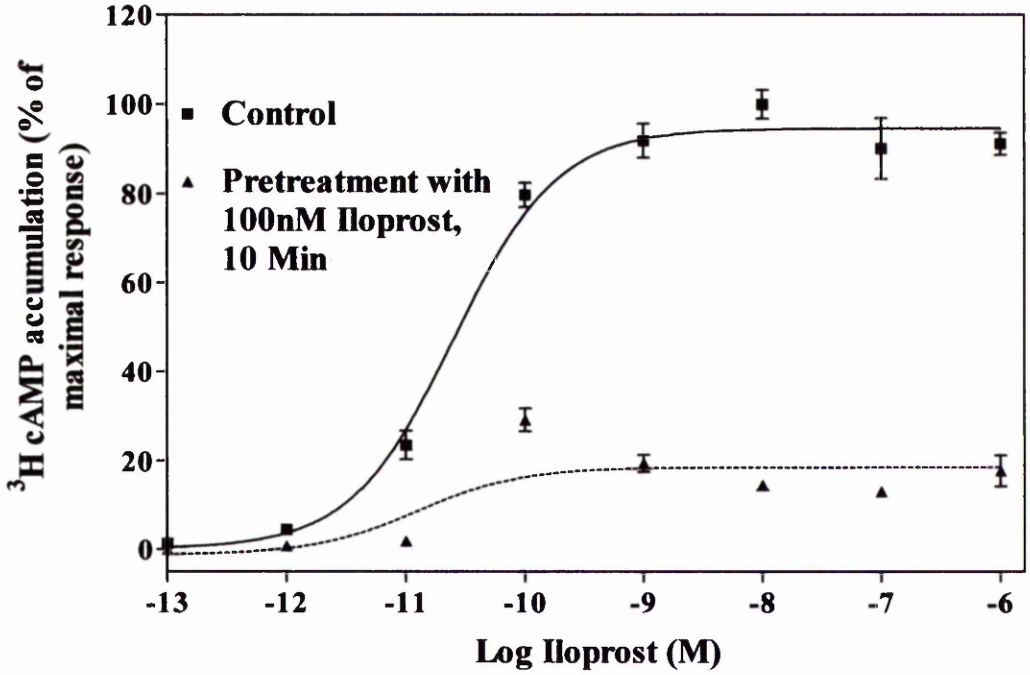
120
100
80
60
40
20
0
Control
Pretreatment with
100nM Iloprost,
10 Min
^{3}H cAMP accumulation (% of maximal response)
-13
-12
-11
-10
-9
-8
-7
-6
Log Iloprost (M)

b)

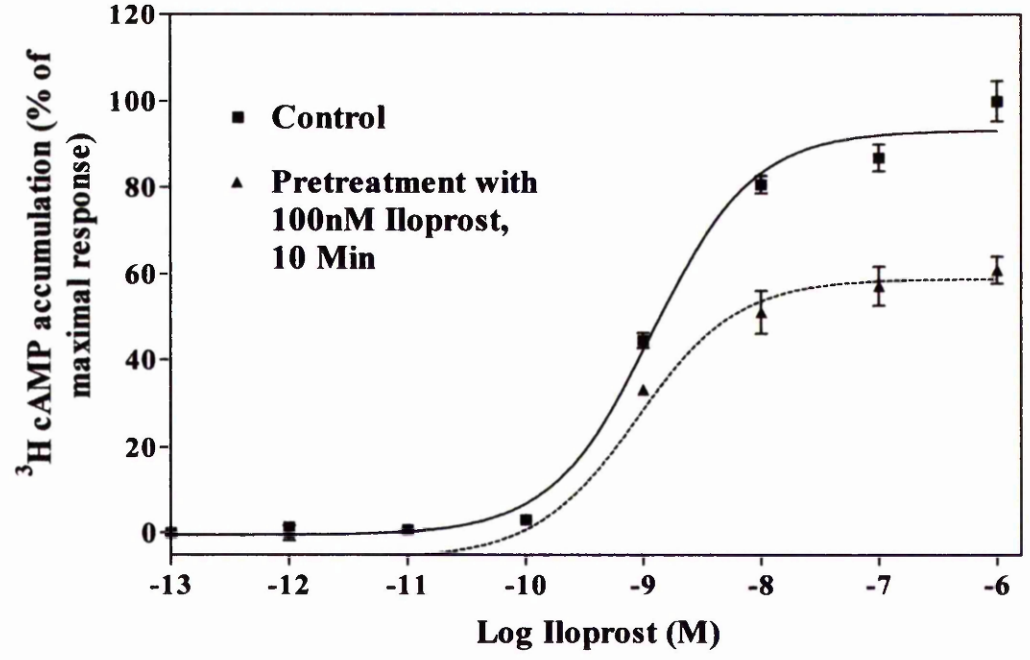
120
100
80
60
40
20
0
Control
Pretreatment with
100nM Iloprost,
10 Min
^{3}H cAMP accumulation (% of maximal response)
-13
-12
-11
-10
-9
-8
-7
-6
Log Iloprost (M)

c)

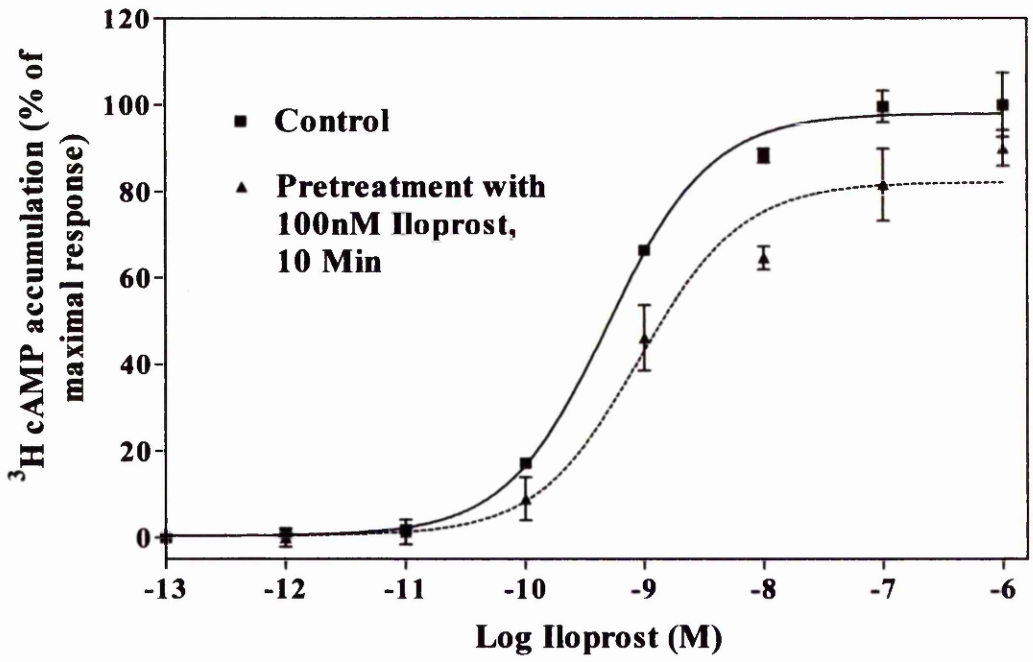
120
100
80
60
40
20
0
^{3}H cAMP accumulation (% of maximal response)
Control
Pretreatment with 100nM Iloprost, 10 Min
-13
-12
-11
-10
-9
-8
-7
-6
Log Iloprost (M)

Figure 5.2

Desensitisation of the chimeric IP receptors in intact cells after prolonged iloprost pre-treatment.

The IP-TRH-GFP (a) and IP-β_2-GFP (b) cell lines were challenged with or without 100nM iloprost for 30 or 60 min intervals. The cAMP generated in desensitised cells was calculated by subtracting the cAMP accumulated after iloprost pre-exposure at zero time. Results for the receptor constructs were normalised to the maximal cAMP accumulation of non-desensitised cells with maximal output being set at 100%. The data shown are representative of three independent experiments which were performed in triplicate.

Figure 5.2

a)

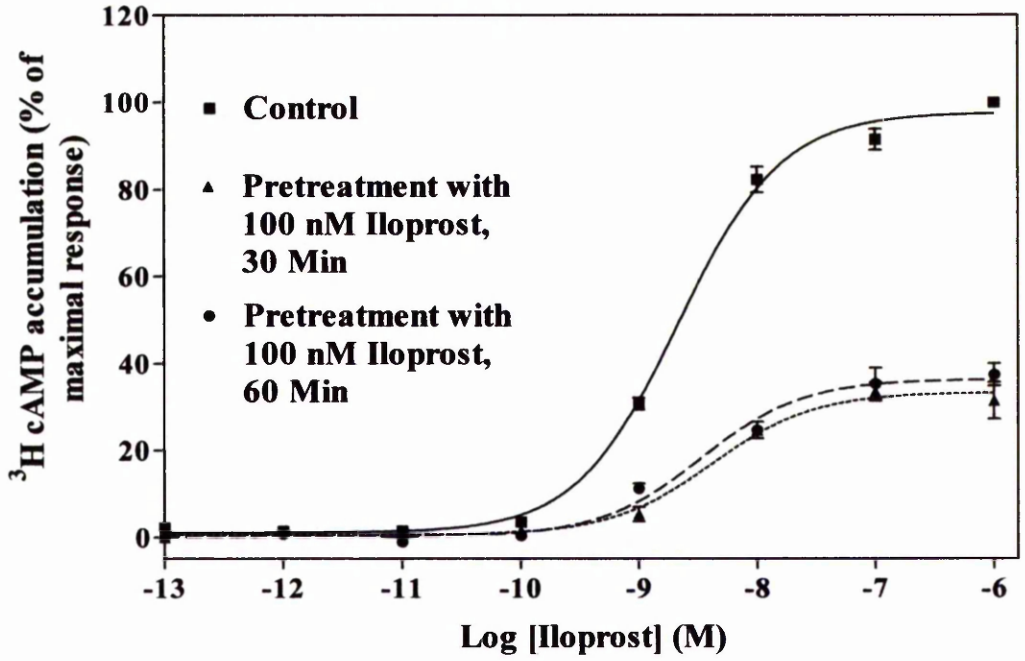
120
100
80
60
40
20
0
^{3}H cAMP accumulation (% of maximal response)
Control
Pretreatment with 100 nM Iloprost, 30 Min
Pretreatment with 100 nM Iloprost, 60 Min
-13
-12
-11
-10
-9
-8
-7
-6
Log [Iloprost] (M)

b)

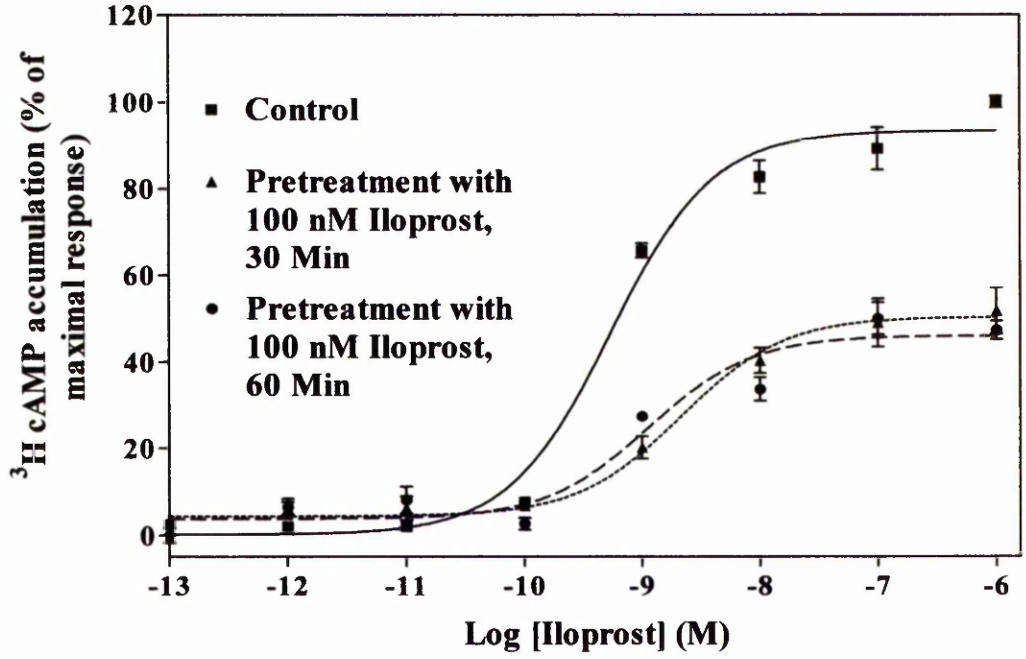
120
100
80
60
40
20
0
^{3}H cAMP accumulation (% of maximal response)
Control
Pretreatment with 100 nM Iloprost, 30 Min
Pretreatment with 100 nM Iloprost, 60 Min
-13
-12
-11
-10
-9
-8
-7
-6
Log [Iloprost] (M)

Figure 5.3

The effects of PKA inhibition on agonist-mediated cAMP accumulation in cell lines expressing the GFP-tagged IP receptor proteins.

Cells expressing the IP-GFP (a), IP-TRH-GFP (b) and IP-β_2-GFP (c) constructs were incubated in medium containing the phosphodiesterase inhibitor IBMX (1mM), prior to treatment with vehicle or 10μM H89 for 30 min. Cells were then challenged with 1μM iloprost for 0-60 min. The cAMP responses are expressed as a fraction of the cAMP accumulation in non-treated cells at 60 min (assigned as a value of 1). Data are means ± S.E.M. from one experiment which was performed three times.

Figure 5.3

a)

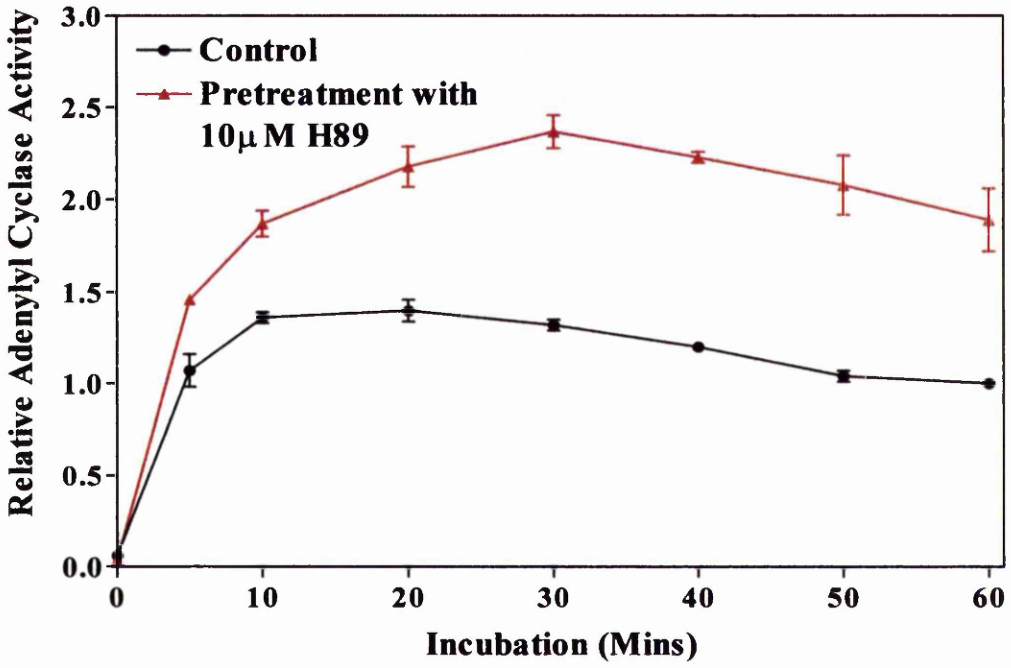
Relative Adenylyl Cyclase Activity
3.0
2.5
2.0
1.5
1.0
0.5
0.0
Control
Pretreatment with
10μM H89
0
10
20
30
40
50
60
Incubation (Mins)

b)

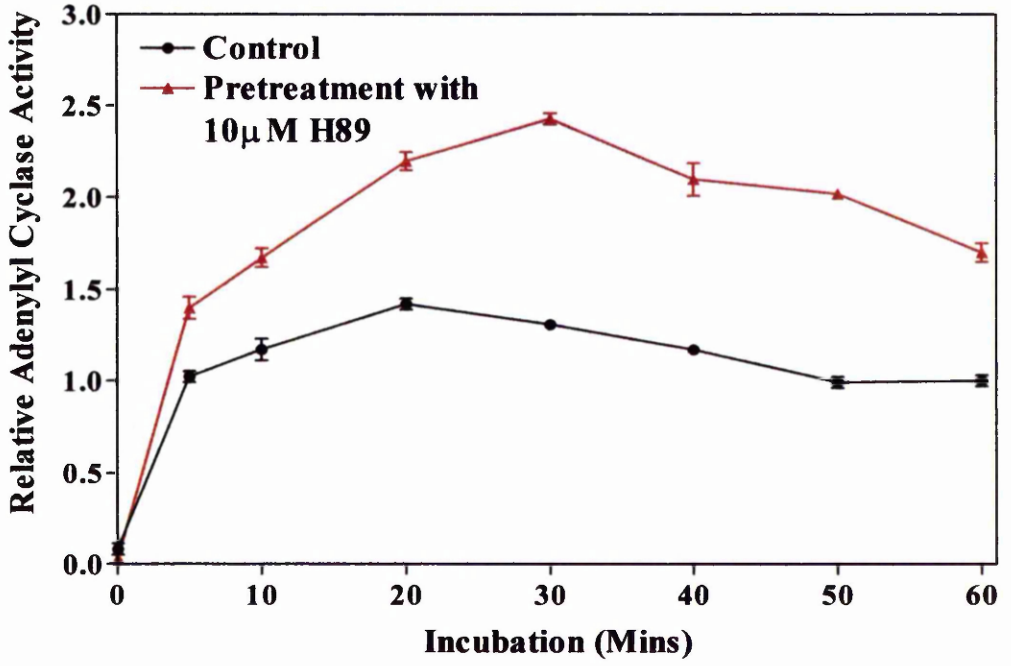
Relative Adenylyl Cyclase Activity
3.0
2.5
2.0
1.5
1.0
0.5
0.0
Control
Pretreatment with
10μM H89
0
10
20
30
40
50
60
Incubation (Mins)

c)

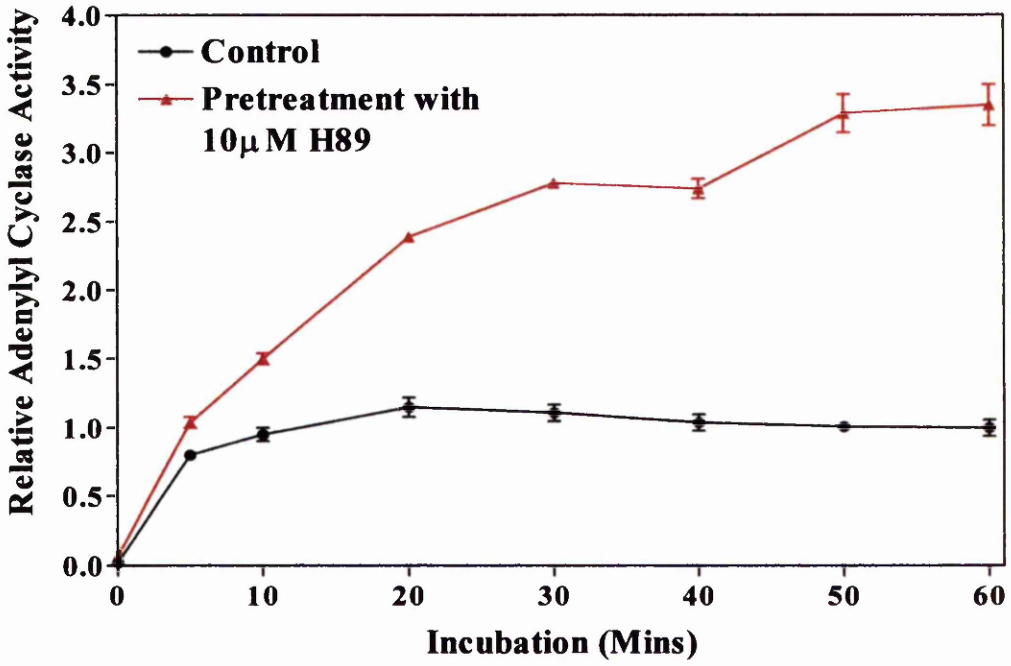
Relative Adenylyl Cyclase Activity
4.0
3.5
3.0
2.5
2.0
1.5
1.0
0.5
0.0
Control
Pretreatment with
10μM H89
0
10
20
30
40
50
60
Incubation (Mins)

Figure 5.4

The effects of PKC inhibition on the agonist-mediated adenylyl cyclase activity of the GFP-tagged IP receptors.

In the presence of 1mM IBMX, the IP-GFP (a), IP-TRH-GFP (b), and IP-β_2-GFP (c) cells were pre-treated with or without 5μM GF109203X for 30 min prior to challenge with 1μM iloprost for up to 60 min. Intracellular cAMP levels are normalised to those in non-treated cells at the 60 min timepoint (set as 1). Data shown are representative of one experiment which was performed three times.

Figure 5.4

a)

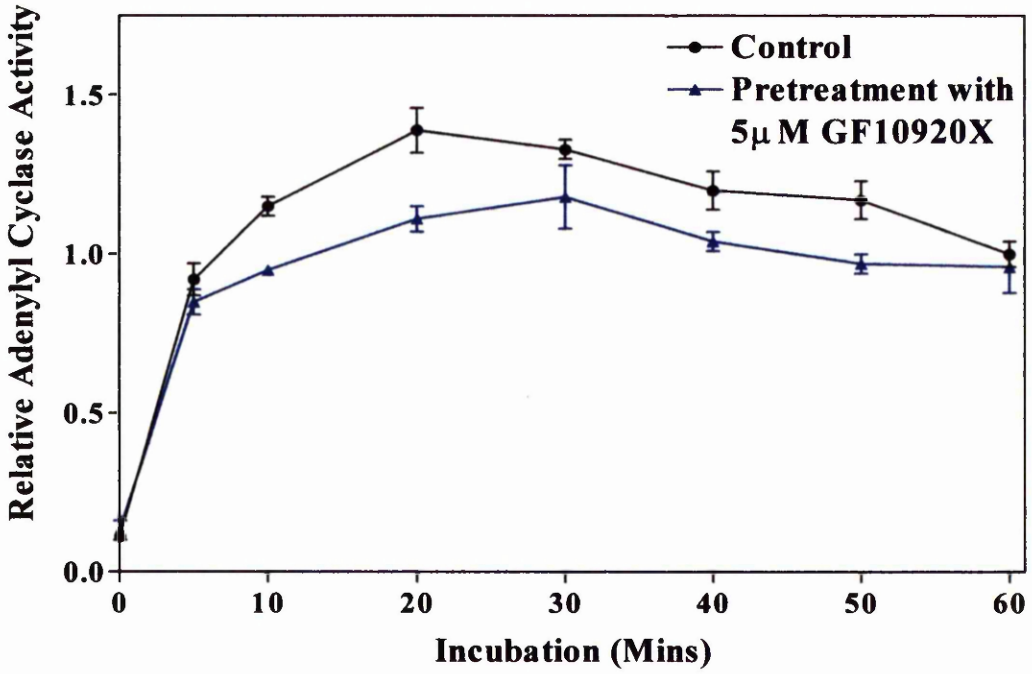
Relative Adenylyl Cyclase Activity
Control
Pretreatment with
5μ M GF10920X
0.0
0.5
1.0
1.5
0
10
20
30
40
50
60
Incubation (Mins)

b)

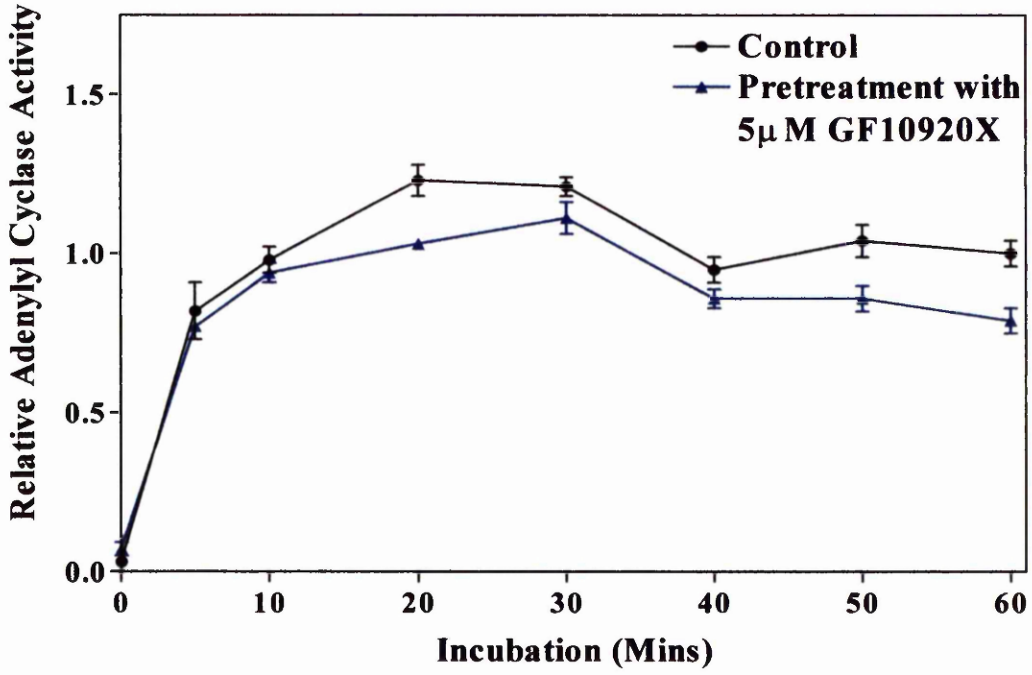
Relative Adenylyl Cyclase Activity
Control
Pretreatment with
5μ M GF10920X
0.0
0.5
1.0
1.5
0
10
20
30
40
50
60
Incubation (Mins)

c)

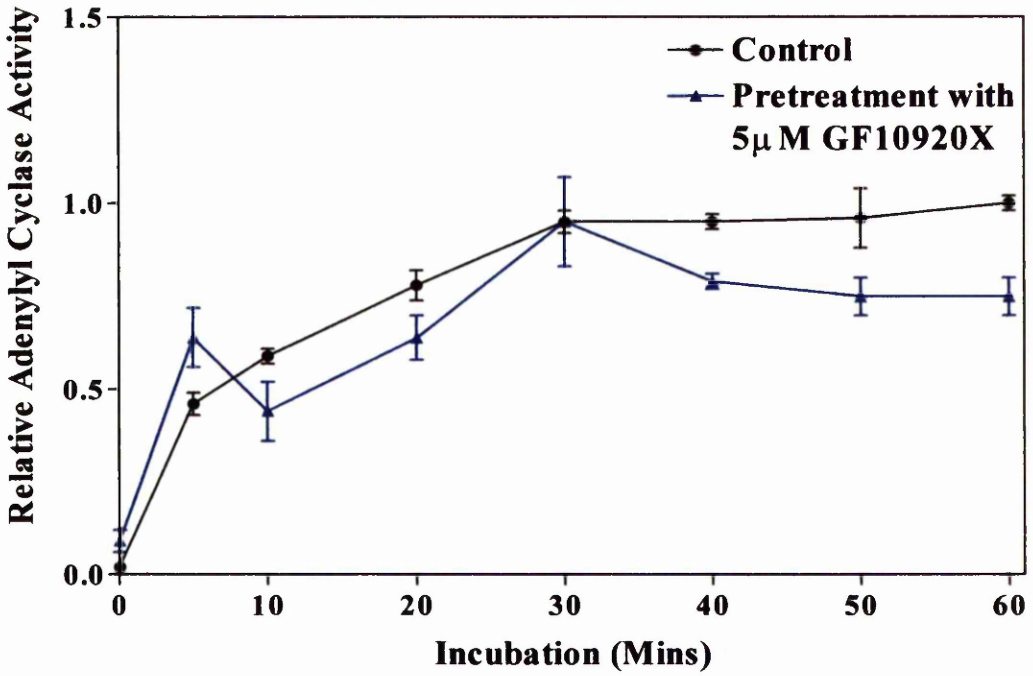
Relative Adenylyl Cyclase Activity
1.5
1.0
0.5
0.0
0
10
20
30
40
50
60
Incubation (Mins)
Control
Pretreatment with
5μM GF10920X

Figure 5.5

The effects of second messenger kinase inhibitors on agonist-mediated sequestration of the HA-tagged prostacyclin receptor constructs.

Cells were pre-treated with vehicle (a, b), 10μM H89 (c), or 5μM GF109203X (d) for 30 min prior to treatment with 1μM iloprost (b, c, d) for 60 min at 37°C. Receptors were visualised by immunostaining with the 12CA5 antibody. The confocal images shown are from a single experiment which was repeated twice. Scale bar = 2.5μM.

Figure 5.5

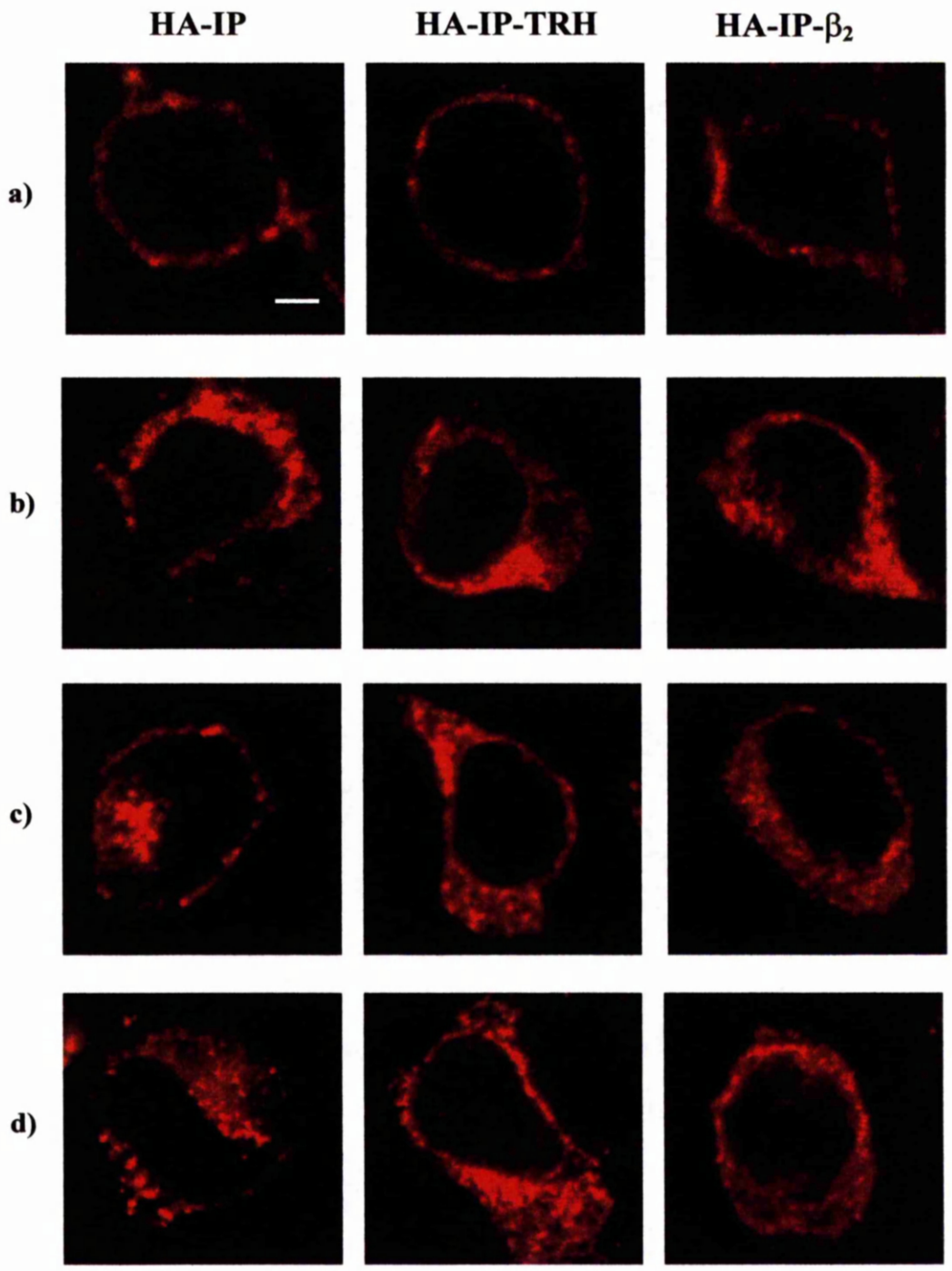

Figure 5.6

Quantitative analysis of the effects of PKA and PKC inhibition on iloprost-induced internalisation of the GFP-tagged IP receptor constructs.

a) The stable cell clones were pre-incubated with vehicle (1, 2), 10μM H89 (3), or 5μM GF109203X (4) prior to 1μM iloprost exposure (2, 3, 4) for 60 min at 37°C. Cell surface glycoproteins were subsequently labelled with biotin and the receptors were immunoprecipitated and visualised as detailed in section 2.7.5. Representative blots are shown. Similar results were obtained from two further experiments.

b) Densitometric scanning of the biotin blots was used to quantify the levels of cell surface receptors. The values shown represent mean ± S.E.M. for three experiments, with the levels of cell surface receptors observed in the absence of agonist set at 100%.

Figure 5.6

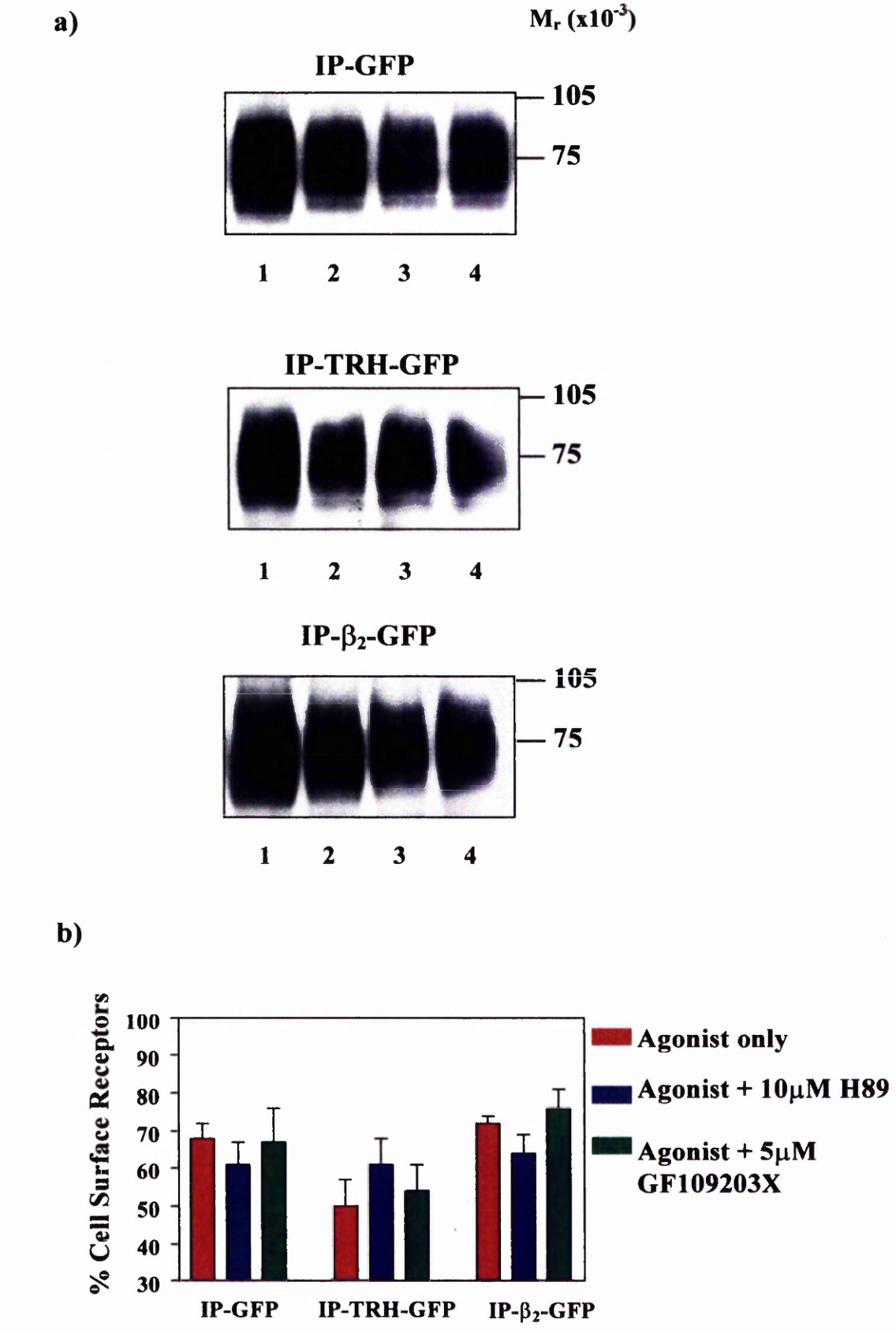
a)
M_r ($x10^{-3}$)
IP-GFP
105
75
1 2 3 4
IP-TRH-GFP
105
75
1 2 3 4
IP-β_2-GFP
105
75
1 2 3 4
b)
% Cell Surface Receptors
100
90
80
70
60
50
40
30
IP-GFP
IP-TRH-GFP
IP-β_2-GFP
Agonist only
Agonist + 10μM H89
Agonist + 5μM GF109203X

Figure 5.7

Confocal visualisation of the effects of second messenger kinase activation on the sequestration of the HA-tagged IP receptor proteins.

Cells transiently expressing the HA-tagged receptor constructs were incubated with vehicle (a), 1μM iloprost (b), 5μM forskolin (c), or 5μM PMA (d) for 60 min at 37°C. Receptors were visualised by immunostaining with the 12CA5 antibody. The confocal images shown are representative of a single experiment which was repeated twice. Scale bar = 2.5μM.

Figure 5.7

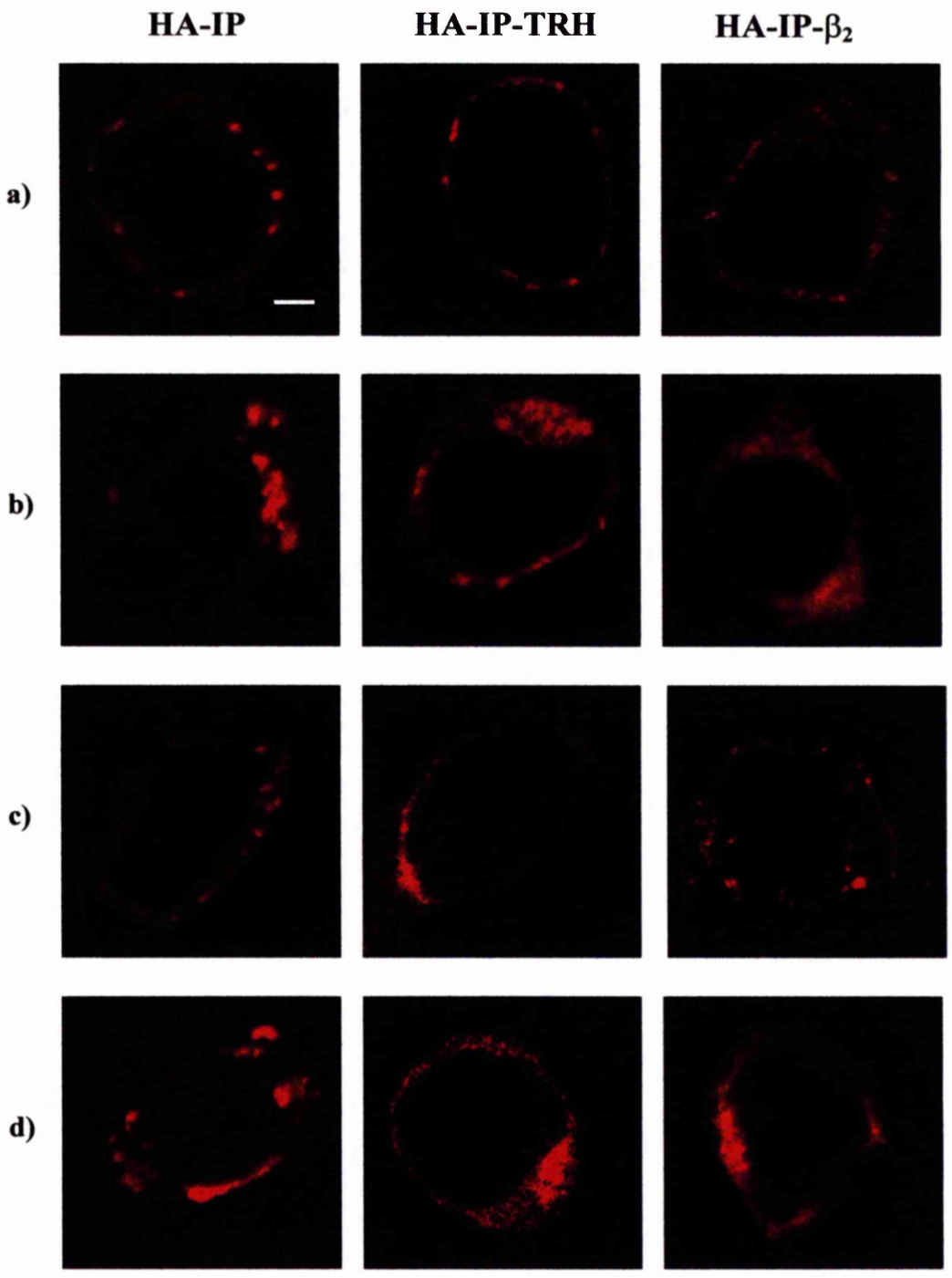

Figure 5.8

Quantitative analysis of the effects of exogenous second messenger kinase activation on the internalisation of the GFP-receptor proteins.

a) Cells were incubated with vehicle (1), 1μM iloprost (2), 5μM forskolin (3), or 5μM PMA (4) for 60 min at 37°C. Cell surface glycoproteins were subsequently labelled with biotin and the receptors were immunoprecipitated and visualised as detailed in section 2.7.5. Representative blots are shown. Similar results were obtained from two further experiments.

b) Densitometric scanning of the biotin blots was used to quantify the levels of cell surface receptors. The values shown represent mean ± S.E.M. for three experiments, with the levels of cell surface receptors observed in non-treated cells set at 100%.

Figure 5.8

a)

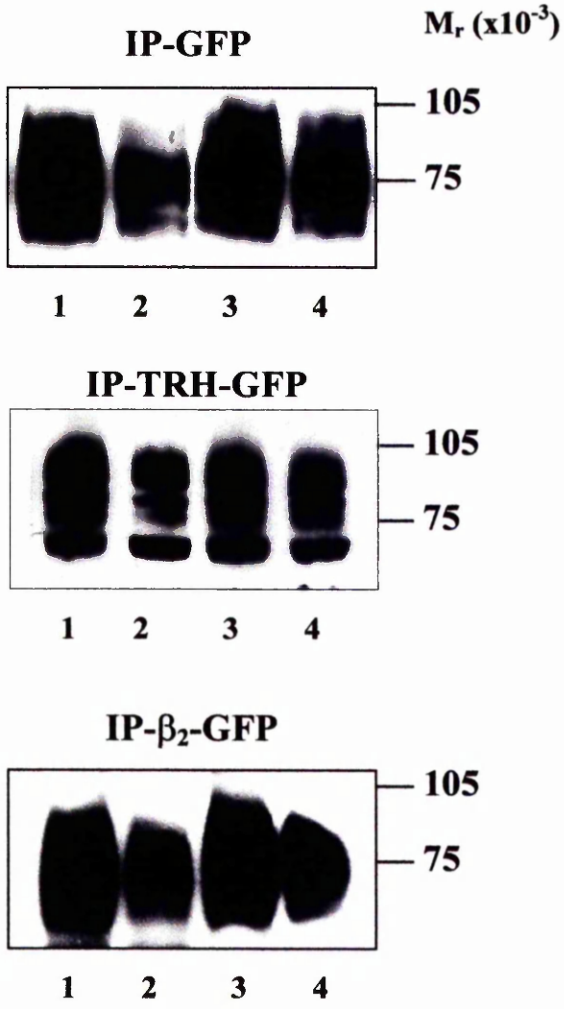
IP-GFP
M_r (x10^{-3})
105
75
1 2 3 4
IP-TRH-GFP
105
75
1 2 3 4
IP-β_2-GFP
105
75
1 2 3 4

b)

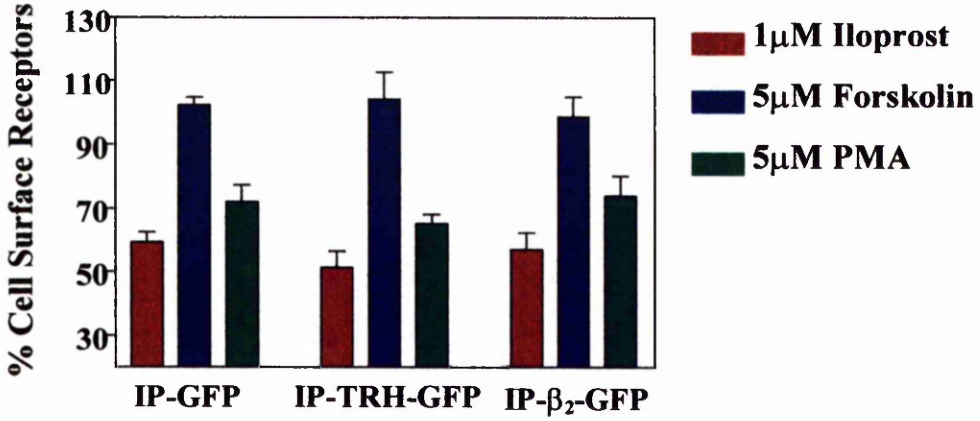
% Cell Surface Receptors
130
110
90
70
50
30
IP-GFP
IP-TRH-GFP
IP-β_2-GFP
1μM Iloprost
5μM Forskolin
5μM PMA

Figure 5.9

Iloprost-induced phosphorylation of the GFP-tagged prostacyclin receptor constructs.

Cells were incubated with vehicle (1), or 1μM iloprost for 30 seconds (2), 1 min (3) 2 min (4), 5 min (5) or 10 min (6). Receptors were then immunoprecipitated as described in 2.6.3b. Dried gels were analysed by autoradiography. Data shown are representative of one experiment which was repeated twice.

Figure 5.9

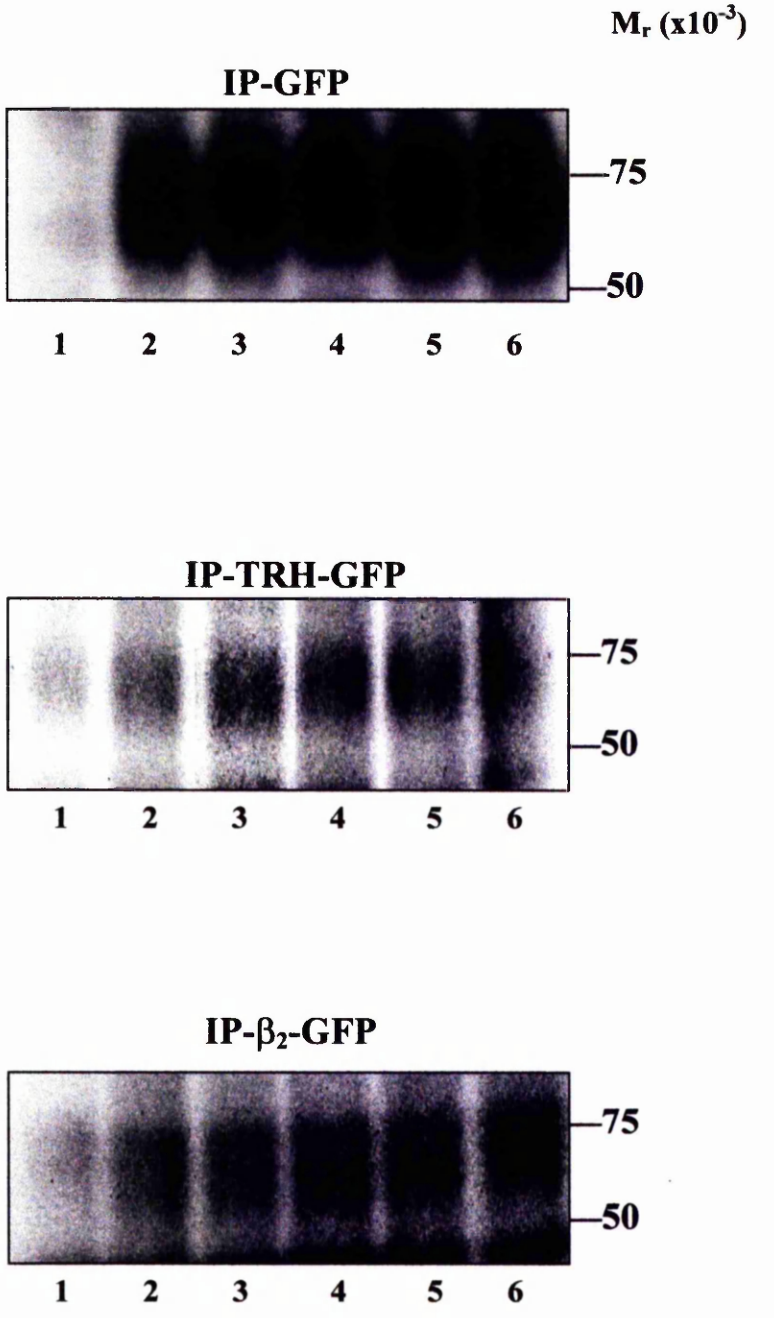
M_r ($x10^{-3}$)
IP-GFP
75
50
1 2 3 4 5 6
IP-TRH-GFP
75
50
1 2 3 4 5 6
IP-β_2-GFP
75
50
1 2 3 4 5 6

Figure 5.10

Effects of second messenger kinases on phosphorylation of the IP receptor-GFP conjugates.

Cells were pre-treated with vehicle (1, 5, 6), 10μM H89 (3) or 5μM GF109203X (4) prior to stimulation with 1μM iloprost (2, 3, 4), 5μM forskolin (5) or 5μM PMA (6) for 10 min at 37°C. Representative autoradiographs of the immunoprecipitated receptors are shown. Similar results were produced with two further experiments.

Figure 5.10

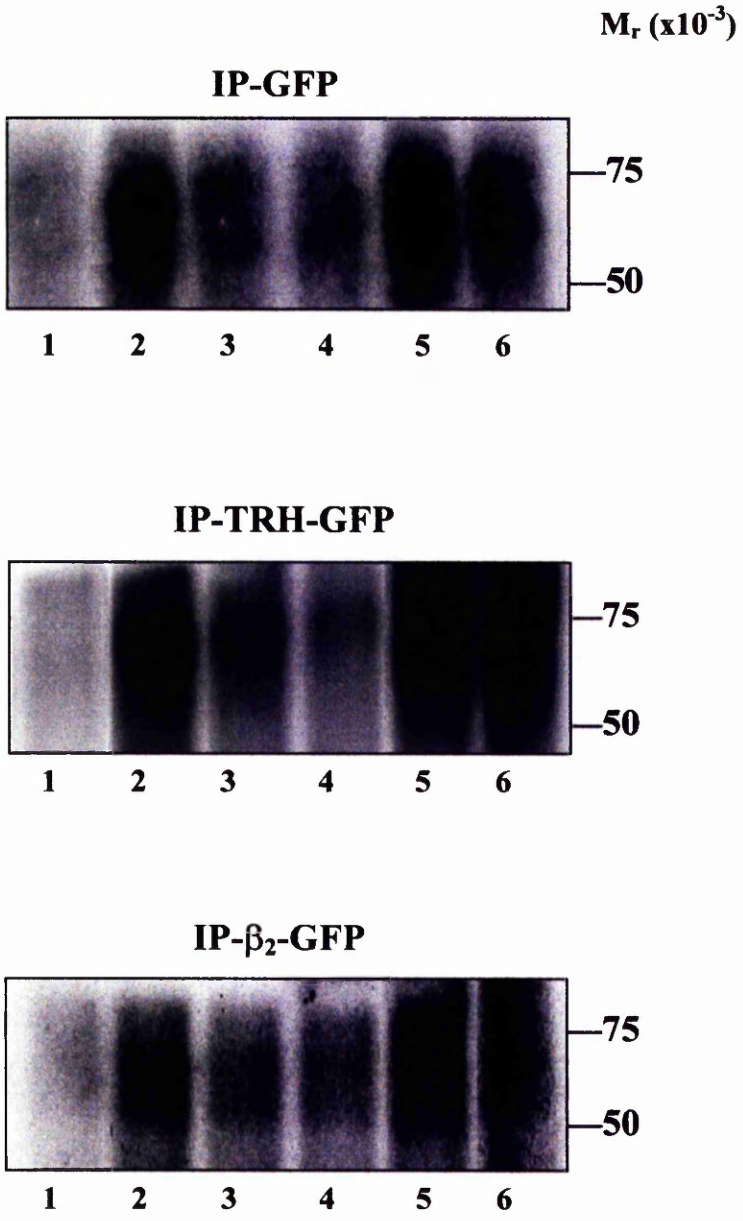
M_r ($x10^{-3}$)
IP-GFP
75
50
1 2 3 4 5 6
IP-TRH-GFP
75
50
1 2 3 4 5 6
IP-β_2-GFP
75
50
1 2 3 4 5 6

Figure 5.11

Resensitisation of the GFP-tagged IP receptor proteins following agonist removal.

The IP-GFP (a), IP-TRH-GFP (b), and IP-β_2-GFP (c) stable cell clones were incubated for 60 min at 37°C in the absence (control) or presence of 100nM iloprost. Cells were then washed to remove agonist and maintained in fresh medium for 30 or 60 min intervals at 37°C. Adenylyl cyclase activity in cells was then assessed in the presence of increasing concentrations of agonist. Net accumulation of intracellular cAMP in recovered cells was measured by subtracting the cAMP accumulation (after pre-exposure) measured at zero time. Results for each receptor are expressed as a percentage of the maximal cAMP accumulation in control cells. The data represent the mean ± S.E.M. of three independent experiments which were performed in triplicate.

Figure 5.11

a)

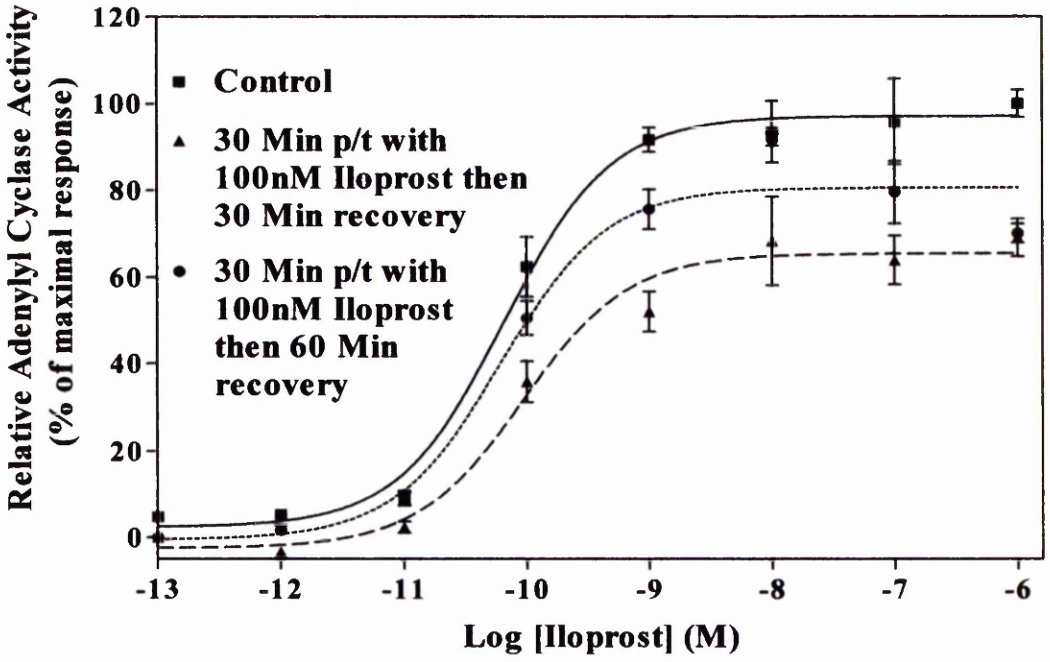

b)

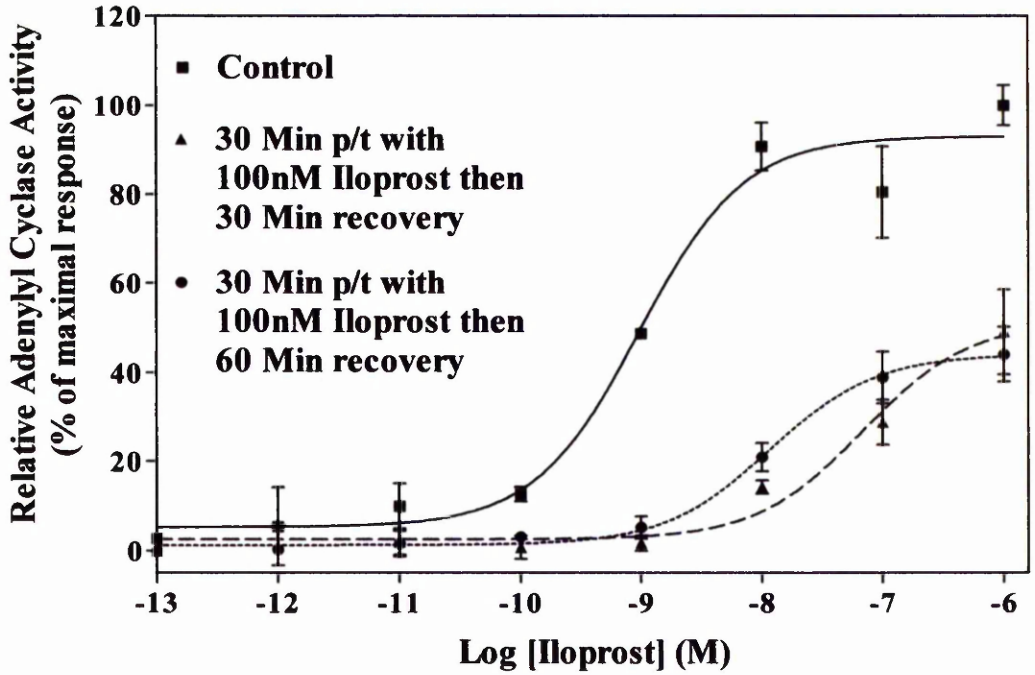

c)

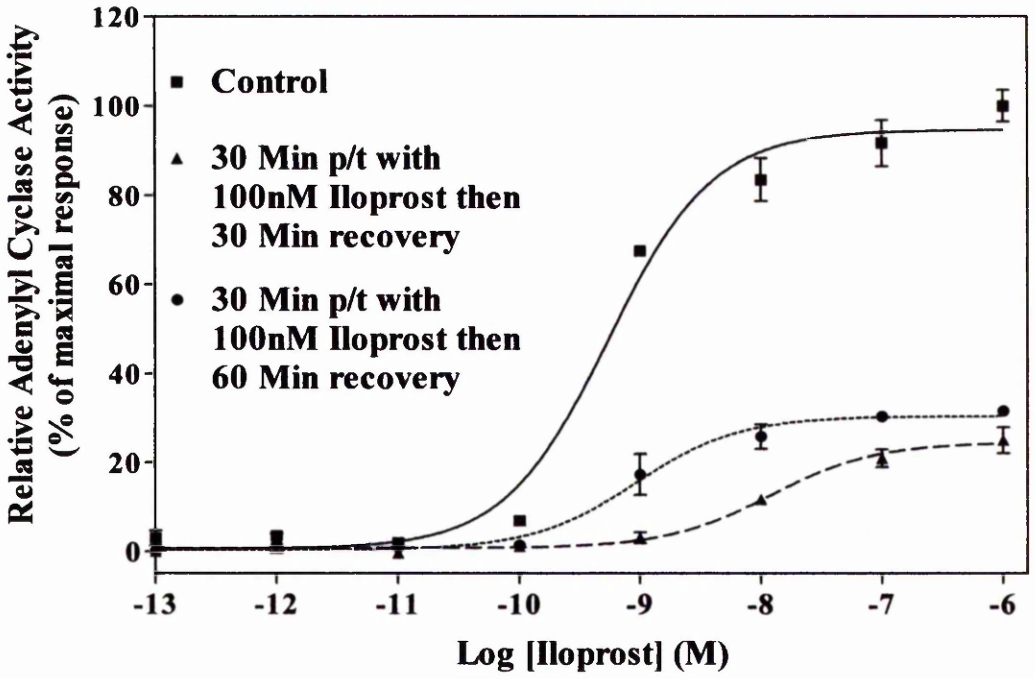
Relative Adenylyl Cyclase Activity
(% of maximal response)
120
100
80
60
40
20
0
Control
30 Min p/t with
100nM Iloprost then
30 Min recovery
30 Min p/t with
100nM Iloprost then
60 Min recovery
-13
-12
-11
-10
-9
-8
-7
-6
Log [Iloprost] (M)

Figure 5.12

Recycling of the sequestered IP receptor-GFP fusion proteins to the plasma membrane.

a) Cells were treated with vehicle (1) or 1μM iloprost for 60 min at 37°C (2, 3, 4) followed by a recovery period of 0 min (2), 30 min (3) or 60 min (4) in agonist-free conditions. Cell surface glycoproteins were subsequently labelled with biotin and the receptors were immunoprecipitated and visualised as detailed in section 2.7.5. Representative blots are shown. Similar results were obtained from two further experiments.

b) Densitometric scanning of the biotin blots was used to quantify the levels of cell surface receptors. The values shown represent mean ± S.E.M. for three experiments, with the levels of cell surface receptors observed in the absence of agonist set at 100%.

Figure 5.12

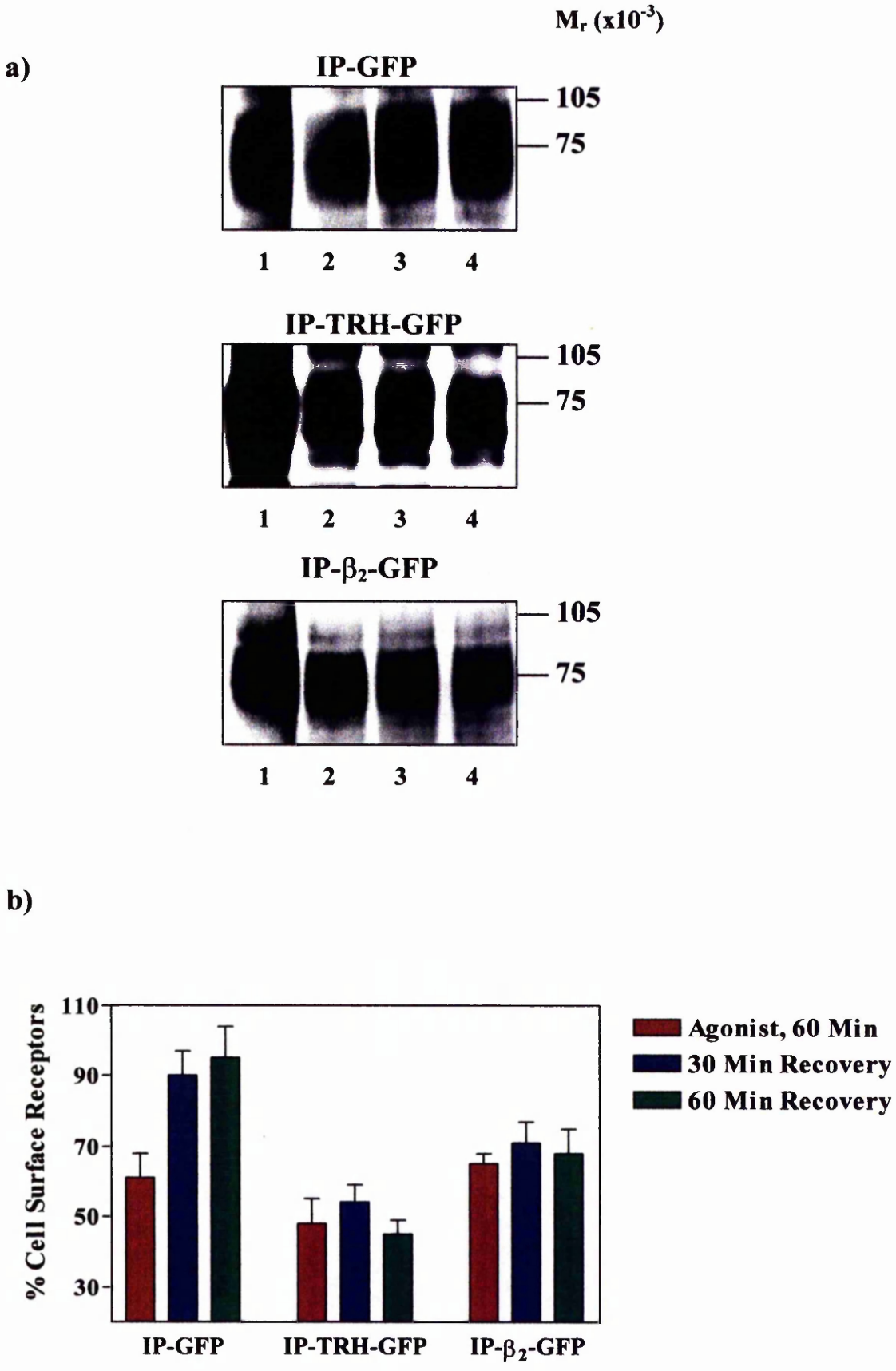
a)
M_r ($x10^{-3}$)
IP-GFP
105
75
1 2 3 4
IP-TRH-GFP
105
75
1 2 3 4
IP-β_2-GFP
105
75
1 2 3 4
b)
% Cell Surface Receptors
110
90
70
50
30
IP-GFP
IP-TRH-GFP
IP-β_2-GFP
Agonist, 60 Min
30 Min Recovery
60 Min Recovery

Figure 5.13

Western blot analysis of IP receptor-GFP constructs: the effects of receptor protein expression upon prolonged iloprost incubation.

a) The stable cell clones were treated with vehicle (control) or 1μM iloprost for 8 hours at 37°C. Cell lysates were then prepared and subjected to Western blot analysis using an anti-GFP antibody. The immunoblots shown are from a single experiment which was repeated twice with similar results. Molecular masses are in kDa.

b) Densitometric scanning of the immunoblots was used to quantify the levels of cell surface receptors. The values shown represent mean ± S.E.M. for three experiments, with the levels of cell surface receptors observed in the absence of agonist set at 100%.

Figure 5.13

a)

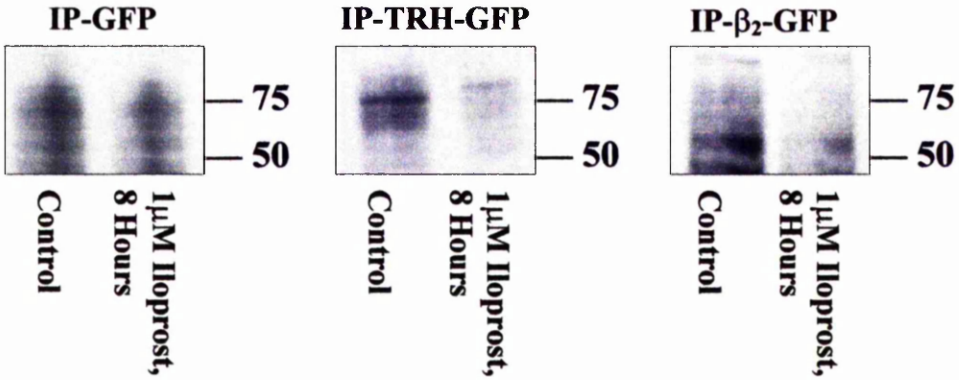

b)

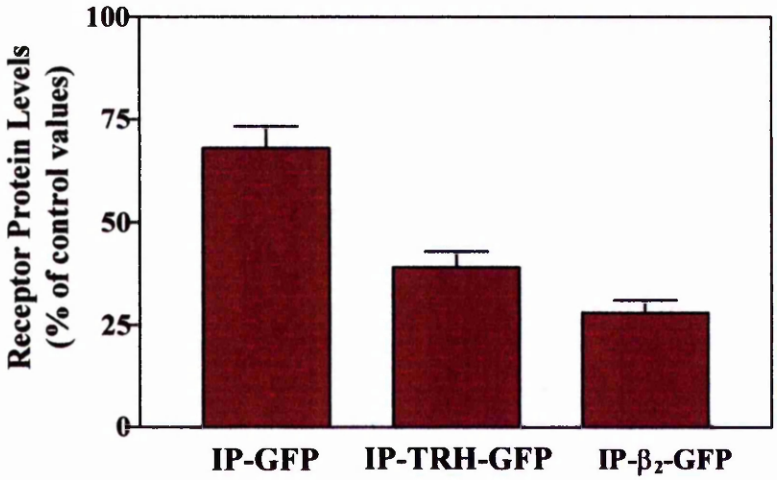

5.7 Discussion

The GPCR carboxyl terminal domain is primarily a site of agonist-mediated phosphorylation and β-arrestin interaction. Therefore, for many receptors, the process of desensitisation is dependent upon the integrity of the intracellular C-tail. In this chapter, the functioning of the carboxyl domain in the desensitisation of a GFP-tagged form of the prostacyclin receptor was examined using the C-tail receptor chimeras, IP-TRH-GFP and IP-β_2-GFP. Whole-cell adenylyl cyclase assays, which were used to monitor G_s coupling, showed that the IP-GFP receptor underwent rapid agonist-mediated desensitisation. Thus, the fusion of the GFP moiety to the receptor's C-terminus did not affect the receptor's ability to desensitise. The degree of receptor desensitisation induced in each cell line seemed to correlate well with the potency of iloprost at the receptors. For the IP-GFP receptor, at which iloprost was found to be the most potent, substantial abrogation of signalling was observed in cells after 10 min iloprost pre-exposure (Figure 5.1). By comparison, the IP-TRH-GFP and IP-β_2-GFP receptors (at which iloprost was approximately one order of magnitude less potent) exhibited a more modest attenuation of signalling after 10 min agonist pre-treatment (Figure 5.1). Therefore, it could be suggested that the reduction in G_s coupling efficiency of the chimeric receptors affected the receptors' capacity to induce full receptor desensitisation. The adenylyl cyclase responses of the IP-TRH-GFP and IP-β_2-GFP receptors were further reduced after a more prolonged period of iloprost pre-exposure (Figure 5.2). This increase in desensitisation may have been due to the onset of receptor sequestration. It could therefore be argued that the mechanisms involved in acute desensitisation of the IP-GFP receptor differ from those of the receptor chimeras.

Earlier prostacyclin receptor studies have demonstrated that mutant receptors lacking the putative PKC phosphorylation sites in the carboxyl terminal domain exhibit minimal agonist-mediated desensitisation in HEK293 cells (Smyth *et al.*, 1998). From this observation it was suggested that PKC is the major desensitising kinase of the prostacyclin receptor. In this chapter, the role of second messenger kinases in the iloprost-mediated desensitisation of the GFP-tagged prostacyclin receptor proteins was analysed in time courses of cAMP formation in the absence and presence of H89 (a PKA inhibitor) and GF109203X (a PKC inhibitor). For each of the constructs, an

increased accumulation of intracellular cAMP was evident in H89-pre-treated cells (Figure 5.3). Surprisingly, PKC inhibition did not appear to have any effects on the agonist-mediated adenylyl cyclase activation of the receptors (Figure 5.4). Taken together, the data indicated that PKA, and not PKC, is of functional significance in the desensitisation of the GFP-tagged prostacyclin receptor and its chimeric forms. The explanation for these unexpected observations is unclear. In the studies of Smyth and coworkers, prostacyclin receptor desensitisation was assessed in membrane preparations while in this investigation the process was examined in live cells. The discrepancy between the results reported here and the observations made by Smyth *et al.* (1998) may therefore simply reflect the different experimental conditions which were used to assay receptor desensitisation. The ineffectiveness of GF109203X in blocking desensitisation of the GFP-tagged prostacyclin receptors may be indicative of the receptors' inability to stimulate PI hydrolysis, and subsequently, activate PKC. Measurement of the receptors' coupling capacity to G_q/G_{11} would have to be performed to test this. It could be suggested that H89's effects on the desensitisation responses elicited by the prostacyclin receptor constructs were not due to the loss of PKA phosphorylation of the receptors. Rather, the inhibition of PKA phosphorylation of downstream effectors such as G proteins and/or adenylyl cyclase isoforms may account for the increased cAMP production seen in the presence of H89. It is also possible that the GFP adjunct alters prostacyclin receptor desensitisation. The fusion of GFP to the receptor's C-terminus may affect receptor signalling by inducing conformational changes in the receptor, indirectly altering kinase phosphorylation of key residues within the intracellular domains.

While in the midst of this investigation Smyth *et al.* (2000) reported that second messenger kinase phosphorylation was not a requirement for sequestration of the prostacyclin receptor. Similarly, in this study, pre-treatment of cells with the kinase inhibitors H89 and GF109203X failed to attenuate iloprost-stimulated sequestration of the HA- and GFP-tagged forms of the receptors when assessed both visually (by confocal analysis) and quantitatively (in biotin labelling assays) (Figures 5.5 and 5.6). The data therefore indicated that second messenger kinase phosphorylation plays only a minor role in mediating sequestration of the IP receptors. Nevertheless, the data cannot rule out a possible involvement of GRKs in receptor sequestration. Previous published findings have suggested that prostacyclin receptor sequestration is independent of GRK-

mediated phosphorylation since overexpression of GRKs did not increase internalisation (Smyth *et al.*, 2000). On this basis, it could be argued that trafficking of the IP receptor and the chimeras proceeds primarily via a phosphorylation-independent mechanism. For many GPCRs, phosphorylation is a prerequisite for receptor sequestration (Ferguson and Caron, 1998). However, phosphorylation-independent trafficking has been reported for GPCRs including the rat follitropin receptor (Nakamura *et al.*, 1998) and chemokine CXCR2 receptor (Fan *et al.*, 2001).

Heterologous desensitisation of GPCRs can involve the phosphorylation of unoccupied as well as agonist-bound receptors by second messenger kinases. The process may also be associated with an increase in receptor internalisation. Indeed, heterologous activation of second messenger kinases has been shown to trigger internalisation of the α_{1B}-adrenergic and δ-opioid receptors in the absence of ligand (Awaji *et al.*, 1998; Xiang *et al.*, 2001). To determine whether heterologous activation of PKA and/or PKC regulated the agonist-independent activities of the prostacyclin receptor constructs, receptor sequestration was monitored after pre-treatment of cells with forskolin or PMA (Figures 5.7 and 5.8). In confocal experiments and biotin labelling assays, exogenous stimulation of PKA by forskolin did not alter the plasmalemmal distribution of unoccupied IP receptor proteins. In contrast, exogenous PKC activation by PMA promoted considerable internalisation of each of the receptor constructs. The data therefore indicated that PKC phosphorylation of the receptors is sufficient to promote internalisation. Why GF109203X did not at least partially inhibit iloprost-mediated internalisation of the receptors is unclear. It is possible that the diacylglycerol formed upon iloprost stimulation of the receptors induces only modest PKC activation. Thus, the contribution of PKC to agonist-stimulated receptor sequestration may be insignificant. It could also be argued that a GF109203X-insensitive PKC isoform directs internalisation of the prostacyclin receptor constructs. Contrary to the hypothesis of Smyth *et al.* (2000), the data presented here cannot rule out the possibility that phosphorylation is a pre-requisite for the sequestration of the prostacyclin receptor proteins. Notably, the extent of PMA-induced receptor internalisation was less than the response mediated by iloprost incubation, indicating that receptor phosphorylation alone is unable to elicit a maximal endocytic response. Receptor occupancy may therefore promote conformational changes which are essential for endocytosis.

The prostacyclin receptor, expressed in HEK293 cells, is rapidly phosphorylated in response to agonist stimulation (Smyth *et al.*, 1996; 1998). Similarly, the GFP-tagged form of the receptor was shown to undergo rapid phosphorylation in response to iloprost challenge (Figure 5.9). The presence of the large GFP group at the carboxyl terminus of the receptor might have been expected to inhibit agonist-mediated receptor phosphorylation but this was not the case. The maintenance of agonist-dependent phosphorylation has also been shown for other GPCR-GFP conjugates including the β_2-AR and cAMP1 receptor (Barak *et al.*, 1997a; Xiao *et al.*, 1997). As anticipated, a time-dependent increase in receptor phosphorylation was also exhibited by the IP-TRH-GFP and IP-β_2-GFP constructs in response to agonist treatment (Figure 5.9). Furthermore, the time courses revealed that the constructs exhibited similar phosphorylation kinetics. In order to determine the role of second messenger kinases in receptor phosphorylation, agonist-stimulated phosphorylation was examined in the presence of H89 and GF109203X (Figure 5.10). Pre-treatment with H89, as well as GF109203X, significantly diminished agonist-mediated phosphorylation of the GFP-tagged prostacyclin receptor. A similar effect was also seen with the receptor chimeras. Thus, the data indicated that both PKA and PKC phosphorylate the receptor proteins. In further support of these findings, exogenous activation of PKA by forskolin and PKC by PMA also induced phosphorylation of the receptors independently of agonist activation (Figure 5.10). Previous reports of prostacyclin receptor phosphorylation by Smyth and coworkers (1996) suggested that IP receptor phosphorylation is primarily catalysed by PKC and not PKA. The reasons for the apparent discrepancy between the data reported here and the findings of Smyth *et al.* (1996) are unclear although the presence of GFP at the receptor C-terminus may have modified receptor phosphorylation. It could be postulated that GFP itself is acting as a substrate for the second messenger kinases. It is impossible to determine from the phosphorylation experiments the sites of kinase action, though sequence analysis has shown that each of the receptor constructs contains multiple consensus sites for PKA (R-X_{1-2}-**S/T**-X) and PKC (X-**S/T**-X-R/K) phosphorylation within their intracellular domains. While it appears that second messenger kinases account for a sizeable proportion of the agonist-induced phosphorylation response of the receptors, the data does not rule out the possibility that other kinases, such as GRKs, regulate the responsiveness of the receptor proteins.

The fine balance between receptor resensitisation and downregulation of desensitised GPCRs determines the magnitude and endurance of a cell's response to further agonist exposure. The fate of the agonist-activated prostacyclin receptor-GFP proteins was examined to further characterise receptor regulation. Upon withdrawal of agonist, adenylyl cyclase activity in IP-GFP cells was restored to levels comparable to those in control cells within a 60 min recovery period (Figure 5.11). Resensitisation of the IP-GFP receptor appeared to coincide with the recycling of sequestered receptors back to the plasma membrane therefore indicating that a significant number of the recycled receptors were fully functional (Figure 5.12). However, no obvious recovery of G_s coupling was evident in IP-TRH-GFP and IP-β_2-GFP cells after 60 min of agonist-free conditions (Figure 5.11). The slow resensitisation of the chimeric receptors was associated with their failure to recycle (Figure 5.12). Earlier investigations by Oakley and coworkers (1999) revealed that stable association of desensitised receptors with β-arrestins protects the receptor from phosphatases, blocking dephosphorylation and resulting in slowed receptor resensitisation. The data from Chapter 4, together with published findings by Smyth *et al.*, (2000), have indicated that prostacyclin receptor sequestration occurs independently of β-arrestins. Therefore consistent with Oakley's hypothesis, it could be argued that β-arrestin-independent trafficking of the IP receptor allows for rapid association with the GPCR phosphatases, enabling dephosphorylation and the rapid recycling of receptors back to the plasma membrane. Likewise, it could be postulated that long-term association of the β-arrestin proteins with the IP-TRH-GFP construct impedes receptor resensitisation. In support of this hypothesis, confocal experiments demonstrated that the TRH-tailed IP receptors endocytose in complexes with β-arrestin 2 (Chapter 4). Furthermore, numerous investigations have confirmed the role of TRH carboxyl tail in mediating high affinity binding with β-arrestins (Willars *et al.*, 1999; Heding *et al.*, 2000; Zhang *et al.*, 1999; Oakley *et al.*, 1999, 2000). For the IP-β_2-GFP construct, which was shown to exhibit β-arrestin-independent sequestration (Chapter 4), the pattern of receptor resensitisation does not fit the model proposed by Oakley and coworkers (1999). The biochemical explanation for this unanticipated result remains undetermined. It is known that dephosphorylation is a prerequisite for the exocytosis of GPCRs including the β_2-adrenergic, δ-opioid and vasopressin V2 receptors (Shih *et al.*, 1999; Hasbi *et al.*, 2000; Innamorati *et al.*, 2001). Therefore it could be suggested that sequestered IP-β_2-GFP receptors exhibit incomplete

dephosphorylation. Interactions between the β_2-GFP tail and the body of the receptor may induce conformational changes which affect the access of phosphatases to desensitised receptors. Another possibility is that the internalised IP-β_2-GFP receptors deviate to an organelle that is not part of the recycling pathway. For the non-recycling vasopressin V2 receptor, sequestered receptors have been shown to diverge from the sorting endosomes to the perinuclear compartment where they are retained (Innamorati *et al.*, 2001).

The retention of sequestered GPCRs intracellularly has been suggested to promote routing of receptors to the lysosomes (Bremnes *et al.*, 2000). Consistent with this hypothesis, an increased downregulation of the non-recycling IP-TRH-GFP and IP-β_2-GFP receptor proteins was detected in comparison to the recycling IP-GFP receptor after 8 hour's of agonist challenge. (Figure 5.13). The different intracellular trafficking routes of the full-length prostacyclin receptor and it chimeric forms may be an important mechanism underlying the distinct physiological responses mediated by the receptors.

In summary, the results show that the GFP-tagged prostacyclin receptor exhibits rapid iloprost-induced desensitisation which is reversible upon agonist withdrawal. Examination of the underlying mechanisms governing IP-GFP signalling has highlighted the critical roles of PKA and PKC in the processes of desensitisation and sequestration. Similarly, for the TRH- and β_2-AR-tailed receptor chimeras, second messenger kinase phosphorylation was found to be of functional importance in receptor regulation. However, comparative analysis of the receptors' G_s coupling clearly demonstrated that the presence of the different carboxyl tails altered the receptor's ability to elicit desensitisation and resensitisation responses. The data would therefore suggest that the carboxyl terminal domain of the prostacyclin receptor contributes to these processes.

In contrast to findings in this study and those previously reported by Smyth *et al.* (1998), in which prostacyclin receptor desensitisation was analysed in overexpression systems, all studies performed with cells naturally expressing the IP receptor describe a much slower time course of desensitisation occurring over a period of several hours

(Krane *et al.*, 1994; Mundell and Kelly, 1998; Giovanazzi *et al.*, 1997; Nilius *et al.*, 2000). The slow desensitisation kinetics in natural systems suggest that mechanisms different from those described for the cloned prostacyclin receptor are likely to be involved. The mechanisms of long-term attenuation of the endogenously expressed IP receptor are much less understood although the process is thought to be independent of receptor phosphorylation and sequestration (Nilius *et al.*, 2000). The signalling responses of the IP receptor in HEK293 cells may therefore be artefacts of the transfection system.

Chapter 6

Final Discussion

Chapter 6

The GPCR superfamily constitutes one of the largest protein families in nature with the identification of approximately 2000 members to date. Despite binding and transducing signals of a wide range of ligands, all GPCRs share the same basic structure comprising an extracellular amino terminal domain followed by a central core domain of seven transmembrane helices (connected by three extracellular and three intracellular loops), and an intracellular carboxyl terminal domain. GPCRs mediate their intracellular actions through the activation of one or more class of heterotrimeric G protein. As well as initiating receptor signalling, agonist binding to GPCRs activates a series of signalling events which lead to receptor desensitisation, a process which is characterised by a reduction in GPCR responsiveness. The molecular mechanisms of receptor desensitisation are primarily the uncoupling of receptors from G proteins and sequestration of plasma membrane receptors to intracellular compartments. To maintain cellular homeostasis, GPCR responsiveness to extracellular stimuli is restored by the process of receptor resensitisation which is achieved mainly through the recycling of receptors back to the cell surface in the pre-ligand exposed state and/or shuttling of newly synthesised receptors to the plasma membrane. Thus, a co-ordinated balance between receptor desensitisation and resensitisation regulate GPCR activity (Ferguson and Caron, 1998).

In addition to determining G protein coupling and specificity, the intracellular domains of GPCRs are also involved in GPCR regulation. Agonist-mediated phosphorylation of residues within the receptor's cytosolic loops and/or C-tail domain promotes the binding of β-arrestins which uncouple GPCR/G protein interactions and target receptors for endocytosis in clathrin-coated pits, thereby inducing receptor desensitisation. Conversely, the release of bound β-arrestin and dephosphorylation of the receptor's intracellular regions are considered to be essential processes for the resensitisation of ligand-activated GPCRs.

For many GPCRs the carboxyl terminal domain is the primary site of agonist-mediated phosphorylation and β-arrestin interaction. Thus, alterations within this region have been shown to influence the processes of desensitisation (Blaukat *et al.*, 2001; Lamey *et*

al., 2002; Maestes *et al.*, 1999; Smith *et al.*, 1998), sequestration (Fukushima *et al.*, 1997; Huang *et al.*, 1995; Hukovic *et al.*, 1998), and resensitisation (Oakley *et al.*, 1999; Innamorati *et al.*, 2001). In many of these investigations, point mutations and/or receptor truncations have been the most common strategies adopted in the study of C-tail function. An alternative strategy is the generation of chimeric receptors. With this approach the predicted outcome is either the retention of receptor function or the conferment of properties of the donor receptor to the recipient. In this study, chimeric GPCRs possessing the intracellular tail regions of the human β_2-adrenergic and rat TRH-1 receptors were constructed in order to examine the role of the carboxyl terminal region in prostacyclin receptor regulation. Furthermore, C-terminally GFP-tagged forms of each receptor were generated, thus providing the opportunity to directly monitor the localisation, and trafficking of receptors in response to extracellular stimuli. Earlier investigations by Smyth and coworkers (1998, 2000) with a recombinant IP receptor construct, overexpressed in HEK293 cells, indicated that the processes of receptor desensitisation and sequestration were dependent upon the integrity of the carboxyl tail.

In chapter 3 experiments were performed to characterise the pharmacological properties and agonist-mediated trafficking of each receptor construct. Ligand binding analysis revealed the GFP-tagged receptors exhibited similar binding affinity for [^{3}H] iloprost thus demonstrating that the IP receptor's carboxyl tail was not a critical factor in agonist binding. The ability of the constructs to mediate intracellular signalling was confirmed in assays of adenylyl cyclase activity. Moreover, the addition of GFP to the C-terminal region did not appear to affect G_s coupling. Iloprost was most potent at the IP-GFP receptor, exhibiting an EC_{50} value similar to that reported earlier for both native and epitope-tagged forms of the receptor (Smyth *et al.*, 1996). The lower receptor expression in the IP-TRH-GFP and IP-β_2-GFP cell lines may account for the observation that iloprost was less potent at stimulating adenylyl cyclase in these stable clones. The relationship between agonist potency and receptor density has previously been established for GPCRs such as the adenosine A1 and β_2-adrenergic receptors (Cordeaux *et al.*, 2000; Whaley *et al.*, 1994). Further desensitisation studies with stable cell lines expressing similar receptor densities would be necessary to test this hypothesis.

Agonist-induced sequestration of the receptor-GFP conjugates was initially determined by confocal analysis. Direct visualisation of sequestered receptors proved to be problematic since each of the selected clones exhibited varying amounts of intracellular GFP-derived autofluorescence in the unstimulated state. Despite this, significant translocation of plasmalemmal receptors to intracellular compartments could be detected in each of the stable cell lines upon agonist incubation. Confocal data suggested that the IP-TRH-GFP receptor displayed enhanced internalisation kinetics whereas the IP-GFP and IP-β_2-GFP receptors internalised more slowly. Quantification of receptor internalisation in biotin labelling experiments further supported these observations, demonstrating that internalisation of the β_2-tailed chimera was comparable to that of the full-length receptor whereas receptor sequestration was augmented by the presence of the TRH receptor carboxyl tail. In internalisation studies of the HA-tagged receptor proteins similar results were obtained. Therefore, the presence of a C-terminal GFP tag did not alter the internalisation kinetics of the receptors, a phenomena which has been reported for other GFP-conjugated GPCRs including the β_2-AR and edg1 receptor (Kallal *et al.*, 1998; Liu *et al.*, 1999).

The native TRH receptor rapidly internalises in response to agonist (Nussenzveig *et al.*, 1993). From various mutational studies, the determinants of receptor sequestration were localised to regions within the receptor's carboxyl domain (Nussenzveig *et al.*, 1993; Drmota and Milligan, 2000). On this basis, it would appear that the fusion of the TRH carboxyl tail to the IP receptor created a receptor chimera possessing the trafficking behaviour of the donor receptor. In accord with such an assumption, internalisation of the mammalian GnRH receptor was reported to be enhanced by the addition of the TRH carboxyl tail to the receptor C-terminus (Heding *et al.*, 1998).

Expression of the β_2-AR carboxyl sequence was unable to switch the sequestration phenotype of the prostacyclin receptor to that of the donor. Rather, the internalisation kinetics remained unaltered from that of the full-length receptor. The role of the carboxyl tail in the sequestration of the β_2-AR is uncertain since mutations of potential phosphorylation sites and C-tail deletions did not inhibit internalisation (Hausdorff *et al.*, 1989; Ferguson *et al.*, 1995, 1996) whereas a dileucine motif within this region was identified as a positive regulator of receptor endocytosis (Gabilondo *et al.*, 1997). In this

study, the internalisation assays revealed that there was no acquisition of function by the expression of the β_2-AR C-tail. It would therefore appear that multiple domains would have to be switched in order to gain β_2-AR-like internalisation properties.

To further characterise the molecular mechanisms governing sequestration of the prostacyclin receptor, in chapter 4 various techniques were employed to identify the pathway involved in its sequestration. The role of the receptor's carboxyl terminal domain in this process was examined using the chimeric receptor constructs. Pharmacological agents which block endocytosis via clathrin coated pits were effective at inhibiting sequestration of each of the receptor constructs. Furthermore, the receptors were shown to traffic in vesicles in close apposition to those containing transferrin. Taken together, these initial data identified the main pathway of internalisation of each of the constructs as clathrin-dependent.

Clathrin-mediated endocytosis of GPCRs invariably displays a dependence on β-arrestin. Therefore, confocal microscopy was used to monitor the association of β-arrestin proteins with the receptors in intact cells. In accordance with previously published reports by Smyth *et al.* (2000), sequestration of the full-length prostacyclin receptors did not appear to be mediated via a β-arrestin dependent route. Switching of the carboxyl domain for the equivalent TRH receptor region increased the receptor's affinity for β-arrestins as revealed by confocal imaging in which the chimeric receptor could be seen to co-internalise with β-arrestin 2. In contrast, the β_2-AR tailed chimeras trafficked independently of β-arrestins, assuming the same pattern of internalisation as the full-length receptor. Confocal analysis also revealed that the prostacyclin receptor proteins were capable of mediating significant levels of agonist-induced internalisation in a cellular milieu deficient of GRKs and arrestins. The predominant endocytic pathway utilised by the receptor constructs may therefore be arrestin-independent, although better cell models would be needed to confirm this.

The colocalisation experiments indicated that the addition of the TRH receptor C-tail sequence conferred β-arrestin sensitivity to the prostacyclin receptor. In support of this, earlier research suggested that the TRH receptor carboxyl domain was the main site of β-arrestin interaction, mediating high affinity binding with both β-arrestin 1 and 2 (Yu

and Hinkle, 1999; Willars *et al.*, 1999; Heding *et al.*, 2000; Oakley *et al.*, 2000). Moreover, the carboxyl tail alone was reported to be sufficient to increase the binding affinity of β-arrestins to various receptor chimeras (Willars *et al.*, 1999; Oakley *et al.*, 2000). Although an increase in the prostacyclin receptor's affinity to β-arrestin was produced by the expression of the TRH carboxyl sequence, the failure of the IP/TRH chimeras to interact with β-arrestin 1 would suggest that, in this instance, the substitution of further intracellular domains would be necessary to reproduce a TRH-like sequestration phenotype.

The wild type β_2-AR receptor has been demonstrated to internalise in a β-arrestin-dependent manner (Zhang *et al.*, 1996; Ferguson *et al.*, 1996; Oakley *et al.*, 2000). Some investigators have suggested that the determinants which regulate the β_2-AR's interactions with β-arrestin are located within the receptor's carboxyl tail (Zhang *et al.*, 1999, Oakley *et al.*, 1999, 2000) while others have intimated that other receptor domains contribute to the process (Jockers *et al.* 1996; Ferguson *et al.*, 1996). The data reported in this study would seem to be in accord with the latter postulation. The exchange of the intracellular loop regions may therefore also be required to generate a β-arrestin-sensitive receptor.

In the final results chapter, the desensitisation and resensitisation properties of the prostacyclin receptors were examined. In overexpression systems, the prostacyclin receptor has been shown to undergo rapid agonist-mediated desensitisation, a process which coincides with receptor phosphorylation (Smyth *et al.*, 1998). Desensitisation studies with the IP-GFP receptor produced similar results, demonstrating that the GFP tag did not prevent signal attenuation. Agonist-stimulated IP-TRH-GFP and IP-β_2-GFP receptors exhibited a similar pattern of phosphorylation. However, the desensitisation responses elicited by the chimeras were more modest in comparison to that of the full-length receptor. The reason for these apparent differences in receptor responsiveness is unclear although it could be suggested that the reduced coupling efficiency displayed by the chimeric proteins was a contributory factor.

PKC has been reported to be the main desensitising kinase of the prostacyclin receptor (Smyth *et al.* 1998). However, experiments performed in this study indicated that PKA,

and not PKC, was involved in the desensitisation of the IP-GFP receptor. Moreover, PKA was found to contribute to the desensitisation of the receptor's chimeric forms. The explanation for the apparent discrepancy between results from this study and the observations made by Smyth *et al.* (1998) is uncertain. The GFP adjunct may alter receptor phosphorylation, and thus affect the signalling processes which induce receptor desensitisation. Consistent with this, the phosphorylation data reported here revealed that both second messenger kinases could stimulate phosphorylation of the constructs whereas Smyth and coworkers (1998) concluded that the IP receptor was not a substrate for PKA phosphorylation. It is possible that GFP may be modifying receptor phosphorylation and desensitisation by acting as a substrate for kinase action. It has been suggested that GRKs do not contribute to the desensitisation of the prostacyclin receptor (Smyth *et al.*, 2000). It remains to be determined whether this is also the case for the GFP-tagged form of the receptor, and if the different carboxyl tails are GRK substrates.

The role of phosphorylation in receptor sequestration has been established for many GPCRs. For the prostacyclin receptor, however, it has been reported that phosphorylation is not a prerequisite for internalisation (Smyth *et al.*, 2000). Contrary to this, the internalisation data in chapter 5 suggested that PKC phosphorylation may be of importance in the sequestration of the prostacyclin receptors; PMA-induced PKC activity stimulated the endocytosis of unoccupied cell surface receptors. Nevertheless, PKC's involvement in the sequestration of agonist-activated receptors may be minimal since PKC inhibition failed to inhibit internalisation of iloprost-stimulated receptors. The data in this study cannot therefore rule out a link between receptor phosphorylation and sequestration for the IP receptor and its chimeric forms.

Upon the removal of agonist, the sequestered IP-GFP receptors were found to rapidly recycle back to the plasma membrane with a concomitant recovery of receptor responsiveness. In contrast, the agonist-activated chimeric receptors did not recycle. The retention of receptors intracellularly coincided with the receptors' failure to resensitise. Various studies have intimated that dephosphorylation is a prerequisite for receptor recycling and resensitisation (Pippig *et al.*, 1995; Shih *et al.*, 1999; Hasbi *et al.*, 2000; Innamorati *et al.*, 2001). The dissociation of the receptor/β-arrestin complexes has

been reported to be the rate-limiting step for receptor dephosphorylation (Oakley *et al.*, 1999). Consistent with this, it could therefore be argued that the β-arrestin-independent trafficking of the IP-GFP receptor allows for rapid association of the sequestered receptors with the phosphatase, enabling rapid recycling and resensitisation. This model may also be applicable to IP-TRH-GFP receptor sequestration; the high affinity β-arrestin interactions mediated by the TRH carboxyl tail may prevent receptor dephosphorylation and recycling. The recycling and resensitisation profile of the β_2-AR tailed chimera did not fit the model proposed by Oakley *et al.* (1999). Although it has been shown that the construct internalises independently of β-arrestin, it is conceivable that conformational effects induced by the presence of the β_2-AR carboxyl domain impede phosphatase access or possibly direct receptor trafficking via a non-recycling pathway. Assessment of the receptors' phosphorylation status after agonist withdrawal would be required to accurately determine the rate of dephosphorylation for each construct, and whether the dephosphorylation step dictates the receptors' resensitisation kinetics. Investigation of the long-term fate of the agonist-stimulated prostacyclin receptor constructs revealed that the non-recycling chimeric receptors underwent downregulation more rapidly compared to the recycling full-length receptor. From this observation, it could therefore be assumed that the retention of receptors intracellularly increases sorting via a degradative pathway, a proposal which has been suggested by other investigators (Oakley *et al.*, 1999; Bremnes *et al.*, 2000).

In conclusion, with the use of receptor chimeras, the carboxyl terminal domain of the prostacyclin receptor has been shown to be of functional significance in various aspects of receptor regulation including desensitisation, sequestration, and resensitisation. The results indicate that the different carboxyl sequences modulate distinct receptor interactions with intracellular signalling components. Although switching of carboxyl tail domain was found to have profound effects on receptor activity, the chimeric receptors did not assume the GPCR characteristics typical of the carboxyl terminal donors. It therefore seems likely that the carboxyl tail, in concert with other intracellular domains, regulate receptor activity.

The use of GFP to directly visualise the trafficking of the prostacyclin receptors in cells provided crucial insight into the mechanisms involved in GPCR regulation.

Nevertheless, it is clear from this investigation that whilst many of the pharmacological properties of the prostacyclin receptor were retained following the C-terminal fusion of the GFP moiety, the IP-GFP receptor elicited discernible differences in receptor activity in comparison to those reported for the non-GFP-tagged form of the protein (Smyth *et al.*, 1996 1998). Therefore, data from GPCR-GFP studies should be viewed with caution.

It is evident from the data presented in this study that further research is required to better characterise the role of the carboxyl terminal domain in prostacyclin receptor signalling. Future work with the prostacyclin receptor constructs would include investigating the G_q/G_{11} coupling efficiency of the receptors to determine the role of PKC activation in receptor desensitisation and internalisation. It would also be of interest to examine the possible role of GRK-mediated phosphorylation in homologous desensitisation of these receptor proteins. Viable β-arrestin knockout cell lines would also be useful tools to delineate the sequestration pathways utilised by the receptors. Furthermore, assessment of the intracellular localisation and phosphorylation status of the agonist-activated receptors would provide greater insight into the mechanisms involved in the resensitisation of the full-length receptor and the carboxyl tail chimeras. Further understanding of prostacyclin receptor regulation could also be achieved by the generation of a series of prostacyclin receptor chimeras in which additional intracellular domains are switched.

Chapter 7

References

References

Abramovitz M, Boie Y, Nguyen T, Rushmore TH, Bayne MA, Metters KM, Slipetz DM and Grygorczyk R (1994) *J. Biol. Chem.* **269:** 2632-2636

Ahn S, Maudsley S, Luttrell LM, Lefkowitz RJ and Daaka Y (1999) *J. Biol. Chem.* **274:** 1185-1188

Ambrose C, James M, Barnes G, Lin C, Bates G, Altherr M, Duyao M, Groot N, Church D and Wasmuth JJ (1992) *Hum. Mol. Genet.* **1:** 697-703

Anborgh PH, Dale L, Seachrist J and Ferguson SSG (2000) *Mol. Endocrinol.* **14:** 2040-2053

Andersen NH, Eggerman TL, Harker LA, Wilson CH and De B (1980) *Prostaglandins* **19:** 711-735

Andersen NH and Ramwell PW (1974) *Arch. Intern. Med.* **133:** 30-50

Aoki J, Katoh H, Yasui H, Yamaguchi Y, Nakamura K, Hasegawa H, Ichikawa A and Negishi M (1999) *Biochem. J.* **340:** 365-369

Aramori I, Ferguson SSG, Bieniasz PD, Zhang J, Cullen BR and Caron MG (1997) *EMBO J.* **16:** 4606-4616

Arora KK, Krsmanovic LZ, Mores N, O'Farrell H and Catt KJ (1998) *J. Biol. Chem.* **273:** 25581-25586

Arora KK, Sakai A and Catt KJ (1995) *J. Biol. Chem.* **270:** 22820-22826

Attramadal H, Arriza JL, Aoki C, Dawson TM, Codina J, Kwatra MM, Snyder SH, Caron MG and Lefkowitz RJ (1992) *J. Biol. Chem.* **267:** 17882-17890

Audoly L and Breyer R (1997a) *Mol. Pharmacol.* **51:** 61-68

Audoly L and Breyer R (1997b) *J. Biol. Chem.* **272:** 13475-13478

Awaji T, Hirasawa A, Kataoka M, Shinoura H, Nakayama Y, Sugawara T, Izumi S and Tsujimoto G (1998) *Mol. Endocrinol.* **12:** 1099-1111

Bakalyar HA and Reed RR (1990) *Science* **250:** 1403-1406

Barak LS, Ferguson SSG, Zhang J and Caron MG (1997b) *J. Biol. Chem.* **272:** 27497-27500

Barak LS, Ferguson SSG, Zhang J, Martenson C, Meyer T and Caron MG (1997a) *Mol. Pharmacol.* **51:** 177-184

Barlic J, Khandaker LS, Mahon MH, Andrews J, DeVries ME, Negrou E, Mitchell GB, Rahimpour R, Ferguson SSG and Kelvin DJ (1999) *J. Biol. Chem.* **274:** 16287-16294

Bastepe M and Ashby B (1999) *Br. J. Pharmacol.* **126:** 365-71

Bastien L, Sawyer N, Grygorczyk R, Metters K and Adam M (1994) *J. Biol. Chem.* **269:** 11873-11877

Benovic JL and Gomez J (1993) *J. Biol. Chem.* **268:** 19521-19527

Benovic JL, De Blasi A, Stone WC, Caron MG and Lefkowitz RJ (1989) *Science* **246:** 235-239

Benovic JL, Kuhn H, Wey I, Codina J, Caron MG and Lefkowitz RJ (1987) *Proc. Natl. Acad. Sci. USA* **84:** 8879-8882

Benovic JL, Onorato JJ, Arriza JL, Stone WC, Lohse MJ, Jenkins NA, Gilbert DJ, Copeland NG, Caron MG and Lefkowitz RJ (1991) *J. Biol. Chem.* **266:** 14939-14946

Benovic JL, Pike LJ, Cerione RA, Staniszewski C, Yoshimasa T, Codina J, Caron MG and Lefkowitz RJ (1985) *J. Biol. Chem.* **260:** 7094-70101

Benovic JL, Strasser RH, Caron MG and Lefkowitz RJ (1986) *Proc. Natl. Acad. Sci. USA* **83:** 2797-2801

Becker KP, Garnovskaya M, Gettys T and Halushka PV (1999) *Biochim. Biophys. Acta* **1450:** 288-296

Bergström S and Sjövall J (1957) *Acta. Chem. Scand.* **11:** 1086

Bhatnagar A, Willins DL, Gray JA, Woods J, Benovic JL and Roth BL (2001) *J. Biol. Chem.* **276:** 8269-8277

Biebermann H, Schoneberg T, Schulz A, Krause G, Gruters A and Schultz G, Gudermann T (1998) *FASEB J.* **14:** 1461-1471

Birnbaumer L and Rodbell M (1969) *J. Biol. Chem.* **244:** 3477-3482

Blaukat A, Pizard A, Breit A, Wernstedt C, Alhenc-Gelas F, Muller-Esterl W and Dikic I (2001) *J. Biol. Chem.* **276:** 40431-40440

Bley KR, Hunter JC, Eglen RM and Smith JA (1998) *Trends Pharmacol. Sci.* **19:** 141-147

Boer U, Neuschafer-Rube F, Moller U and Puschel GP (2000) *Biochem. J.* **350:** 839-847

Bohm SK, Khitin LM, Smeekens SP, Grady EF, Payan DG and Bunnett NW (1997) *J. Biol. Chem.* **272:** 2363-2372

Boie Y, Rushmore TH, Darmon-Goodwin A, Grygorczyk R, Slipetz DM, Metters KM and Abramovitz M (1994) *J. Biol. Chem.* **269:** 12173-12178

Boie Y, Sawyer N, Slipetz D, Metters K and Abramovitz M (1995) *J. Biol. Chem.* **270:** 18910-18916

Bol GF, Gros C, Hulster A, Bosel A and Pfeufer T (1997) *Biochem. Biophys. Res. Commun.* **237:** 251-256

Bouvier M, Collins S, O'Dowd BF, Campbell PT, de Blasi A, Kobilka BK, MacGregor C, Irons GP, Caron MG and Lefkowitz RJ (1989) *J. Biol. Chem.* **264:** 16786-16792

Bouvier M, Hausdorff WP, De Blasi A, O'Dowd BF, Kobilka BK, Caron MG and Lefkowitz RJ (1988) *Nature* **333:** 370-373

Bownds D, Dawes J, Miller J and Stahlman M (1972) *Nature* **237:** 125-127

Bremnes T, Paasche JD, Mehlum A, Sandberg C, Bremnes B and Attramadal H (2000) *J. Biol. Chem.* **275:** 17596-17604

Budd DC, McDonald JE and Tobin AB (2000) *J. Biol. Chem.* **275:** 19667-19675

Cali JJ, Zwaagstra JC, Mons N, Cooper DM and Krupinski J (1994) *J. Biol. Chem.* **269:** 12190-121905

Camps M, Hou C, Sidiropoulos D, Stock JB, Jakobs KH and Gierschik P (1992) *Eur. J. Biochem.* **206:** 821-831

Casey PJ, Moomaw JF, Zhang FL, Higgins YB and Thissen JA (1994) *Recent Prog. Horm. Res.* **49:** 215-238

Cassel D and Selinger Z (1978) *Proc. Natl. Acad. Sci. USA* **75:** 4155-4159

Castellani S, Paladini B, Paniccia R, Di Serio C, Vallotti B, Ungar A, Fumagalli S, Cantini C, Poggesi L and Neri Serneri GG (1997) *Am. Heart J.* **133:** 94-100

Liu Y, Ruoho AE, Rao VD and Hurley JH (1997) *Proc. Natl. Acad. Sci. USA* **94:** 13414-13419

Liu CH, Thangada S, Lee MJ, Van Brocklyn JR, Spiegel S and Hla T (1999) *Mol. Biol. Cell* **10:** 1179-1190

Logothetis DE, Kurachi Y, Galper J, Neer EJ and Clapham DE (1987) *Nature* **325:** 321-326

Lohse MJ, Andexinger S, Pitcher J, Trukawinski S, Codina J, Faure J-P, Caron MG and Lefkowitz RJ (1992) *J. Biol. Chem.* **267:** 8558-8564

Lohse MJ, Benovic JL, Caron MG and Lefkowitz RJ (1990b) *J. Biol. Chem.* **265:** 3202-3209

Lohse MJ, Benovic JL, Codina J, Caron MG and Lefkowitz RJ (1990a) *Science* **248:** 1547-1550

Lorenz W, Inglese J, Palczewski K, Onorato JJ, Caron MG, and Lefkowitz RJ (1991) *Proc. Natl. Acad. Sci. USA* **88:** 8715-8719

Luttrell LM, Daaka Y, Della Rocca GJ and Lefkowitz RJ (1997) *J. Biol. Chem.* **272:** 31648-31656

Maestes DC, Potter RM and Prossnitz ER (1999) *J. Biol. Chem.* **274:** 29791-29795

Matharu A-L, Mundell SJ, Benovic JL and Kelly E (2001) *J. Biol. Chem.* **276:** 30199-30207

Menard L, Ferguson SSG, Barak LS, Bertrand L, Premont RT, Colapietro AM, Lefkowitz RJ and Caron MG (1996) *Biochemistry* **35:** 4155-4160

Menard L, Ferguson SSG, Zhang J, Lin F, Lefkowitz RJ, Caron MG and Barak LS (1997) *Mol. Pharmacol.* **51:** 800-808

Miller WE and Lefkowitz RJ (2001) *Curr. Opin. Cell Biol.* **13:** 139-145

Miller WE, Maudsley S, Ahn S, Khan KD, Luttrell LM and Lefkowitz RJ (2000) *J. Biol. Chem.* **275:** 11312-11319

Min L, Galet C and Ascoli M (2002) *J. Biol. Chem.* **277:** 702-710

Moore RH, Tuffaha A, Millman EE, Dai W, Hall HS, Dickey BF and Knoll BJ (1999) *J. Cell. Sci.* **112:** 329-338

Moro O, Lameh J and Sadee W (1993) *J. Biol. Chem.* **268:** 6862-6865

Moro O, Shockley MS, Lameh J and Sadée W (1994) *J. Biol. Chem.* **269:** 6651-6655

Morrison KJ, Moore RH, Carsrud NDY, Trial J, Millman EE, Tuvim M, Clark RB, Barber R, Dickey BF and Knoll BJ (1996) *Mol. Pharmacol.* **50:** 692-699

Mundell SJ, Benovic JL and Kelly E (1997) *Mol. Pharmacol.* **51:** 991-998

Mundell SJ and Kelly E (1998) *Br. J. Pharmacol.* **125:** 1594-1600

Murakami A, Yajima T, Sakuma H, McLaren MJ and Inana G (1993) *FEBS Lett.* **334:** 203-209

Murata T, Ushikubi F, Matsuoka T, Hirata M, Yamasaki A, Sugimoto Y, Ichikawa A, Aze Y, Tanaka T, Yoshida N, Ueno A, Oh-ishi S and Narumiya S (1997) *Nature* **388:** 678-682

Nakamura K and Ascoli M (1999) *Mol. Pharmacol.* **56:** 728-736

Nakamura K, Krupnick JG, Benovic JL and Ascoli M (1998) *J. Biol. Chem.* **273:** 24346-24354

Namba T, Oida H, Sugimoto Y, Kakizuka A, Negishi M, Ichikawa A and Narumiya S (1994) *J. Biol. Chem.* **269:** 9986-9992

Namba T, Sugimoto Y, Negishi M, Irie A, Ushikubi F, Kakizuka A, Ito S, Ichikawa A and Narumiya S (1993) *Nature* **365:** 166-170

Negishi M, Sugimoto Y and Ichikawa A (1995) *Biochim. Biophys. Acta.* **1259:** 109-119
Ng GYK, Trogadis J, Stevens J, Bouvier M, O'Dowd BF and George SR (1995) *Proc. Natl. Acad. Sci. USA* **92:** 10157-10161

Nilius SM, Hasse A, Kuger P, Schror K and Meyer-Kirchrath J (2000) *FEBS Lett.* **484:** 211-216

Nishigaki N, Negishi M and Ichikawa A (1996) *Mol. Pharmacol.* **50:** 1031-1037

Noda K, Saad Y, Kinoshita A, Boyle TP, Graham RM, Husain A and Karnik SS (1995) *J. Biol. Chem.* **270:** 2284-2289

Nussenzveig DR, Heinflink M and Gershengorn MC (1993) *J. Biol. Chem.* **268:** 2389-2392

Nussenzveig DR, Thaw CN and Gershengorn MC (1994) *J. Biol. Chem.* **269:** 28123-28129

Oakley RH, Laporte SA, Holt JA, Barak LS and Caron MG (1999) *J. Biol. Chem.* **274:** 32248-32257

Oakley RH, Laporte SA, Holt JA, Caron MG and Barak LS (2000) *J. Biol. Chem.* **275:** 17201-17210

Oates JA, Fitzgerald GA, Branch RA, Jackson EK, Knapp HR and Roberts LJD (1988) *N. Engl. J. Med.* **319:** 689-698

O'Dowd BF, Hnatowich M, Regan JW, Leader WM, Caron MG and Lefkowitz RJ (1988) *J. Biol. Chem.* **263:** 15985-15992

Offermanns S, Laugwitz KL, Spicher K and Schultz G (1994) *Proc. Natl. Acad. Sci. USA* **91:** 504-508

Ohguro H, Van Hooser JP, Milam AH and Palczewski K (1995) *J. Biol. Chem.* **270:** 14259-14262

Oida H, Namba T, Sugimoto Y, Ushikubi F, Ohishi H, Ichikawa A and Narumiya S (1995) *Br. J. Pharmacol.* **116:** 2828-2837

Okuda-Ashitaka E, Sakamoto K, Ezashi T, Miwa K, Ito S and Hayaishi O (1996) *J. Biol. Chem.* **271:** 31255-31261

Opperman M, Freedman NJ, Alexander RW and Lefkowitz RJ (1996) *J. Biol. Chem.* **271:** 13266-13272

Orly J and Schramm M (1976) *Proc. Natl. Acad. Sci. USA* **73:** 4410-4414

Orsini MJ, Parent J-L, Mundell SJ and Benovic JL (1999) *J. Biol. Chem.* **274:** 31076-31086

Pak Y, O'Dowd BF, Wang JB and George SR (1999) *J. Biol. Chem.* **274:** 27610-27616

Palczewski K, Buczylko J, Kaplan MW, Polans AS and Crabb JW (1991) *J. Biol. Chem.* **266:** 12949-12955

Palczewski K, Buczylko J, Ohguro H, Annan RS, Carr SA, Crabb JW, Kaplan MW, Johnson RS and Walsh KA (1994) *Protein Sci.* **3:** 319-329

Palmer TM, Benovic JL and Stiles GL (1995) *J. Biol. Chem.* **270:** 29607-29613

Pals-Rylaarsdam R, Gurevich VV, Lee KB, Ptasienski JA, Benovic JL and Hosey MM (1997) *J. Biol. Chem.* **272:** 23682-23689

Pals-Rylaarsdam R, Xu Y, Witt-Enderby P, Benovic JL and Hosey MM (1995) *J. Biol. Chem.* **270:** 29004-29011

Parent J-L, Labrecque P, Orsini MJ and Benovic JL (1999) *J. Biol. Chem.* **274:** 8941-8948

Parenti M, Vigano MA, Newman CM, Milligan G and Magee AI (1993) *Biochem. J.* **291:** 349-353

Parruti G, Peracchia F, Sallese M, Ambrosini G, Masini M, Rotilio D and De Blasi A (1993) *J. Biol. Chem.* **268:** 9753-9761

Pavord ID, Wisniewski A, Mathur R, Wahedna I, Knox AJ and Tattersfield AE. (1991) *Thorax* **46:** 633-637

Pebay-Peyroula E, Rummel G, Rosenbusch JP and Landau EM (1997) *Science* **277:** 1676-1681

Pei G, Kieffer BL, Lefkowitz RJ and Freedman NJ (1995) *Mol. Pharmacol.* **48:** 173-177

Pfeufer T and Helmreich EJ (1975) *J. Biol. Chem.* **250:** 867-876

Pfister C, Chabre M, Plouet J, Tuyen VV, De Kozak Y, Faure JP and Kuhn H (1985) *Science* **228:** 891-893

Pierce KL, Fujino H, Srinivasan D and Regan JW (1999) *J. Biol. Chem.* **274:** 35944-35949

Pippig S, Andexinger S, Daniel K, Puzicha M, Caron MG, Lefkowitz RJ and Lohse MJ (1993) *J. Biol. Chem.* **268:** 3201-3208

Pippig S, Andexinger S and Lohse MJ (1995) *Mol. Pharmacol.* **47:** 666-676

Pitcher JA, Freedman NJ and Lefkowitz RJ (1998) *Ann. Rev. Biochem.* **67:** 653-692

Pitcher JA, Inglese J, Higgins JB, Arriza JL, Casey PJ, Kim C, Benovic JL, Kwatra MM, Caron MG and Lefkowitz RJ (1992) *Science* **257:** 1264-1267

Pitcher JA, Payne ES, Csortos C, DePaoli-Roach AA and Lefkowitz RJ (1995b) *Proc. Natl. Acad. Sci. USA* **92:** 8343-8347

Pitcher JA, Touhara K, Payne ES and Lefkowitz RJ (1995a) *J. Biol. Chem.* **270:** 11707-11710

Premont RT, Chen J, Ma HW, Ponnapalli M and Iyengar R (1992a) *Proc. Natl. Acad. Sci. USA* **89:** 9809-9813

Premont RT, Inglese J and Lefkowitz RJ (1995) *FASEB J.* **9:** 175-182

Premont RT, Jacobowitz O and Iyengar R (1992b) *Endocrinology* **131:** 2774-2784

Premont RT, Macrae AD, Stoffel RH, Chung N, Pitcher JA, Ambrose C, Inglese J, MacDonald ME and Lefkowitz RJ (1996) *J. Biol. Chem.* **271:** 6403-6410

Pronin AN and Benovic JL (1997) *J. Biol. Chem.* **272:** 3806-3812

Pronin AN, Satpaev DK, Slepak VZ and Benovic JL (1997) *J. Biol. Chem.* **272:** 18273-18280

Prou D, Gu WJ, Le Crom S, Vincent JD, Salamero J and Vernier P (2001) *J. Cell. Sci.* **114:** 3517-3527

Qian H, Pipolo L and Thomas WG (2001) *Mol Endocrinol.* **15:** 1706-1719

Rall TW, Sutherland EW, and Berhet J (1957) *J. Biol. Chem.* **224:** 463-475

Raposo G, Dunia I, Delavier-Klutchko C, Kaveri S, Strosberg AD and Benedetti EL (1989) *Eur. J. Cell Biol.* **50:** 340-352

Raposo G, Dunia I, Marullo S, Andre C, Guillet JG, Strosberg AD, Benedetti EL and Hoebeke (1987) *J. Biol. Cell* **60:** 117-123

Rasmanis G, Vesterqvist O, Green K and Henriksson P (1995) *Prostaglandins* **49:** 247-253

Ray K, Clapp P, Goldsmith PK and Spiegel AM (1998) *J. Biol. Chem.* **273:** 34558-34567

Raychowdhury MK, Yukawa M, Collins LJ, McGrail SH, Kent KC and Ware JA (1994) *J. Biol. Chem.* **269:** 19256-19261

Regan JW, Bailey TJ, Donello JE, Pierce KL, Pepperl DJ, Zhang D, Kedzie KM, Fairbairn CE, Bogardus AM, Woodward DF, *et al.* (1994b) *Br. J. Pharmacol.* **112:** 6163-6169

Regan JW, Bailey TJ, Pepperl DJ, Pierce KL, Bogardus AM, Donello JE, Fairbairn CE, Kedzie KM, Woodward DF and Gil DW (1994a) *Mol. Pharmacol.* **46:** 213-220

Rehwald M, Neuschafer-Rube F, de Vries C and Puschel GP (1999) *FEBS Lett.* **443:** 357-362

Richardson RM, Kim C, Benovic JL and Hosey MM (1993) *J. Biol. Chem.* **268:** 13650-13656

Rockman HA, Choi D-J, Rahman NU, Akhter SA, Lefkowitz RJ and Koch WJ (1996) *Proc. Natl. Acad. Sci. USA* **93:** 9954-9959

Rodbell M, Birnbaumer L, Pohl SL and Krans HM (1971) *J. Biol. Chem.* **246:** 1877-1882

Ross EM and Gilman AG (1977) *J. Biol. Chem.* **252:** 6966-6969

Sakai A, Yajima M and Nishio S (1990) *Life Sci.* **47:** 711-719

Schlador ML and Nathanson NM (1997) *J. Biol. Chem.* **272:** 18882-18890

Schleicher A, Kuhn H and Hofmann KP (1989) *Biochemistry* **28:** 1770-1775

Schmid A, Thierauch KH, Schleuning WD and Dinter H (1995) *Eur. J. Biochem.* **228:** 23-30

Schneider WP, Pike JE and Kupiecki FP (1966) *Biochim. Biophys. Acta.* **125:** 611-613

Schulein R, Lorenz D, Oksche A, Wiesner B, Hermosilla R, Ebert J and Rosenthal W (1998) *FEBS Lett.* **441:** 170-176

Schwaner I, Seifert R and Schultz G (1992) *Biochem. J.* **281:** 301-307

Sealfon SC, Weinstein H and Millar RP (1997) *Endocr. Rev.* **18:** 180-205

Segi E, Sugimoto Y, Yamasaki A, Aze Y, Oida H, Nishimura T, Murata T, Matsuoka T, Ushikubi F, Hirose M, Tanaka T, Yoshida N, Narumiya S and Ichikawa A (1998) *Biochem. Biophys. Res. Commun.* **246:** 7-12

Shapiro MJ and Coughlin SR (1998) *J. Biol. Chem.* **273:** 29009-29014

Shapiro MJ, Trejo J, Zeng D and Coughlin SR (1996) *J. Biol. Chem.* **271:** 32874-32880

Shayo C, Fernandez N, Legnazzi BL, Monczor F, Mladovan A, Baldi A and Davio C (2001) *Mol. Pharmacol.* **60:** 1049-1056

Shear M, Insel PA, Melmon KL and Coffino P (1976) *J. Biol. Chem.* **252:** 7572-76

Shih M, Lin F, Scott JD, Wang HY and Malbon CC (1999) *J. Biol. Chem.* **274:** 1588-1595

Shinohara T, Dietzschold B, Craft CM, Wistow G, Early JJ, Donoso LA, Horwitz J and Tao R (1987) *Proc. Natl. Acad. Sci. USA* **84:** 6975-6979

Shorr RG, Lefkowitz RJ and Caron MG (1981) *J. Biol. Chem* **256:** 5820-5826

Sibley DR, Benovic JL, Caron MG and Lefkowitz RJ (1987) *Cell* **48:** 913-922

Sibley DR and Lefkowitz RJ (1985) *Nature* **317:** 124-129

Sibley DR, Strasser RH, Benovic JL, Daniel K and Lefkowitz RJ (1986) *Proc. Natl. Acad. Sci. USA* **83:** 9408-9412

Silvius JR and l'Heureux F (1994) *Biochemistry* **33:** 3014-3022

Simonds WF, Goldsmith PK, Codina J, Unson CG and Spiegel AM (1989) *Proc. Natl. Acad. Sci. USA* **86:** 7809-7813

Slice LW, Yee HF Jr and Walsh JH (1998) *Receptor Channels* **6:** 201-212

Smith RD, Hunyady L, Olivares-Reyes JA, Mihalik B, Jayadev S and Catt KJ (1998) *Mol. Pharmacol.* **54:** 935-941

Smith WC, Milam AH, Dugger D, Arendt A, Hargrave PA and Palczewski K (1994) *J. Biol. Chem.* **269:** 15407-15410

Smyth EM, Austin SC, Reilly MP and Fitzgerald GA (2000) *J. Biol. Chem.* **275:** 32037-32045

Smyth EM, Li WH and Fitzgerald GA (1998) *J. Biol. Chem.* **273:** 23258-23266

Smyth EM, Nestor PV and Fitzgerald GA (1996) *J. Biol. Chem.* **271:** 33698-33704

Sohlemann P, Hekman M, Puzicha M, Buchen C and Lohse MJ (1995) *Eur. J. Biochem.* **232:** 464-472

Sondek J, Bohm A, Lambright DG, Hamm HE and Sigler PB (1996) *Nature* **379:** 369-374

Sorkin A and Carpenter G (1993) *Science* **261:** 612-615

Spiegel AM (1987) *Mol. Cell Endocrinol.* **49:** 1-16

Sprang SR (1997) *Ann. Rev. Biochem.* **66:** 639-678

Spring DJ and Neer EJ (1994) *J. Biol. Chem.* **269:** 22882-22886

Spurney RF, Ruiz P, Pisetsky DS and Coffman TM (1992) *Kidney Int.* **41:** 973-982

Sri Kantha S, Matsumura H, Kubo E, Kawase K, Takahata R, Serhan CN and Hayaishi O (1994) *Prostaglandins Leukot. Essent. Fatty Acids* **51:** 87-93

Stadel JM, Nambi P, Lavin TN, Heald SL, Caron MG, and Lefkowitz RJ (1982) *J. Biol. Chem.* **257:** 9242-9245

Stadel JM, Nambi P, Shorr RG, Sawyer DF, Caron MG and Lefkowitz RJ (1983a) *Proc. Natl. Acad. Sci. USA.* **80:** 3173-3177

Stadel JM, Strulovici B, Nambi P, Lavin TN, Briggs MM, Caron MG and Lefkowitz RJ (1983b) *J. Biol. Chem.* **258:** 3032-3038

Staehelin M and Simons P (1982) *EMBO J.* **1:** 187-190

Sterne-Marr R, Gurevich VV, Goldsmith P, Bodine RC, Sanders C, Donoso LA and Benovic JL (1993) *J. Biol. Chem.* **268:** 15640-15648

Stoffel RH, Inglese J, Macrae AD, Lefkowitz RJ and Premont RT (1998) *Biochemistry* **37:** 16053-16059

Stoffel RH, Randall RR, Premont RT, Lefkowitz RJ and Inglese J (1994) *J. Biol. Chem.* **269:** 27791-27794

Strader CD, Fong TM, Graziano MP and Tota MR (1995) *FASEB J.* **9:** 745-754

Strader CD, Sigal IS, Register RB, Candelore MR, Rands E and Dixon RA (1987) *Proc. Natl. Acad. Sci. USA* **84:** 4384-4388

Strasser RH, Sibley DR and Lefkowitz RJ (1986) *Biochemistry* **25:** 1371-1377

Strathmann M and Simon MI (1990) *Proc. Natl. Acad. Sci. USA* **87:** 9113-9117

Strulovici B, Cerione RA, Kilpatrick BF, Caron MG and Lefkowitz RJ (1984) *Science* **225:** 837-840

Strulovici B, Stadel JM and Lefkowitz RJ (1983) *J. Biol. Chem.* **258:** 6410-6414

Su Y-F, Harden TK and Perkins JP (1979) *J. Biol. Chem.* **254:** 38-41

Sugimoto Y, Yamasaki A, Segi E, Tsuboi K, Aze Y, Nishimura T, Oida H, Yoshida N, Tanaka T, Katsuyama M, Hasumoto K, Murata T, Hirata M, Ushikubi F, Negishi M, Ichikawa A and Narumiya S (1997) *Science* **277:** 681-683

Sullivan KA, Miller RT, Masters SB, Beiderman B, Heideman W and Bourne HR (1987) *Nature* **330:** 758-760

Sutherland EW and Rall TW (1958) *J. Biol. Chem.* **232:** 1077-1091

Takahashi K, Tsuchida K, Tanabe Y, Masu M and Nakanishi S (1993) *J. Biol. Chem.* **268:** 19341-19345

Tang WG and Gilman AG (1991) *Science* **254:** 1500-1503

Tarasova NI, Stauber RH and Michejda CJ (1998) *J. Biol. Chem.* **273:** 15883-15886

Taussig R and Gilman AG (1995) *J. Biol. Chem.* **270:** 1-4

Tholanikunnel BG and Malbon CC (1997) *J. Biol. Chem.* **272:** 11471-11478

Thomas WG, Thekkumkara TJ, Motel TJ and Baker KM (1995) *J. Biol. Chem.* **270:** 207-213

Tobin AB, Totty NF, Sterlin AE and Nahorski SR (1997) *J. Biol. Chem.* **272:** 20844-20849

Trapaidze N, Keith DE, Cvejic S, Evans CJ and Devi LA (1996) *J. Biol. Chem.* **271:** 29279-85

Trejo J, Altschuler Y, Fu HW, Mostov KE and Coughlin SR (2000) *J. Biol. Chem.* **275:** 31255-31265

Trejo J and Coughlin SR (1999) *J. Biol. Chem.* **274:** 2216-2224

Tseng MJ, Detjen K, Struk V and Logsdon CD (1995) *J. Biol. Chem.* **270:** 18858-18864

Tsuga H, Kameyama K, Haga T, Honma T, Lameh J and Sadee W (1998) *J. Biol. Chem.* **273:** 5323-5330

Tsuga H, Kameyama K, Haga T, Kurose H and Nagao T (1994) *J. Biol. Chem.* **269:** 32522-32527

Unger VM, Hargrave PA, Baldwin JM and Schertler GF (1997) *Nature* **389:** 203-206

Urade Y and Hayaishi O (1999) *Biochim. Biophys. Acta.* **1436:** 606-615

Valiquette M, Bonin H, Hnatowich M, Caron MG, Lefkowitz RJ and Bouvier M (1990) *Proc. Natl. Acad. Sci. USA* **87:** 5089-5093

Valiquette M, Parent S, Loisel TP and Bouvier M (1995) *EMBO J.* **14:** 5542-5549

van Dorp, Beerthuis RK, Nugteren DH and Vonkerman H (1964) *Biochim. Biophys. Acta.* **90:** 204-207

Vane JR and Botting RM (1995) *Am. J. Cardiol.* **75:** 3A-10A

Venkatesan S, Petrovic A, Locati M, Kim YO, Weissman D and Murphy PM (2001) *J. Biol. Chem.* **276:** 40133-40145

Vickery RJ and von Zastrow M (1999) *J. Cell. Biol.* **144:** 31-43

Vilardaga J-P, Krasel C, Chauvin S, Bambino T, Lohse MJ and Nissenson RA (2002*) J. Biol. Chem.* **277:** 8121-8129

Vogler O, Bogatkewitsch GS, Wriske C, Krummenerl P, Jakobs KH and van Koppen CJ (1998) *J. Biol. Chem.* **273:** 12155-12160

Vogler O, Nolte B, Voss M, Schmidt M, Jakobs KH and van Koppen CJ (1999) *J. Biol. Chem.* **274:** 12333-12338

von Euler US (1934) *Naunyn-Schmiedebergs Arch. Pharmacol.* **175:** 78-84

von Zastrow M (2001) *Parkinsonism Relat. Disord.* **7:** 265-271

von Zastrow M and Kobilka BK (1992) *J. Biol. Chem.* **267:** 3530-3538

von Zastrow M, Link R, Daunt D, Barsh G and Kobilka B (1993) *J. Biol. Chem.* **268:** 763-766

Vrecl M, Anderson L, Hanyaloglu A, McGregor AM, Groarke AD, Milligan G, Taylor P and Eidne KA (1998) *Mol. Endocrinol.* **12:** 1818-1829

Walsh MT, Foley JF and Kinsella BT (1998) *J. Pharmacol. Exp. Ther.* **286:** 1026-1036

Walsh MT, Foley JF and Kinsella BT (2000) *J. Biol. Chem.* **275:** 20412-20423

Watson S and Arkinstall S (1994) *The G-protein Linked Receptor Facts Book* 1st ed. Academic Press, San Diego.

Wedegaertner PB, Chu DH, Wilson PT, Levis MJ and Bourne HR (1993) *J. Biol. Chem.* **268:** 25001-25008

Weiss ER, Raman D, Shirakawa S, Ducceschi MH, Bertram PT, Wong F, Kraft TW and Osawa S (1998) *Mol. Vis.* **4:** 27

Werbonat Y, Kleutges N, Jakobs KH and van Koppen CJ (2000) *J. Biol. Chem.* **275:** 21969-21972

Wess J (1993) *Trends Pharmacol. Sci.* **14:** 308-313

Wess J, Bonner TI, Dorje F and Brann MR (1990) *Mol. Pharmacol.* **38:** 517-523

West RE Jr, Moss J, Vaughan M, Liu T and Liu TY (1985) *J. Biol. Chem.* **260:** 14428-14430

Whaley BS, Yuan N, Birnbaumer L, Clark RB and Barber R (1994) *Mol. Pharmacol.* **45:** 481-489

Wilden U, Hall SW and Kuhn H (1986b*) Proc. Natl. Acad. Sci. USA*. **83:** 1174-1178

Wilden U, Wust E, Wey I and Kuhn H (1986a) *FEBS Lett.* **207:** 292-295

Willars GB, Heding A, Vrecl M, Sellar R, Blomenrohr M, Nahorski SR and Eidne KA (1999) *J. Biol. Chem.* **274:** 30146-30153

Willets J M, Challiss RAJ, Kelly E and Nahorski SR (2001) *Mol. Pharmacol.* **60:** 321-330

Wilson S, Chambers JK, Park JE, Ladurner A, Cronk DW, Chapman CG, Kallender H, Browne MJ, Murphy GJ and Young PW (1996) *J. Pharmacol. Exp. Ther.* **279:** 214-221

Wise H (1999) *Eur. J. Pharmacol.* **386:** 89-96

Woods JW, Goodhouse J and Farquhar MG (1989) *Eur J. Cell. Biol.* **50:** 132-143

Wu G, Krupnick JG, Benovic JL and Lanier SM (1997) *J. Biol. Chem.* **272:** 17836-17842

Xiang B, Yu GH, Guo J, Chen L, Hu W, Pei G and Ma L (2001) *J. Biol. Chem.* **276:** 4709-4716

Xiao Z, Zhang N, Murphy DB and Devreotes PN (1997) *J. Cell Biol.* **139:** 365-374

Yamaki K, Tsuda M, Kikuchi T, Chen KH, Huang KP and Shinohara T (1990) *J. Biol. Chem.* **265:** 20757-20762

Yan SZ, Huang ZH, Rao VD, Hurley JH and Tang WJ (1997) *J. Biol. Chem.* **272:** 18849-18854

Yoshimura M and Cooper DM (1992) *Proc. Natl. Acad. Sci.* **89:** 6716-6720

Yu R and Hinkle PM (1999) *J. Biol. Chem.* **274:** 15745-15750

Yu SS and Lefkowitz RJ (1993) *J. Biol. Chem.* **268:** 337-341

Zhang Z, Austin SC and Smyth EM (2001) *Mol. Pharmacol.* **60:** 480-487

Zhang J, Barak LS, Anborgh PH, Laporte SA, Caron MG and Ferguson SSG (1999) *J. Biol. Chem.* **274:** 10999-11006

Zhang J, Barak LS, Winkler KE, Caron MG and Ferguson SSG (1997) *J. Biol. Chem.* **272:** 27005-27014

Zhang J, Ferguson SSG, Barak LS, Menard L and Caron MG (1996) *J. Biol. Chem.* **271:** 18302-18305